PIEZO ACTUATED FLEXURAL STAGE

FOR

SUB-MICRON PRECISION MEASUREMENT

David Madigan

M.Eng

Waterford Institute of Technology

Internal Supervisor: Mr. Joseph Phelan

Submitted to Waterford Institute of Technology,

October 2008

Declaration

FLEXURAL-HINGE GUIDED STAGE FOR SUB-MICRON PRECISION MEASUREMENT

Presented to: Mr. Joe Phelan

Department of Engineering Technology

Waterford Institute of Technology

This Thesis is presented in fulfillment of the requirements for the degree of Masters of Engineering. It is entirely of my own work and has not been submitted to any other college or higher institution, or for any other academic award in this College. Where use has been made of the work of other people it has been fully acknowledged and fully referenced.

Signed: _____

David Madigan

Date: _____

Acknowledgements

I would like to thank those who gave help and advice during the course of this project. Their help proved invaluable.

I would like, in particular, to thank my supervisor, Mr. Joe Phelan for his continuous help, encouragement and guidance and also the following people whose help I greatly appreciated:

Mr. David Walsh	Lecturer
Mr. Colman Shouldice	Post-graduate Student
Mr. Paul Allen	Lecturer
Mr. Albert Byrne	Head of Department of Engineering Technology
Mr. Mark Maher	Manufacturing Technician
Mr. Seamus Scully	Engineering Manager, NN Euroball
Mr. Keith Pheasey	Quality Engineer, NN Euroball
Mr. Christy Hayes	Managing Director, NN Euroball
Mr. Tom O'Shea	Maintenance Manager, NN Euroball
Mr. Joe Egan	Store Manager, NN Euroball
Mr. Patrick Sweeney	Graduate
Mr. Eoin Scally	Graduate
Mr. Nick Fenelon	Graduate
Mr. Kevin Irish	Graduate
Mr. Ian Brennan	Graduate
Mr. Niall Thompson	Graduate

Table of Contents

List of Figures

List of Tables

PIEZO ACTUATED FLEXURAL STAGE FOR SUB-MICRON PRECISION MEASUREMENT

David Madigan

Abstract

This thesis presents the design of a novel piezo-driven, sub-micron, comparative measurement stage for an automatic high-speed in-process industrial control system. The design features the use of precision solid flexures to transmit motion from a low voltage piezo stack to the measurement tip. This motion is used to determine height differences between a reference standard and a sample ball bearing. The key product diameter dimension is computed from this and is the basis of the feedback for automatic control of the production process.

The aim of the automated measurement system is to precisely control the multiple continuous and repetitive metal reduction stages throughout a ball bearing manufacturing process. This thesis largely concentrates on the design, construction, control and testing of the piezo based measurement instrument, but also discusses the automatic sampling and delivery process, process control and the communication methods between the measurement system and the manufacturing process.

Throughout the initial design stage of the measurement instrument, the focus is on the first two phases of the design: analytical design and finite element analysis (FEA). Design equations developed to predict the behaviour of the stages are used to compute the stiffness, displacement, stress and resonant frequency of the stage; modifications of dimensions enables the control and optimisation of the response of the measurement stage to achieve the desired outcome. Finite element analysis is then used to verify estimations obtained from the analytical design phase.

Testing of the measurement instrument focuses on specifying the in-production system capabilities in terms of trueness and precision of measurements; the tests prove and validate the functionality of the instrument within the production facility.

Keywords: Sub-Micron Measurement; Comparative Measurement; Flexure Stage; Piezo Actuation

1 Introduction

1.1 Background

Ball bearing manufacture at the specific production facility which is the focus of this project, can be characterised briefly as follows: a batch production industry using multiple parallel high-volume standalone machines: eight common production stages – heading, flashing, heat treatment, grinding, coarse-lapping, finish-lapping, defect-detection and classification, and packaging; ball diameter measurement is the key control issue in each stage. Machine adjustment is currently carried out manually on the basis of hourly measurement checks built into cut-down charts. An unavoidable feature of this industry is the difficult working conditions: very high acoustic and electrical noise, vibration, large heat generation as well as high humidity, all arising from the huge metal removal processes involved.

The economics of current ball bearing production mainly hinges on the efficient control of batch grinding and lapping processes (for minimum cost) and the effective production and classification of finished balls into tight tolerance ranges, to maximise value; within the production facility (and indeed throughout the world), ball diameter measurement is the critical process in both of these factors. The machine adjustment process must balance a desire for rapid size reduction (cost minimisation) against essential quality requirements (value creation), precision, sphericity and surface finish.

Currently the in-process measurement of product in the facility is carried out manually on a laboratory type instrument, see Figure 12 (feedback and machine adjustment are also completed manually). Comparative measurement is used in this manual process: the nominal measurement accuracy achieved is 1μm: both the production samples and the standard components are held for a defined period in a temperature normalising fluid prior to measurement in order to equalise their temperatures.

This project targets the development of an automatic in-line, high resolution, high-speed piezo measurement instrument to service a representative section of production within the facility, (with a view to total plant servicing in the future). The total integration (both physically and electronically) of the instrument with targeted production machines in cooperation with a parallel postgraduate project is also addressed in the project.

In order to service a higher quality, higher value product, the company has targeted a measurement accuracy of 0.1μm. The possibilities of achieving this with the current manual process, without significant labour cost increase, is not a realistic prospect for the company. Manual measurement must therefore be replaced by an automated system: and measurement accuracy must be improved by a factor of ten, putting it into the sub-micron scale.

The current product range is 10–13.5mm diameter, thereby defining a 3.5mm measuring range for the measurement process. Approximately 60 component measurements per hour are currently taken. It is estimated that any new automated system needs to be capable of measuring 280 products hourly (a measurement cycle time of 12.85 seconds). The vision is that measurements will be taken at more frequent intervals and in greater sample sizes; this will be necessary to service both improved product tolerances and improved machine performance, allowing both improved confidence levels and the tightening of machine control limits.

The key development in this project is the design of the piezo-based measurement instrument. A feasibility study had confirmed the feasibility of piezo-based measurement for the specific application: further cycles of research, prototyping and improvement are necessary to optimise performance and provide the required accuracy in the production instrument.

2 Technical Review

2.1 Current Ball Bearing Industry Standards

2.1.1 Introduction

A bearing is the support and guide for a rotating, oscillating or sliding shaft, pivot or wheel [30]: a device to permit constrained relative motion between two parts, typically rotation or linear movement. Ever since objects have been moved, round rollers were used to make the job easier; Egyptians used logs to roll huge blocks of stone for pyramids. Eventually the idea was developed of securing the roller to whatever was being moved, creating the first vehicle with wheels. However, these used bearings known as plain bearings made from materials rubbing on each other instead of rolling on each other. A typical plain bearing is made of two parts; a rotary plain bearing can be just a shaft running through a hole. It was not until the late eighteenth century that the basic design for bearings was developed. Philip Vaughan was a Welsh inventor and ironmaster who patented the first design for a ball bearing in Carmarthen in 1794 [32]; his design ran along a track in an axle assembly, known as a ball race, thus originating the modern ball bearing design [33]. Development continued through the nineteenth and early twentieth centuries, spurred by the advancement of the bicycle and the automobile.

The purpose of a bearing is to reduce friction and support radial loads (load applied perpendicular to the bearing axis of rotation) and axial loads (thrust load, applied to the bearing parallel with the bearing axis of rotation). Bearings reduce friction by providing smooth metal balls or rollers and a smooth inner and outer metal surface for the balls to roll against. These balls or rollers "bear" the load, allowing the device to spin smoothly. Generally one of the races is fixed; this allows the second race to rotate which also causes the balls to rotate. This rotation causes a lower coefficient of friction, than if the two flat surfaces were rotating on each other.

2.1.2 Bearing Types

Bearings may be classified broadly according to the motions they allow and according to their principle of operation as well as by the directions of applied loads they can handle. Depending on where the bearing is being used, it may see all radial loading, all thrust loading or a combination of both. Typically, bearings that support the shafts of motors and pulleys are subject to a radial load; in this case, most of the load comes from the tension in the belt connecting the two pulleys. Thrust bearings that support axial loads can be found in the clutch of a car. Other bearings like the one in the hub of a car wheel are required to support both a radial load and a thrust load; the radial load comes from the weight of the car and the thrust load comes from the cornering forces as the car turns on a bend.

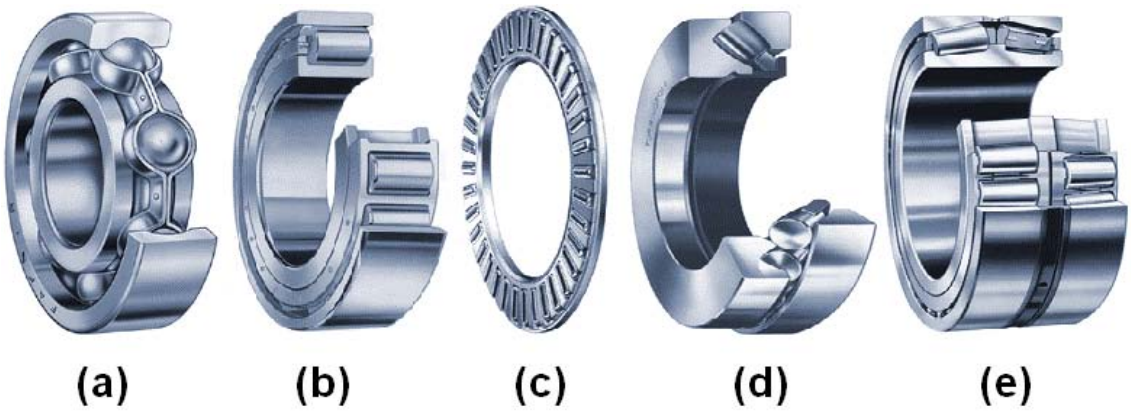

Figure 1 Types of Bearings [31]

There are thousands of sizes, shapes and kinds of bearings; ball bearings, roller bearings, needle bearings, thrust and tapered roller bearings are the major kinds. Ball bearings as shown in Figure 1 (a) are probably the most common type of bearing. These bearings can handle both radial and thrusts loads and are usually found in applications where the load is relatively small; for lightly loaded bearings, balls offer lower friction than rollers. In a ball bearing, the load is transmitted from the outer race to the ball and from the ball to the inner race. Since the ball is a sphere, it only contacts the inner and outer race over a very small area, which helps the bearing to rotate very smoothly. On the other hand this means that load is spread over a very small area and if the bearing is overloaded, the balls can easily deform ruining the bearing.

Common roller bearings like the one illustrated in Figure 1 (b) use cylinders of slightly greater length than diameter as the rolling element and are used in applications

like conveyor belt rollers, where they must hold heavy radial loads. Using rollers means that the contact between the inner and outer race is not a point but a line; this spreads the load out over a large area, allowing the bearing to handle much greater loads than a ball bearing. However this type of bearing is not designed to handle much thrust loading; any misalignment of the outer and inner races greatly reduces the bearing capacity. A variation of this type of bearing, called a needle bearing uses very long cylindrical rollers with very small diameters to reduce friction of rotating surfaces in very tight spaces. Since the rollers are very thin, the difference between the diameter of the shaft and the diameter of the bearing is greatly reduced, allowing for a compact design. The drive shaft of a rear wheel drive vehicle typically has at least eight needle bearings, four in each universal joint.

The type of bearing illustrated in Figure 1 (c) is known as a roller thrust bearing and is designed to support large thrust loads. They are often used to support a vertical shaft against gravitational loads, but are most commonly found in car transmissions between gears and between the housing and the rotating shafts; the helical gears used in transmissions have angled teeth, which cause a thrust load that must be supported by a bearing.

Illustrated in Figure 1 (d) and (e) are tapered roller bearings, tapered roller bearings use conical rollers that run on conical races. The inner and outer ring raceways are segments of cones and the rollers are also made with at taper; therefore if projected, the conical surfaces of the raceways and the roller axes would all meet at a common point on the main axis of the bearing. As mentioned, most roller bearings are only suitable to take radial loads, but tapered roller bearings can support both radial and axial loads and can carry higher loads than ball bearings due to greater contact area. For that reason, tapered roller bearings are most commonly used as the wheel bearings of most cars. The complexity of the manufacturing process is the greatest downside to this type of bearing; hence tapered roller bearings are usually more expensive than ball bearings. Also, under heavy loads the tapered roller acts like a wedge and the bearing loads tend to try eject the roller; the force from the collar which keeps the roller in the bearing adds to bearing friction compared to ball bearings.

There is a vast variety in the sizes for all types of bearings. Sizes vary from being small enough to run miniature motors, to huge bearings typically used to support rotating parts in hydroelectric power plants and cranes; these large bearings can be over

3 meters in diameter. The most common sizes can fit in one hand and are used in things like electric motors.

Generally ball bearings are the less expensive choice in small sizes under lighter loads, while roller bearings are less expensive for larger sizes and heavier loads; roller bearings are more satisfactory under shock or impact loading. A ball bearing cannot rotate forever, even if ball bearings are properly installed, adequately lubricated, protected from foreign matter and are not subjected to extreme operating conditions, sooner or later material fatigue will occur. The period until the first sign of fatigue occurs is a function of the number of cycles performed by the bearing and the magnitude of the load. Fatigue is the result of shear stresses appearing immediately below the load-carrying surface: after time stresses cause cracks which gradually extend up the surface. As the balls pass over the cracks, fragments of the material break away and this is known as flaking or spalling [34]. The flaking progressively increases and eventually makes the bearing unusable; the life of a ball bearing is defined as the number of revolutions the bearing can perform before incipient (beginning to appear) flaking occurs.

The trueness and precision of the measurement instrument used to measure the balls for bearings is a very important factor in relation to the life of the complete ball bearing; if the measurements are biased in either direction, the balls can ultimately be either too large or too small for the space between the inner and outer races. A loose fit between the balls and the raceways can cause relative motion between mating parts. If the relative motion between mating parts is slight but continuous, fretting occurs. Fretting is the generation of fine metal particles that oxidize, leaving a distinctive brown colour. This material is abrasive and will aggravate the looseness; if the looseness is enough to allow considerable movement of the inner or outer ring, the mounting surfaces (bore, outer diameters, faces) will wear and heat, causing run-out problems. In contrast, a tight fit between the balls and the raceways will lead to a heavy wear path in the bottom of the raceway around the entire circumference of the inner and outer races. When interference fits exceed the radial clearance at the operating temperature, the balls become excessively loaded and this results in a rapid temperature rise accompanied by high torque. Continued operation under such conditions can lead to rapid wear and fatigue.

2.1.3 Bearing Ball Materials

Bearing steels must posses high strengths, toughness, wear resistance, dimensional stability, annealability, machinability, manufacturing reliability, mechanical and rolling contact fatigue resistance and freedom from internal defects [36]. There are essentially two choices for the material used in balls for bearings, stainless steel or chrome steel.

Stainless steel balls are preferred in environments where corrosion and chemical resistance are required. These materials have evolved in response to different manufacturing and application needs; they are also commonly specified for food and beverage processing machinery, medical applications, medicine equipment and aerospace applications. 400 series martensitic (A structure in quenched steel which has the maximum hardness of any of the structures resulting from the decomposition or transformation of austenite [37]) stainless steel is the standard material where corrosion resistance is more important than load bearing capacity. Three of the most common types of stainless steel used are DR Stainless steel, AISI 440C Stainless steel and ES1 Stainless steel. DR Stainless steel is used in the manufacture of most corrosion resistant balls; the chemical composition for this material is shown in Table 1. DR Stainless steel has been specially developed to give excellent lifetime and low noise characteristics, combined with superior corrosion-resistance.

DR Stainless Steel Chemical Composition (%)						
C Carbon	Si Silicon	Mn Manganese	P Phosphorous	S Sulphur	Cr Chromium	Mo Molybdenum
0.6-0.7	Max1.0	Max1.0	Max0.03	Max 0.01	12-13.5	Max 0.25

Table 1 DR Stainless Steel Chemical Composition

The chemical composition of AISI 440C is shown in Table 2, this materials very high carbon content is responsible for exhibiting excellent toughness and hardness properties: following heat treatment, type 440C attains the highest hardness of any stainless steel, while maintaining a good resistance to corrosion. This material is used extensively for balls in bearing applications where precise tolerances and surfaces are required. The use of 440C stainless steel has declined in favour of other, more modern stainless steel formulations.

AISI 440C Stainless Steel Chemical Composition (%)						
C Carbon	Si Silicon	Mn Manganese	P Phosphorous	S Sulphur	Cr Chromium	Mo Molybdenum
0.95-1.2	Max1.0	Max 1.0	Max 0.04	Max 0.03	16-18	Max 0.75

Table 2 AISI 440C Stainless Steel Chemical Composition

ES1 Stainless steel shown in Table 3 is a relatively new stainless steel. This formulation has excellent machinability (relative ease of machining a metal [37]); this allows for ball finish characteristics approaching those of chrome steel, combined with a corrosion resistance at least equal to AISI 440C.

ES1 Stainless Steel Chemical Composition (%)						
C Carbon	Si Silicon	Mn Manganese	P Phosphorous	S Sulphur	Cr Chromium	Mo Molybdenum
0.44	0.2-0.4	0.2-0.4	Max 0.03	Max 0.01	12.8-13.2	Max 0.25

Table 3 ES1 Stainless Steel Chemical Composition

The vast majority of balls to be measured using the automatic in-line, high resolution piezo measurement instrument for the specific production facility are made of chromium steel in the form of hot rolled spheroidized wire rod and small diameter cold drown spheroidized rod. This material is supplied in coils by mills in the spheroidized-annealed condition, which is a heating process to create globular carbides in the rod [37]. The specific chromium steel used is SAE-AISI 52100: this is the standard material used for ball bearing applications where load capacity is the consideration. This steel is relatively inexpensive and is the most widely used steel for the manufacture of balls for bearings: its hardness, at about 62 HRC (Hardness on the Rockwell “C” scale) leads to good wear resistance and rolling contact resistance. The machinability of this steel is excellent; giving smooth, low noise ball finishes, together with superior life. In corrosive environments it is not recommended to use chrome steel balls.

SAE-AISI 52100		
Element	**Minimum Percent**	**Maximum Percent**
Carbon C	0.98	1.05
Manganese Mn	0.25	0.45
Phosphorus P	-	0.02
Sulphur S	-	0.008
Silicon Si	0.15	0.35
Chromium Cr	1.35	1.6
Copper Cu	-	0.2
Nickel Ni	-	0.25
Molybdenum Mo	-	0.08
Oxygen O	-	9.0 ppm max
Titanium Ti	-	30.0 ppm max
Aluminium Al	0.01	0.05

Table 4 SAE-AISI 52100 Chromium Steel Chemical Composition

The 52100 steel is a high-carbon chromium alloy steel, (Table 4). The hardness of steel is increased by the addition of more carbon. Adding carbon up to about 1.5% can increase the wear resistance of the steel: beyond this point the increase of carbon reduces toughness and increases brittleness.

The addition of chromium in the steel increases the hardness penetration and also increases the toughness and wear resistance. The amount of chromium in the AISI 52100 steel is what distinguishes it from the stainless steels previously discussed; steels with 12% or more chromium are referred to as stainless steels. The Manganese and Silicon in the steel when used with other alloys help increase the toughness and hardness penetration of the steel.

In the annealed condition this steel is comparatively easy to machine, however very high hardness and abrasion resistance can be developed by heat-treatment to make the steel particularly suitable for ball bearing applications where extreme wear resistance is required.

2.1.4 Technical Requirements of Balls for Bearings

In the 20th century the highest quality ball bearings were made by German manufactures; hence ball bearings have generally been sized in millimetres, but the balls themselves were frequently sized in inches. Over the last decade this has slowly changed, balls are now commonly sized in mm while still producing imperial ball sizes e.g. 7/16 inch ball is now termed as a 11.112mm ball. The preferred nominal ball diameters are given in Table 5: where applicable, the corresponding inch sizes are given for reference purpose only. The nominal ball diameter D_W is the diameter value, which is used for the general identification of a ball size [8]. The specific range of balls required to be measured using the proposed piezo measurement instrument are highlighted in the red box.

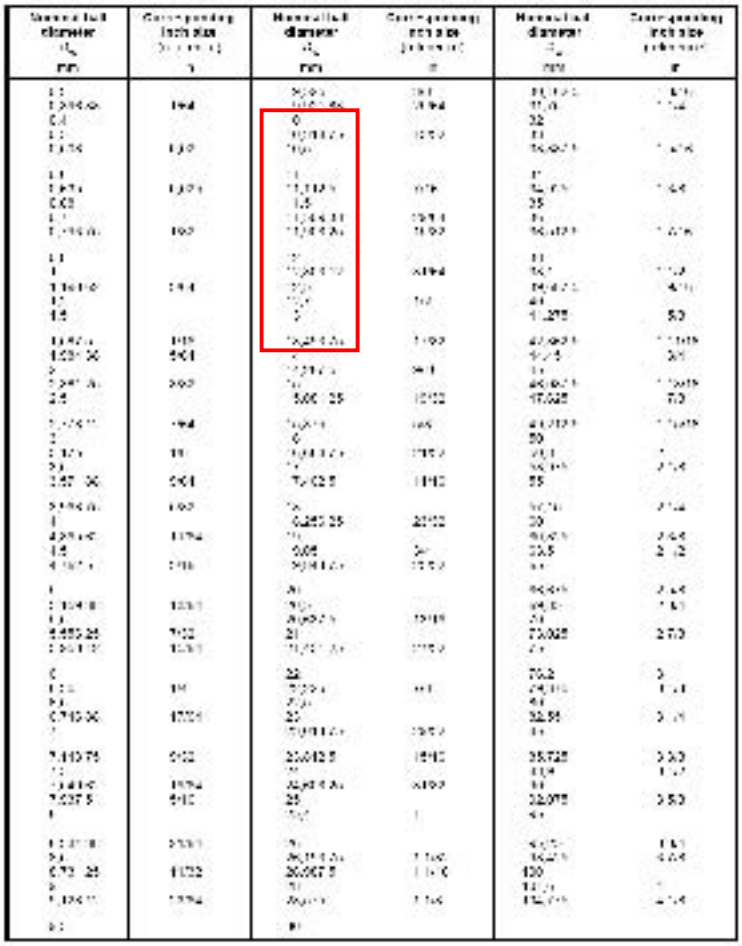

Table 5 Preferred Nominal Ball Diameters [8]

Precision bearing balls are specified by grades; these ball grades designate a manufacturing tolerance system for the bearing balls. Ball grade is the specific combination of dimensional, form, surface roughness and sorting tolerances for balls

[8]. As shown in Table 6, the letter G and a number identify ball grade; the lower the grade number the higher the accuracy requirements for each of the bearing balls. There is less geometrical variation and higher surface quality in higher-grade balls. High-grade balls offer superior contact surfaces, which cause less vibration in high-speed applications; this lowers the fatigue and increases the lifetime of the bearing. The variation of ball diameter V_{Dws} is the difference between the largest and the smallest of the single diameters of a ball [8]. Deviation from spherical form is the greatest radial distance, in any equatorial plane (plane passing through the equator of a ball), between the smallest circumscribed sphere and the greatest inscribed sphere, with their centres common to the least square sphere centre [8]. The measurement of deviation from the spherical form of balls is carried out by the measurement of roundness deviation in a required number of single equatorial planes: roundness deviation being measured in three equatorial planes 90˚ to each other. The level of sphericity is expressed in millionths of an inch (.0254μm); for example a Grade 10 ball must have a roundness (circularity) of each spherical element within 10 millionths of an inch (.25μm). The surface roughness of each ball must also be within certain tolerances for each grade; surface roughness includes irregularities with relatively small spacing, which usually include irregularities resulting from the method of manufacture being used and/or other influences. Grades 5, 10 and 16 bearings are generally used for white goods, industrial applications and car hub bearings respectively.

Grade	Variation of ball diameter V_{Dws} max.	Deviation from spherical form max.	Surface roughness Ra max.
G 3	0,08	0,08	0,010
G 5	0,13	0,13	0,014
G 10	0,25	0,25	0,020
G 16	0,4	0,4	0,025
G 20	0,5	0,5	0,032
G 24	0,6	0,6	0,040
G 28	0,7	0,7	0,050
G 40	1	1	0,060
G 60	1,5	1,5	0,080
G 100	2,5	2,5	0,100
G 200	5	5	0,150
NOTE The values given in this table do not take into account surface defects; hence measurement must be taken outside such defects.			

Table 6 Form and Surface Roughness Tolerances [8]

The ordered size of a ball lot (definite quantity of balls manufactured under conditions presumed uniform and which is considered as an entity [8]) is usually

expressed as the nominal diameter plus ball gauge; the ball gauge is defined as the amount by which the mean diameter of a ball lot should differ from the nominal ball diameter [8]. Maintaining tight tolerances while manufacturing the inner and outer raceways is very difficult; therefore bearing balls are ordered with different gauge values to suit the varying ring diameters. It is assumed for forecasting purposes that the manufacturing errors of the raceways are normally distributed; this allows the manufacturer to decide what percentage of each gauge value to produce. The preferred gauge values are shown in Table 7: gauge values can be characterised as P, N or M to indicate respectively a positive, nominal and negative diameter. For example, a 12.7mm (P3) is the basic diameter of a ball lot having a mean diameter of 12.7mm +0.003mm (12.703mm).

GRADE	GAUGE INTERVAL	GAUGE FRAME	GAUGE INTERSECT DEVIATION
G5 to G16	3	M9...M3, P0, P3...P9	± 0,5
G20 to G24	3	M9...M3, P0, P3...P9	± 1,0
G28 to G60	3	M9...M3, P0, P3...P9	± 2.0
G100 and G200	4	M12...M4, P0, P4...P12	± 2,0

Table 7 Preferred Gauges

A ball gauge, in combination with the ball grade and nominal diameter is considered as the most exact ball specification and therefore for ordering purposes the customer must specify these three characteristics for each ball lot. For example, to order a 13mm, Grade 5, P3 ball lot, the customer designations should be filled in as shown in Table 8.

1	2	3	4	5	6	7	8	9	10	11	12	13
0	1	3	0	0	0	G	0	0	5	P	0	3
Dw						**ID**	**Grade**			**Gauge**		

Table 8 Customer Designation

- Dw: This area consists of 6 characters and represents the ball diameter expressed in mm.
- ID: This area consists of 1 character and is "G" for steel balls
- Grade: This area consists of 3 characters and details the ball quality grade.
- Gauge: This area consists of 3 characters and specifies the ball gauge.

The economics of bearing ball production is largely dependent on the effective production and classification of finished balls into the tight tolerance ranges shown in Table 6 and Table 7. Unbiased and precise measurement is extremely important when dealing with these extreme small tolerances; the distinguishing geometry for ovality and roundness between one to another quality grade is in the sub-micron range.

The requirements are even higher for surface roughness measurements. Currently, there is no calibrated equipment that could be used for roughness measurements at the range required; to distinguish between the surface roughness tolerances of different high grade balls the response of the measurement instrument to changes in the measured balls surface roughness i.e. the sensitivity, is required to be 1 nanometer. Sensitivity is defined as the smallest input that results in a detectable (useable) output signal [23].

Currently, the bearing balls manufactured at the specific production facility range from G5 to G20. The tolerances for the highest quality G5 ball, specify that the max variation of ball diameter is 0.13μm and the max variation of ball lot diameter is 0.25μm; the variation of ball lot diameter is the difference between the mean diameters of the largest and the smallest ball in a ball lot [8]. Since higher grade balls have less variation, it is anticipated that higher grade balls will yield more accurate and precise measurements. The nominal measurement accuracy currently being achieved with the manual measurement process is 1μm; therefore to improve the measurement process, the target measurement accuracy for the automatic piezo measurement instrument is 0.1μm.

2.2 Company and Process Description

2.2.1 Company Overview

NN, Inc (NN) manufactures precision balls, cylindrical and tapered rollers, bearing retainers, plastic injection moulded products, precision bearing seals and precision metal components. The Company's balls, rollers, retainers and bearing seals are used primarily in the domestic and automotive bearing industry. The plastic injection moulded products are used in the bearing, automotive, instrumentation and fibre optic industries. The Company's precision metal components products are used in automotive, diesel engine and refrigeration industries.

NN operates in the US, Europe, Asia, Canada, Mexico and South America and primarily operates through three business segments: metal bearing components, plastic and rubber components and precision metal components. The Company's metal bearing components segment manufactures and sells steel balls in sizes ranging in diameter from 3.968mm(5/32") to 63.5mm(2 ½") in grades ranging from grade G3 to grade G100. The segment also manufactures steel cylindrical rollers and tapered rollers. The Company's metal bearing components segments has eight manufacturing locations around the world. The segment manufactures cylindrical rollers in two manufacturing facilities located in Erwin, Tennessee and Mountain City, Tennessee; the Erwin and Mountain City plants have approximately 11,612m^2 and 8,035m^2 of manufacturing space, respectively. The Company's Asian subsidiary, NN Asia officially began manufacturing of precision steel balls at a new factory located in Kunshan, China.

The Company's European subsidiary, NN Europe provides precision steel balls, tapered rollers and stamped steel components for various applications including bearing and automotive parts. NN Europe includes a total of five manufacturing facilities within the European Union; these are located in Kilkenny, Ireland; Eltmann, Germany; Pinerolo, Italy; Kysucke Nove Mesto, Slovakia and Veenendal, The Netherlands. Table 9 gives some brief information about each of the European facilities.

The selected facility for the In-line Piezo Measurement Instrument is the Irish facility located in Kilkenny. The Kilkenny facility was established in May 1997 to deal with the European market; the facility has approximately 80 employees and has a capacity of over 12,000 tons of balls per year (1,422 million pieces).

Facility	Ireland	Germany	Italy	Slovakia	Netherlands
Manuf. Space m2	11,612	16,257	30,657	12,541	14,771
Ball or Roller	B	B	B	B	R
Manuf. Range mm	10-13.494	30-400	3.968-9.921	14-28.575	
Typical Use	Hub Bearing Industrial Quality	Rolling Press Cranes	Elect. Motor Quality Elect. Standard Quality	CV Joints	

Table 9 Manufacturing Facility Information

2.2.2 The Manufacturing Process

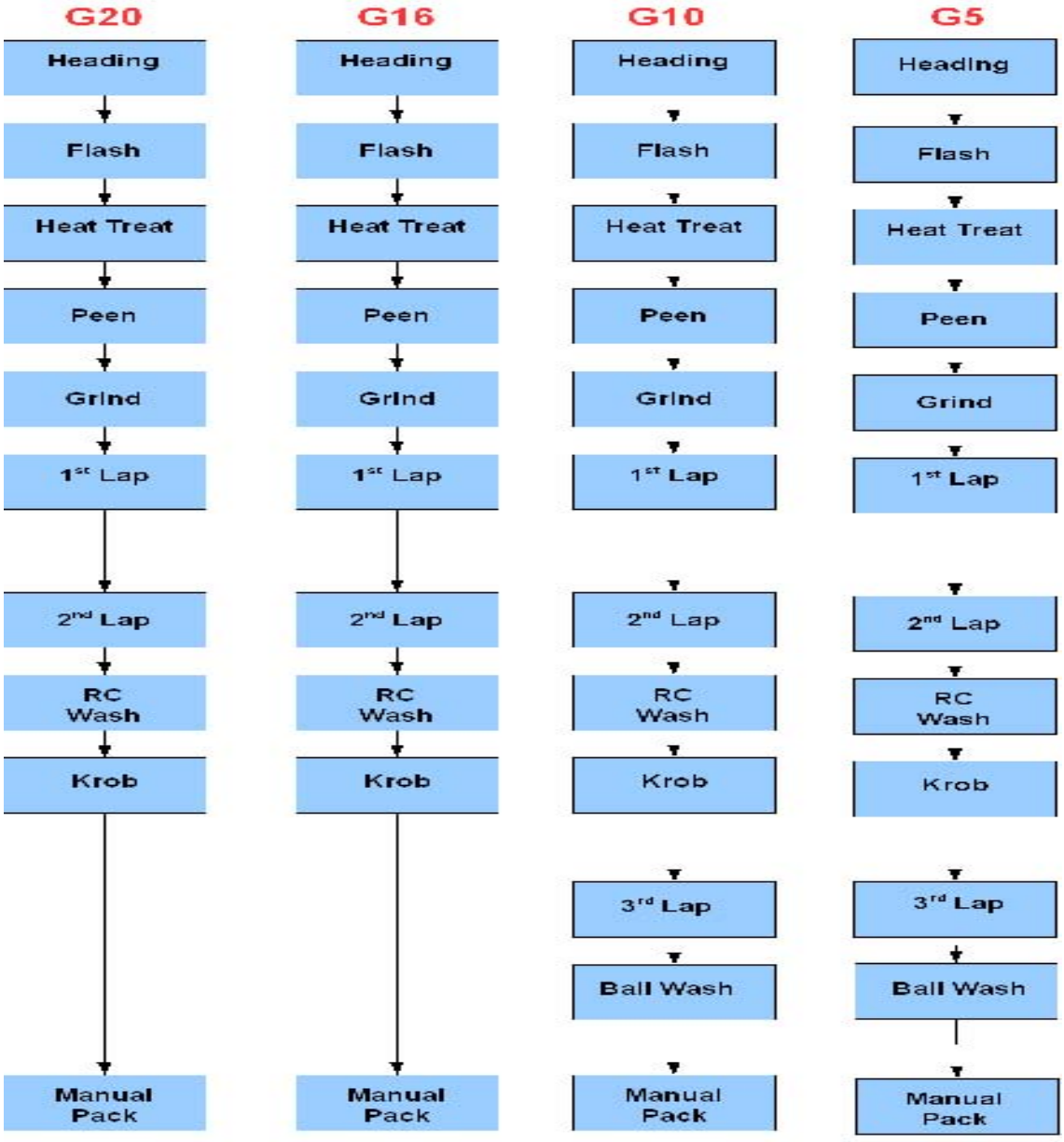

Figure 2 Bearing Ball Process Flow Chart

The process flow for different ball grades is shown in Figure 2; the basic manufacturing process is similar for the entire range of grades, the only difference being that high-grade balls require some extra finishing processes.

The first stage in the process is a cold forming operation. A steel wire approximately the diameter of the finished ball is fed from a roll through a heading machine; this machine cuts the wire into slugs similar to the one shown in Figure 3. This machine also has a metal cavity in the shape of a sphere; each slug is placed into the cavity and it presses shut on the wire, forcing the slug into the shape of a ball. As shown in Figure 4, the process leaves a ring of metal known as flash around the equator of the ball, leaving the balls something like the planet Saturn. This process is called cold heading; its name comes from the fact that the wire is not heated before being formed and the that the original use for the process was to put the heads on nails.

Figure 3 Wire Slug

Figure 4 Headed Ball

Next the balls go into a machine that removes the flash; the specific machine used is a Noonan Ball Machine shown in Figure 6. The Noonan Ball Machine has been serving the ball manufacturing industry for over forty years and its rugged design allows it to process low carbon steel, stainless steel, alloy steel, ceramic, plastic and various other materials from 2.5mm to 50mm in diameter. The basic machine can be utilized for de-flashing the headed ball, hard or soft grinding and lapping the finished ball, simply by altering horsepower and RPM or changing the wear plates. This machine rolls the ball between two very hardened steel plates called wear plates, shown in Figure 5. One plate rotates, while the second plate remains stationary. The plates have concentric circle grooves machined into them that guide the balls around in a circular path. The stationary plate has a section cut out of it; this is where the balls enter and exit the grooves. The machine is self-contained: it uses an automatic turntable to continuously feed balls into the grooves and to remove them from the grooves when a full rotation is completed. When the machine is running, the grooves are completely filled with balls and as the ball travels through the groove, it spins and tumbles; this breaks off the rough edges and the ball forms into a spherical shape. The balls cycle through the machine a number of times; each time they randomly enter one of a number of grooves and travel the length of the groove and rotate freely on their own axis under constant pressure. Since the balls circulate at random, the grooves remain uniform and balls in the batch

achieve a high degree of precision in both sphericity and size. This operation generates a considerable amount of heat, so water based coolant pours over the balls to cool them and to wash away the swarf. The most important and significant variables in this process are the pressure that squeezes the plates together, the speed at which the plates spin and the duration of time the balls are left in the machine; properly setting these variables will consistently produce balls of the correct size. The balls are machined continuously until they are about 150μm above the required finished size; the balls are left oversize so that they can be ground to their finished size after heat treatment.

Figure 5 Rill Plates

Figure 6 Noonan Machine

Following the de-flashing operation the balls are heat-treated to harden the balls. Metallic materials consist of a microstructure of small crystals called grains; the nature of the grains (grain size and composition) largely determines the overall mechanical behaviour of the metal. Heat-treatment provides an efficient way to manipulate the properties of the metal by controlling the rate of diffusion and the rate of cooling within the microstructure. The balls are fed through a heat-treating furnace at about 843˚C (1,550˚F) for several hours, depending on the size of the balls. Subsequently the balls are dipped into an oil bath, which cools them and also makes them very hard. This hardening process also makes the balls very brittle. Therefore the next step is to temper the balls; this is done by heating the balls in a second oven to about 148˚C (300˚F) and then letting them cool in air. A heat-treated ball is shown in Figure 7: following the heat-treatment process the balls are both hard and tough.

Figure 7 Heat-Treated Ball

The next process after heat-treatment is peening; peening is the cold working process of working the surface of a material to improve its material properties. Peening is usually by mechanical means such as hammer blows or by blasting with shot, but bearing ball peening is carried out by rotating the batch of balls in a peening barrel causing the surfaces of the balls to repeatedly hit off each other. These repeated collisions tend to expand the surface of the cold metal, relieving tensile stresses already present. Peening also encourages strain hardening of the surface; this increases the balls yield strength but decreases its ductility and makes cracks less likely to form at the surface and provides resistance to abrasion.

After the peening process the balls go through a grinding operation. The balls are put back into a machine that works the same way as the de-flasher, except that the RPM is altered and the hardened balls are precision ground by rolling them between a fixed iron plate and a very hard fine-grit rotating grind wheel. Once again the fixed iron plate has concentric circle grooves that guide the balls around in a circular path. This hard grinding operation generates a considerable amount of heat, so a continuous flow of water based coolant cools the batch of balls and the grinding wheel. A ball following the hard-grinding operation is shown in Figure 8. The grinding wheel grinds the balls down so that they are within 20μm of their finished size. The number of balls produced per hour depends on a number of variables, such as the quality of the rough ball entering the machine and the required finished size and tolerance. The most important factor is the diameter of the balls being produced; the quantity of balls the machine is processing and the number of balls in a batch increases exponentially with smaller diameters.

Figure 8 Hard-Grinded Ball

The developed automatic on-line piezo measurement instrument will service the grind process shown in Figure 9; the grind process consists of twenty-four machines and will represent a section of production within the facility. The targeted production machines will be integrated both physically and electronically with the

Figure 9 Grind Process

measurement instrument. Successful control of this process will lead to the eventual control of the entire plant centred around this instrument. It will also allow the development of information systems for effective data analysis and the road mapping of future product tolerance/value improvement in the plant.

The ball gauge for each batch of manufactured balls is decided at the hard grinding process; during this process, each batch is assigned a certain gauge value using appropriate production forecasts. Prior to the hard-grind process batches are only categorized by their nominal ball diameters. The measurement instrument is required to control the grinding process until the batch has reached the correct dump size; the dump size is the finished hard-grinding ball diameter. For example, a 13mm (P3) leaving the grinding operation is required to be dumped at 13.003mm + 20µm (13.023mm).

The grinding process is very labour intensive; currently the process runs three eight-hour shifts a day with a minimum of two operators per shift. Outlined below is the procedure that an operator must follow to successfully operate a single grinding machine and to provide appropriate process control for a single load of balls. The procedure consists of the qualification of a load from the de-flashing process, machine checks, machine operation and qualification of a load for the lapping process. The purpose of this work instruction is to establish the current methods and guidelines used for the correct operation of a grinding machine and to give a clear indication of the entire manually operated grinding process.

1. Flash Qualification

1.1. Verify that all Heading, Flash, and Heat-Treatment information has been properly recorded. Fill out the grind load record and attach to the move ticket.

2. Set-up and Check-Off Details

2.1. Check the grind machine using the machine audit section of the grind load record, as shown in Figure 10.

MACHINE AUDIT		
	DATE: _____	BY: _____
LEADS		
WEAR POCKETS IN PICKER		
FEED OUT CHUTE ALIGNMENT		
APPROACH PL. ALIGNMENT		
STONE DEPTH	**0.185/0.204**	
RING DEPTH	**0.204 max**	
DIAMOND ALIGNMENT		
DIAMOND USAGE		
DRESSER BOLTS, GUIDES & STRAIGHTNESS		
CLEAN SUMP DITCH		
STRAY BALLS-MACH.,APRON,T-TABLE & HUB		
T-TABLE LEVEL & LINER		
ALL STRAY BALLS CLEARED		

Figure 10 Machine Audit

3. Loading

3.1. Using the overhead gantry system, lift the hopper of bearing balls onto the knife – edge trolley.

3.2. Measure two balls for size from the load using a micrometer and put under knife-edge. The function of the knife-edge is to ensure that oversize stray balls from previous batches do not enter the load; oversize balls entering the grind machine can cause catastrophic failure of the grinding wheel.

3.3. Close the iron ring and grinding stone to ensure that no balls can fall between them. Do not allow the grinding stone to touch the diamond picker.

3.4. Using a knife edged trolley or pre bar-grated load, load a lot of balls into the turntable.

3.5. Spread the balls evenly around turntable

4. **Start-Up**

4.1. With pressure on manual, open up the iron ring and grinding stone until balls begin to fall into the grooves.

4.2. Jog the grinding stone on manual pressure until balls barely pull through the iron ring and grinding stone.

4.3. Again, with pressure on manual, start machine at approx. 50 PSI above the pressure required to move the rotating grinding stone. Continue to increase the pressure until all the grooves in the iron ring begin to feed.

4.4. Adjust the pressure to approx. 500 PSI over the pressure required to move the grinding stone.

4.5. Allow the lot to cycle through the grind machine until there is no variation in colour between balls; this ensures each ball has been through the machine an adequate amount of times to remove all high spots that could damage the grinding stone at high pressure.

4.6. The amount of pressure that is been applied to the production balls between the iron ring and the grinding stone is set by controlling the amount of current that the main motor can pull. The greater the pressure on the ball, the greater the current used by the motor and vice-versa.

4.7. Set ammeter minimum and maximum to hold between 40 and 45 amps. Switch pressure to automatic and cycle.

4.8. Ensure the feed-board to the approach plate is completely full of balls and that all grooves are feeding into the iron ring at the correct angle. Ensure also that no separation of the balls is occurring within the approach plate. Coolant should not be used to force feed the balls to the stone.

5. Running

5.1. Ensure that all the grooves continue to feed correctly

5.2. Ensure adequate coolant flow throughout the grinding process

5.3. While running normal product at +10µm above the dump size, put the machine on round-up cycle by reducing the pressure to 800 PSI. When running 10Q product, start the round up cycle at +20µm above the dump size. Only run 10Q product in a machine carrying the 10Q compliant sign. This sign will be placed on the machine by the production controller.

6. **Quality Checks**

6.1. Handheld Micrometer

6.1.1. While the average ball diameter of the lot is +20µm above the dump size, use a micrometer to measure 3 balls from the lot; record and plot the ball diameter on the cut-down chart as required, see Figure 11. To minimise the variation of ball lot diameter and the deviation from spherical form, follow "Road Map Line" outlined in Figure 11.

6.1.2. Too steep of a cut rate is often caused by variables such as: Too much pressure, Stone groove's too deep or insufficient coolant. Adjust the appropriate variable accordingly and verify with smaller intervals between gauge checks.

6.1.3. Too shallow of a cut rate is often caused by variables such as: insufficient pressure, stone groove's too shallow or ring groove's too deep. Adjust the appropriate variable accordingly and verify with smaller intervals between gauge checks.

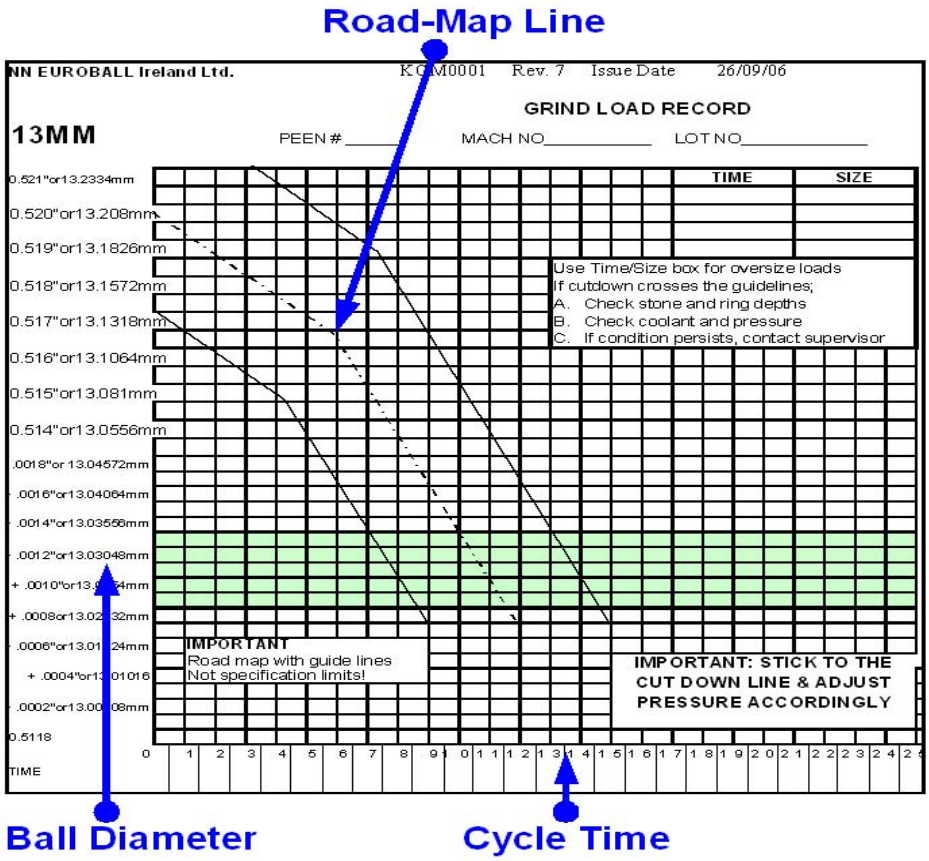

Figure 11 Grind Cut Down Chart

6.2. Dorsey-Heidenhain Digital Display Gauge

6.2.1. When the average ball diameter of the lot is within +20μm of the dump size, the micrometer is not adequately true or precise enough to measure to the tight tolerances required for each ball grade. At this point the quality checks must be carried out using a Dorsey-Heidenhain Gauge and digital display lab type instrument. Each hour, it is required to measure 3 balls from the lot, record and plot the ball diameter on the cut-down chart as required.

6.2.2. Each hour, randomly pick 3 balls from the turntable of the grind machine and deliver them to the measurement area.

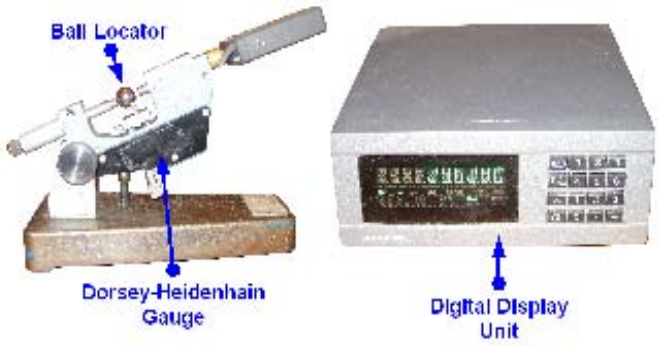

Figure 12 Dorsey-Heidenhain Gauge and Digital Display

6.2.3. Place the 3 samples along with the appropriate reference ball in the temperature normalizing solution for a minimum of 5 minutes.

6.2.4. After the normalizing period, centre the reference ball on the gauge ball locator as shown in Figure 12 by utilizing the backstop and micrometer fine tail adjustment screw. Adjust the ball upwards until it comes in contact with the top plunger.

6.2.5. With the master ball inserted, manually zero the gauge utilizing the keypad.

6.2.6. Return the master ball to the stabilizing solution for a minimum of 5 minutes.

6.2.7. Reinsert the reference ball to recheck set up. This gauge is extremely sensitive and the reference ball will need to be re-inserted continuously to achieve the actual zero point of the finished ball

6.2.8. Proceed to measure the 3 samples taken from the grind machine. Record the reading and plot the ball diameter on the cut-down chart

7. Load Completion - Qualification for Lapping

7.1. The batch of balls must be dumped to within ± 2.54µm of their specified dump size.

7.2. Using Dorsey-Heidenhain Gauge, once again measure three sample balls for size variation.

7.3. Complete all move tags, load records, and control charts.

7.4. The addition of the operator's initials to the Move Tag indicates he/she has checked and verified that the quality meets the specified requirements.

8. Process Control Grind

8.1. At the completion of a load, the Operator must fill out the following: Date, Lot Number, Ball Size, Cycle time and Operators initials.

9. Unloading

9.1. Shut the grind machine down and switch the hydraulic pressure to manual.

9.2. Depress the “pressure release” and “out” buttons simultaneously until the balls at the top of the iron ring exit the take-off chute into the turntable.

9.3. Verify that the diamonds are not in contact with the grinding stone. This will prevent stone damage while running the turntable to unload the batch of balls.

9.4. Finally with the hydraulic pressure gauge reading zero, all balls are then jogged out of the machine.

9.5. Inspect the turntable and hub for stray balls

After the grinding process, the bearing balls are moved to the lapping process. This process gives the balls their perfect smooth and shiny surface, while removing very little material. Again, the same kind of Noonan machine used in the de-flashing and hard-grinding processes is used; this time the plates are made of softer cast iron and the coolant contains a very fine abrasive slurry which is used to polish the balls to get an almost mirror finish. The pressure to squeeze the balls between the plates and RPM on the lapping machine is much less than the grind or flash machines. There are three lapping processes in total, 1st Lap, 2nd Lap and 3rd Lap; the required precision of the batch of balls determines how many lapping processes are required. For example, G20 and G16 balls are processed through 1st Lap and 2nd Lap, while to obtain higher tolerances higher grades balls such as G10 and G5 balls require further processing in 3rd Lap higher tolerance.

After precision washing and oiling (before packing), sample balls are taken from each batch and are sent to a laboratory for a final audit to check if surface roughness, roundness, waviness, lot size variation and hardness are adequate for the specified ball grade.

Also at this point, every single ball in every single batch is tested using a Krob ball scanner; this is a testing and sorting machine for the non-destructive examination of the surface-quality of ball bearings. This machine uses an optical method (EOT) and an eddy-current method (ECT) to detect defects; the two testing methods enable a simultaneous examination for point and polish defects (the optical method) and for cracks, flats or shape defects (the eddy-current method). If a ball that has passed through the scanner is found to be defective, the machine will sort the balls in two categories:

Repairable (optical defects)-these balls can be washed and tested again, because dirt is very often the reason for the optical errors and Non-Repairable- defects found by the eddy-current method.

Following the quality assurance process, the batch of balls are ready to be packed: depending on the customer some balls are packed in boxes and others are packed in bottles. Each gauge lot is packed separately and is supplied with corrosion protection applied. The packaging is marked with the ball nominal diameter, grade, gauge and material number or material designation and is now ready to be shipped.

2.2.3 Proposed Process Automation System

The ball bearing manufacturing process is very labour intensive and can be characterised briefly as follows: a batch production industry using multiple parallel high-volume standalone machines: nine common production stages- heading, de-flashing, heat-treatment, peening, hard-grinding, coarse lapping, finish lapping, defect detection/classification and packaging. Measurement is a generic issue throughout each of the processes; currently a sample of three balls is taken each hour, it is measured off line with a laboratory type comparative measurement instrument, logged onto a control chart and the appropriate machine adjustments are made – all manual operations.

The machine adjustment process must balance a desire for rapid size reduction (cost minimisation) against essential sphericity and surface finish requirements (value creation); this balance is currently a somewhat rough compromise at the Kilkenny facility, partially arising from the need to reduce the manual inputs. The process operators control the pressure that influences the cut-down rate and will often increase the pressure to finish the batch of balls before the end of a shift or a predetermined lunch break. This often leads to a variation in cycle times of up to 30% in many of the processes. The economics of ball bearing production mainly hinges on the effective control of each process cycle time; standardising cycle times will add value to each batch by guaranteeing precise high tolerance balls.

As mentioned in Section 2.1.4, the Kilkenny facility currently manufacture balls for bearings in the 10-13.494mm size range. The production is targeted at the lower end of the quality/value market (car industry mainly), for which relatively loose tolerances on the bearings are satisfactory. These products are currently vulnerable to competition from low cost countries; therefore the company is urgently pursuing cost reductions throughout the production cycle in the plant. The company needs to migrate production in order to service a higher quality, higher value market, which will require the ongoing tightening of ball tolerances.

The nominal measurement accuracy achieved with the manual instrument is 1μm; in order to service a higher quality product, the company has targeted a measurement accuracy of 0.1μm. The possibilities of achieving this with the current manual process, but without significant labour cost increase, is not a realistic prospect for the company. To standardise cycle times and to improve the measurement accuracy

by a factor of ten, manual measurement must therefore be replaced by an automated system.

Redesign/redevelopment of the production processes into something akin to a continuous production process, which might provide scope for continuous measurement and control is a long-term plan for the facility. The immediate objectives are therefore to automate the manual measurement and control of the existing machine systems and to build a driving information system for progressive product (diameter tolerance) improvement. Discussions with the plant engineers verify that while the initial cost of research and installation may be significant, the long term potential for reduced labour costs and increased product quality makes this practicable.

The high gross volume of product from the plant linked to the innate batch production processes used in the industry results in very high activity volume in measurement and very distributed control. It is envisaged that a single piezo-based measurement instrument will service all the machines within the hard-grinding process, thereby changing the nature of the control to a more centralised process. An inescapable feature of this industry is the difficult working conditions: very high levels of acoustic and electrical noise, vibration and heat generation as well as high humidity all arising from the metal removal processes involved. For this reason, the piezo measurement instrument will be located in a reasonably undisturbed section of the facility, 200 meters away from the mass grinding machines.

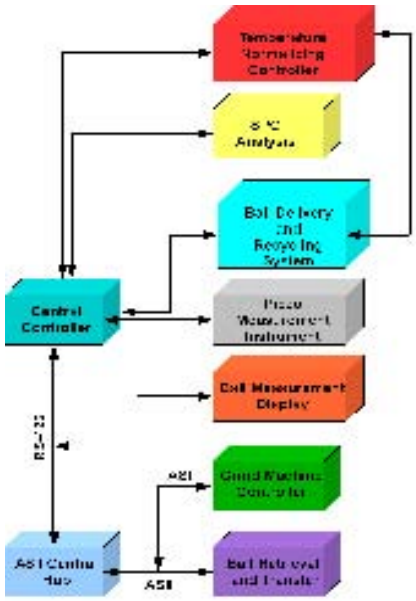

Figure 13 Communication Links for the Complete Automated System

A central controller will control the proposed sampling and measuring system; the central controller will be linked to the grind machine controllers via a network, which will allow communication to and from the central controller. The block diagram in Figure 13 illustrates how the individual processes will link together in the proposed automatic sampling and measurement project. The operation sequence of the proposed automated sampling and measurement system is as follows:

1. Retrieval of Samples from the Grinding Machine

An automated sampling system takes samples from the grind machine at regular intervals; the system as shown in Figure 14 consists of a pick and place arm mounted on the external housing of the grind machine. The retrieval system selects five balls at random from the machine turntable and delivers them to the ball propulsion system

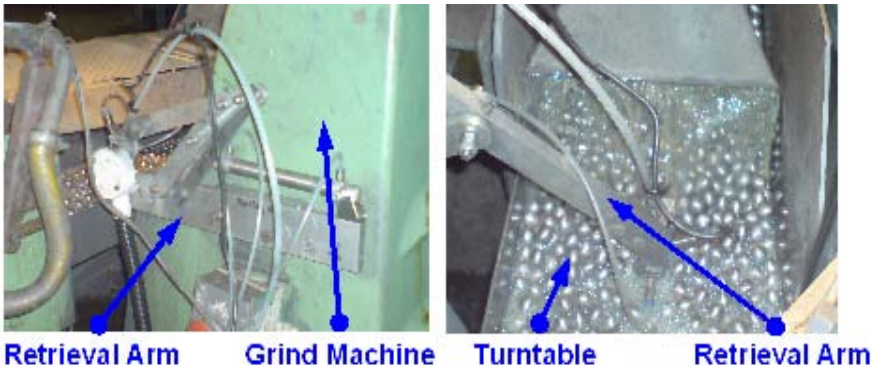

Figure 14 Retrieval System

2. Transportation of Sample to the Measuring Area

The transfer system delivers each machine sample the 200 meters or so to the centralised measuring location; the system is capable of transferring balls ranging from 10mm-13.494mm. This system is also capable of transporting the sample balls relatively quickly without causing damage or inadvertently altering its properties. A blast of compressed air propels the five-ball sample vertically 6 meters through an enclosed PVC conduit piping network. Subsequently, the force of gravity aided by compressed air transports the five-ball sample through the piping network to the measuring location.

3. Temperature Normalizing

On arrival at the measurement location, the five-ball sample is submerged under a temperature-controlled fluid within holding pipes at the temperature-normalizing station. The sample is held along with the maximum and minimum reference standard balls at a fixed temperature for a pre-determined length of time (both sets of balls are held in the same fluid in order to equalize their temperatures). The number of machine samples measured between re-calibrations of the measurement instrument (using the reference balls) is limited to one sample batch of five balls: any errors due to thermal changes between reference standard balls and sample balls will thereby be minimised.

4. Measurement of the Bearing Ball Diameter using the Custom-Built Piezo Measurement Instrument

Following temperature normalizing, the sample ball diameter is measured using the automated piezo measurement instrument. When the measurement instrument is ready, the reference balls followed by the sample balls are released from the temperature normalizing station and inserted into the instrument. Calibration of the instrument is carried out by measuring the minimum reference ball and maximum ball; each sample ball diameter is then measured in comparison to the reference balls. Subsequent to the measurement process, the reference balls are recycled through the system and the sample balls are ejected from the system.

5. Statistical Process Control

Based on stock removal trials, the average of the five sample ball measurements is then plotted on a developed automatic cut down “road mapping” chart. Statistical process control is used to determine control limits for the process; if the average diameter falls outside the limits, then the process is out of control and corrections are made to the process.

6. Machine Adjustment

Grind machine adjustment by the central controller creates a closed loop system; following the SPC analysis the central controller can increase or decrease the pressure between the grinding stone and iron plate. If the average measurement is above or

below the control limits on the cut-down chart, the grind machine is automatically altered to correct the cut down rate.

7. Measurement display

To assist the operator to interface with each machine a digital display unit is mounted on the control panel of each machine; this is controlled automatically by the central controller and is updated after each machine is sampled. This unit shows the average measured diameter and the time the sample was taken, allowing the operator to identify with great ease the exact period in the cycle for each machine.

Figure 15 illustrates the control structure and the delivery piping-network for each machine; a hierarchal control structure is implemented for the central controller to communicate with each grinding machine PLC, each measurement display (MD), the normalizing station and the measurement instrument.

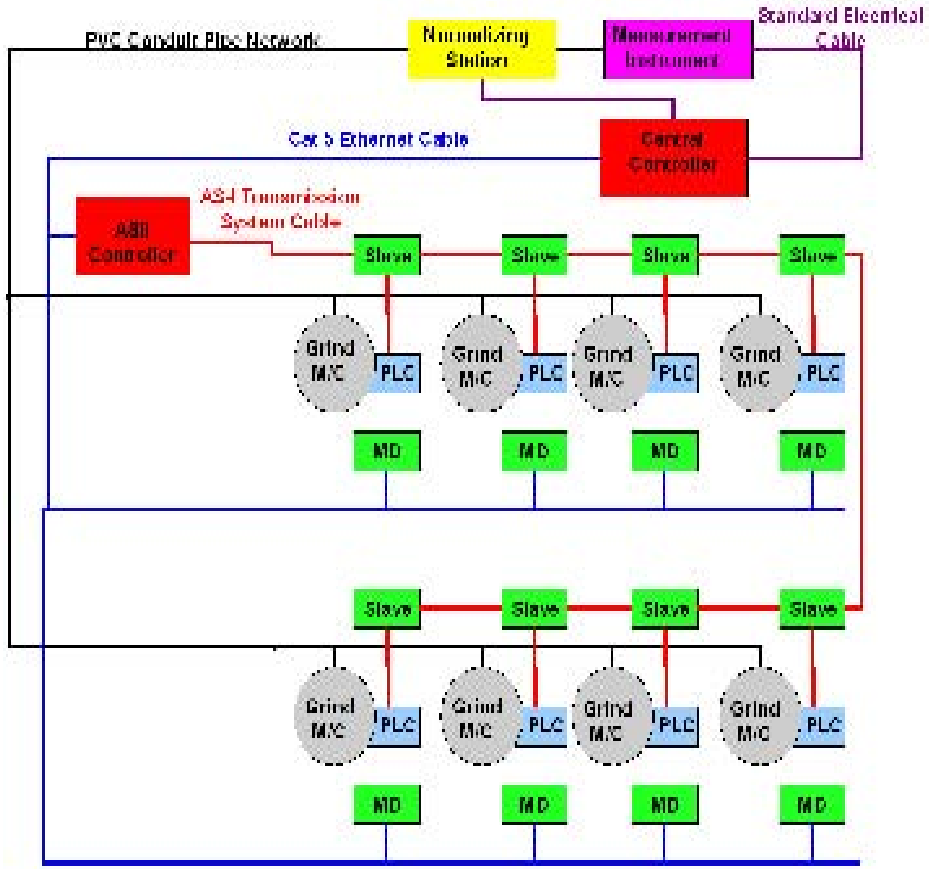

Figure 15 Process Automation Overview

Having indicated the proposed automation system, it is necessary to discuss the measuring parameters and elements that will be used within the system.

2.3 Measurement

2.3.1 Introduction

As suggested in Section 1.1, ball diameter measurement is the critical process in ball bearing production for the efficient control of batch grinding and lapping processes and the effective production and classification of finished balls into tight tolerance ranges. With this in mind this chapter will discuss measurement and measurement instrument variation.

Measurement as defined by C.Eisenhart (1963) [23] is the assignment of numbers or values to material things to represent the relationship among them with respect to particular properties. The process of assigning numbers is defined as the measurement process and the value assigned is defined as the measurement value. The measurement process consists of a set of operations for the purpose of determining the value of a quantity to establish the magnitude of some attribute of an object, such as its length or weight, relative to a unit of measurement [25]. Measurement usually involves using a measuring instrument, such as a ruler or scale, which is calibrated to compare some standard, such as a meter or a kilogram.

Any quantitative data, facts, observations, and information that come from investigations obtained from a measuring instrument is referred to as measurement data. This data can be used in a variety of ways; the decision to adjust a manufacturing process or not is commonly based on measurement data. Statistical control limits of a process can be compared with measurement data, or some statistic derived from them. If the process is deemed out of control, then an adjustment of some kind can be made. Alternatively if the process is in control, the process is allowed to run without adjustment. Measurement data can also be used to determine if a significant relationship exists between two or more variables e.g. the relationship of speed and pressure in a grinding process. Studies that investigate such relationships are called analytic studies. Studies of this kind lead to a greater understanding of processes; they enhance knowledge about the system of causes that affect the process.

The quality of the measurement data determines how beneficial the data is to the manufacturing process or to an analytical study. The quality of measurement data is defined by the statistical properties of multiple measurements obtained from a measurement system operating under stable conditions [23]. For example, if a

measuring instrument is used to make several measurements of a particular characteristic of a manufactured component, the quality of data is high, if all the measurements are consistent and close to an accepted reference value (a value that serves as an agreed-upon reference for comparison) [7]. On the other hand if the measurements are far away from the accepted reference value, the quality of data is low.

2.3.2 Measurement Variation

Frequently the analysis and conclusions of a process or analytical study are based upon the assumption that measurements are exact. It is often forgotten that there is variation in the measurement instrument which effects the individual measurements and subsequently the decisions based upon the data.

Variation is one of the most frequent explanations for low quality measurement data. A common cause of variation in measurement data is the interaction between the measurement instrument and its environment. If a measuring instrument used to measure the length of a certain characteristic of a component is sensitive to the ambient temperature of the environment, then the variation may be due to changes in length of components or to changes in the ambient temperature. A measurement instrument with a large amount of variation may hide the variation in a manufacturing process and hence would not be appropriate for analyzing that particular process.

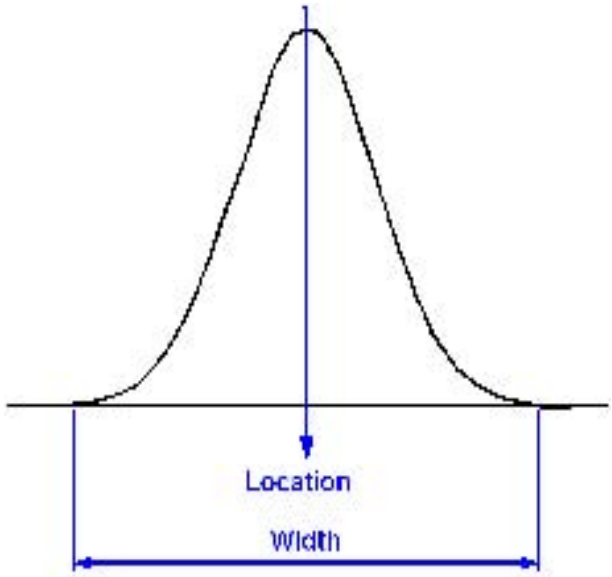

Figure 16 Characteristics of the Measurement Process Variation

Measurements always have errors and therefore uncertainties. In fact, the reduction of uncertainty is central to the concept of measurement. The general assumption is that measurement errors are often normally distributed about the true value of the measured quantity (the actual measure of the part) [23]; repeated measurements of the same quantity are expected to yield results which are clustered

around a particular value. If all the major sources of errors have been taken into account, it is assumed that the remaining error is the result of a large number of very small effects, and hence normal. Deviations from normality are interpreted as indications of systematic errors, which have not been taken into account: A systematic error is any biasing effect, in the environment, methods of observation, or instruments used, which introduces error into an experiment and is such that it always affects the results of an experiment in the same direction [21].

The characteristics of measurement process variation consists of location variation and width variation, Figure 16. Location variation is related to the trueness of a measurement; trueness refers to the closeness of agreement between the arithmetic mean of a large number of test results and the true or accepted reference value [7]. Width variation is related to the precision of a measurement; precision refers to the closeness of agreement between test results [7].

The discussion of measurement instruments can become confusing and misleading without an established set of terms to refer to the common statistical properties and related elements of a measurement system. Hence, this section provides a discussion of such terms, which are used to describe the quality of measurement within this document.

2.3.2.1 Accuracy / Location Variation

Accuracy is a generic term to describe the concept of exactness related to the closeness of agreement between the average of one or more measured results and a reference value [23]. In the past, the term accuracy was used to describe the component now named as “trueness”: trueness is the closeness of agreement between the average value obtained from a large series of test results and an accepted reference value [7]. The trueness of a measurement method is examined by comparing the obtained set of measurement results with the accepted reference value. It is desired that any individual measurement should be as close to the true value as possible. This

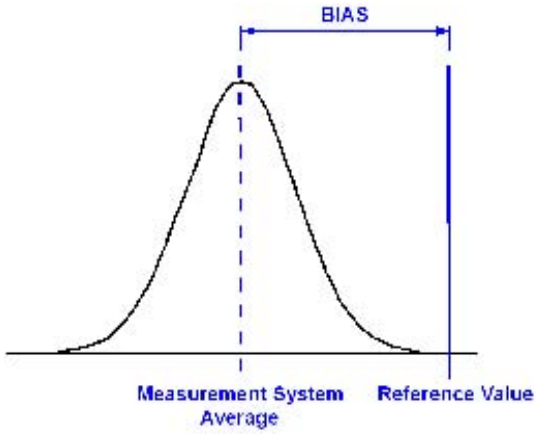

Figure 17 Bias

value is frequently unknown for many measurement processes; therefore the accepted reference value is used as an approximation of the true value.

Trueness is normally expressed in terms of bias. Bias is the difference between the true value (accepted reference value) and the observed average of measurements on the same characteristic on the same part [23], see Figure 17. Bias is the measure of systematic error as contrasted to random error e.g. an incorrectly calibrated thermostat may consistently read, that is 'be biased' several degrees hotter or colder than the actual temperature. There may be one or more systematic error components contributing to the bias. A larger systematic difference from the accepted reference value is reflected by a larger bias value. To reduce the bias of the system, the measurement procedure employed in calibration process using the reference masters should be as identical as possible to the normal operations measurement procedure

Some possible causes for excessive bias are:

- Instrument needs calibration
- Instrument or fixture is worn
- Worn or damaged reference standard
- Distortion of instrument or part
- Environmental influences such as temperature, humidity, vibration and cleanliness
- Application: part size, position, operator skill, fatigue, observation error (readability)

A factor that also has to be considered is the change in bias over time known as stability, Figure 18. Stability is the total variation in the measurements obtained with a measurement system on the same master or parts when measuring a single characteristic over an extended time period [23]. Instability of the measuring instrument is evident, if the biases of a group measurement vary over time. Stability measures the change in systematic errors over time. Systematic errors, which change during an experiment, are usually easy to detect; measurements show trends with time rather than varying randomly about the mean e.g. for example if each measurement is higher than the previous measurement, this would perhaps suggest that the instrument becomes warmer during the measurement period. Long-term instability should not be a problem for comparator measurements, but short-term can be a problem.

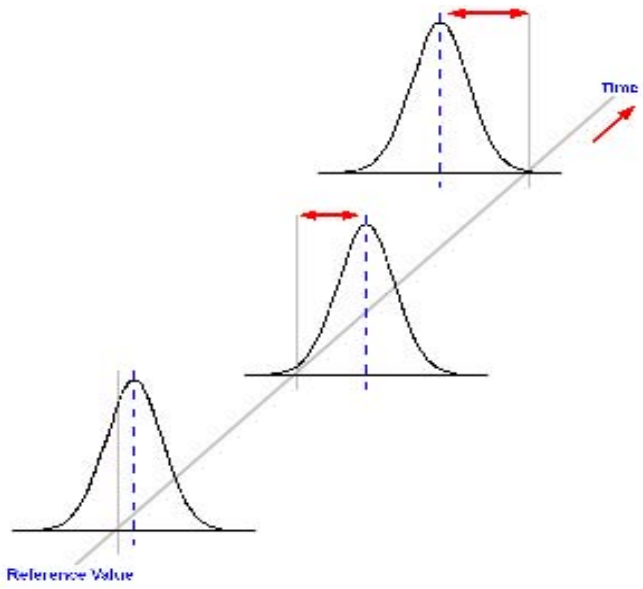

Figure 18 Stability

The factors, which frequently contribute to the instability of the observed values obtained, are:

- The time interval between calibrations is excessively long
- Normal aging or obsolescence of the measuring instrument
- Poor maintenance of the measuring instrument
- Worn or damaged reference standard
- Improper calibration or use of the reference standard
- Measuring Techniques differ- setup, loading, clamping
- Environmental drift- temperature, humidity, vibration, cleanliness
- Application: part size, position, operator skill, fatigue, observation error (readability)

Linearity is the change in bias over the entire measurement range of the measurement instrument, Figure 19; it is the difference of bias throughout the expected operating (measurement) range of the equipment [23]. Linearity can be thought of as a change in bias with respect to size and it is the correlation of multiple and independent bias errors over the operating range. If the instrument bias remains constant throughout the measuring range, the instrument is said to have constant bias, on the other hand if the bias varies over the operating range the instrument has nonconstant bias (linearity). As shown in Figure 20, unacceptable linearity can come in a variety of different forms and all the possible causes of excessive bias and instability can also cause linearity.

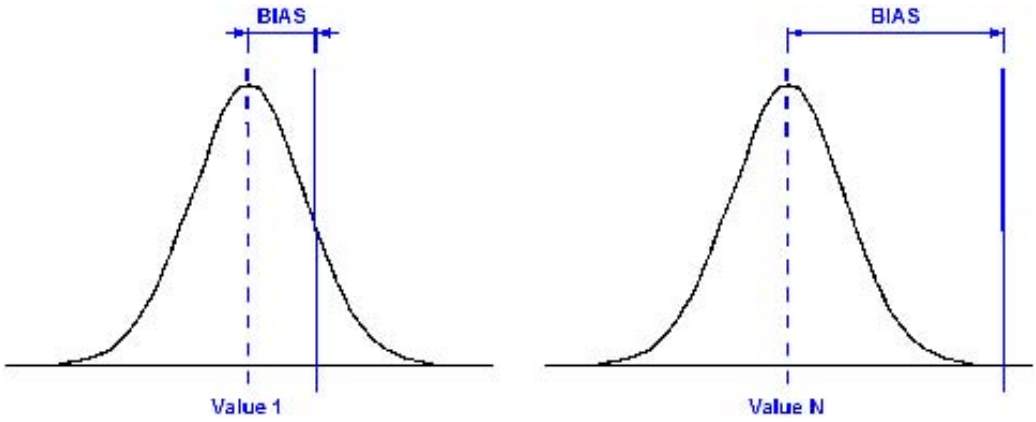

Figure 19 Linearity

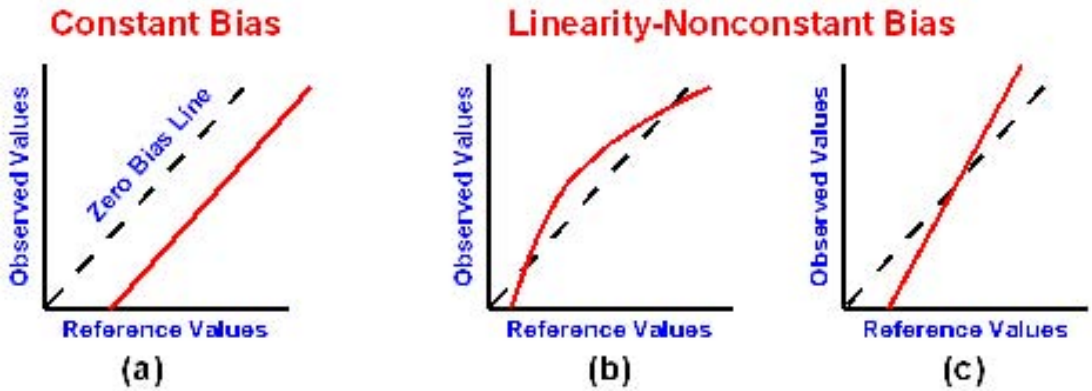

Figure 20 Observed Values vs. Reference Values

2.3.2.2 Precision / Width Variation

Tests performed on presumably identical materials in presumably identical circumstances generally do not give identical results. The general term for variability between repeated measurements is precision. Precision is the closeness of agreement between independent test results obtained under stipulated conditions [7]; the closeness of repeated readings to each other. A precise measuring instrument will give very nearly the same result each time it is used.

Precision measures the dispersion of a set of results, usually computed as a standard deviation of the test results. It depends only on the distribution of random errors inherent in every measurement and does not relate to the true value or the accepted reference value: a random error is a deviation of an observed from a true value, which behaves like a variate in the sense that any particular value occurs as though chosen at random from a probability distribution of such errors [28]. The variability due to random errors must be taken into account when interpreting measurement data, e.g. comparing test results from two batches of ball bearings will not indicate a fundamental quality difference between them, if the difference can be credited to the inherent variation in the measurement process.

Many different factors other than variations between supposedly identical parts may contribute to the variability of results from a measurement method, including the operator, equipment used, calibration of the equipment, environment (temperature, humidity etc.) and the time between measurements. The variability between measurements performed by different operators and/or with different equipment will usually be greater than the variability between measurements carried out within a short interval of time by a single operator using the same equipment [7].

To describe the variation within the measuring process, precision is often classified into two groups, repeatability and reproducibility. Repeatability and reproducibility are the two extremes of precision, the first describing the minimum and the second the maximum variability in results

Repeatability is defined as precision under repeatability conditions [27]; repeatability conditions are conditions where independent test results are obtained with the same method on identical test items in the same laboratory by the same operator using the same equipment within short intervals of time [27]. The measure of repeatability is the standard deviation qualified with the term: ‘repeatability’ as

repeatability standard deviation, Figure 21. A measurement may be said to be repeatable when the variation in measurements is smaller than some agreed limit. Repeatability is often referred to as the within appraiser variability; variation in measurements obtained with one measurement instrument used several times by one operator while measuring the one characteristic on the same part. This variation or capability will permanently exist within the measuring equipment; repeatability is the random error variation from successive trials under defined conditions of measurement [23].

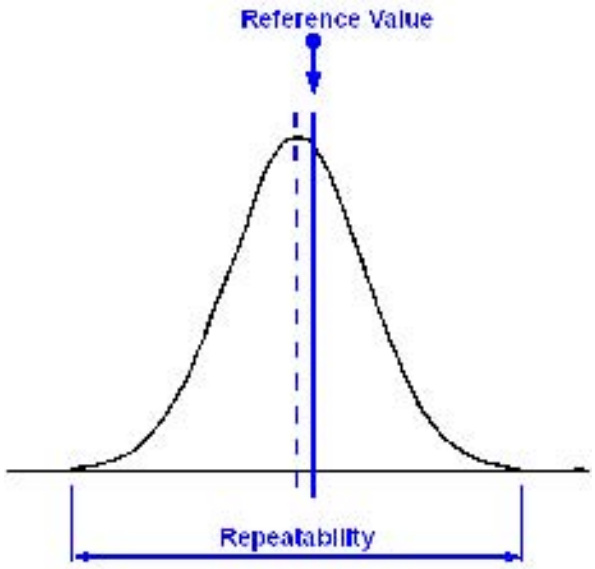

Figure 21 Repeatability

Some possible causes for poor repeatability are:

- Within Part (Sample): form, position, and surface finish
- Within Instrument: wear, equipment or fixture failure, poor quality or maintenance
- Within Standard: quality, class, wear
- Within Method: variation in setup, technique, zeroing, holding, clamping
- Within Appraiser (Operator): technique, position, fatigue, lack of experience, manipulation skill or training
- Within Environment: short-cycle fluctuations in temperature, humidity, vibration, cleanliness
- Instrument design or method lacks robustness, poor uniformity

Reproducibility is different from repeatability, which measures the success rate in successive experiments: Reproducibility relates to the agreement of test results with different operators, test apparatus, and laboratory locations, Figure 22.Reproducibility is defined as precision under reproducibility conditions [27]; reproducibility conditions are conditions where test results are obtained with the same method on identical test items in different laboratories with different operators using different equipment [27]. The measure of reproducibility is the standard deviation qualified with the term 'reproducibility' as reproducibility standard deviation. Under reproducibility conditions observations are carried out at different laboratories; i.e. not only do all the factors such as operator, equipment used, calibration, environment and the time between measurements vary but also with additional effects due to the difference between laboratories in management and maintenance of the laboratory, stability checking of the observations, etc.

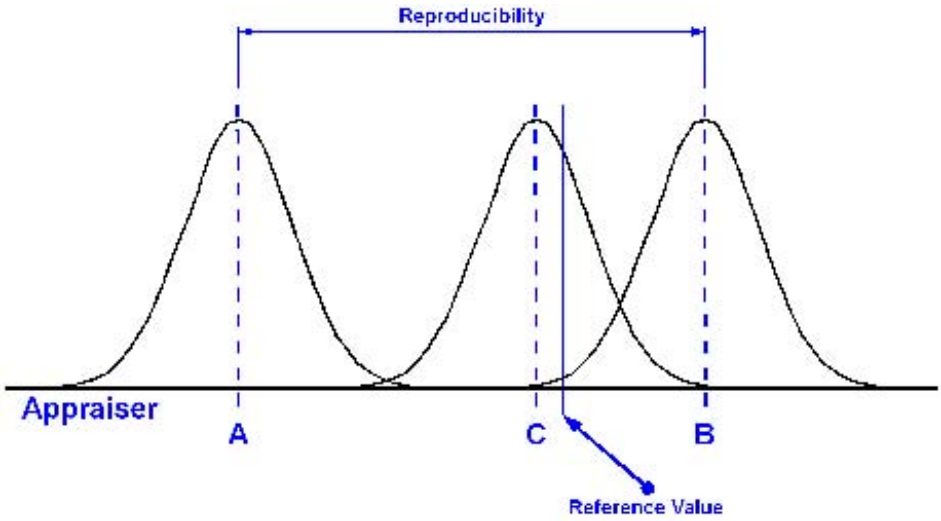

Figure 22 Reproducibility

In relation to research, the results of an experiment performed by a particular researcher are generally evaluated by other independent researchers by reproducing the original experiment; the experiment is repeated based on the original experimental description, to see if similar results are obtained. The result values are said to be commensurate (having a common measure [30]), if they are obtained according to the same reproducible experimental description and procedure.

Reproducibility is often referred to as the between appraiser variability. This is often true for manual instruments influenced by the skill of the operator; however it is not true for automated measurement processes where the operator is not a major source

of variation. Therefore reproducibility is referred to as the average variation between systems or between conditions of measurement.

Factors, which are potential sources of reproducibility error include:

- Between Parts (samples): average difference when measuring types of parts A, B, C, D, using the same instrument, operators and method
- Between Instruments: average difference using instruments A, B, C, D for the same parts, operators and environment
- Between Standards: average influence of different setting standards in the measurement process
- Between Methods: average difference caused by zeroing, holding or clamping methods
- Between Appraisers (Operators): average difference between appraisers A, B, C, D, caused by training, technique, skill and experience
- Between Environment: average difference in measurements over time 1,2,3, caused by environmental cycles; this is the most common cause for automated measurement systems

A factor that also has to be considered is the repeatability over time known as consistency, Figure 23; consistency is the difference in the width variation of the measurements taken over time [23]

Special causes of variation impact consistency such as:

- Temperature of parts
- Often a warm up period is required for equipment
- Equipment wears over time

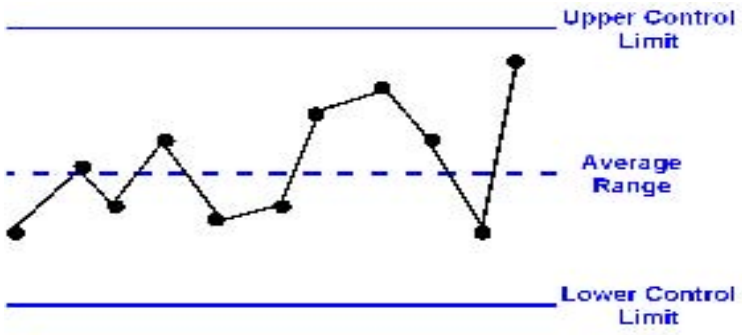

Figure 23 Consistency

Stability is the change of systematic errors (bias) with respect to time, the change in random errors (precision) with respect to time is known as uniformity. Uniformity is the difference in variation throughout the operating range of the gauge [23]. It is considered to be the homogeneity (sameness) of the repeatability over size, see Figure 24.

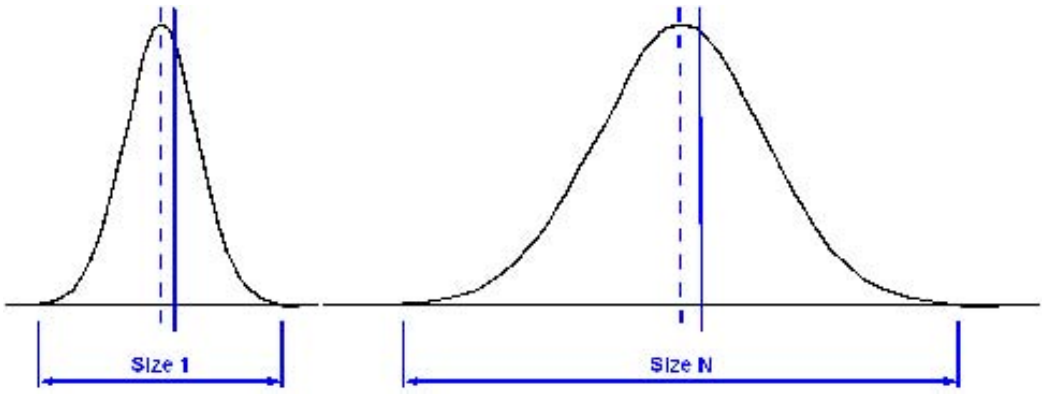

Figure 24 Uniformity

Finally, under repeatability conditions, the factors that contribute to the variability of results are kept constant and do not add to the variability, while under reproducibility conditions they vary and do add to the variability of the test results. Therefore repeatability and reproducibility are the two extremes of precision, the first describing the minimum and the second the maximum variability in results.

Bias is the difference between the true value and the observed average of measurements on the same characteristic on the same part, while repeatability is the variation in these measurements taken by a single instrument on the same item and under the same conditions. A target comparison analogy is used to give a clear explanation of the relationship between bias and repeatability, Figure 25. Bias describes the closeness of the paintballs to the bullseye at the target center, the location error. Paintballs that strike closer to the bullseye are relatively unbiased; the closer a systems measurements to the accepted value the greater the trueness(accuracy) of the system. If a large number of paintballs are fired, the repeatability would be the size of the paintball cluster. When all the shots are grouped tightly together, the cluster is considered repeatable since they all struck close to the same spot, if not necessarily near the bullseye; the measurements are repeatable (precise), though biased (untrue, inacurate).

However it is not possible to reliably achieve trueness without precision; if the paintballs are not all grouped together, they cannot all be close to the bullseye. Their average position might be an accurate estimation of the of the bullseye, but the individual shots are biased (untrue, inacurate). The results of measurements can be unbiased but not repeatable, repeatable but biased, neither or both. Measurement data is valid if it is both unbiased and repeatable.

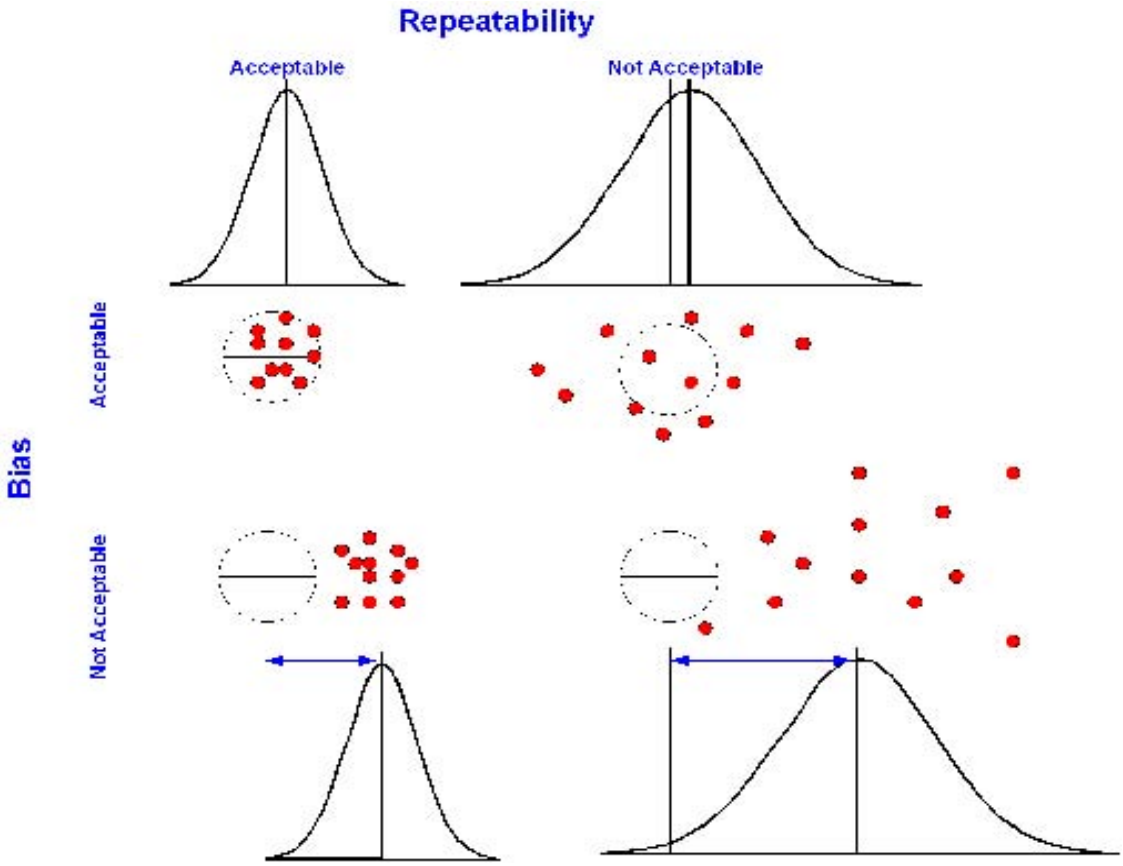

Figure 25 Relationship between Bias and Repeatability

Having discussed the ball bearing industry (standards, manufacturing processes) and the process issue of measurement, some of the technical issues associated with flexure-piezo systems as well as issues related to the integration of these systems into the plant will now be discussed.

2.4 Flexure Systems

2.4.1 Flexure Mechanisms

Sub-micron level positioning resolution is a critical performance objective in a micro/nanopositioning stage design: friction and backlash, which are common features of conventional mechanical systems, are anathema to such high precision resolution. In micro/nanopositioning stages, joint friction/resistance can account for a sizable fraction of actuator output and joint clearances can often be much larger than the systems resolution and sometimes of the same order of magnitude as the dimensions of the system workspace. Monolithic flexure hinges, which eliminate backlash and friction, therefore replace conventional joints such as revolute joints, universal joints and prismatic joints in many of these designs.

The three main categories of flexure hinges are: single-axis, two-axis and multiple-axis [56]. Single-axis flexures are generally used in two-dimensional applications and are fabricated by removing material from a blank piece. The manufacturing processes that are being utilized for this purpose include end-milling, electrodischarge machining (EDM), laser cutting, metal stamping or photolithographic techniques for microelectrical systems (MEMS). In two-dimensional applications, the flexure is designed to be compliant about one axis only and stiff about all other axes and motions [56]. The two-dimensional flexure hinges are usually symmetric about the longitudinal and middle transverse axes

Two-axis and multiple-axis flexures are used in three-dimensional applications. The flexure hinge can be manufactured by lathe-turning or precision casting. Two-axis flexure hinges, for instance, enable bending about two mutually perpendicular compliant axes generally at different spring rates [55]. Multi-axis flexure hinge configurations that have rotational symmetry (they are revolute) are implemented in

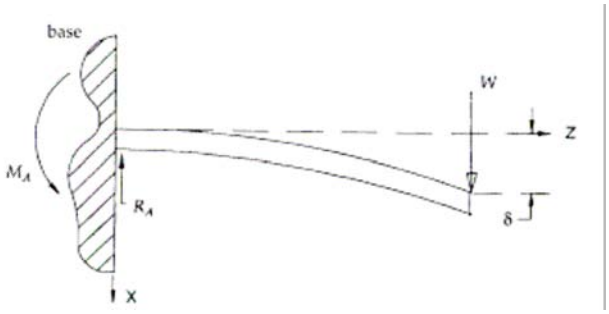

Figure 26 Simple Cantilever Beam [1]

three-dimensional applications in order to take advantage of the capacity of producing rotation about two or more compliant axes.

The cantilever shown in Figure 26 is considered the simplest single-axis flexure mechanism [1]. The simple cantilever is rarely usable because an arched locus is traced out by any point on the beam [3]. To design a mechanism for linear or angular motion, geometries that exploit symmetry are used. This is achieved by applying a couple to negate the twisting effect of the actuation load; one simple approach is shown in Figure 27. To provide an end deflection that is free of rotation, the beam is driven midway between the base and its end; this very simple design is not very stable because the beam is susceptible to buckling and more importantly twisting [3]. Thus misalignment of the force may cause large parasitic deflections.

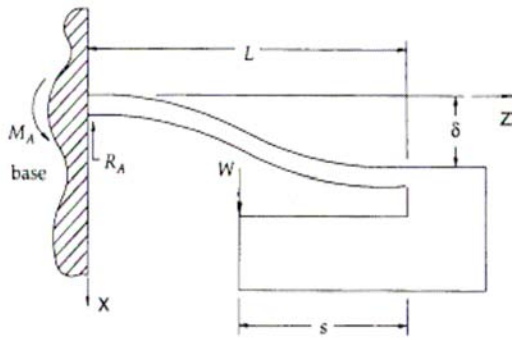

Figure 27 Deflection of a cantilever beam in the presence of an applied couple [1]

The resistance to torsional deflection is commonly improved by attaching two or more of these flexures together to form a linear spring mechanism as shown in Figure 28 [1]. Any mechanism in which displacements are achieved with little or no rotation is classified as a linear mechanism; although the mechanism will not rotate, it will follow a curvilinear path. Parasitic errors (change in height) from a curvilinear path have been presented by Jones, [57] and [58]: he found that a simple linear spring mechanism driven through 1mm gave a parasitic height variation h of approximately 28.5μm, see Figure 28; this is a rather disappointing error of 35:1. These mechanisms also have the

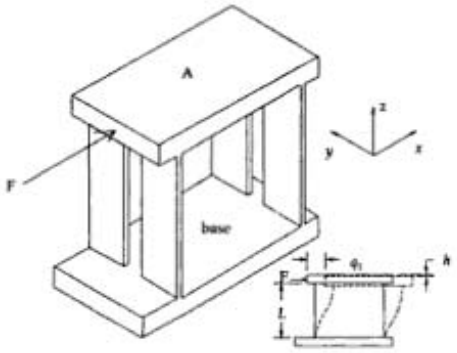

Figure 28 Simple Linear Spring [1]

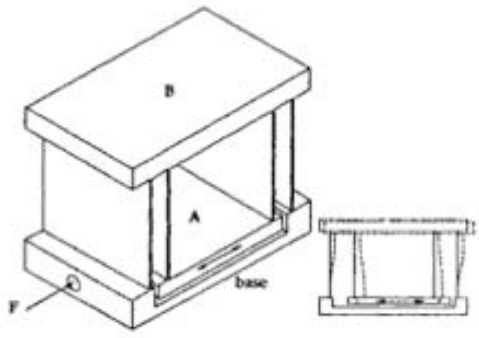

Figure 29 Compound Linear Spring

disadvantage that they have a relatively low stiffness in directions other than the drive axis.

Compensation for the curvilinear motion can be achieved by combining two simple springs in a more symmetrical design to produce the compound spring illustrated in Figure 29.

A second type of single-axis flexure mechanism is the notch hinge as shown in Figure 30. This type of flexure is constructed by drilling two holes close together in a solid blank and removing the excess material. The accuracy of the spring is primarily dependent upon the accuracy of the centre and the alignment of the holes [5].

Figure 31 shows a linear spring mechanism constructed from four notch hinges; applying a force at the platform causes exactly the same behaviour as with the leaf spring preciously mentioned.

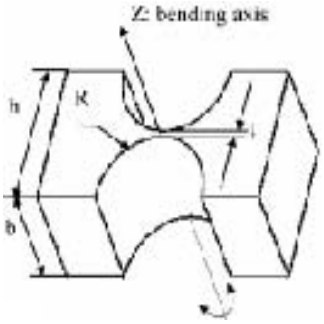

Figure 30 Notch Hinge [5]

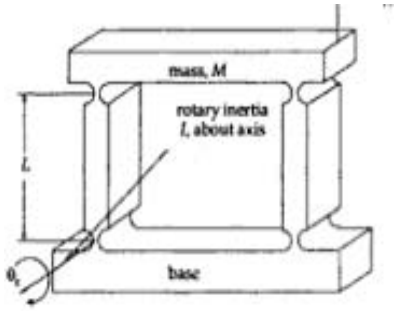

Figure 31 Notch Type Linear Spring [3]

So far only single-axis systems with one degree of freedom have been considered. Elastic mechanisms can be easily extended to develop two-axis and multi-axis systems; Figure 32 (a) is a two-axis hinge and it consists of two notch hinges with axes perpendicular to each other, while Figure 32 (b) is multi-axis universal circular hinge. Such flexures can be used to form simple or compound linear springs to provide motion in two dimensions with relatively predictable stiffness [3].

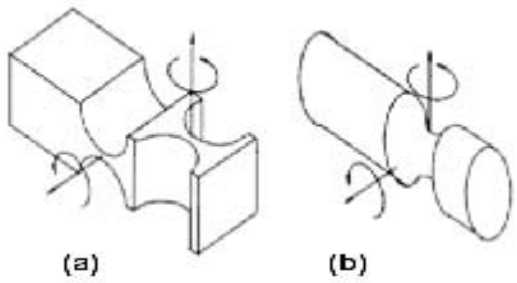

Figure 32 Two-Axis Hinge and Multi-Axis Hinge

To conclude, flexure hinges of different designs can be used to replace conventional revolute joints, universal joints and prismatic joints [5]. While taking advantage of the inherent material compliance, flexures are wear free and provided they are not distorted beyond their elastic limit, their line of action will remain constant throughout their life. In addition, flexures can be manufactured from a single piece of material to provide a monolithic mechanism, which eliminates interface wear. Displacements of flexures are smooth and continuous at all levels, therefore displacements can be accurately predicted from the application of known forces and conversely, predictable forces can be generated by controlled displacements.

However, with these advantages come disadvantages: limited travel ranges due to the elastic limits of the material used; vulnerability to fatigue when subjected to cyclic motions because high stress concentration arises in the neck area of the flexure joint; there will be hysteresis due to dislocation movement in most materials. Flexures cannot tolerate large loads: unless precautions are taken, accidental overloads can lead to fatigue, work hardening and eventually to catastrophic failure. [3]

To drive the flexure system, of course an actuator of some sort is required. Piezo based actuation will be the focus of the next section, to be followed (Section 0) by a discussion of sensing systems for measurement of the resulting flexure system movement.

2.4.2 Precision Actuation Devices

Actuators affect virtually every performance attribute of a measurement system. While standard considerations of forces, motion range and size continue to be important, others such as linearity/hysteresis and friction become very important. Conventional actuators, including mechanical micrometers and friction drives have been used for measurement systems. Many of these actuators use sliding surface contacts and require transmissions and bearings that introduce friction. Actuators with high positioning resolution, such as electromagnetic actuators and piezoelectric actuators, are now commonly used to drive micro measurement stages [5].

When specifying an actuator for applications in nanotechnology, the decision is usually based upon the three following criteria [3]:

- Stiffness, which determines both the dynamic response and the magnitude of the transmissible forces.
- Positional Accuracy, which limits repeatability and is often enhanced by feedback control; this usually, but not always increases the cost of the actuator.
- Range, at a nanometre resolution tends to be rather restricted in terms of normal engineering applications. Generally, costs can be considered roughly proportional to the range/accuracy ratio for a given resolution.

Mechanical micrometers provide a low cost solution to many large to medium range measurement applications. However, micrometer screws are invariably hysteretic due to the non-linearity of contact forces and will display backlash unless the system is well designed [3]. Due to the complex and precise shape of components that make up a micrometer screw, it is only economical to make them using metals; therefore thermal properties of micrometers are reasonably poor. Standard micrometers can be manually controlled to a micrometer: To operate at the sub-micron level a positional feedback system is commonly necessary with these mechanical instruments.

A friction drive consists of a polished bar that is squeezed between two rollers; as the rollers are precisely rotated, the bar translates at a rate of one circumferential length per revolution. The main advantage of this mechanism is that the contact forces between the drive roller and driven bar remain relatively constant and the range of movement is virtually unlimited [3]. On the other hand, problems associated with rotary accuracy resolution, performance of bearings supporting the squeeze roller, surface

finish of the contact surfaces and alignment of the driven bar axis relative to the squeeze rollers limit the performance of a friction drive. There is little information on friction drives for ultra-high precision applications although many such drives have been designed and used to achieve long-range motion at relatively high velocities of 100mm/sec, with sub-micron resolution [59].

There are a large number of variations of electromagnetic actuation; in precision electromagnetic devices, a saturated permanent magnet is surrounding by a coil or vice versa. A force is generated between the magnet and the coil that is proportional to both the strength of the magnet and the gradient of the field from the coil perpendicular to the axis of the magnet; therefore, for a fixed geometry, the force depends directly on the coil current [3]. This type of actuator requires some sort of stiffness against which to act since it is a pure force generator; to obtain a controlled displacement, the force is applied to a linear spring and it is this which limits the achievable accuracy of such devices. Using a spring manufactured from single crystal silicon, open-loop displacements of up to 100nm have been obtained with a resolution of 5pm as measured using x-ray interferometry [61]. Linear range is restricted by the spring stiffness and the field uniformity. They are relatively cheap and easy to implement and can have a good dynamic response. Near zero stiffness designs allow good vibration decoupling, but unless well screened, they may be sensitive to the proximity of ferromagnetic materials [3].

In contrast to electronic devices; hydraulic actuators are capable of generating very large forces. Conventional rams and hydraulic motors are used in large machines of their power to weight ratio. These characteristics are commonly not as important for precision actuators; hence not many precision hydraulic systems exist. A very stiff short-range actuator can be made in the form of a servo-controlled hydrostatic bearing; displacements are obtained by applying a differential pressure. These have been used for the fine feed mechanism in ductile grinding machines to obtain displacements of up to 100μm with a resolution of 1nm [62].

Another hydraulic approach is to use the deflection of a pressure vessel, as if hydraulic pressure were to pressurize a very stiff balloon. Pressures of 300x105 Pa are achievable and controllable; therefore the tube can be subjected to a tensile force of 236 KN [3]. This method seems not to have been tried in practice and it is not yet certain if

it would be linear (although with pressures so far below the yield stress of steel, it should behave relatively linearly) [3].

The main difficulty with hydraulic systems is the elimination, or at least reduction of noise transmitted through the fluid from pumps and control valves. Also, hydraulic pressure generation units are both expensive and bulky and the dynamic response is usually restricted by the hydraulic control.

Piezo-electric materials show a physical relation between mechanical load and electric charge; external loads cause a shift of ions in the crystalline structure resulting in a polarization of the material. Thus, an electric charge can be generated from the surface. This direct piezo-electric effect is utilized for the design of sensors such as piezo-electric accelerometers. Furthermore, this effect can be inverted (inverse piezo-electric effect); piezo materials driven by an electric voltage show an alteration of length. Certain ceramic materials, which are used to build actuators, such as lead-zirconium-titanate (PbZrTi or short PZT), have very large piezo-electric strains. These materials are permanently polarized by a strong electric field during the process of production. When an actuator is driven by an electric field, acting in the same direction, it extends in the field direction (longitudinal effect) and contracts in the perpendicular direction (transversal effect) [60]. The precise motion that results when an electric potential is applied to a piezoelectric material is of prime importance for nanopositioning; piezo actuators can perform sub-nanometer moves at high frequencies because they derive their motion from solid-state crystalline effects. They have no rotating or sliding parts to cause friction. Piezo actuators can move high loads, up to several tons and present capacitive loads that dissipate virtually no power in static operation.

Two types of piezo actuators have become established: low voltage actuators and high-voltage actuators. Monolithic low-voltage actuators (LVPZT) operate with potential differences up to 100V and are made from ceramic layers from 20 to 100µm in thickness. High-voltage actuators (HVPZT) on the other hand, are made from ceramic layers of 0.5 to 1mm thickness and operate with potential differences of up to 1000V. HVPZT can be made with larger cross sections, making them suitable for larger loads than the more compact LVPZT.

A piezo can be approximated as a spring and mass system; the stiffness of the actuator depends on the Young's Modulus of the ceramic (25% that of steel), the cross

section and length of the active material. Typical actuators have stiffness between 1 and 2,000 N/µm and compressive limits between 10 and 100,000 N [4].

Travel ranges of linear piezo actuators are typically between a few tens and a few hundreds of µm. Bender actuators and lever-amplified systems can achieve a few mm, while piezomotors can be used for longer travel ranges. Piezo ceramics are not subject to the stick-slip effect and therefore offer theoretically unlimited resolution. In practice, the resolution actually attainable is limited by electronic and mechanical factors [4]: Sensor and servo-control electronics (amplifier) noise and sensitivity to electromagnetic interference affect the position stability. Mechanical parameters such as the design and mounting precision issues (concerning the sensor, actuator and preload) can induce micro-friction which limits resolution and accuracy.

There are several drawbacks to using piezo elements in an open-loop fashion. The voltage-to-displacement relationship is non-linear and exhibits hysteresis, see Figure 33; hystersis is based on crystalline polarization affects and molecular effects within the piezoelectric material. The non-linear relationship implies that for a given increase in voltage, the piezo will expand by a varying amount across its full range of extension. The amount of hysteresis increases with increasing voltage applied to the actuator; from this it can be concluded that the smaller the move the smaller the uncertainty.

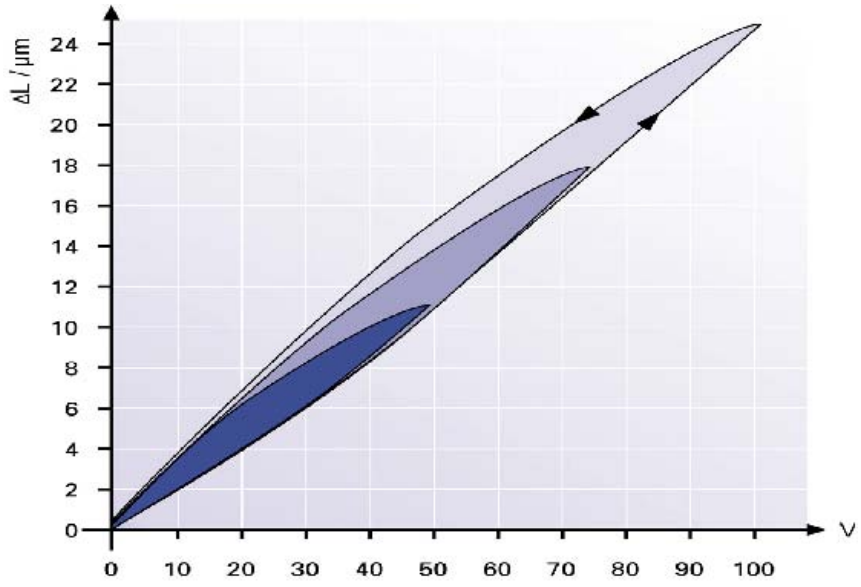

Figure 33 Hystersis Curves of an Open-Loop Piezo Actuator [4]

The same material properties responsible for hysteresis also cause drift or creep; creep is a change in displacement with time without any accompanying change in the control voltage. If the operating voltage of a piezo is changed the piezo gain continues to change, manifesting itself in a slow change of position. The rate of creep decreases logarithmically with time [4]. In general use, maximum creep after a few hours can add up to a few percent of the commanded motion.

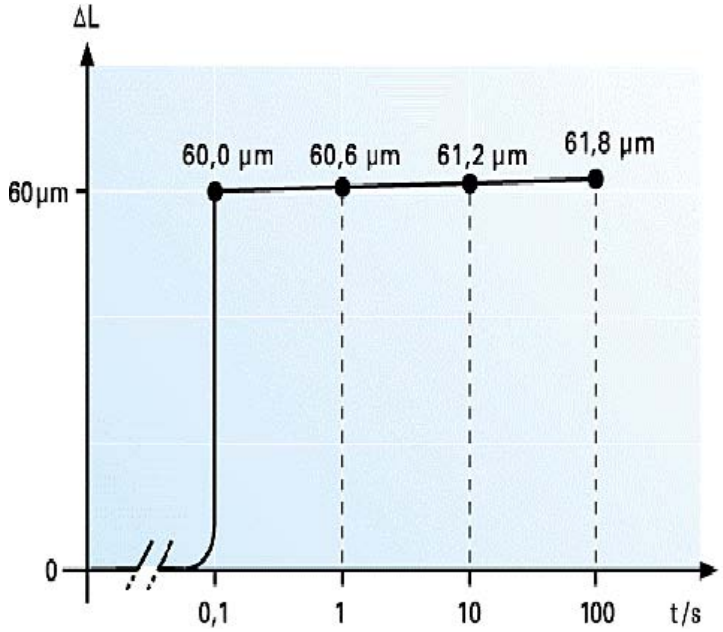

Figure 34 Creep of Open-Loop Piezo Actuator after a 60µm Change in Length as a Function of Time [4]

Chapter 5 will demonstrate how the limitations of piezos (hysteresis and creep) amongst others can be overcome to create an effective measurement instrument for this production scenario.

2.4.3 Displacement Sensors

Displacement sensors can be used to build a closed-loop measurement system that compensates for hysteresis, creep and thereby improves accuracy. Sensors can be categorized based on their working principles, such as resistive sensors, inductive sensors, capacitive sensors and optical sensors.

Resistive sensors, e.g. potentiometers, measure the changes in electrical resistance of a circuit as the target moves; they are easy to use and cost-effective, but being a contact sensor, friction and wear are introduced into the system [5].

Inductive sensors use the change of inductance to measure the corresponding displacement; they have low force coupling and impose little influence on the measurement. A typical example is the linear variable differential transformers (LVDT). As shown in Figure 35, the transformer consists of three coils: a primary coil and two secondary coils. A cylindrical ferromagnetic core, attached to the object whose position is to be measured, slides between the primary coil and the secondary coils. An alternating current is driven through the primary coil, causing a voltage to be induced in each secondary coil proportional to its mutual inductance with the primary; for small displacements of the core about the central position, the amplitude of the output across the secondary windings will be linearly proportional to displacement. Since the sliding core does not touch the coils, it can move without friction, making the LVDT a highly reliable device.

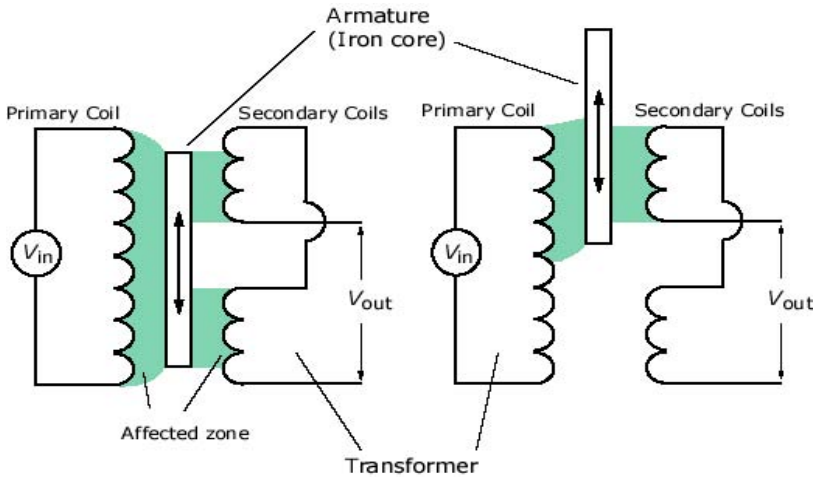

Figure 35 Linear Variable Differential Transformer

Capacitive sensors use the change in capacitance between a moving target and a fixed electrode to measure displacement [5]; two-plate capacitive sensors consist of two RF-excited plates that are part of a capacitive bridge, see Figure 36. One plate is fixed, the other is connected to the object to be positioned. The distance between the plates is inversely proportional to the capacitance, from which the displacement is calculated. Short range, two plate sensors can achieve resolution in the order of picometers [4]. However, capacitance sensors have limited measurement ranges, non-linearities at the extremities of this range and fringe field effects.

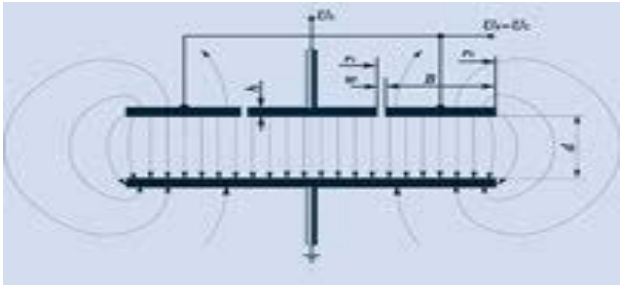

Figure 36 Working Principle of Capacitive Position Sensor

Optical sensors, such as laser interferometers, can potentially achieve sub-nanometer resolution and accuracy. The vast majority of displacement measuring optical transducers use the interference of two coherent light beams, usually from a single source; the beam is split into two with one beam reflecting from a datum surface while the other reflects from the surface being measured. The beams returning from the reflectors then combine and interfere; the intensity after inference will depend upon the difference in path lengths of the two beams. For an ideal beam passing through ideal optics there will be a sinusoidal variation in intensity as the reflector is moved and so the phase of the sine wave may be interpreted as displacement. Measurement stabilities of the order of 20nm with a resolution of 5nm are typical with optical sensors. However, large disturbances due to atmospheric temperature and humidity variations, air turbulence and vibrations caused by a harsh working environment would greatly reduce the practicality of such sensors. Further, the equipment and its calibration can be very expensive and complicated.

The third realistic option for displacement sensing in the sub-micron range is the strain gauge. They operate on the principle that as a length of wire is subjected to strain, the electrical resistance of the wire varies in direct proportion to the strain applied to it. Strain gauges are relatively cheap and can be used to measure the expansion of piezo

translators. In most of the standard products, two strain gauges are attached on opposite sides of the ceramic stack. Together with two bridge completion resistors, the strain gauges are wired in diagonal positions to form a Wheatstone bridge. The bridge is balanced if all four elements have the same resistance. The resistance of the strain gauges depends on the expansion of the piezo elements.

In summary, a plethora of technologies exist for actuating and sensing to suit different application requirements. Flexure joints and piezoelectric actuators are predominantly used for sub-micron measurement stages.

2.5 Automation Mechanisms and Control Systems

Whilst the development of the measuring system is paramount in this project, it is also necessary to automate the feeding mechanisms and control systems. This will include the use of positioning devices, networks and control software.

2.5.1 Positioning Devices

Positioning devices use a wide range of pneumatic, hydraulic and electrical devices coupled to ball screws cams etc. to move components. It is however outside the scope of this project to discuss the units in detail, and an explanation of these can be found in [63]. However it is envisaged that linear motion guides and stepper motors will be an inherent part of the design and will be discussed in Appendix G.

2.5.2 Network Communication

The control system utilises Actuator Sensor Interface (ASI) as a networking standard, coupled with RS-232 and RS-422 links. A brief description of theses can be found in Appendix H.

2.5.3 LabView Application Software

Software transforms the PC and the DAQ hardware into a complete data acquisition, analysis and presentation tool; there are two types of software required, driver and application. Driver software is the layer of software for communicating with the DAQ hardware; it forms the middle layer between the application software and the hardware. Application software adds analysis and presentation capabilities to the driver software; the software sends the driver commands to acquire and generate signals and manipulates the raw data into a form that is understandable.

The specific application software used for the measurement instrument control and central controller is National Instruments Labview 8.0. LabView (**Lab**oratory **V**irtual **I**nstrumentation **E**ngineering **W**orkbench) is a platform and development environment for a visual programming language from National Instruments, commonly known as G; a visual programming language is any programming language that lets users specify programs by manipulating program elements graphically rather than specifying textually. Program execution is determined by the structure of a graphical block diagram, (the LV-source code) on which the programmer connects different

function nodes by drawing wires; these wires transmit variables and any node can execute as soon as all its input data become available.

LabView programs are called virtual instruments, or VI's, because their appearance and operation imitate physical instruments, such as oscilloscopes and multimeters. LabView contains a comprehensive set of tools for acquiring, analysing, displaying and storing data. In LabView, you build a user interface, or front panel, with controls and indicators; controls are knobs, push buttons, dials and other input mechanisms, indicators are graphs, L.E.D. and other output displays. After building the user interface, code is added to the block diagram using VI's and structures to control the front panel objects. Each VI has three components: a block diagram, a front panel and a connector pane. The last is used to represent the VI in the block diagrams of other calling VI's. Controls and indicators on the front panel allow an operator to input or extract data; however, the front panel can also serve as programmatic interface. Thus a virtual instrument can either be run as a grogram, with the front panel serving as a user interface, or when dropped as a node onto the block diagram, the front panel defines the inputs and outputs for the given node through the connector pane. This implies that each VI can be easily tested before being embedded as a subroutine into a larger program. Figure 37 illustrates the block diagram and front panel of the central controller VI.

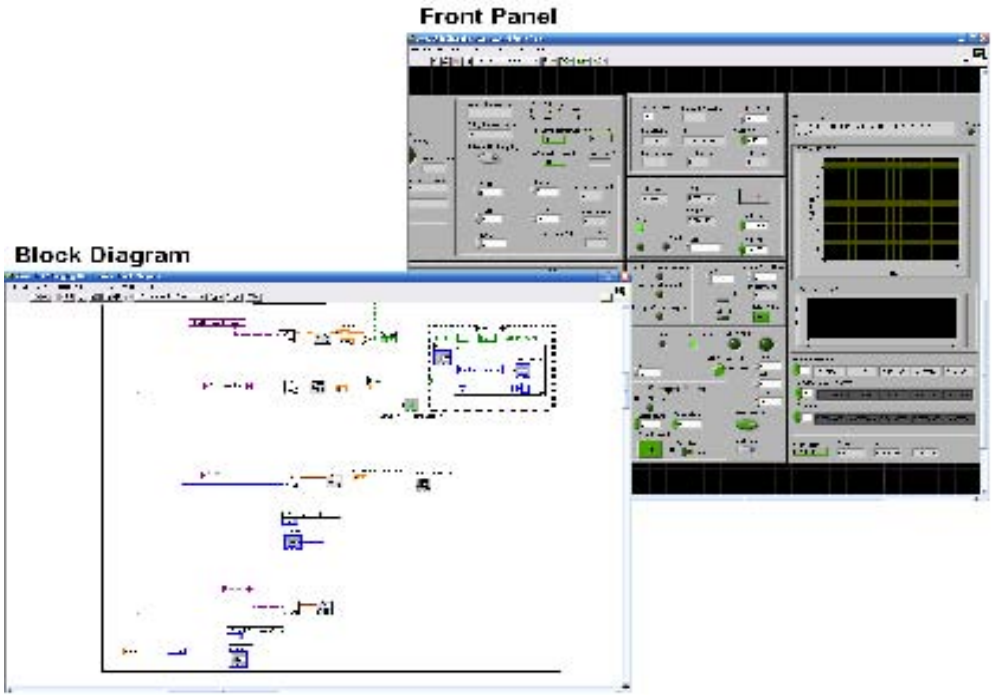

Figure 37 Labview Front Panel and Block Diagram

2.6 Project Aims and Objectives

2.6.1 Objectives

Having discussed the general elements of a possible measuring system, the objectives of the project can be defined as:

Objective 1: Research and develop a 'piezo-flexure-based' sensor system for multi-diameter ball bearing tolerance measurement to 0.1micron accuracy using FEA simulation and flexure design analysis

Objective 2: Simulate, design and build the measurement instrument to meet the production requirements of the client plant.

Objective 3: Test, prove and validate this measurement instrument in the Laboratory.

Objective 4: Install and commission the instrument in the plant: this includes the necessary temperature, humidity and vibration isolation and service access.

Objective 5: Prove and validate the instrument on-site, for the in-process measurement task. This involves the full integration of the measurement station with the grinding machines to allow closed-loop feedback control in cooperation with a parallel project

Objective 6: Study and improve the performance of the measurement system over a lengthy production cycle

Objective 7: Develop a measurement display unit to ease the change over from manual to automatic control.

2.6.2 Aims

In terms of the overall project, the aim was the total automation of the long established and universal labour intensive batch production technology of ball bearing production. Within this overall aim, the aim of this specific project is as follows:

- The development of a high-speed, high-precision measurement instrument to meet the requirements of the plant into the future
- The development of a measurement station around this new measurement instrument, making it the core of a new plant wide automation scheme.

3 Measurement Instrument Design

3.1 Prototype 1 Measurement Instrument

A feasibility study carried out by Mr. T. Wemyss [64] had already confirmed the suitability of piezo-based measurement for the ball bearing application prior to the start of this project. In this study a simple experimental prototype was built (Figure 38). This measurement instrument (Prototype 1) used the dramatic change in sensor feedback (a jump in the range of 0.1703V was observed), which occurs when a sinusoidal excited piezo contacts a solid surface. This effect was combined with tried and proven reference ball measurement techniques in order to achieve high resolution and accurate and repeatable measurement.

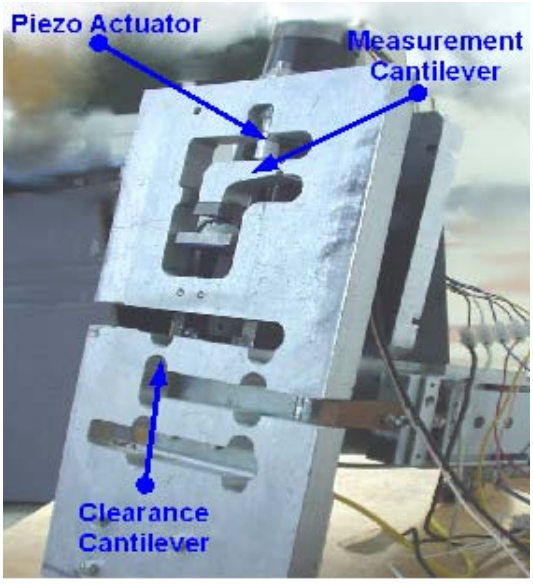

Figure 38 Prototype1 Measurement Instrument [64]

Two reference balls of known diameter were used to calibrate the monolithic piezo driven cantilever. Each ball was fed in turn to a fixed position locator beneath the cantilever tip; a piezo actuator controls the displacement of the cantilever tip. When the ball is in position, the cantilever is lowered by means of a piezo actuator. The extension of the piezo stack is then tracked by means of two inbuilt strain gauges mounted in a Wheatstone bridge. The DC voltage feedback value immediately prior to extension is recorded.

During the measurement process a continuous sinusoidal voltage of ≈ 1Khz (resonant frequency of the cantilever hinge as predicted by FEA and found experimentally) was applied to the piezo actuator, the frequency and amplitude of the

resulting feedback wave is constantly monitored throughout the measurement cycle. As the hinge is being excited at resonance, the dynamic stiffness of the hinge is at its minimal (resonance is the tendency of a system to oscillate at maximum amplitude at certain frequencies) and at these frequencies, even small periodic driving forces can produce large amplitude vibrations because the system stores vibrational energy. Therefore the displacement of the hinge and the strain gauge wave amplitude is at its greatest, for the piezo excitation voltage. When the measurement tip makes full contact with a sample ball, stiffness is added to the system; causing both to vibrate in unison. This additional stiffness increases the resonant frequency of the system. However as the piezo excitation frequency remains constant, the system is no longer excited at resonance; the magnitude of the vibration of the measurement tip is therefore decreased. As shown in Figure 39, it is this sudden change in feedback wave amplitude that is used to detect contact with a sample ball.

Having recorded the DC voltage feedback of the piezo actuator at point of contact and also prior to extension, a Labview VI routine computes the actual distance travelled by piezo actuator. This is then compared to the equivalent maximum and minimum reference component travel distance to establish the actual diameter of the product.

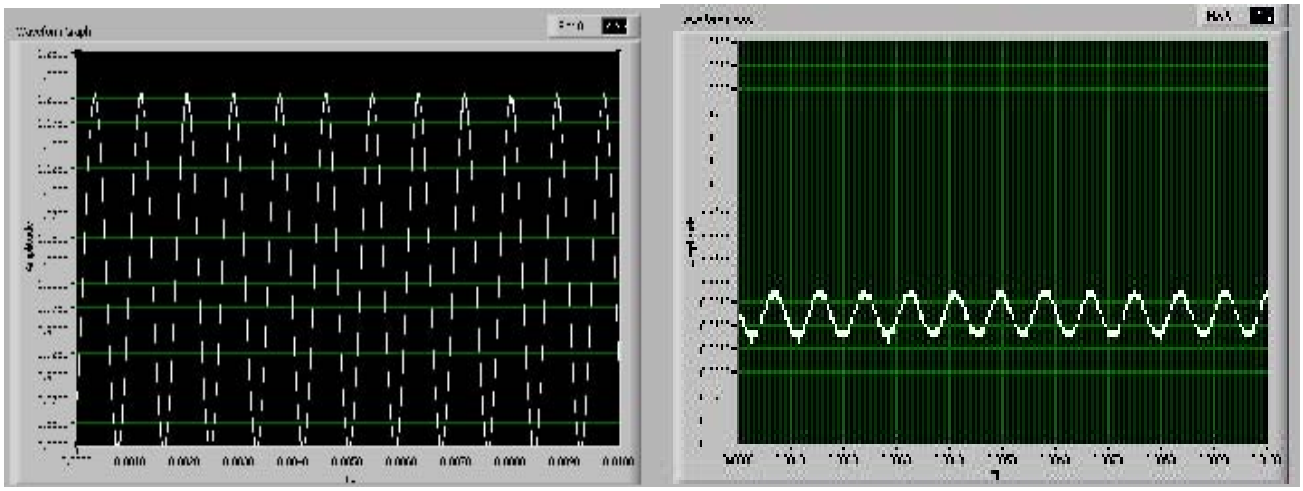

No Touch
Wave Frequency: 1.1730KHz
Wave Amplitude: 0.1903v

Touch
Wave Frequency: 1.1724KHz
Wave Amplitude: 0.020v

Figure 39 Strain Gauge Feedback Wave

To allow adequate clearance for ball positioning/ejection, the frame to which the cantilever is attached must undergo a relatively large movement. As illustrated in Figure 38 (the clearance cantilever), this was achieved by using a second cantilever hinge arrangement.

The measurement bearings were located against two hemispheres (Figure 40). This arrangement ensured that centres of differing diameter balls were located close to the same spot relative to the measuring tip.

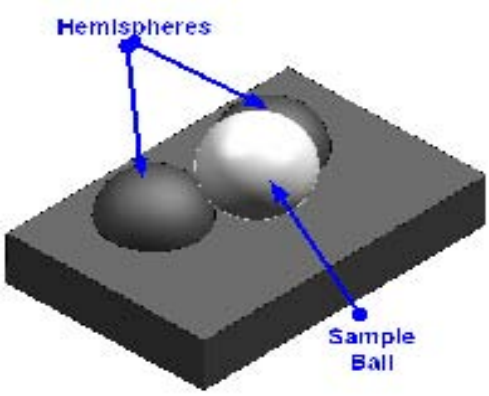

Figure 40 Prototype1 Ball Locator

This instrument is intended to measure different gauge bearings, which can be at different stages of their production cycle, as well as bearings of different sizes in the 10-35mm range. This demanded a measurement range far greater than can be offered by a piezo driven cantilever operating within the elastic range of the material. To address this need for flexibility, a stepper motor driven lead screw, giving a resolution of 5µm, was developed to move the bearing-locating platform to within the range of the measuring cantilever before it is pneumatically clamped.

The Prototype1 measurement instrument was situated in an open room, where it was mounted on a granite block. This left the device very susceptibly to mechanical and electronic noise and temperature changes. Temperature variations have significant effects on the device. The coefficient of linear expansion of aluminium is 23.6µm/m°C and the overall dimensions of the unit are 400x200mm. As illustrated in Figure 41, FEA simulations of the effect of temperature variation on the aluminium plate have been carried out: it was shown that with a 1°C temperature rise, the tip of the measurement cantilever is displaced by 0.11mm. To some extent this is counterbalanced by the expansion of the lead screw,

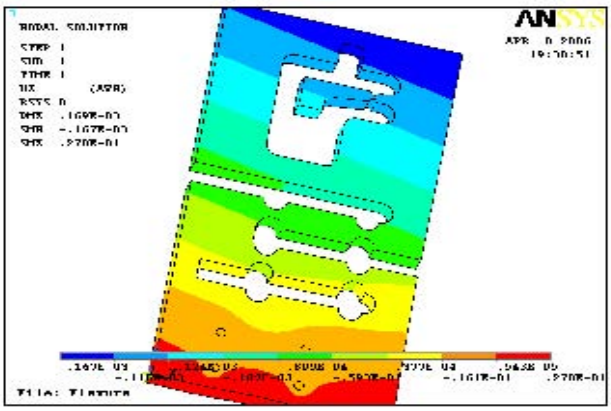

Figure 41 Expansion of Prototype Measurement Instrument along the Z direction due to 1C rise in Temperature

ball locator and clamping mechanism, but the relative displacements can be assumed to be large and relatively unpredictable.

For practical purposes in terms of the plant requirements, Prototype 1 has some important limitations. In the periodic samples taken from the grinding machine, the sample ball diameter can be +150µm from the nominal diameter. Therefore the effective working range for the measurement device (without adjusting the moving platform) is required to be 150µm. Prototype1 measurement instrument was designed with a lever motion amplifier; an available piezo actuator of 15µm stroke was used and the cantilever amplification ratio used was 2:1. Thus the max measurement range of the device is 30µm. Also and perhaps the most limiting factor is the sinusoidal voltage applied to the piezo actuator to detect the touch of the ball. When a frequency (1KHz in this case) is applied to a Low Voltage Piezo Actuator the electrical capacitance of the actuator and the average power of the amplifier limits the movement of the actuator. As illustrated in Figure 42, with 1KHz sinusoidal voltage applied, the actuator will travel 20% of its full range. As a result the actual movement of the measurement tip is reduced from 30µm to 6µm.

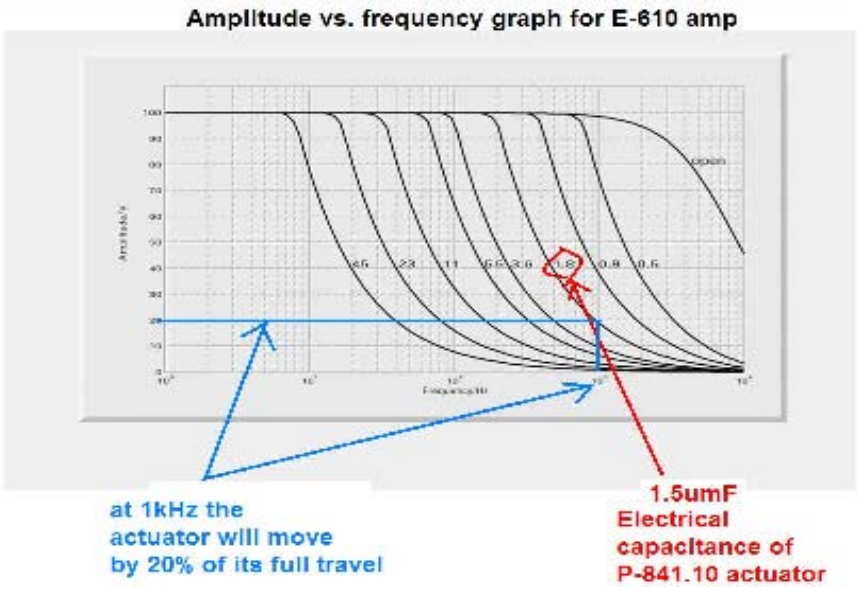

Figure 42 E-610 Piezo Driver Open-Loop Frequency Response with various Piezo Loads

Another limitation of this first design was that as the measurement tip extends, the cantilever rotates about the hinge point (Figure 43). Consequently, varying sample ball diameters touch the measurement tip at different points, introducing errors not just due to surface roughness but also due to the changing angle of the upper contact surface.

These limitations were known beforehand but allowed for the development of the fitting and control of the piezo actuators, the LabView visualisation and measurement routines and the study of the ball seating and delivery issue, as well as investigating the touch phenomena.

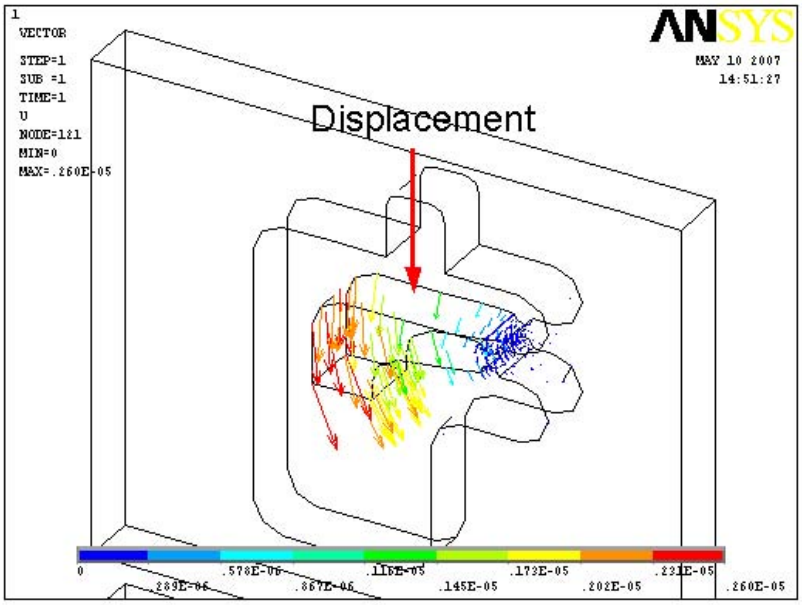

Figure 43 Rotation of Cantilever

Using Prototype 1 as the basis of a measurement system for ball bearings, a system suitable for a production line was developed and will be discussed in the next section.

3.2 Production Measurement Instrument

3.2.1 Description

Prototyping proved essential for clarifying the functional requirements of the production measurement instrument and also significantly assisted the design process of the instrument. The testing of Prototype1 confirmed that ball bearing piezo-based measurement is a practical solution for the ball bearing application.

The production measurement instrument consists of a primary flexural-hinge guided stage driven by a piezoelectric actuator Pa (Figure 44); in-built into the primary stage is a secondary flexural-hinge guided stage, which again is driven by a piezoelectric actuator Pb. The primary piezo actuator is used to drive the stage through long-travel positioning and the secondary acts as a touch sensor to detect contact between the measurement stage and the product. For full working drawings see Appendix E.

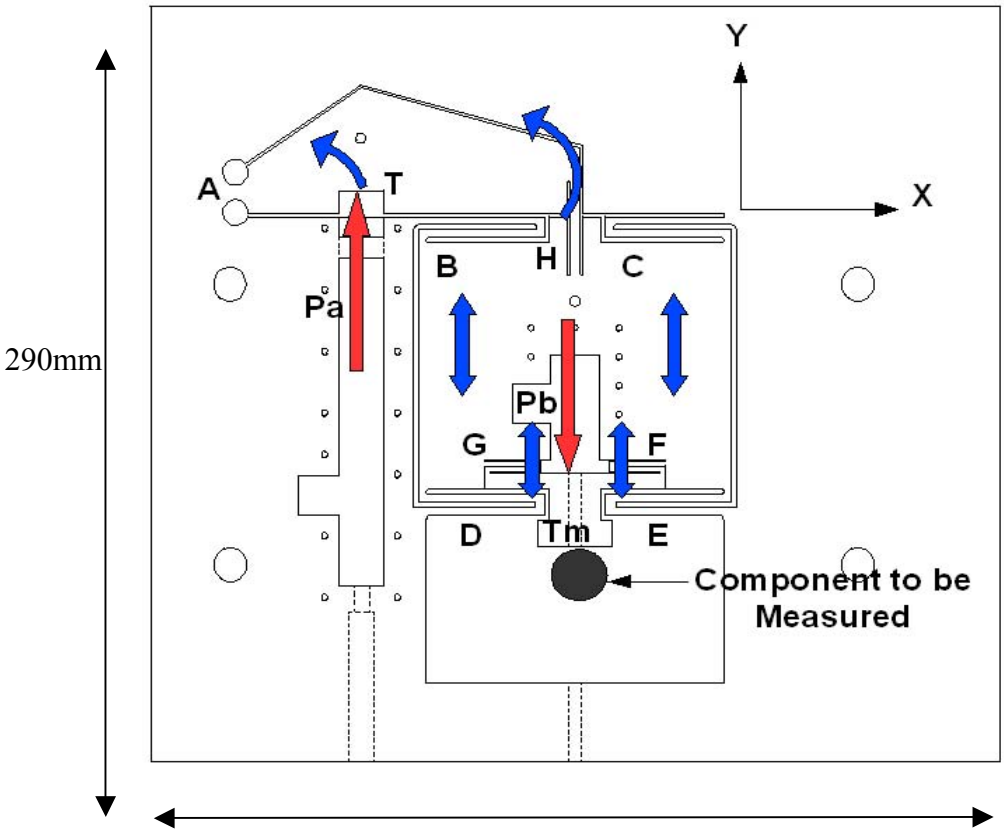

Figure 44 Measurement Instrument Schematic

Figure 44 presents a schematic illustration of the developed measurement device. In this arrangement, a displacement (0-90μm) at point T caused by movement of the primary piezoelectric actuator *Pa* is amplified through the lever mechanism. The displacement in the y-direction causes the entire stage to move in the upward direction, hence resulting in displacement amplification. As shown the displacement at point T causes the lever to rotate about point A; this rotation results in displacement offset of 12.3μm in the x-direction. The transmission of this offset to the measurement point is reduced to 1.14μm by flexure H and by four leaf flexures B, C, D and E. Therefore the amplified displacement at point Tm will be linear and in the y-direction only.

3.2.2 Measurement Principle

Maximum and minimum reference components of known diameter are used to calibrate the system; a continuous cycle of calibration followed by measurement is used. Sample balls are selected automatically from the process and delivered to a temperature normalizing station: they are stored there along with the reference components for a specific period of time (sufficient for complete temperature equalization) in a temperature controlled fluid at slightly above ambient temperature. The number of samples measured between calibrations is kept to a minimum so that the effects of environmental variability are minimized: it is expected that any errors due to thermal changes in the entire measurement device will thereby be minimized.

The expansion and contraction of the piezo actuators Pa and Pb are tracked by means of two inbuilt strain gauges mounted in a Wheatstone bridge. When a sample ball is in place, the measurement process begins with the piezo actuator Pa being retracted: the DC voltage feedback value immediately prior to retraction is recorded. During the measurement cycle the amplitude of the touch sensor piezo Pb feedback signal is constantly monitored: When the tip makes full contact with the sample ball the strain on the piezo drops instantly (since contacting the ball causes the piezo to compress). It is this sudden change in feedback amplitude that is used to detect contact with the sample ball. The exact amplitude of the voltage feedback on Pa is again recorded at this contact point. (Unlike Prototype1 a continuous sinusoidal voltage is not applied to the piezo actuator; therefore instead of sinusoidal feedback wave, the feedback from the touch

sensor piezo within the production measurement instrument is a constant amplitude signal).

Having recorded the DC voltage feedback of the piezo actuator at point of contact and also prior to retraction, a Labview VI computes the actual distance travelled by the piezo actuator. This is then compared to the equivalent maximum and minimum reference ball travel distance to establish the precise diameter of the sample ball.

3.2.3 Material Selection

3.2.3.1 Introduction

This section describes the flexure material selection process and explains the theory behind materials selection in precision mechanical design; different properties of materials will be examined to discover how each affect the performance of designs in relation to ability to carry loads, deflections due to loads and thermal effects etc.

Material properties limit performance, but seldom does that performance depends on just one property. It is generally a combination or several combinations of properties that have the greatest affect on performance e.g. Strength to Weight ratio σ_f/ρ or stiffness to weight ratio E/ρ. Property charts with logarithmic scales are used to plot one property against another. These charts are helpful in condensing a large body of data into a compact but accessible form and they reveal correlations between material properties, which aid in checking and estimating data. The property charts are used as a tool to swiftly eliminate unsuitable materials and to identify potential areas for more careful exploration. Subsequently, a short-list of appropriate materials can be made. Property profiles are used for cross-comparison of the selected short-list of materials. Property profiles summarize graphically the quality of a material over a wider range of property groupings.

The two most important areas in the design of precision mechanisms are the stability of the system under mechanical load and the stability of the system under thermal load. In this material selection process, material properties are therefore divided into groups: the mechanical property group and the thermal property group. The final outcome of this materials study was the selection of a more appropriate Aluminium Alloy (7075) than that used in Prototype 1 (6082).

3.2.3.2 Mechanical Property Group

The mechanical functionality required of a precision system commonly involves: the minimization of deflection under external and/or self-weight loads and the maximization of load capacity in small members or conversely, the maximization of elastic deflection in a flexure mechanism. The control of resonant frequencies may also be important [3].

The deflection (Δd) of a cantilevered beam of constant rectangular cross section from a point load (W) at its end, varies as

$$\Delta d = \frac{WL^3}{EI} \qquad \textbf{(1)}$$

Where (b), (d), (L) is the width, depth and length of the beam respectively, (E) is the modulus of elasticity and $I=bd^3/12$

The deflection due to its own weight varies as

$$\Delta d = \frac{\rho AgL^4}{EI} \qquad \textbf{(2)}$$

Where (ρ) is density of material, (A) is the cross sectional area and (g) is gravitational acceleration. The max bending moment (M_{max}) that the beam can carry without yielding is

$$M_{\max} = \frac{2YI}{d} \qquad \textbf{(3)}$$

Where (Y) is the yield stress. From Equation (2) the deflection due to gravity is minimized by minimizing (ρ) and maximizing (E). Therefore a material should be chosen with a minimum ρ/E ratio or maximum specific strength E/ρ.

From Equation (1) the stiffness (K) can be calculated as

$$K = \frac{Ebd^3}{L^3} \qquad \textbf{(4)}$$

As the weight is ρLbdg, both stiffness and weight depend on (b), (L) and (d). With both (b) and (L) fixed, (d) can be varied to minimize weight while maintaining the specified stiffness. From Equation (4), if the other terms are fixed, to maintain the stiffness

$$d \propto \frac{1}{E^{\frac{1}{3}}} \Rightarrow weight \propto \rho d$$

therefore

$$weight \propto \frac{\rho}{E^{\frac{1}{3}}} \qquad \textbf{(5)}$$

$\rho/E^{1/3}$ is the best ratio to use for minimum weight design of stiff beams [3]. From Figure 45, the value of constant C ($E^{1/2}/\rho$) increases as the lines are displaced upwards and to the left, therefore the materials offering the greatest stiffness-to-weight ratio lie towards the upper left corner. For example Aluminium alloys are better than steels for a minimum weight strut that must support a specified buckling load.

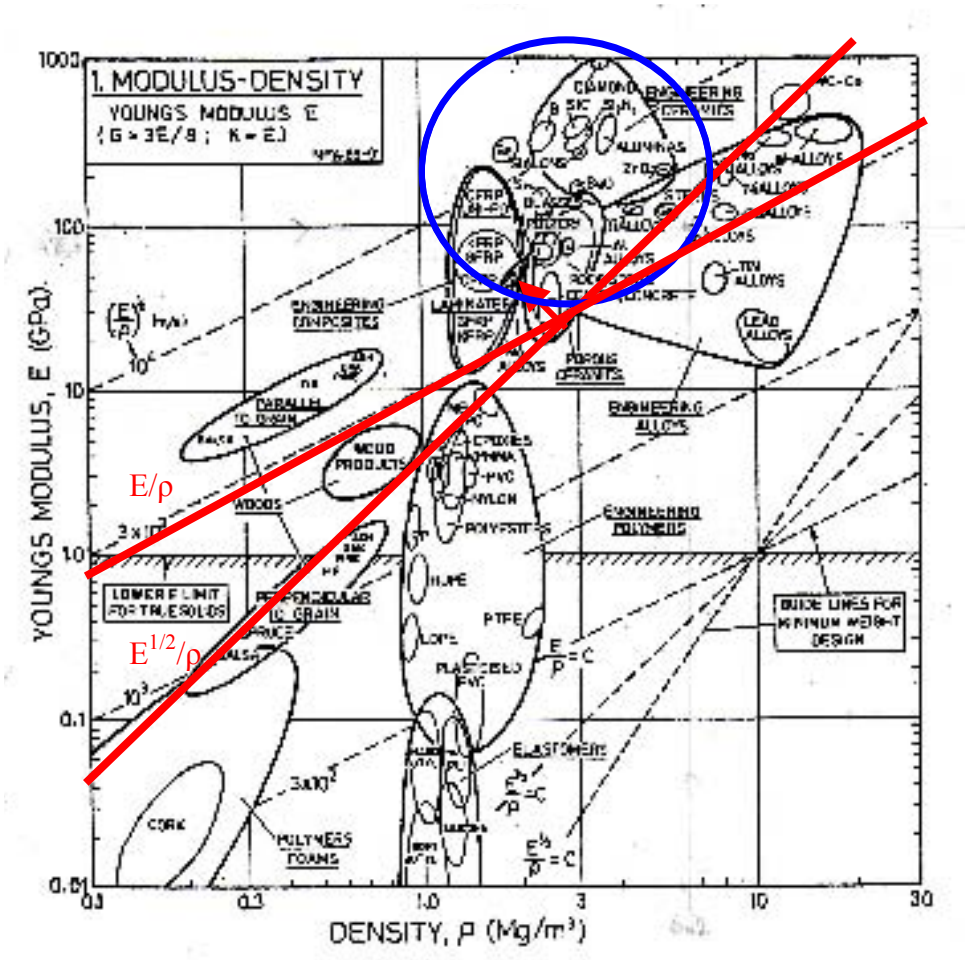

Figure 45 Modulus-Density Property Chart

For free vibration of a simple beam the natural frequency (f) is given by [1]

$$f = \left(\frac{1}{2\pi}\right)\left(\sqrt{\frac{k}{m}}\right) \qquad \textbf{(6)}$$

Where (m) is the mass of the beam. In most situations, decoupling unwanted vibrations from a system is made easier if its resonances are at high frequencies [3]. From Equation (7), increasing the resonant frequency of a system is possible by maximizing the stiffness and minimizing the mass.

$$f = \left(\frac{1}{2\pi}\right)\left(\frac{\left(\frac{Ebd^3}{L^3}\right)}{((V)(\rho)}\right) \quad \textbf{(7)}$$

Since $mass = volume \times density$. If the volume is fixed, then to minimize the mass of the system, choose a material with a low value for density.

From Equation (4), if (b), (L) and (d) are all fixed values, then the stiffness can only be increased by using a material with a high value for Young's Modulus.

$$f \propto \frac{E}{\rho} \quad \textbf{(8)}$$

Therefore, to increase the resonant frequency of the system, choose a material with a maximum E/ρ ratio.

Flexures exploit linear strain, so a material with a low modulus of elasticity might appear preferable. However, repeatability in flexures requires avoidance of plastic strain and thus operation must be within the elastic region of the material. Since, the maximum strain (ε) is limited by the yield strength (σ_y)

$$\sigma_y = E\varepsilon \quad \textbf{(9)}$$

$$\text{Therefore } \varepsilon = \frac{\sigma_y}{E} \quad \textbf{(10)}$$

For flexure applications therefore, selection of a material with a high σ_y/E ratio is desirable. From Figure 46, the value of constant C (σ_y/E) increases as the lines are displaced downwards and the right, therefore the materials that can be flexed the most without yielding or failing lie towards the bottom right corner. A lower limit for the modulus of elasticity has to be set to maintain the required rigidity of the mechanism.

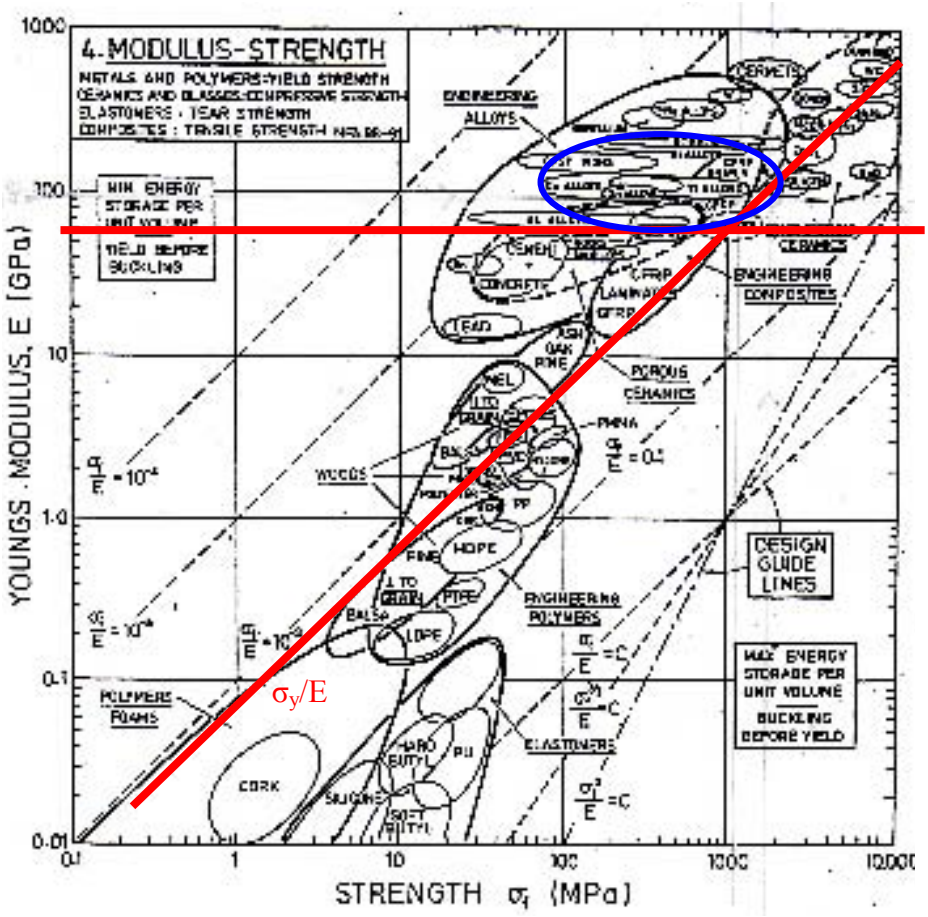

Figure 46 Modulus Strength Property Chart

3.2.3.3 Thermal Property Groups

Thermal disturbances in a mechanical device can be caused by environmental changes or by localized power/energy sources such as actuators. Almost all solids expand on heating and for that reason the usual requirement is to choose a material with a low coefficient for thermal expansion (α). Also, a body is sometimes tightly constrained such that little or no change in dimension is possible. Forces are then generated at the constraints that cause compression in the member exactly compensating for its attempted thermal expansion [3]. For homogeneous, isotropic materials, the stress (σ) generated by a change in temperature (ΔT) is given by

$$\sigma = E\alpha\Delta T \qquad \textbf{(11)}$$

To minimize the stress caused by thermal expansion (Eα) should be minimised by selecting a material with a combination of a low modulus of elasticity and a low coefficient of thermal expansion.

If the device carries an actuator, then it may be conducting a steady heat flow. Using Fourier's Law for conduction along a uniform rod of length (L) and cross sectional area (A), carrying a heat flow (q), implies a temperature differential between the ends such that

$$q = \frac{kA\Delta T}{L} or \Delta T = \frac{qL}{kA} \qquad \textbf{(12)}$$

Where (k) is the thermal conductivity of the material. If the end of the rod is at room temperature, then there will be a uniform temperature gradient towards the heat source and the average rise in the rod will be ΔT/2. In most solids, thermal expansion relates directly to temperature. Thus, the strain (ε) due to a temperature change is given by

$$\varepsilon = \alpha\Delta T \Rightarrow \alpha\frac{\Delta T}{2} \qquad \textbf{(13)}$$

From (12) $\frac{\Delta T}{2} = \frac{qL}{2kA}$

Substituting in (13) $\varepsilon = \frac{qL\alpha}{2KA}$

To reduce strain it is better to use a material with a low value of α/k. Reduced strain can be achieved by choosing a material with a high thermal conductivity to conduct the heat away and a low expansion coefficient to reduce thermal strains, hence a material with a high k/α ratio is desirable. Figure 47 is the chart for assessing thermal distortion: the contours show constant value C of the ratio k/α. Materials with a large value of C show small thermal distortion: the value of the constant C increases towards the bottom right corner.

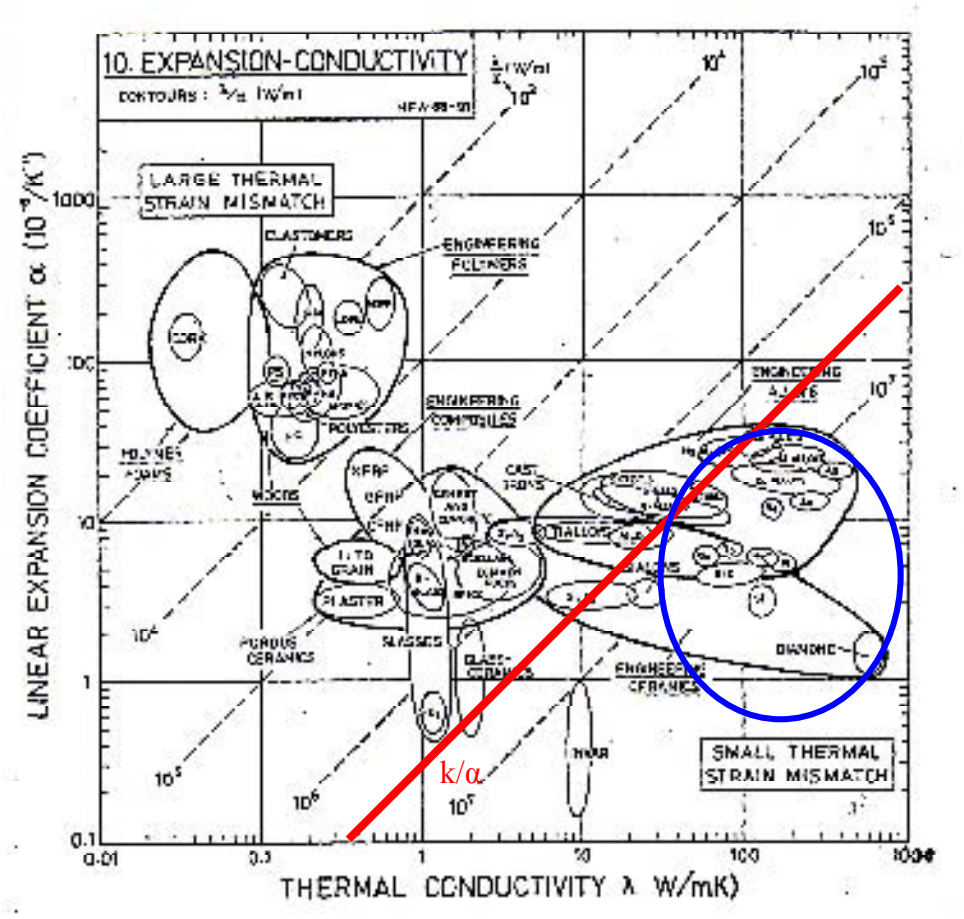

Figure 47 Thermal Distortion Chart

However, if the thermal disturbance is not steady, then normally a rapid return to equilibrium is desirable. The simplest case of the one dimensional heat equation is [3]

$$\frac{d\theta}{dt} = \frac{k}{Cp} \cdot \frac{d^2\theta}{dx^2} \qquad \textbf{(14)}$$

Where (θ) is temperature relative to ambient, (t) is time, (x) is spatial distance and (Cp) is the volume specific heat. The time behaviour is an exponential decay from the disturbed state at a rate governed directly by the diffusivity k/Cp [3]. To ensure a rapid return to equilibrium a material with a high k/Cp ratio should be selected.

3.2.3.4 The Material Selection Decision

The property charts from the previous section were used in this project to eliminate a significant amount of unsuitable materials and allow attention to be rapidly focused on material that could be useful in the precision flexure design. Members of the engineering alloys class were the most consistent throughout all the property ratios. Steels, Aluminium alloys, Tungsten alloys and Titanium alloys were short listed as potential successful materials.

Property profiles were used to cross-compare the selected short-list of materials; these summarize graphically the quality of a material over the wide range of property groupings discussed earlier. Several scales are required to be compared and it is much easier to read the chart if they are normalized in a standard way. Therefore, the value for of each ratio of a material is divided by the same ratio value for a standard material. Smith and Chetwynd [3] propose that a model material, which has ideal values for each property, should be used to normalize the chart. Table 10 shows properties of a model material for use in flexure hinges.

Property	Value	Typical of
Youngs Modulus	200 GPa	Steel
Max Strength	300MPa	Steel
Density	4000 kg m^{-3}	Ceramic
Thermal Expansion	7x10^{-6} K^{-1}	Ceramic
Thermal Conductivity	150 $Wm^{-1}K^{-1}$	Brass
Specific Heat	750 J $kg^{-1}K^{-1}$	Metals

Table 10 Properties of Model Material [3]

Error! Reference source not found. illustrates the property profile for the short listed materials. Factors influencing mechanical performance are placed to the left and those relating to thermal performance are to the right. As previously mentioned, deflection is related to σ/E, and resonance and lightweight design are related to E/ρ. External environmental influences are very likely in the context of this project (a harsh operating environment); therefore great attention is paid to $1/E\alpha$, k/α and k/Cp, which relate to stress, strain and response to temperature change respectively.

Of the short listed material, Tungsten performs well on all characteristics except E/ρ, hence increasing the weight of the design and lowering the resonant frequency. Titanium looks very impressive mechanically but performs poorly for thermal characteristics leaving the design very susceptible to temperature variations. Mild Steel is consistently modest for all characteristics both mechanically and thermally.

The profile for Aluminium gives an immediate impression of a material that is never really good, but rarely bad. Aluminium performs consistently well throughout all the characteristics; therefore, Aluminium was selected as the material for the flexure mechanism. It was chosen because it is easy to work with in applications that are not at the limits of performance and low density permits an increase in resonant frequency and faster response. The combination of a low thermal expansion coefficient and high thermal conductivity promotes short-lived transient gradients, rapid thermal equilibrium and minimal thermal induced stress.

	E	σ	E/ρ	σ/E	1/Eα	k/α	k/Cp
Aluminium	0.35	0.4	0.5	1.1	0.8	0.45	1.9
Titanium	0.6	2.3	0.55	3.9	1.3	0.1	0.6
Tungsten	2.1	4.5	0.45	2.2	0.75	1.7	1.3
Mildsteel	1.1	1	0.55	0.95	0.6	0.25	0.35

Table 11 Property Group Values Expressed Relative to Model Material

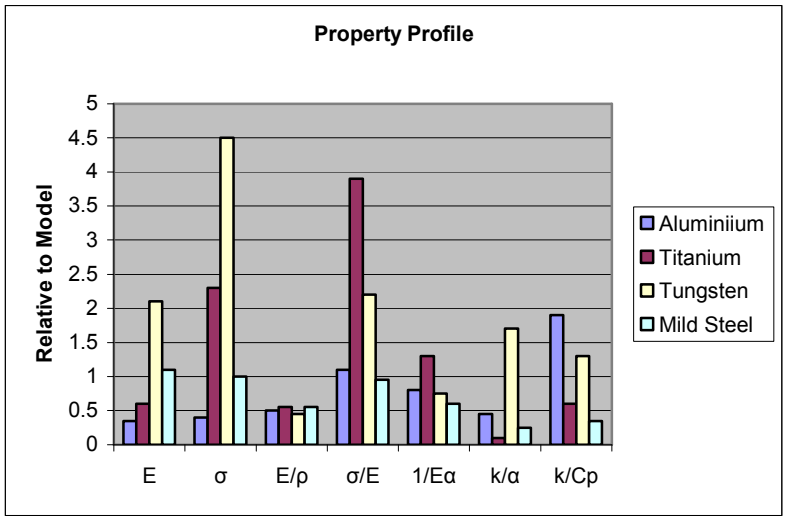

Figure 48 Property Profile

The specific Aluminium alloy chosen is Aluminium 7075 T6. This is an Aluminium alloy with zinc as the alloying element. T6 denotes the type of temper used; in this case it is solution treated, then artificially aged. [see Appendix A]. It is a very high strength material: it is one of the highest strength Aluminium alloys available, with a yield strength of 503Mpa[13], compared to 250Mpa for Aluminium 6082 T6 used in Prototype 1(Figure 49). As previously mentioned, repeatability in flexures requires avoidance of plastic strain and thus the maximum strain is limited by the yield strength of the material; therefore Aluminium 7075 T6 allows for 1.96 times the strain of Aluminium 6082, increasing the measurement range of the production measurement instrument. Aluminium 7075's strength-to weight ratio is also excellent and it is ideally used for highly stressed parts [11]. It is also strong, with a good fatigue strength of 159Mpa at $5x10^8$ cycles, compared to 83Mpa for Aluminium 6082 T6; therefore the amount of measurement cycles performed before the material will fail is far superior than the Prototype 1 material.

7075 is widely used for the construction of aircraft fittings, gears and shafts, fuse parts, meter shafts and gears, missile parts, regulating valve parts, worm gears, keys, aircraft, aerospace and defence applications [11]. Its strength and light weight are also desirable in other fields; rock climbing equipment and bicycle components are commonly made from 7075 aluminum alloy.

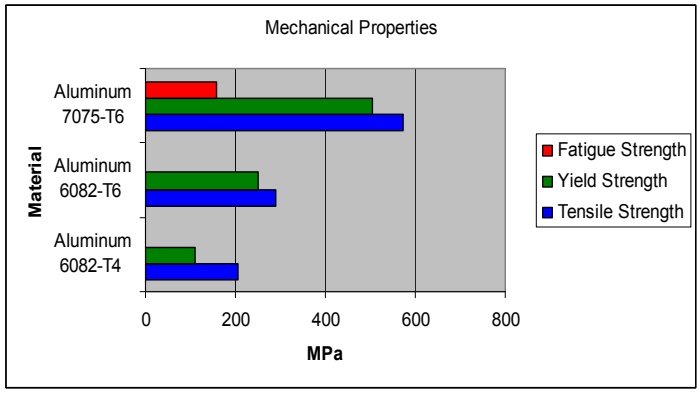

Figure 49 Comparison of Aluminium Strengths

3.2.4 The Mechanical Design

3.2.4.1 Cantilever Notch Hinge

The design involves two different types of simple flexure arrangements. The first type is a cantilever with a simple notch hinge: this is used to amplify the displacement of the piezo actuator *Pa* (Figure 50).

3.2.4.1.1 Linear Stiffness of Cantilever Hinge

The angle of rotation of the cantilever about Point *A* due to the force applied at point *Ta* is

$$\theta radians = \frac{9\pi r^{0.5} M}{2Ebt^{2.5}} \quad \textbf{(15)}$$

Where r is the hinge radius, M is the bending moment on point A, E is Young's Modulus, b is the material thickness and t is the thickness of the hinge [3].

Since for very small θ,

Sinθ° ≈ θradians,

Therefore θ° = Sin^{-1}θradians

$$\Rightarrow \theta° = \sin^{-1}\left(\frac{9\pi r^{0.5} M}{2Ebt^{2.5}}\right)$$

Using simple trigonometric functions, the distance moved Dy can be calculated by Dy=(Df)(Sinθ°), the equation can be simplified to

$$\Rightarrow Dy = Df \sin\left(\sin^{-1}\left(\frac{9\pi r^{0.5} M}{2Ebt^{2.5}}\right)\right)$$

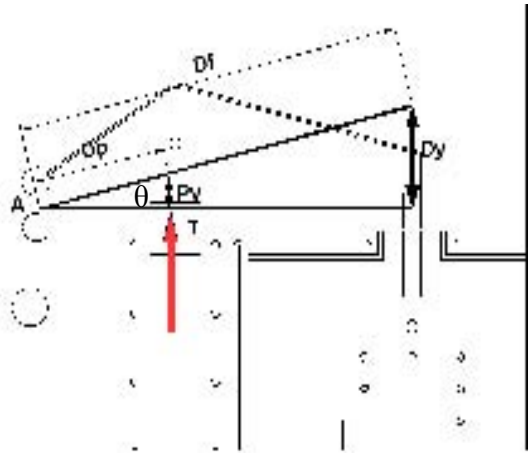

Figure 50 Cantilever Notch Hinge Schematic

Also M=Force x Distance, so M=(F)x(Dp)

Therefore the displacement at the end of the cantilever due to the force applied by the piezo actuator is given by

$$Dy = \frac{9\pi r^{0.5} FDpDf}{2Ebt^{2.5}} \quad \textbf{(16)}$$

The linear stiffness of cantilever hinge K_c along the axis of Dy is given by

$$K_c = \frac{F_1}{Dy} \qquad \textbf{(17)}$$

F_1 is the force applied by the piezo at point T

Substituting

$$K_c = \frac{F_1}{\left(\frac{9\pi r^{0.5} F_1 DpDf}{2Ebt^{2.5}}\right)} = \frac{F_1}{1} \times \frac{2Ebt^{2.5}}{9\pi r^{0.5} F_1 DpDf}$$

$$\therefore K_c = \frac{2Ebt^{2.5}}{9\pi r^{0.5} DpDf}$$

For a notch radius (r) of 5mm, plate thickness (b) of 20mm, cantilever length (Df) of 135mm, distance from hinge to piezo (Dp) of 50mm, flexure thickness (t) of 5.5mm and Young's Modulus of 72 Gpa (Aluminium 7075), the flexure stiffness Kc is calculated as

$$K_c = \frac{2(72x10^9)(0.02)(0.055^{2.5})}{9\pi(0.005^{0.5})(0.05)(0.135)} = 478769.173N/m = .4787N/\mu m$$

3.2.4.1.2 Relationship Between the Angle at which the Cantilever is Rotated and the Rotation of the Link Beam

As shown in Figure 51, the piezo force acts to rotate the cantilever in an anti-clockwise direction about point A, the angle of rotation is denoted θ. There is a vertical link beam at the end of the main flexure: the objective is to try to isolate a moving block (connected via a second flexure hinge to the other end of this vertical link) from the rotation of the cantilever. When the cantilever is rotated θ˚, the link beam will rotate α˚. Using the schematic an expression for the relationship between θ and α can be derived.

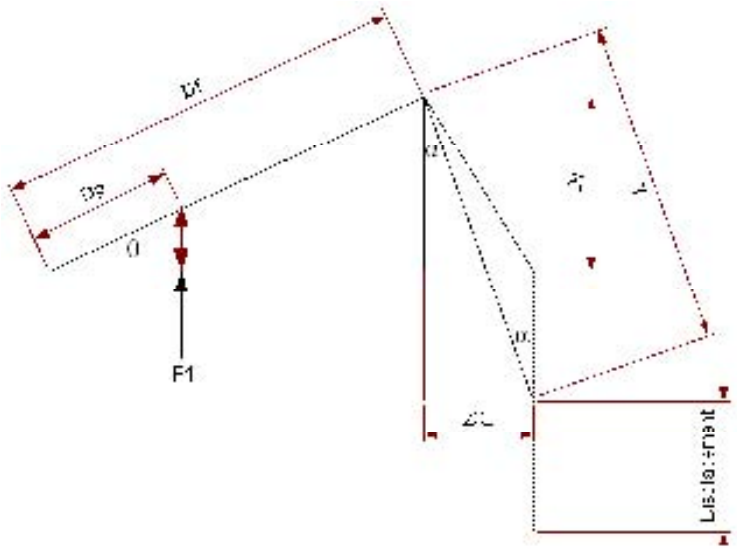

Figure 51 Cantilever and Link Beam Schematic

$$Sin\theta = \frac{Dy}{Df} \Rightarrow Dy = DfSin\theta$$

$$Tan\alpha = \frac{O}{A} = \frac{2XL}{L} \approx Sin\alpha = \frac{2XL}{L} \quad (\alpha \text{ small})$$

Where XL is the linear movement of the link beam and L is the length of the link beam

$$Tan\alpha = \frac{2XL}{L} \Rightarrow 2XL = L(Tan\alpha)$$

$$Tan\theta = \frac{Dy}{Df - 2XL} \Rightarrow Tan\theta = \frac{Dy}{Df - \{L(Tan\alpha)\}} \Rightarrow Dy = Tan\theta[Df - \{L(Tan\alpha)\}]$$

$$\frac{Dy}{Tan\theta} = Df - \{L(Tan\alpha)\} \Rightarrow Df - \frac{Dy}{Tan\theta} = L(Tan\alpha)$$

$$\Rightarrow Tan\alpha = \frac{1}{L}(Df - \frac{Dy}{Tan\theta})$$

Since $Dy = DfSin\theta$

$$\Rightarrow Tan\alpha = \frac{1}{L}(Df - \frac{DfSin\theta}{Tan\theta}) \Rightarrow Tan\alpha = \frac{1}{L}\left\{Df(1 - \frac{Sin\theta}{Tan\theta})\right\}$$

$$Cos\theta = \frac{Sin\theta}{Tan\theta}$$

Simplifying

$$Tan\alpha = \frac{Df(1 - Cos\theta)}{L}$$

Therefore the relationship between the angle at which the cantilever is rotated θ and the rotation of the link beam α is given by

$$\alpha = Tan^{-1}\left\{\frac{Df(1 - Cos\theta)}{L}\right\}$$

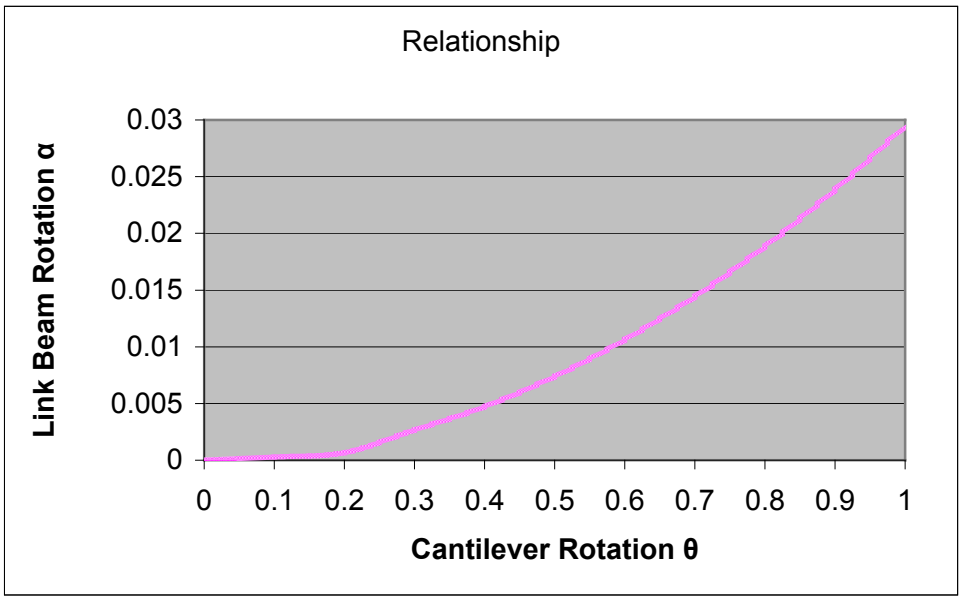

Figure 52 Graph Relating α and θ

3.2.4.1.3 The Horizontal and Vertical Component of the Force Acting on the Link Beam when the Cantilever is Rotated

The rotational stiffness of the link beam is

$$K_{RL} = \frac{M}{\alpha} = \frac{EI}{L} = \frac{Ebd^3}{12L} \text{ (Since } I = \frac{bd^3}{12}\text{)} \qquad \textbf{(18)}$$

Where (L) is the length of the link beam, (b) the plate thickness, (d) the thickness of the beam.

$$\alpha radians = \frac{12LF_H}{Ebd^3}$$

Where F_H is the horizontal component of the force acting on the link beam.

From earlier

$$Tan\alpha \approx Sin\alpha = \frac{2XL}{L}$$

$$\alpha radians = Sin\alpha^\circ \Rightarrow \alpha radians = \frac{2XL}{L}$$

$$XL = \frac{\alpha radians L}{2}$$

$$\Rightarrow XL = \frac{(\frac{12LF_H}{Ebd^3})L}{2} = \frac{6L^2F_H}{Ebd^3}$$

Therefore the linear stiffness of the link beam K_H is

$$K_H = \frac{F_H}{XL} = \frac{F_H}{\left(\frac{6L^2F_H}{Ebd^3}\right)} = \frac{Ebd^3}{6L^2} \qquad \textbf{(19)}$$

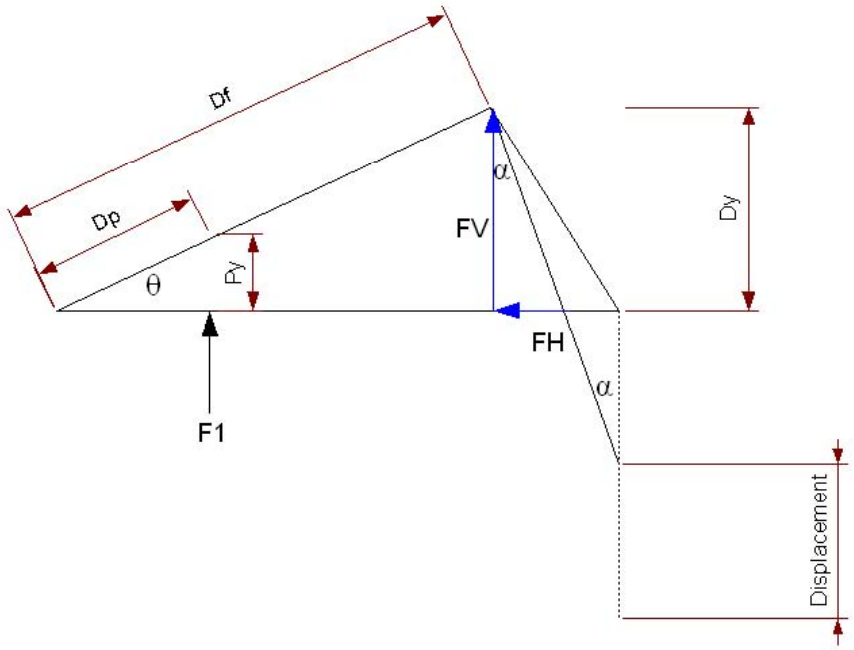

Figure 53 Force Diagram

The force in the horizontal direction F_H is

$$\frac{F_H}{XL} = \frac{Ebd^3}{6L^2} \Rightarrow F_H = \frac{Ebd^3 XL}{6L^2}$$

$$\frac{Dp}{Df} = \frac{Py}{Dy} \Rightarrow DyDp = PyDf \Rightarrow Dy = \frac{PyDf}{Dp}$$

$$Tan\alpha = \frac{O}{A} = \frac{XL}{Dy} = \frac{Df(1-Cos\theta)}{L} \Rightarrow \frac{XL}{\left(\frac{PyDf}{Dp}\right)} = \frac{Df(1-Cos\theta)}{L} \Rightarrow \frac{XLDp}{PyDf} = \frac{Df(1-Cos\theta)}{L}$$

$$\Rightarrow XL = \frac{PyDf^2(1-Cos\theta)}{LDp}$$

Therefore the horizontal component of the force acting on the link beam when the cantilever is rotated through θ is

$$F_H = \frac{Ebd^3\left(\frac{PyDf^2(1-Cos\theta)}{LDp}\right)}{6L^2} \qquad \textbf{(20)}$$

$$Tan\alpha = \frac{F_H}{F_V} \Rightarrow F_V = \frac{F_H}{Tan\alpha}$$

$$F_V = \frac{F_H}{\left(\frac{Df(1-Cos\theta)}{L}\right)} = \frac{F_H L}{Df(1-Cos\theta)} = \frac{\left(\frac{Ebd^3 PyDf^2(1-Cos\theta)}{6L^3 Dp}\right)L}{Df(1-Cos\theta)}$$

$$F_V = \frac{LEbd^3 PyDf^2(1-Cos\theta)}{6L^3 DpDf(1-Cos\theta)}$$

Therefore the vertical component of the force acting on the link beam when the cantilever is rotated through θ is

$$F_V = \frac{Ebd^3 PyDf}{6L^2 Dp} \qquad \textbf{(21)}$$

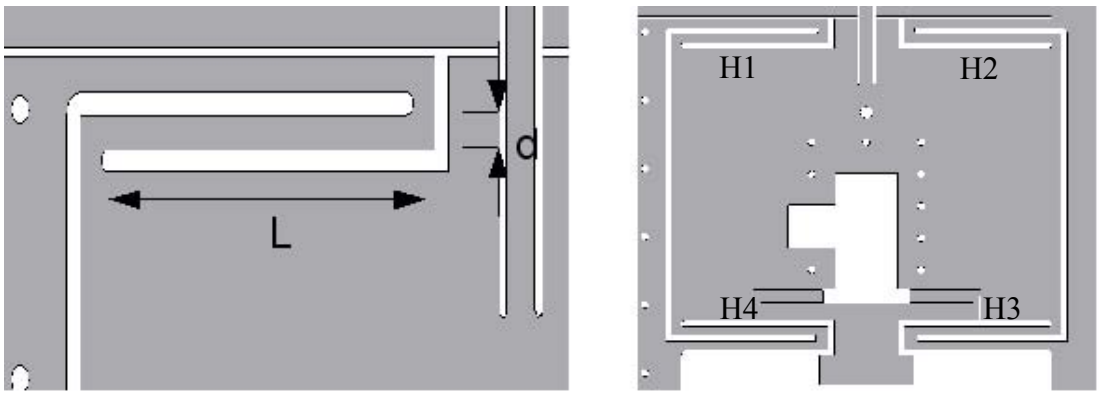

(a) **Figure 54 Compound Flexure** (b)

3.2.4.2 Compound Flexure

The second type of flexure is a linear compound flexure hinge; the objective of the flexure is to eliminate the displacement offset in the *x*-direction caused by the rotation about point *A* (Figure 44). As shown in Figure 54 (b), the compound flexure consists of four separate flexure hinges H1, H2, H3 and H4; each of these flexure hinges consists of two bracketed cantilevers in series [9].

3.2.4.2.1 Effective Stiffness of the Compound Flexure

The end deflection Δd of a single cantilever hinge, is given by [3]

$$\Delta d = \frac{FL^3}{12EI} \quad \textbf{(22)}$$

Where (F) is the force applied to a rectangular beam of plate thickness (b), thickness of hinge (d) and length (L)

Therefore the stiffness of a single cantilever is K is F/Δd

$$K = \frac{F}{\Delta d} = \frac{F}{\left(\frac{FL^3}{12EI}\right)} \Rightarrow \frac{F}{1} \times \frac{12EI}{FL^3}$$

$$K = \frac{12EI}{L^3} \Rightarrow \frac{Ebd^3}{L^3} \textbf{ (Since moment of area I = bd}^3\textbf{/12)} \quad \textbf{(23)}$$

Since the cantilevers are in series, the effective stiffness of a single flexure H1, H2, H3 or H4 is $\frac{1}{K_{H1,H2,H3,H4}} = \frac{1}{K_1} + \frac{1}{K_2}$

$$\frac{1}{K_{H1,H2,H3,H4}} = \frac{1}{\left(\frac{Ebd^3}{L^3}\right)} + \frac{1}{\left(\frac{Ebd^3}{L^3}\right)} = \frac{2}{\left(\frac{Ebd^3}{L^3}\right)}$$

$$K_{H1,H2,H3,H4} = \frac{\left(\frac{Ebd^3}{L^3}\right)}{2} = \frac{1}{2}\left(\frac{Ebd^3}{L^3}\right) \quad \textbf{(24)}$$

The linear compound flexure consists of four of these hinges in parallel; the effective stiffness of compound flexure is

$$K_{compound} = K_{H1} + K_{H2} + K_{H3} + K_{H4}$$

$$K_{compound} = \frac{1}{2}\left(\frac{Ebd^3}{L^3}\right) + \frac{1}{2}\left(\frac{Ebd^3}{L^3}\right) + \frac{1}{2}\left(\frac{Ebd^3}{L^3}\right) + \frac{1}{2}\left(\frac{Ebd^3}{L^3}\right) = \frac{4}{2}\left(\frac{Ebd^3}{L^3}\right)$$

$$\Rightarrow K_{compound} = \frac{2Ebd^3}{L^3} \quad \textbf{(25)}$$

As shown in Figure 55 varying *d,* and *L* will have the greatest impact on stiffness of the flexure hinge. In relation to Equation (22), the flexural hinge force F represents the force applied to a single cantilever hinge. The total force applied to the linear compound flexure hinge from the piezo actuator is 4F.

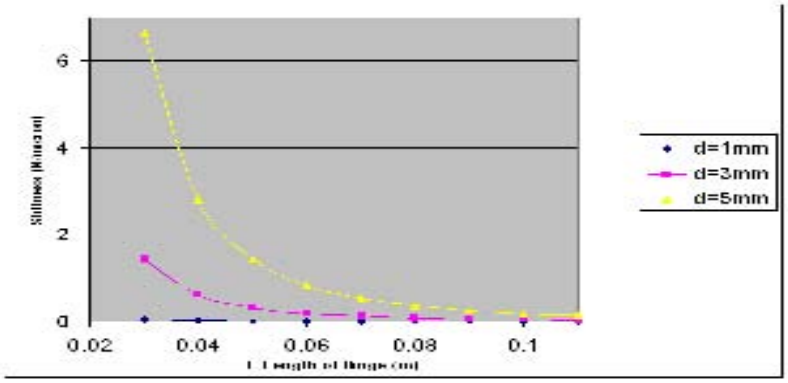

Figure 55 Stiffness versus hinge length, for different hinge length and width

The stage is 20mm thick; hinges are 3mm thick and 47mm long and using a Young's modulus of 72 GPa the linear stiffness of the linear compound flexure is calculated using Equation (25)

$$K_{compound} = \frac{(2)(72\times10^9)(.02)(.003^3)}{.047^3} = 748966.99N/m = 0.748966N/\mu m$$

3.2.4.2.2 The Max Acceptable Displacement of the Flexure Hinges

The range of motion of the stage will be restricted either by the stiffness of the flexural hinges through maximum force applied to the hinges, or the necessity not to exceed its elastic properties of the material. The max acceptable displacement is given by

$$\Delta d_{\max} = \frac{\sigma_{\max} l^2}{3Ed} \qquad \textbf{(26)}$$

Where (σmax) is the max allowable bending tensile strength [3]. From this equation, if the range of motion is specified and (L), (d), and (E) are known, the design can be checked for the stresses not to exceed the maximum allowable stress to insure linear elastic deflection of the hinges.

Therefore applying Equation (26) with a max allowable bending tensile strength of 101Mpa (20% of yield strength); the max acceptable displacement of the flexure hinges is calculated as

$$\Delta d_{\max} = \frac{(101\times10^6)(0.047^2)}{3(72\times10^9)(0.003)}$$

$$\Delta d_{\max} = 344.3\mu m$$

3.2.4.3 Combined System

In this section, resonance frequencies, necessary pre-load piezo accommodating gap sizes, stroke lengths and stress levels are calculated for the combined cantilever and linear compound flexure. Firstly an expression had to be derived for the linear stiffness of the combined system.

3.2.4.3.1 Linear Stiffness of the Combined System

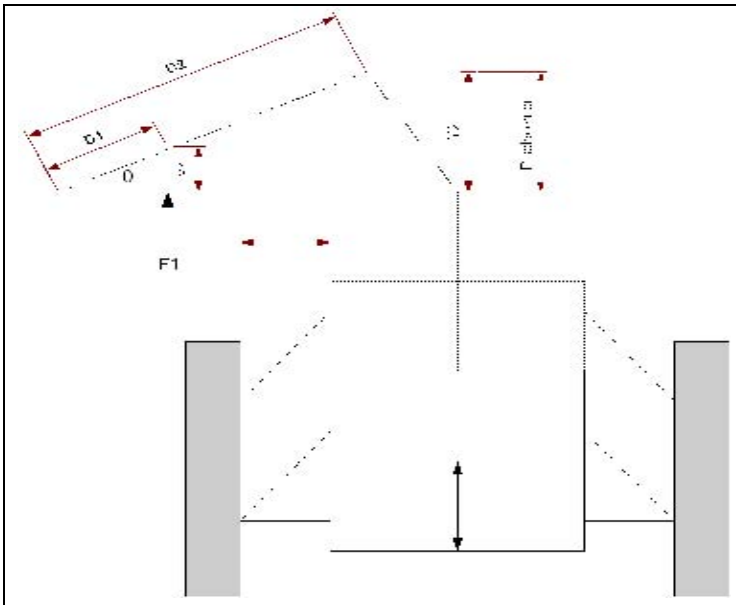

Figure 56 Combined System

K_1 = Linear stiffness of cantilever hinge at the point where the piezo exerts force on the system

$$Y_1 = D_2 Sin\theta$$

Substituting

$$Y_1 = \frac{D_2 9\pi\sqrt{r}M}{2Ebt^{2.5}} \Rightarrow \frac{D_2 9\pi\sqrt{r}F_1 D_1}{2Ebt^{2.5}} \text{ (Since M= } F_1D_1\text{)}$$

$$K_1 = \frac{F_1}{Y_1} = \frac{F_1}{\frac{D_2 9\pi\sqrt{r}F_1 D_1}{2Ebt^{2.5}}}$$

$$\Rightarrow K_1 = \frac{2Ebt^{2.5}}{9\pi\sqrt{r}D_1^{\,2}}$$

K_2 = Linear stiffness of guiding flexure

$$K_2 = \frac{2Ebd^3}{L^3}$$

The same equation as used by Wemyss et al. [9] was used to derive an expression for the rotation of the cantilever

$$\theta rad = \frac{9\pi\sqrt{r}F_1D_1}{2Ebt^{2.5}} - \frac{9\pi\sqrt{r}F_2D_2}{2Ebt^{2.5}}$$

$$\theta rad = \frac{9\pi\sqrt{r}}{2Ebt^{2.5}}\left(F_1D_1 - F_2D_2\right)$$

$F_1=Y_1K_1$

$F_2=Y_2K_2$

$$\frac{D_1}{D_2} = \frac{Y_1}{Y_2} \Rightarrow Y_2 = \frac{Y_1D_2}{D_1}$$

Since Sinθ° ≈ θradians (θ small)

$$Sin\theta = \frac{Y_1}{D_1} = \frac{9\pi\sqrt{r}}{2Ebt^{2.5}}\left(Y_1K_1D_1 - Y_2K_2D_2\right) = \frac{9\pi\sqrt{r}}{2Ebt^{2.5}}\left(Y_1K_1D_1 - K_2\frac{D_2}{D_1}Y_1D_2\right)$$

$$Y_1 = \frac{9\pi\sqrt{r}D_1}{2Ebt^{2.5}}\left(Y_1K_1D_1 - K_2\frac{D_2}{D_1}Y_1D_2\right)$$

$$K_{eff} = \frac{F_1}{Y_1}$$

$$K_{eff} = \frac{F_1}{\frac{9\pi\sqrt{r}D_1}{2Ebt^{2.5}}\left(Y_1K_1D_1 - K_2\frac{D_2}{D_1}Y_1D_2\right)}$$

$$K_{eff} = \frac{2Ebt^{2.5}F_1}{9\pi\sqrt{r}D_1\left(Y_1K_1D_1 - K_2\frac{D_2}{D_1}Y_1D_2\right)}$$

$$K_{eff} = \frac{2Ebt^{2.5}Y_1K_1}{9\pi\sqrt{r}D_1\left(Y_1K_1D_1 - K_2\frac{D_2}{D_1}Y_1D_2\right)}$$

$$K_{eff} = \frac{2Ebt^{2.5}Y_1\left(\frac{2Ebt^{2.5}}{9\pi\sqrt{r}D_1^{\,2}}\right)}{9\pi\sqrt{r}D_1\left(\left(\frac{2Ebt^{2.5}}{9\pi\sqrt{r}D_1^{\,2}}\right)Y_1D_1 - \left(\frac{2Ebd^3}{L^3}\right)\frac{D_2}{D_1}Y_1D_2\right)}$$

Take out Y_1

$$K_{eff} = \frac{2Ebt^{2.5}Y_1\left(\frac{2Ebt^{2.5}}{9\pi\sqrt{r}D_1^{\,2}}\right)}{9\pi\sqrt{r}D_1Y_1\left(\left(\frac{2Ebt^{2.5}}{9\pi\sqrt{r}D_1}\right) - \left(\frac{2Ebd^3}{L^3}\right)\frac{D_2}{D_1}D_2\right)}$$

Take out 2Eb and Y_1 cancel

$$K_{eff} = \frac{2Ebt^{2.5}\left(\frac{2Ebt^{2.5}}{9\pi\sqrt{r}D_1^{\,2}}\right)}{9\pi\sqrt{r}D_1 2Eb\left(\left(\frac{t^{2.5}}{9\pi\sqrt{r}D_1}\right) - \left(\frac{d^3}{L^3}\right)\frac{D_2^{\,2}}{D_1}\right)}$$

2Eb cancels

$$K_{eff} = \frac{\left(\frac{2Ebt^{5}}{9\pi\sqrt{r}D_1^{\,2}}\right)}{9\pi\sqrt{r}D_1\left(\left(\frac{t^{2.5}}{9\pi\sqrt{r}D_1}\right) - \left(\frac{d^3}{L^3}\right)\frac{D_2^{\,2}}{D_1}\right)}$$

Take out $1/D_1$

$$K_{eff} = \frac{\left(\frac{2Ebt^{5}}{9\pi\sqrt{r}D_1^{\,2}}\right)}{\frac{9\pi\sqrt{r}D_1}{D_1}\left(\left(\frac{t^{2.5}}{9\pi\sqrt{r}}\right) - \left(\frac{d^3}{L^3}\right)D_2^{\,2}\right)}$$

$$K_{eff} = \frac{\left(\frac{2Ebt^5}{9\pi\sqrt{r}D_1^{\,2}}\right)}{9\pi\sqrt{r}\left(\left(\frac{t^{2.5}}{9\pi\sqrt{r}}\right)-\left(\frac{d^3}{L^3}\right)D_2^{\,2}\right)}$$

$$K_{eff} = \left(\frac{2Ebt^5}{9\pi\sqrt{r}D_1^{\,2}}\right)\times\frac{1}{9\pi\sqrt{r}\left(\left(\frac{t^{2.5}}{9\pi\sqrt{r}}\right)-\left(\frac{d^3}{L^3}\right)D_2^{\,2}\right)}$$

Finally

$$\Rightarrow K_{eff} == \frac{2Ebt^5}{\left(9\pi\sqrt{r}D_1\right)^2\left(\left(\frac{t^{2.5}}{9\pi\sqrt{r}}\right)-\left(\frac{d^3}{L^3}\right)D_2^{\,2}\right)} \qquad \textbf{(27)}$$

The effective stiffness of 5.524861 N/µm as predicted using the derived expression for the design would give an 18.1µm deflection for a force of 100N along the axis of force application. As illustrated in Figure 61, FEA simulation predicts this deflection to be 18.178µm

3.2.4.3.2 Resonant Frequency of the Combined System

The same free vibration equations as used by Elmustafa [1] were used to calculate the resonant frequency of the design. For free vibration of a simple beam the natural frequency is given by

$$f = \left(\frac{1}{2\pi}\right)\left(\sqrt{\frac{k}{m}}\right) \qquad \textbf{(28)}$$

(f) is the natural frequency, (k) is the stiffness and (m) is the mass of the beam.

First of all, the mass of the system must be calculated

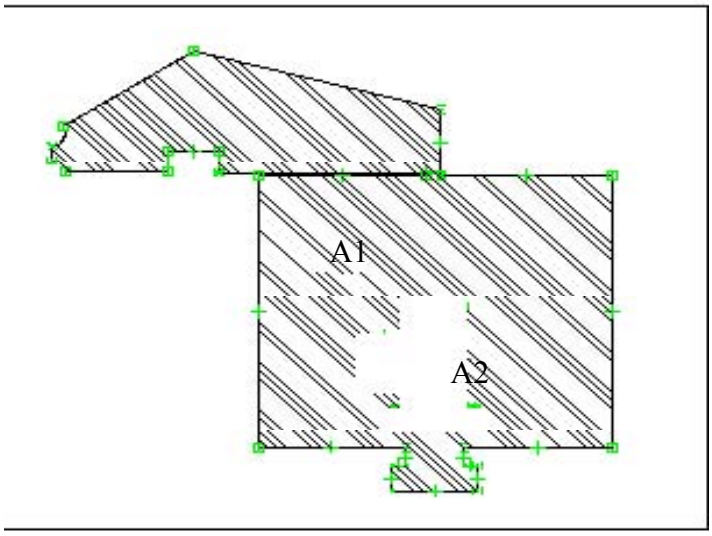

Figure 57 Effective are of Flexure

Area 1(A1) = 0.01861208 m^2

Area 2(A2) = 0.00186120 m^2

From Figure 57, the total area of the flexure (A_f) is

A_f = A1-A2 = 0.01861208 – 0.00186120 = 0.016750 m^2

Volume of flexure (V_f) = (0.016750 m^2) (0.02 m) = 33.501x10^{-5} m^3

The density of Aluminium 7075 is given as 2810 kg/m^3, therefore the mass of the flexure M_f is

M_f = (33.501x10^{-5} m^3) (2810 kg/m^3) = 0.94139 kg

Therefore natural frequency of the flexure f_f is calculated as

$$f_f = \left(\frac{1}{2\pi}\right)\left(\sqrt{\frac{5524861}{0.94139}}\right)$$

$$f_f = 385.43Hz$$

3.2.4.3.3 Primary Piezoelectric Actuator

The primary piezo actuator that is used to drive the stage through long-travel positioning is a P-841.60, closed loop LVPZT translator with a max nominal displacement of 90μm.

A piezo actuator can reach its nominal displacement in approximately 1/3 of the period of the resonant frequency of the piezo translator and therefore the minimum rise time of the P-841.60 piezo actuator is

$$T_{\min} \approx \frac{1}{3f_0} = \frac{1}{3(6000)} \approx 55.5\mu\sec \qquad \textbf{(29)}$$

The max force that this piezo actuator can generate in an infinitely rigid constraint is

$$F_{\max} = K_t \Delta L_o = (10000000)(90 \times 10^{-6}) \qquad \textbf{(30)}$$
$$F_{\max} = 900N$$

Where (ΔL_o) is the max nominal displacement without an external force or restraint and (K_T) is the piezo actuator stiffness. In this design the piezo actuator is not constrained in an infinitely rigid constraint; it is acting against a spring. Thus, the max effective force the piezo can generate against the yielding constraint (spring) is

$$F_{\max eff} = K_t \Delta L_o \left(1 - \frac{K_t}{K_t + K_s}\right) \qquad \textbf{(31)}$$
$$F_{\max eff} = (10000000)(90 \times 10^{-6})\left(1 - \frac{10000000}{10000000 + 5524861}\right) = 320.3N$$

Where (K_s) is the effective linear stiffness of the system [4]

As shown in Figure 58, for a piezo actuator operation against an elastic load, part of the displacement generated by the piezo effect is lost due to the elasticity of the piezo element [4]. The maximum displacement of a piezo actuator acting against a spring load (ΔL) is given by Equation (32):

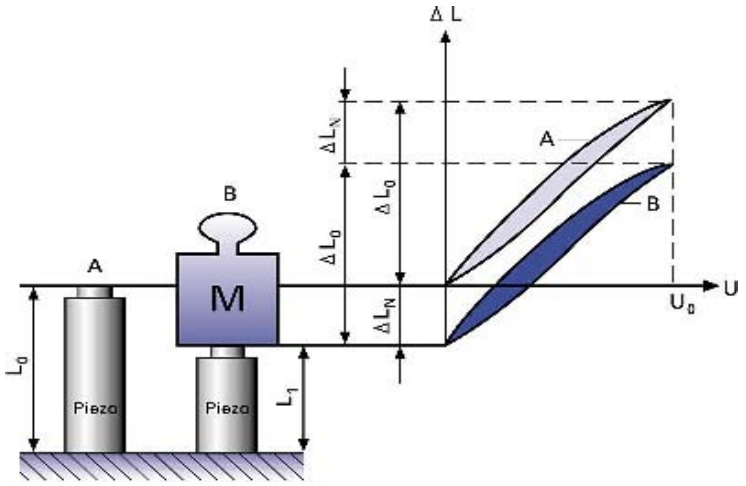

Figure 58 Effective displacement of a piezo actuator acting against a spring load [4]

$$\Delta L = \Delta L_o \left(\frac{K_t}{K_t + K_s} \right)$$
$$\Delta L = (90 \times 10^{-6}) \left(\frac{10000000}{10000000 + 5524861} \right) = 57.97 \mu m \quad \textbf{(32)}$$

The load on the flexure system due to maximum piezo expansion (F_L) is the product of effective flexure stiffness and the maximum displacement of the piezo actuator

$$F_L = K_s \Delta L = (5524861)(57.97 \times 10^{-6}) = 320.276N \quad \textbf{(33)}$$

A preload must be applied so that the piezo actuator does not break contact with the stage at resonance and it must be greater than the maximum dynamic force generated due to resonance. The amplitude of the dynamic load (F_d) due to the resonant frequency of the guiding unit is given by Equation (34)

$$F_d = ma = m.4.\pi^2 f_f{}^2 A$$
$$F_d = (0.94139)4\pi^2 (385.43^2) \left(\frac{57.97 \times 10^{-6}}{2} \right) = 159.9N \quad \textbf{(34)}$$

Where (m) is the effective mass and (A) is the amplitude. The amplitude is taken to be half the maximum stroke length (ΔL). Using a factor of safety of two the piezo stack preload (F_p) is set to 319.8 N. The preload is provided by displacing the flexures to accommodate the piezo stack and shim, which must have a combined length greater than the available space with undeformed flexures.

Based on the desired preload and flexure stiffness, the required flexure displacement (X_f) is:

$$X_f = \frac{F_p}{K_s} = 57.8\mu m \quad \textbf{(35)} \; [2]$$

The thickness of the shim is machined accordingly; this is only a minimum value and it is not necessary to machine the shim to this accuracy. So long as the pre-load is not so great as to effect stroke length, then a thicker shim can be used. The resultant maximum load (F_r) on the flexure system is a combination of the load on the flexure system due to maximum piezo expansion and the preload.

$$F_R = F_L + F_p = 640N \qquad \textbf{(36)}$$

3.2.4.4 Touch Sensor

In-built into the primary stage is a secondary flexural-hinge guided stage, the secondary stage acts as a touch sensor to detect contact between the measurement stage and the product. The touch sensor uses the change in strain of the piezo actuator to detect when contact is made with product. The strain of the piezo stack is given as

$$\varepsilon = \frac{l - lo}{lo} \qquad \textbf{(37)}$$

(ε) is the strain in the measured direction, (l) is the original length and (lo) is the current length of the piezo stack. When contact is made with the product, this causes a reduction in length (compression) of the piezo stack and therefore a negative value for strain; it is this change in strain that is used to detect contact.

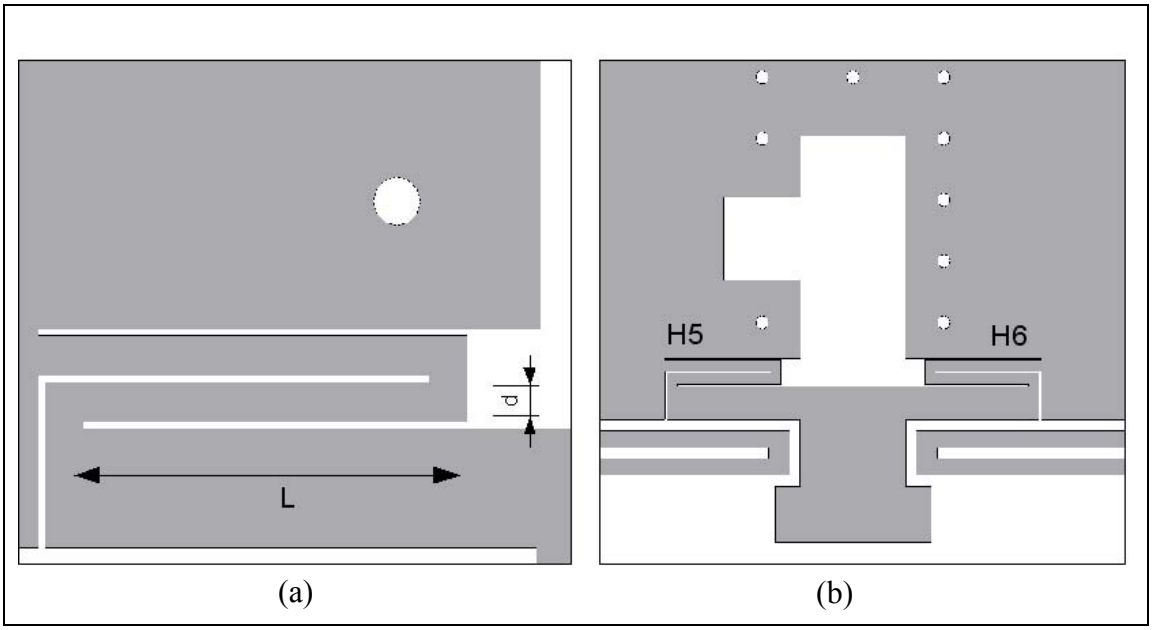

Figure 59 Touch Sensor Flexure

3.2.4.4.1 Linear Stiffness of the Touch Sensor Flexure

The flexure used for the touch sensor consists of two flexure hinges H5 and H6 and again each of these flexure hinges consists of two bracketed cantilevers in series. As previously stated, the stiffness of a single cantilever is given by Equation (23):

$$K = \frac{Ebd^3}{L^3}$$

Since the cantilevers are in series, the effective stiffness of a single flexure H5 or H6 is $\frac{1}{K_{H5,H6}} = \frac{1}{K_1} + \frac{1}{K_2}$

$$\frac{1}{K_{H5,H6}} = \frac{1}{\left(\frac{Ebd^3}{L^3}\right)} + \frac{1}{\left(\frac{Ebd^3}{L^3}\right)} = \frac{2}{\left(\frac{Ebd^3}{L^3}\right)}$$

$$K_{H5,H6} = \frac{1}{2}\left(\frac{Ebd^3}{L^3}\right) \quad \textbf{(38)}$$

The touch sensor flexure consists of two of these hinges in parallel; the effective stiffness of the touch sensor flexure is

$$K_{touch} = K_{H5} + K_{H6} = \frac{1}{2}\left(\frac{Ebd^3}{L^3}\right) + \frac{1}{2}\left(\frac{Ebd^3}{L^3}\right) = \frac{2}{2}\left(\frac{Ebd^3}{L^3}\right)$$

$$\Rightarrow K_{touch} = \frac{Ebd^3}{L^3} \quad \textbf{(39)}$$

The stage is 20mm thick, hinges are 2mm thick and 20mm long and using a Young's modulus of 72 GPa the linear stiffness of the touch sensor flexure is calculated as

$$K_{touch} = \frac{(72\times10^9)(0.02)(0.002^3)}{(0.02^3)} = 1440000N/m = 1.44N/\mu m$$

3.2.4.4.2 The Max Acceptable Displacement of the Touch Sensor Flexures

Applying Equation (26) with a max allowable bending tensile strength of 101Mpa (20% of yield strength); the max acceptable displacement of H5 or H6 is calculated as

$$\Delta d_{\max} = \frac{(101\times10^6)(0.02^2)}{3(72\times10^9)(.002)}$$

$$\Delta d_{\max} = 93.6\mu m$$

This is well above the max displacement of 15μm that can be created by the piezo actuator that is used as the touch sensor.

3.2.4.4.3 Resonant Frequency of the Touch Sensor Flexure

The mass of the touch sensor flexure is calculated as

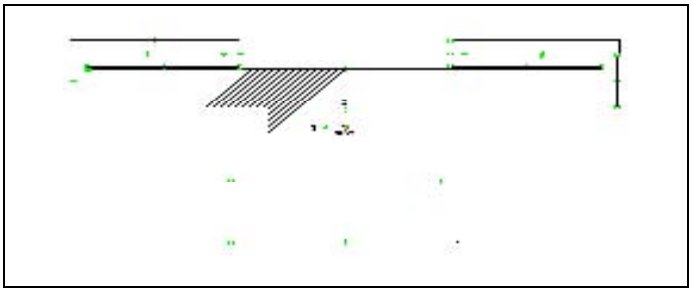

Figure 60Touch Sensor Area

The total area of the touch sensor flexure (A_{ts})= 0.00115559 m^2

Volume of flexure (V_{ts}) = (0.00115559 m^2) (0.02 m) = 2.311x10^{-5} m^3

Once more, using a density of 2810 kg/m^3 the mass of the flexure M_f is

M_f = (2.311x10^{-5} m^3) (2810 kg/m^3) = 0.064944 kg

Therefore using Equation (28), the natural frequency of the touch sensor flexure (f_{ts}) is calculated as

$$f_{ts} = \left(\frac{1}{2\pi}\right)\left(\sqrt{\frac{1440000}{0.064944}}\right)$$

$$f_{ts} = 749.4Hz$$

3.2.4.4.4 Touch Sensor Piezoelectric Actuator

The secondary piezo actuator that acts as a touch sensor is a P-841.10, closed loop LVPZT translator with a max nominal displacement of 15µm.

Applying the same equations as described in the previous section for the long travel piezo, the minimum rise time (T_{min}), max force that the piezo actuator can generate in an infinitely rigid constraint (F_{max}), the max effective force the piezo can generate against the yielding constraint ($F_{max\,eff}$), the maximum displacement of a piezo actuator acting against a spring load (ΔL), the load on the flexure system due to maximum piezo expansion (F_L), the amplitude of the dynamic load (F_d), preload (Fp), the required flexure displacement (shim thickness) (X_f) and the resultant maximum load (F_r) on the flexure system are calculated as below for the short travel touch sensor piezo.

T_{min} = 18.5µsec

F_{max} = 855N

F_{maxeff} = 20.52N

ΔL = 14.64µm

F_L = 21.0816N

F_d = 10.53N

F_p = 21N

X_p=14.5µm

F_r = 42.08N

The most distinct change between Prototype 1 and the Production instrument is that the production instrument consists of a primary flexural-hinge guided stage driven by a piezoelectric actuator and in-built into the primary stage is a secondary flexural-hinge guided stage, which again is driven by a piezoelectric actuator. The primary piezo actuator is used to drive the stage through long-travel positioning and the secondary acts as a touch sensor to detect contact between the measurement stage and the product. Unlike Prototype1 a continuous sinusoidal voltage is not applied to the touch sensor piezo actuator; instead of sinusoidal feedback wave, the feedback from the touch sensor piezo within the production measurement instrument is a constant amplitude signal.

Also, a limitation with Prototype 1 was that as the measurement tip extends, the cantilever rotates about the hinge point. Consequently, varying sample ball diameters touch the measurement tip at different points, introducing errors not just due to surface roughness but also due to the changing angle of the upper contact surface. With the production measurement instrument, the transmission of this offset to the measurement point is largely eliminated by flexure H and by four leaf flexures B, C, D and E. Therefore the amplified displacement at the measurement point will be linear and in the y-direction only.

Having defined the values of the relevant parameters of the stage, it is now necessary to model the system to ensure that the values fit within the required limits. This will be achieved using an FEA package, which will be discussed in the next section.

3.2.5 Finite Element Analysis

A full description of FEA is outside the scope of this project but can be found in [54]. Throughout this project ANSYS FEA software has been used to create and analyse finite element models to define whether the design is suitable; this software is a comprehensive general finite element computer program that is capable of performing static, dynamic, heat transfer, fluid flow and electromagnetism analysis.

Within the ANSYS program, there are three processors that are used most frequently: the preprocessor, the solution processor and the general postprocessor. The preprocessor contains the commands needed to build a model:

- Define element types and options
- Define element real constants
- Define material properties
- Create model geometry
- Define meshing controls
- Mesh the object created

The solution processor has the commands that apply boundary conditions and loads. For example, for structural problems displacement boundary conditions and forces can be defined. Once all the information is made available to the solution processor, it solves for the nodal solutions.

The general postprocessor contains the commands that list and display results of an analysis:

- Read results data from results file
- Read element results data
- Plot results
- List results

Simulations of forces, resonant frequency and stresses were performed using ANSYS to verify the analytical design stage. Three types of analysis were performed: static analysis, modal analysis and thermal analysis. To simplify the analysis, the design was modelled as a 2D problem. ANSYS provides more than one hundred various elements to be used to analyse different problems; selecting the correct element type is a

very important part of the analysis process. 2D solid elements all have the category name PLANE. The standard PLANE42 element is a four-node quadrilateral element used to model structural solid problems; the element is defined by four nodes having two degrees of freedom at each node, i.e. translation in the X and Y-directions. The element type used to analyse the flexure measurement instrument is PLANE82; this is an eight-node (four corner points and four midside nodes) quadrilateral element. It is a higher order version of the two-dimensional, four-node quadrilateral element type. Therefore, PLANE82 offers more accuracy when modelling problems with curved boundaries, such as flexure hinges [54]. As the overall dimensions of the design are extremely large compared to the dimensions of the hinges, the meshes near the hinges need to be very fine in order to illustrate the deformation, stresses and modal frequency with sufficient accuracy.

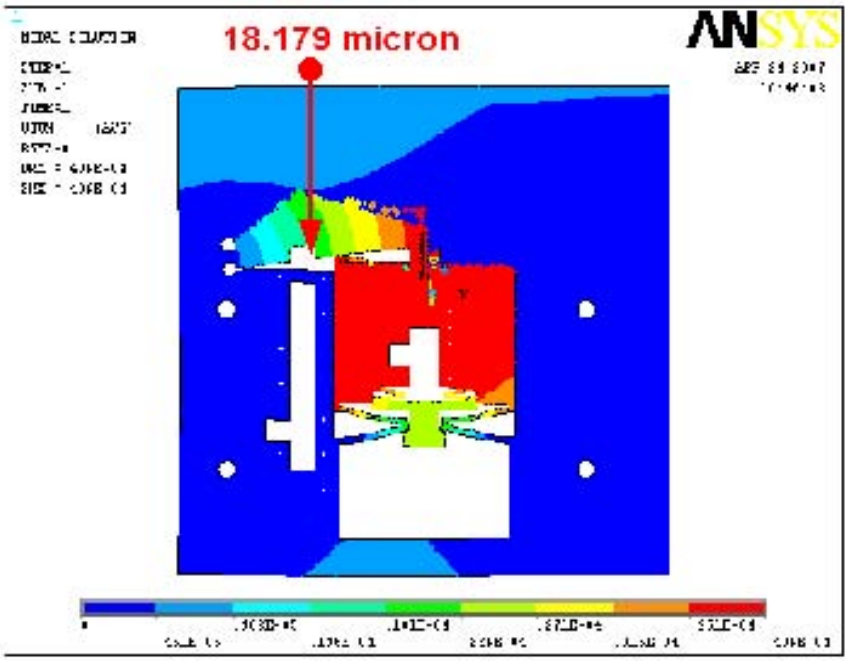

Figure 61 Displacement of Flexure Stage form an Input Force of 100N

To determine the stiffness of the measurement stage, an arbitrary vertical input force (100N) was applied to the flexure stage. The obtained vertical movement along the axis of force application is 18.178μm; therefore the stiffness can be calculated as 5.50N/μm. The corresponding differences between the analytical estimation of (5.52 N/μm) and the FEA simulation are in the range of 0.43%; therefore, the FEA model is satisfactory in terms of verifying the estimations obtained from the analytical design phase.

To avoid introducing plastic deformation into the design, the stress must be monitored. A displacement of 90μm was applied to the model. This is the maximum possible stroke of the piezo actuator and will introduce the highest stress into the design. As can be seen from Figure 62, the max stress introduced is 39.5MPa: this is well below the yield point of 505MPa and the fatigue strength of 160Mpa for Aluminium 7075.

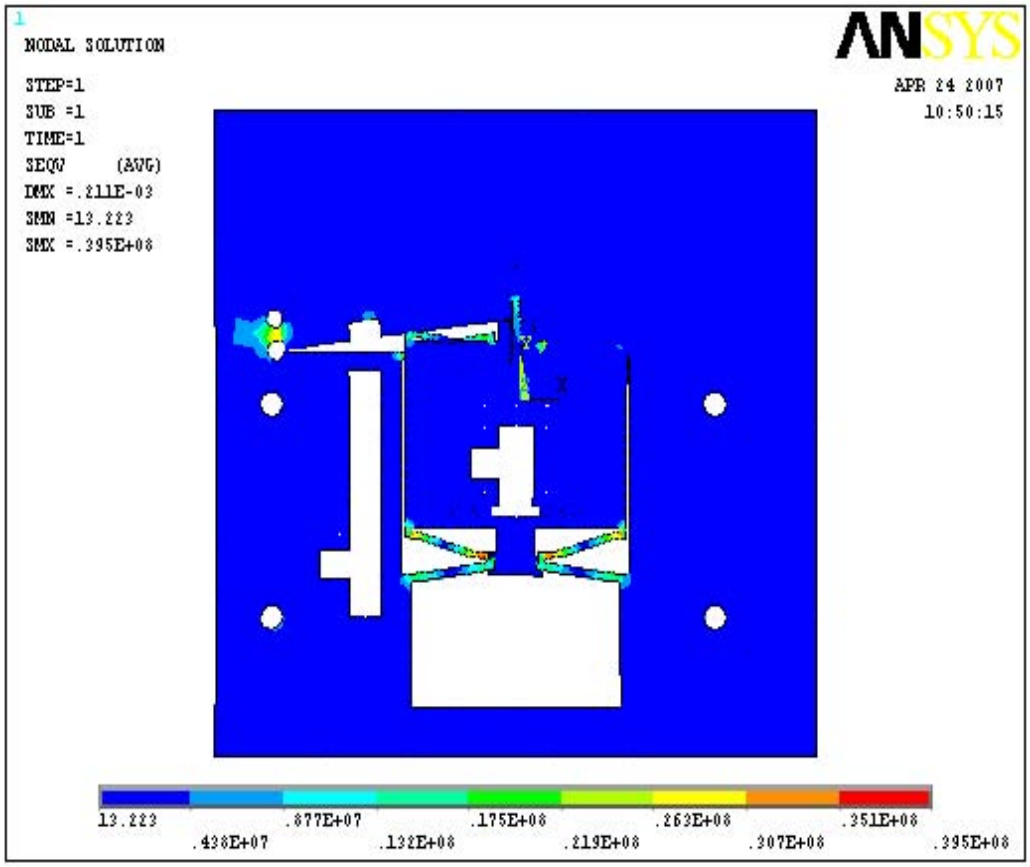

Figure 62 Stress of Flexure Stage caused by Maximum Stroke of Piezo Actuator

As shown in Figure 63, the max stroke of the piezo actuator causes a max flexure displacement of 211μm: this is less than that the 344.3μm max displacement tolerable in the flexure material as established from Equation (26); therefore the measurement stage will operate well within the limits set by the choice of material. In addition, the actual movement of the measurement tip in the y-direction due to the max possible piezo stroke is 211μm: this is well above the 150μm range required for the system.

The resulting displacement offset in the *x*-direction caused by the rotation about the notch hinge is reduced to 1.14μm as shown in Figure 64. This gives 0.54% offset

over the entire measurement range and therefore a significant amount of cantilever rotation is eliminated.

Figure 63 Y-Direction Flexure Displacement caused by Maximum Stroke of Piezo Actuator

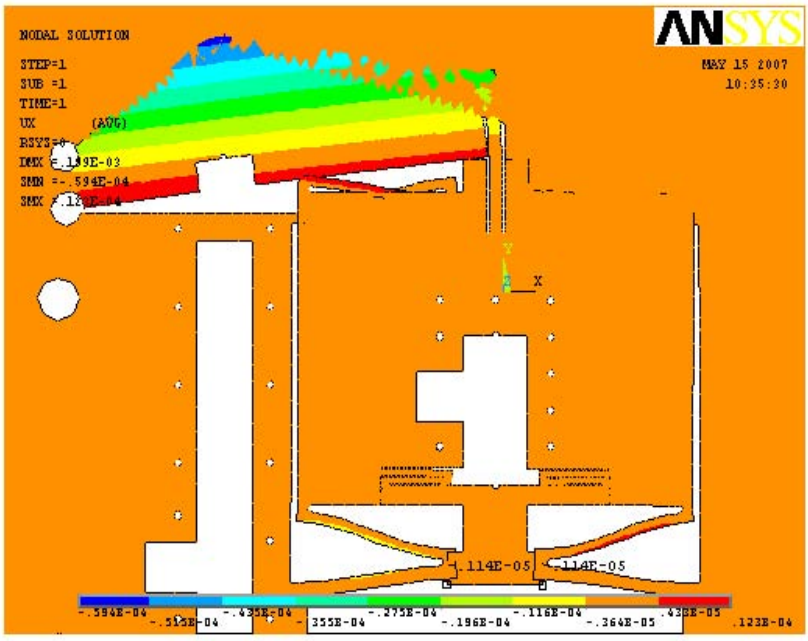

Figure 64 X-Direction Flexure Displacement caused by Minimum Stroke of Piezo Actuator

The deformation of the stage due to a 1° rise in temperature is shown in Figure 65. The key points of interest are those where the long-range piezo actuator is mounted, as temperature driven expansion/contraction here will affect the metrology system. As can be seen the expansion along the axis of the long-range piezo actuator is up to 4μm. Although, to some extent this expansion is counteracted by the expansion of the measurement tip and the ball locator, the level of expansion compared to the targeted measurement resolution required is large. It is hoped that environmental fluctuations of temperature as well as noise radiation (caused by the vibrational excitation of mechanical devices) and electrical noise will be monitored using purpose built Labview VI's and corrections for these fluctuations will be built into the system in the future.

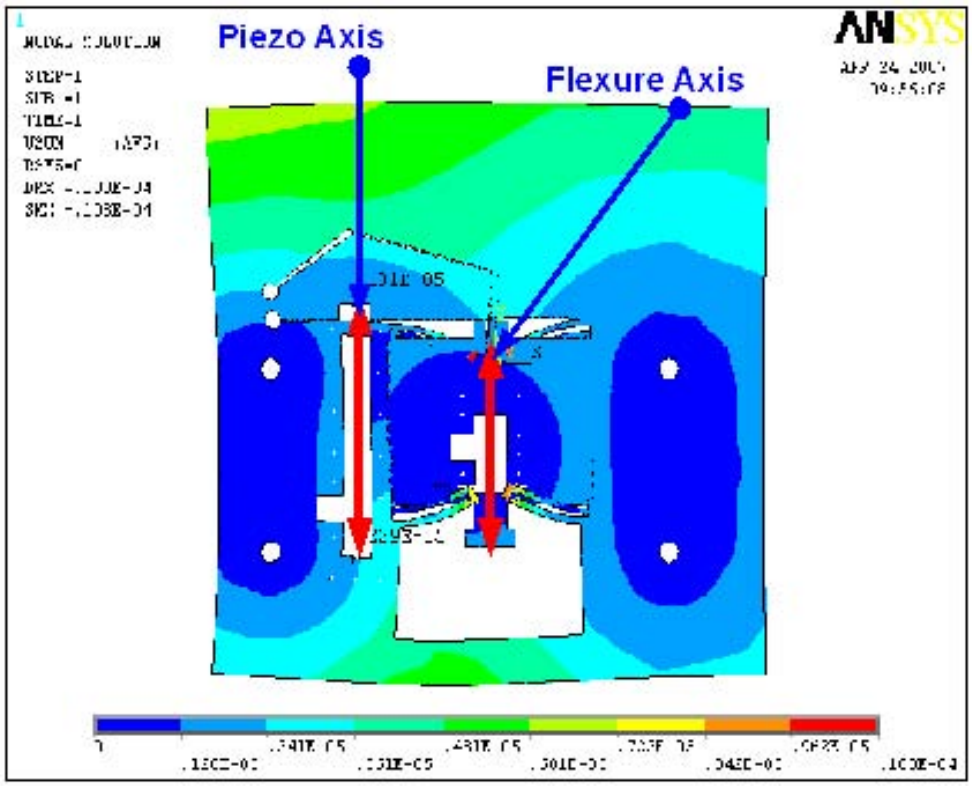

Figure 65 Deformation of Flexure due to 1° Temperature Change

Five modal frequencies were calculated. These calculations represent modal analysis of the stage excluding the effect of the piezo actuators. The modal analysis in ANSYS produced a result of 390.15 Hz and 729.87 Hz for the primary flexure stage and secondary touch sensor flexure stage: this is consistent with the 385.43Hz and 738.6 Hz found using the analytical approach.

3.3 Ball Location

The measurement of a sample ball takes place when the ball, which is sitting on the bottom-measurement surface, is contacted by the top-measuring surface. The distance travelled by the top measurement surface before contact is made, determines the diameter of the ball. As the measuring surfaces can never be produced with a perfect finish and without errors of form, the distant the top measuring surface moves before contact is made with the same sample ball located at different points along the bottom measurement surface will vary (as demonstrated in Figure 66). Therefore each individual measurement of the same sample ball will be different. Consequently if a reference ball and sample ball lie on different points on the measurement surface; then this will introduce an error into the measurement and will affect the accuracy (bias) and precision (repeatability) of the sample measurement. To eliminate or at least minimise this error the sample balls are required to be located closest to the same point as the reference balls and the surface finish of the two measuring surfaces must be of high quality

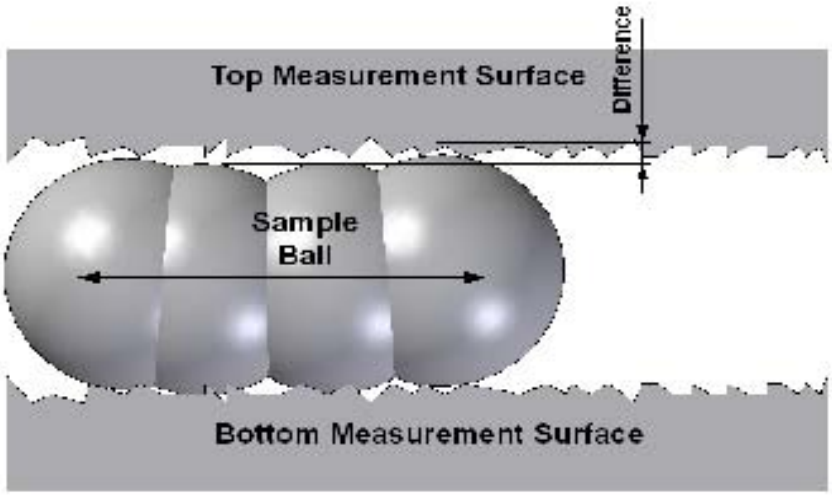

Figure 66 Surface Roughness

Figure 67 shows a single degree of freedom constraint; assuming that there is no friction at the interface, the number of degrees of freedom can be deduced from the Cartesian coordinates. The ball can rotate about all of the three axes α, β and γ. The ball can also slide in the X and Y axes; therefore motion is only restricted in the vertical direction, Z.

Ideally, to eliminate the location error between the reference and the sample balls, they should be constrained on the X, Y and Z axes. For that reason, numerous different methods for constraining the measurement ball were considered; these consisted of two-degree of freedom constraints such as V-grooves on the Y-axis or in the Z-axis. Also examined were a 3-locating sphere arrangement, a trihedral hole and a drilled conical hole which are all three degrees of freedom constraints. A three-degree of freedom constraint seemed very attractive, but the measurement unit is required to function automatically and placing or removing a measurement ball from these constraints would prove to be very difficult: it would be necessary for the measurement ball to sit into them, hence a substantial amount of movement (0.5-3mm) along the Z-axis is required to place or remove a ball. During the measurement cycle the maximum distance between the measurement ball and the top measurement surface in the Z-axis is 170µm, thus a constraint where the measurement ball sits into the constraint is unsuitable.

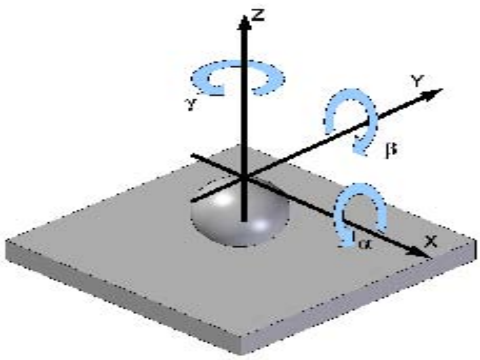

Figure 67 Single Degree of Freedom Constraint

To allow for ease of automatic insertion and ejection, it was decided that balls would have to be free to slide or roll in the Y-axis. A two-degree of freedom constraint ball locator was designed to constrain the ball in the Z and X axes. The ball locator consists of two spheres embedded in a mounting plate, which locate the test ball during the measurement process, Figure 68. This arrangement ensures that the centres of test balls are located identically relative to the measuring surface along the X-axis. However, as the diameter of the ball changes, the seating of the ball on the Y-axis varies also. A mathematical

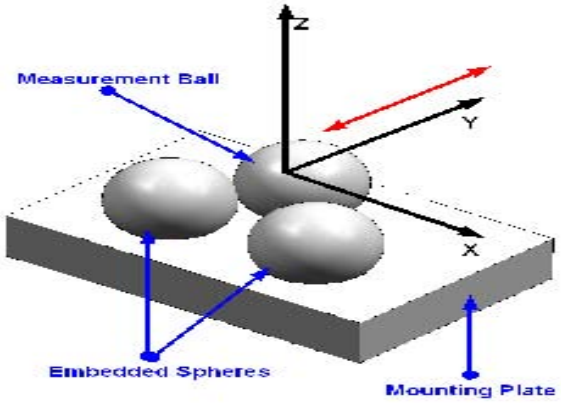

Figure 68 Ball Locator

model [65] was created to represent the ball locator: the objective is to minimise the variation along the X-axis by optimising the diameter of the locating spheres and the distance between them as well as the depth that the spheres are embedded into the locator, see Appendix I.

To determine the actual location effectiveness of the optimal solution a prototype was developed. Locating tests were carried out using sample balls that ranged from 10-13.5mm. The sample balls were located against the embedded spheres using only the force of gravity; therefore the angle of the platform was varied throughout the tests to determine optimal force between the sample balls and embedded spheres when contact is made. Each test consisted of placing the sample ball at the insertion point and allowing the sample ball to locate against the embedded spheres using only the force of gravity, (Figure 69). Observations showed that if the sample ball was released at the exact midpoint between the two embedded spheres on the x-axis: the ball rolled into the embedded balls and was located perfectly each time. On the other hand, if the insertion point is varied along the x-axis, it was very common that the sample ball would not make contact with both embedded spheres at the same time; therefore causing the ball to hit only one of the spheres and bounce out of the locating platform.

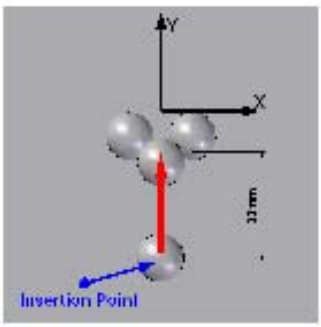

Figure 69 Locating Tests

One hundred percent reliability is required from the locating platform in order for the automatic measuring unit to be effective. The initial prototype was found to be unreliable; the distance between the two embedded spheres did not create a large enough pocket to constrain the measurement ball. Releasing balls from the exact midpoint between the two spheres proved almost impossible over the entire range of sample balls: design of a release system that would automatically adjust to varying ball diameters proved to be to complex. Therefore it was decided to increase the distance between the embedded spheres to 20mm, to allow for a variation of the release point along the x-axis. The diameter of the embedded spheres were also increased to 15mm and embedded 5.5mm into the platform Figure 70, this created a larger pocket to locate the sample balls and eliminated any sample balls bouncing out of the locating platform.

As mentioned earlier, the surface finishes as well as the alignment of the measuring surfaces will affect the accuracy and precision of a sample measurement. This is difficult and expensive to control in the manufacturing process: improvements in the roughness of a surface will usually lead to an exponential increase in the manufacturing costs. The roughness of the measuring surfaces also determines how they will interact with the environment. Rough surfaces usually wear more quickly and have higher friction coefficients than smooth surfaces: therefore effecting the movement of the sample ball.

To obtain a smooth finish on the measuring surfaces without greatly increasing the manufacturing costs of the entire measuring unit, 5mm precision gauge blocks were mounted on each measuring surface. This provides a very hard, temperature stable, corrosion resistant, high quality finish for the two measuring surfaces [16]. Slots were machined into the mild steel measuring surfaces, the two gauge blocks were wrung together and bonded while in the wrung state into the top and bottom slots, Figure 70; assuming no movement after seperation of the gauge blocks, the measuring surfaces should remain parallel and will minimize errors due to surface roughness.

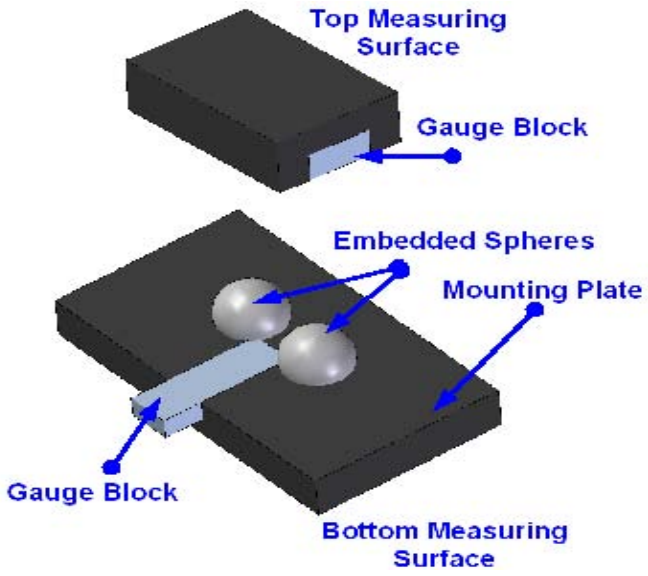

Figure 70 Measuring Surfaces

A fibre optic sensor is used to detect if a sample ball is located accurately against the two embedded spheres. The sensor is positioned between the two embedded spheres and is triggered at the point of contact between the sample ball and embedded spheres, Figure 71.

The type of sensor used on the locating platform is a reflective type Keyence FS-V20 series, dual display digital feedback sensor equipped with a FU-35FZ fibre optic head. The principle of operation is that an optical fibre transmits a light beam onto a sample ball located against the embedded spheres; the light beam reflects off the surface of the sample ball and the light is reflected back through a separate optical fibre mounted on the same sensor head and picked up by the receiver.

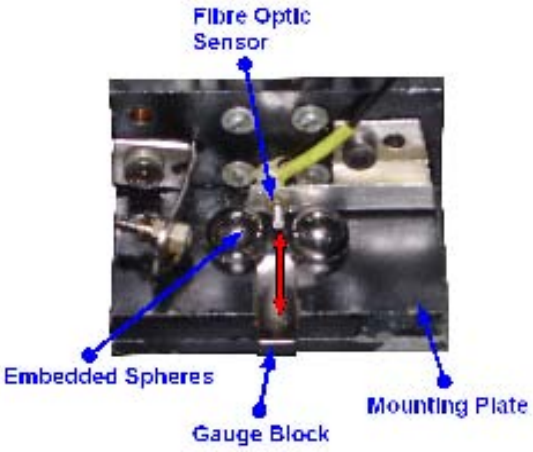

Figure 71 Fibre Optic Sensor

The flexible optical fibre allowed for versatile installation; the optical fibre has a minimum bend radius of 2mm and the sensor head is only 17mm long and has a diameter of 3mm. This allowed the sensor head to be mounted discreetly between the two embedded spheres without physically effecting the surrounding environment. The optical fibres are unaffected by electrical noise as no electric current flows through them, thus are ideally suited to the harsh working environment and they will not introduce electrical noise to the electrically sensitive piezo actuators surrounding them.

4 Measurement Station Design

4.1 Mounting System

4.1.1 Introduction

This section discusses the design of the mounting system for the flexure based measuring unit and the theory that drove the design. The mounting system not only serves a functional purpose in terms of the chassis for the measuring instrument to operate correctly, but also connects the measuring instrument to the surrounding environment. Factors such as vibration, noise, and temperature of the working environment will greatly influence the design of the mounting system. Precision mechanical instruments are very susceptible to small-scale oscillatory behaviour that can limit their ability to function effectively. Noise and vibrations in the surrounding environment are often the source of this oscillatory behaviour. Typically such disturbance is transmitted through the floor from nearby traffic, machinery or people: in a production environment, mechanical vibration from machinery is usually a major issue in this regard. The instrument will also be connected to the outside world by cables and pipes and these can also transmit vibrations to the instrument.

4.1.2 Instrument Base and Chassis Design

A reduction of disturbing noise can be considered at two distinct locations; at the origin of radiation and at the location of vibration reception. Within the environment of this project, the majority of the noise and vibration originates from the mass grinding and lapping machines. Some active (controlling the source of disturbance [3]) shock and vibration isolation measures have been taken to reduce the radiation of noise and vibration at the machines. This section will concentrate only on the passive isolation; reducing the noise transferred to the measuring instrument. Isolation of the instrument from the floor can reduce the amount of noise and vibration transmitted to the measuring instrument. Therefore the mounting system in this case is not just to designed to constrain the measuring instrument but also to operate as vibration isolation system.

A vibration isolation system can be considered to consist of the object being isolated (measuring instrument), the supporting surfaces (floor, foundation) and the vibration isolator (mounting system) placed between them. Figure 72 illustrates the simplest vibration isolation system and Figure 73 illustrates a schematic of the flexure

measuring instrument and mounting system. The measuring instrument must be protected from the vibratory motions of the supporting surface.

Any vibrations transmitted from the floor will cause displacements of the stationary base of the measuring instrument and will cause accelerations of the measuring system and so tend to excite resonant behaviour. The dynamic behaviour of the measuring instrument and mounting system will particularly limit the performance of the system; response to sudden changes of input and sensitivity to vibration are the main concerns. Resonance in individual elements and complete structures is of importance to both. Decoupling unwanted vibrations from a system is made easier if the system resonance is at high frequencies. Therefore, as mentioned in Section 3.2.3.2 the measuring instrument was designed to maximise its natural frequency.

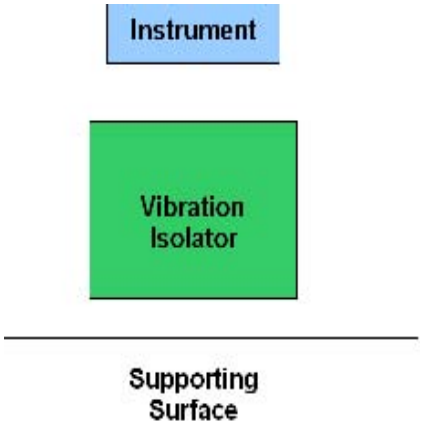

Figure 72 Simple Vibration Isolation System

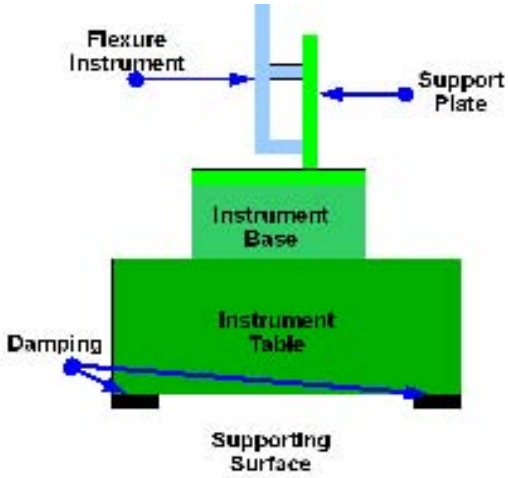

Figure 73 Schematic Side View of Flexure Instrument and Mounting System

Vibration transmission is a low-pass process [3] and so for the design of a general purpose low vibration table, the first priority is to set its natural frequency as low as is compatible with other design constraints. To achieve reasonably effective attenuation of foundation noise, it is desirable that the natural frequency of the measuring instrument be at least an order of magnitude greater than the instrument base and instrument table and sufficient damping must also be present to prevent excessive dynamic amplification near to the natural frequencies [3]. The natural frequency of an undamped spring-mass system is given by

$$f = \sqrt{\frac{K}{m}} \qquad \textbf{(40)}$$

Therefore increasing the mass of the instrument table and instrument base will reduce resonant frequency. Increasing the mass of the table and base, and reducing that of the measuring instrument moves the resonant frequencies apart. The two systems have little influence on each other as the resonances move apart; any vibrations transmitted through the floor will have little influence on the measuring area.

To maximize the mass and minimise the resonant frequency of the instrument base, the base was constructed from granite see Figure 74. This base supports the measuring instrument, the ball-locating platform and the support system. The mass of the base is calculated as

$$mass = (0.24 \times 0.24 \times 0.40) \times 2740 = 63.13Kg$$

Granite is commonly used as a base for high accuracy measurement due to its low vibrancy (high vibration absorption) and low thermal expansion. Also for a variety of other reasons including low cost (cheaper than traditional materials such as cast iron), high rigidity, non-magnetic properties, inert (no external coating required), corrosion resistant (does not rust and long wearing properties), stress free, unrivalled flatness straightness and perpendicularity, high durability (warp resistant) and low maintenance (Appendix A).

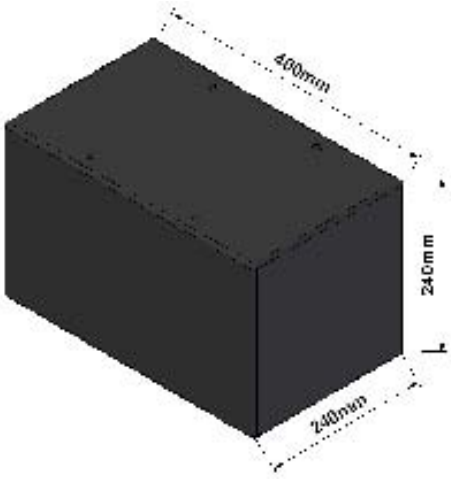

Figure 74 Granite Instrument Base

The support frame (chassis) that constrains the measuring instrument and the locating platform consists of an assembly of two flat plates and two brackets, as shown in Figure 75. As mentioned in Section 3.2.3 the flexure is made from Aluminium7075; an aluminium chassis would eliminate any thermal miss-match and relative expansions between the chassis and the measuring instrument. Aluminium however has a low density making the chassis lightweight; thus making it susceptible to

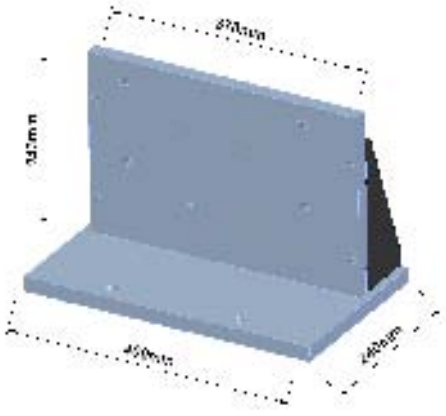

Figure 75 Support Frame

foundation vibrations. Also aluminium's relatively low Young's modulus would lower the stiffness of the support frame. The chassis was therefore made from steel; its high density increased the mass without increasing the overall dimensions compared with aluminium and hence lowered the resonant frequency of the support frame (the mass of the steel chassis is 29.52kg compared to 10.53kg for the same aluminium support frame). If the back plate was less rigid than the rest of the components in the mounting system, this would have the possibility of introducing relatively large vibrations between the top measuring surface and the ball locating platform. These vibrations would be measured as noise by the metrology system and would introduce errors into sample measurements.

As discussed earlier the deformation of the measuring instrument at the axis of the long-range piezo movement and the axis of the flexure movement must be minimized. Temperature driven expansion /contraction at these key points will affect the metrology system. Deformation at these areas is reduced by constraining the measuring instrument in close proximity to the axis of the piezo and the axis of flexure movement: the objective is to allow the measuring instrument to expand away from the measuring areas, Figure 65. Thus it is important that the measuring instrument is free to expand in all other directions in order to minimise thermal induced stresses.

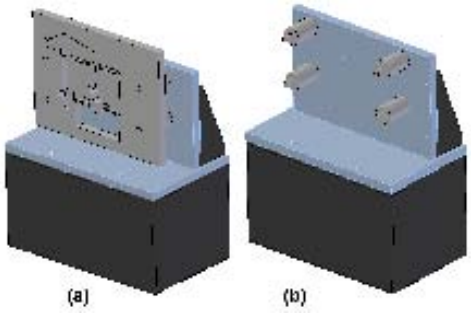

Figure 76 Mounting Pins

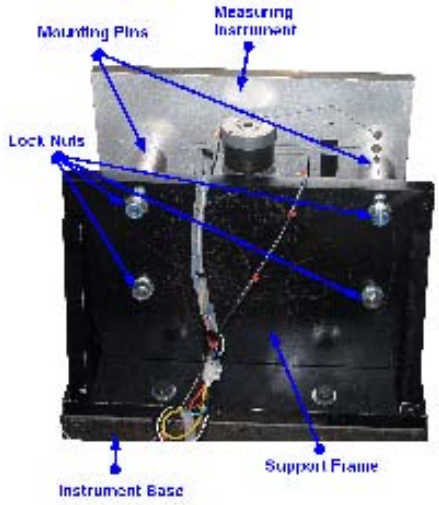

Figure 77 Mounting System

To minimize the deformation of the measuring instrument in the key areas, the monolithic flexure-measuring instrument is constrained at four points to the mounting frame using four pins, Figure 76 (a) and (b). The pins are positioned to allow the measuring instrument to expand in all directions away from the metrology areas. There is an interference fit between the 13mm holes in the measuring instrument and the

13.2mm ends of the pins. The M12 thread ends of the mounting pins are used to fasten the pins and measuring instrument to the support frame. The pins are fastened using spring washers and lock nuts, to guarantee that they do not release over extended periods of use (Figure 77).

4.1.3 Instrument Table

To protect the measuring instrument, the chassis and the instrument base from the vibratory motions of the supporting surface; the complete structure is mounted on the instrument table. Maximum vibration absorption of the instrument table is achieved by increasing the mass of the table to reduce its natural frequency. The assembled table consists of two 20mmx30mm, 5mm thick cast iron main beams, three transverse 20mmx20mm, 5mm thick cast iron beams, four steel side plates and an aluminium top plate, Figure 78. The overall weight of the table is approximately 600kg: this mass provides a good basis for decoupling unwanted vibrations from the system. This structure was originally the base of a proprietary CMM and was used as the mounting platform for the granite instrument base.

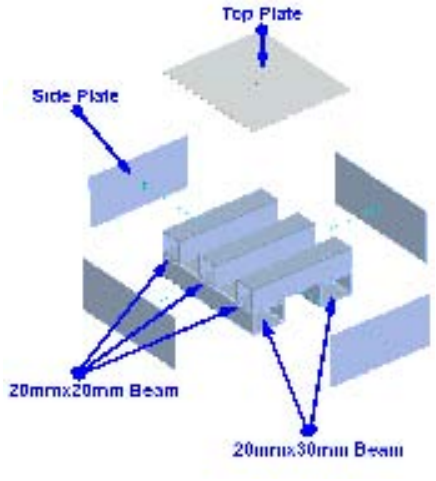

Figure 78 Instrument Table Exploded View

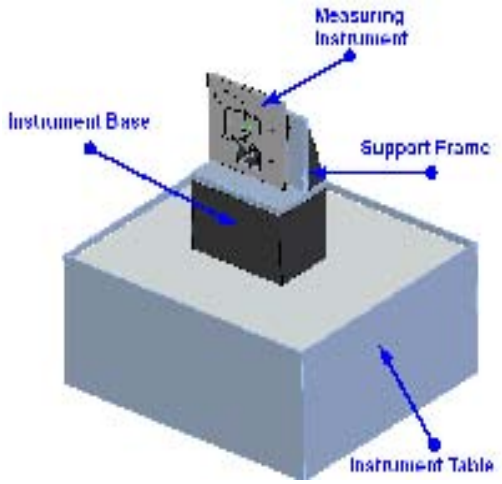

Figure 79 Complete Mounting System

The dynamic stiffness (k_{dyn}) of a system is the ratio of force to unit displacement during simple harmonic motion, Equation (41)

$$k_{dyn} = \frac{F_{dyn}}{Y_{dyn}} \qquad \textbf{(41)}$$

(F_{dyn}) is the applied dynamic force and (Y_{dyn}) is the magnitude of the output under dynamic loading [55]. A static force (F_{st}) will give a displacement Y_{st}; if an

equivalent dynamic force is applied the deformation will increase (A) times, Equation (42), where (A) is the ratio of the dynamic to static amplitude, the dynamic amplification factor (the ratio of dynamic deflection to static deflection).

$$Y_{dyn} = Y_{st}.A \qquad \textbf{(42)}$$

Since $Y_{st} = \frac{F_{st}}{K_{st}}$

$$A = \frac{Y_{dyn}}{\left(\frac{F_{st}}{K_{st}}\right)}$$

Consequently the dynamic stiffness of a system is generally less than the static stiffness (k_{st}); the higher the dynamic amplification factor the lower the dynamic stiffness, Equation (43).

$$k_{dyn} = \frac{k_{st}}{A} \qquad \textbf{(43)}$$

Therefore, the maximum magnitude of the output under dynamic loading is related to the magnitude of deflection under static load. If the amplitude of the exciting force is independent of the excitation frequency, then (A) is given as

$$A = \frac{Y_{dyn}}{\left(\frac{F_{st}}{K_{st}}\right)} = \frac{1}{\sqrt{(1-\eta^2)^2 + (2\xi\eta)^2}} \qquad \textbf{(44)}$$

The level of dynamic amplification depends on the damping factor ξ of the system and the normalised frequency η, the ratio of the frequency of excitation (ω) and the natural frequency of the system (ω_n), Equation (45).

$$\eta = \frac{\omega}{\omega_n} \qquad \textbf{(45)}$$

Therefore, the dynamic stiffness will vary with the applied force frequency and can be increased by increasing the damping and avoiding the natural frequencies of the system. External damping is required to increase the dynamic stiffness of the complete measuring system (mounting system and measuring instrument). An appropriate method

to damp the system is to mount an anti-vibration material between the instrument table and the supporting surface.

There are various types of anti-vibration materials available where the reduction in amplitude or attenuation of vibration depends greatly on the damping factor of the material. Figure 80 shows the dynamic amplification, Equation (44) plotted against a range of normalised frequencies for a series of damping factors of ξ=0.09, 0.16, 0.36, 0.64 and 1.

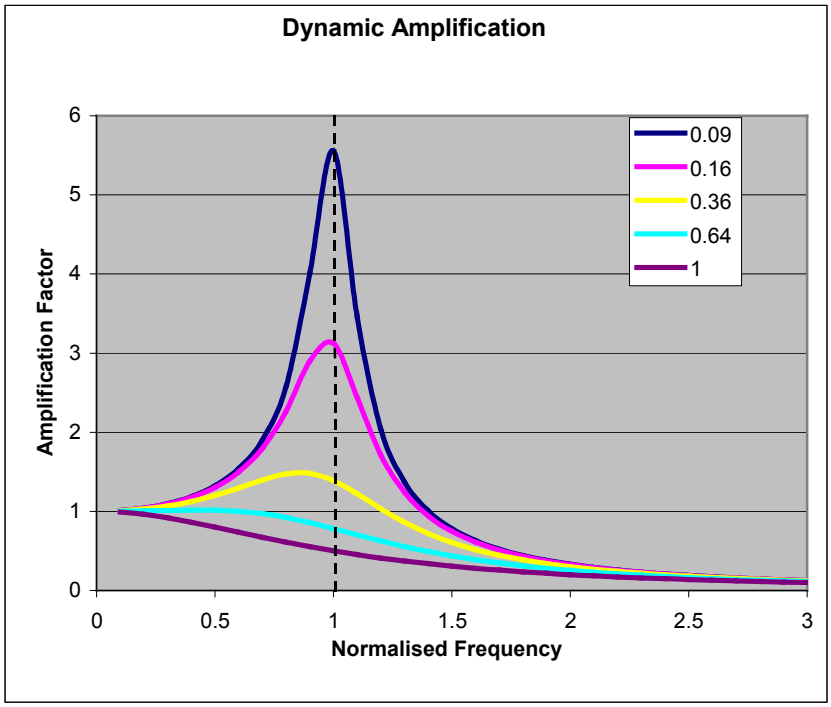

Figure 80 Amplitude Response of a Damped System

The shape of the transfer function is characteristic of all second order systems and also, closely approximates the response of many higher order systems up to and beyond their first natural frequency [3]. Clearly it can be seen that increasing the damping factor can reduce the dynamic amplification close to resonance and the amplification is close to unity for low frequencies well below the resonant frequency and gradually increases up to maximum when the normalised frequency equals 1(resonant frequency). Practically for $\eta < 0.4$ and $\eta > 2.5$ the displacement under static loading is the same as under dynamic loading. As shown, when the system is damped the peak amplification occurs at a point lower than the resonant frequency; increasing the damping factor will also decrease the resonant frequency, but not enough to be

useful at reasonable levels. Equation (46) gives the frequency at which the peak amplification occurs.

$$\omega = \omega_n \sqrt{1-2\xi^2} \qquad \textbf{(46)}$$

Another aspect, which is very important while choosing a damping factor, is the vibration transmissibility of the system. Vibration transmissibility is the percentage or fraction of the vibration that the isolators transmit to the supported equipment [21], or the ratio of the peak output displacement to the peak input displacement. The Transmissibility (TR) is calculated using Equation (47)

$$TR = A\sqrt{1+(2\xi\eta)^2} \qquad \textbf{(47)}$$

If TR > 1, the vibration transmission is increased, = 1 no vibration isolation and < 1 there is vibration isolation. Figure 81 shows the transmissibility plotted against a range of normalised frequencies for a series of damping factors of ξ=0.09, 0.16, 0.36, 0.64 and 1.

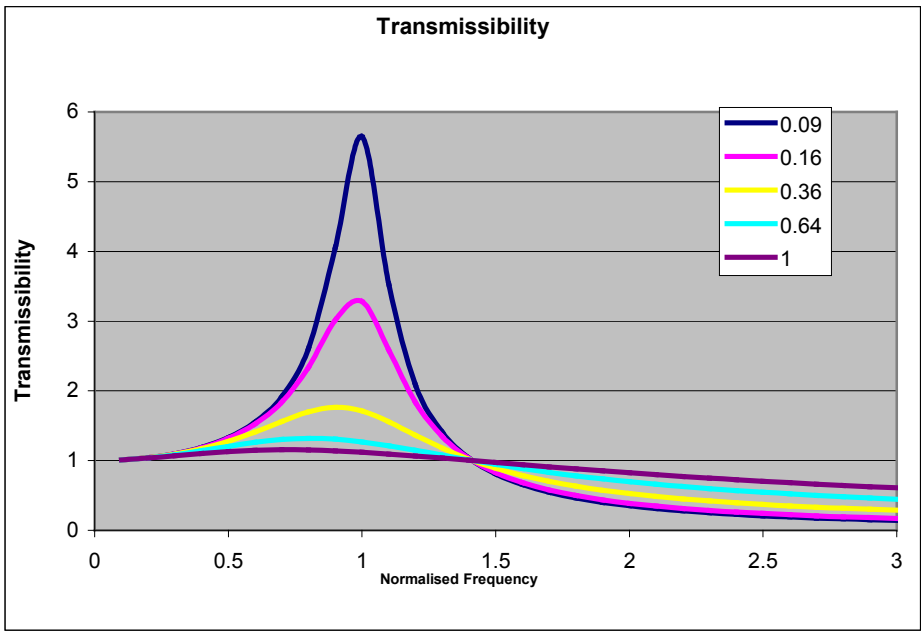

Figure 81 Vibration Transmissibility

A very important aspect of the curves shown in Figure 81 is that the transmissibility never falls below 1 until the normalized frequency is equal to 1.414 ($\omega/\omega_n=2^{0.5}$). Above this frequency, the attenuation is dependent upon the damping factor. As the frequencies increases above this point, small damping factors give more rapid

attenuation. High damping reduces the attenuation at high frequencies and increases the settling time.

The choice of damping factor depends largely on the separation of the resonant frequencies of the instrument table and the measuring instrument. A low value is a good choice to provide rapid attenuation at high frequencies, provided that it is sufficient to prevent a large dynamic amplification near the instrument table resonance. As the damping factor increases, the amplification factor is reduced at the expense of an increased sensitivity to frequencies away from resonance. As stated by Snowden [22], if the mass of the instrument is much less than that of the table, a good compromise is a critical damping factor in the region of 0.1 or less. The 4.66 kg mass of the measuring instrument is much less than the 600kg mass of the instrument table. Therefore, based on the work carried out by Snowden [22], it was decided that the appropriate ant-vibration material must have a damping factor of 0.09.

The anti-vibration material chosen was an elastic vibration damping material with high shock and vibration damping properties molded from high-grade nitrile (NBR) rubber. The NBR can be used for active vibration isolation of pumps, compressors, power presses, forging machines, diesel generators and hydraulic equipment but it is highly suited for passive isolation of highly sensitive equipment such as scientific, measuring and test equipment, Appendix A. The anti-vibration material is placed between the 80mmx80mmx50mm mounting legs of the instrument table and supporting floor.

Figure 82 NBR Anti-Vibration Material

Whilst the development of the measurement instrument is paramount in this project, it is necessary to automate the feeding mechanisms and control systems. This will include the temperature normalizing system, the ball delivery and removal system, the reference ball return and sorting system which are discussed in the remainder of this chapter.

4.2 Sample and Reference Ball Delivery

This section discusses the delivery from the cooling tank to the measurement instrument. The delivery system is required to place the sample balls and reference balls into the ball locator as described in Section 3.3. The measurement instrument carries out a continuous cycle of calibration using a maximum and a minimum reference ball followed by measurement of a sample (typically 5) of production balls.

4.2.1 Temperature Normalizing

As mentioned earlier sample components must be selected automatically from the grinding and lapping process and delivered to the temperature normalizing station. Figure 83 shows a schematic of the temperature normalizing station, indicating the paths of the sample balls and reference balls. The sample balls are stacked five high within individual holding pipes and stored alongside separate holding pipes containing maximum and minimum reference balls. The complete sets of holding pipes are submerged within the temperature-normalizing tank, Figure 84. The entire set of balls remains submerged for a specific period of time (sufficient for complete temperature equalization) in the temperature-controlled fluid at slightly above ambient temperature. The number of samples measured between calibrations is kept to a minimum of one batch so that the effects of environmental variability are minimized: it is expected that any errors due to thermal changes in the entire measurement system will thereby be minimized. The temperature control in the normalizing fluid is at a level of ±0.1ºC [24].

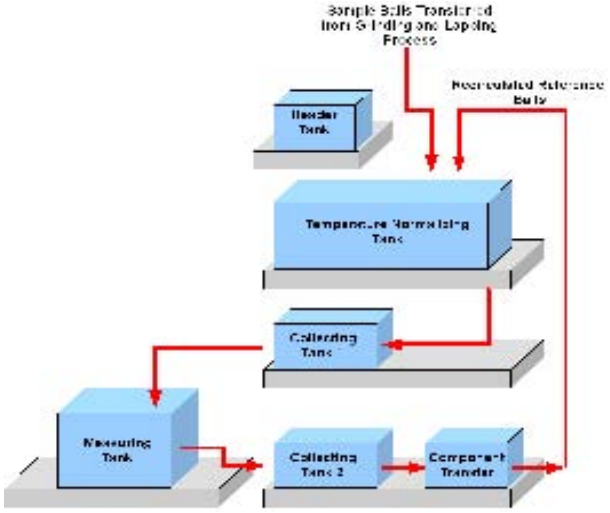

Figure 83 Schematic of Temperature Normalizing Station

Operation of the measuring instrument requires that the balls be measured in sequence; measuring the minimum reference ball followed by the maximum reference ball carries out the calibration of the instrument. To maximise the range of measurement, the ball-locator platform is positioned at a height such that the measurement surface contacts the minimum reference ball at the point minimum piezo extension. The maximum reference ball is then fed in and measured. Each sample ball is then fed in turn and measured in comparison to the reference balls.

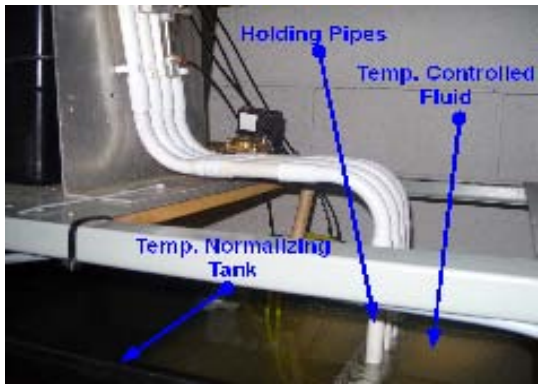

Figure 84 Temperature Normalizing Tank

Figure 85 shows the operation of the release mechanism from the temperature normalizing station tank: during temperature normalizing the pin cylinder remains extended and when the balls are normalized, the pin cylinder retracts, releasing the set of balls into the tank.

The base of the temperature-normalizing tank is tapered so that all released balls are fed into a vertical exit pipe; by releasing the balls at different times the balls are stacked in the proper sequence for measurement (min ref ball, max ref. ball, sample balls). A pneumatic valve then releases the sequenced balls from the normalizing tank outlet pipe and the complete set of balls flow through Collecting Tank 1. The excess fluid, which escapes from the normalizing tank outlet pipe along with the set of balls, is released into this tank. The set of balls roll from the collector tank and flow into the measurement area (sequence unchanged): they are held there awaiting their individual release onto the measurement platform.

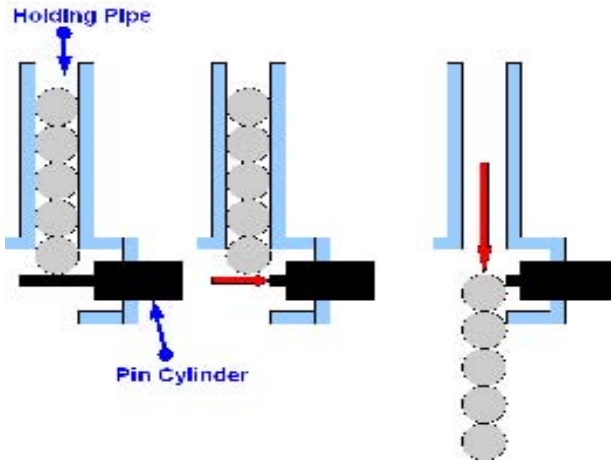

Figure 85 Ball Release Mechanism

4.2.2 Measurement Instrument Ball Delivery/Removal System

This section discusses the design of the ball delivery system; the ball delivery/removal system consists of two units, firstly a unit that places the ball onto the locating platform and secondly a unit that subsequently removes the ball from the locating platform. The primary design issue was to develop a method to accurately place the ball on the locating platform while minimising the location variation and to remove the ball without affecting the surrounds. Errors of consistency (the difference in the variation taken over time) and uniformity (the difference in variation throughout the operating range) in positioning would have to be assessed and reduced to a minimum in order to create a suitable measurement set-up. To avoid interference (vibrational) with the measurement process, the ball delivery/removal system was not linked mechanically with the measurement instrument itself.

4.2.2.1 Rotary Indexer Concept

The use of a rotary indexer unit was an initial concept to move the balls into the locating platform and a prototype was developed as an undergraduate project [66]. The prototype consisted of an indexer housing, rotary indexer and a top cover, Figure 86. With this particular design, each ball to be measured entered through the hole in the top cover and settled in one of the 16 slots in the rotary indexer. A stepper motor with a step angle of 7.5˚ drove the indexer; to rotate the indexer by a single slot, three steps of the stepper motor were required. With the device mounted on a slight incline, the slot in the indexer housing allowed each ball to roll out of the indexer under gravity, onto the locating platform.

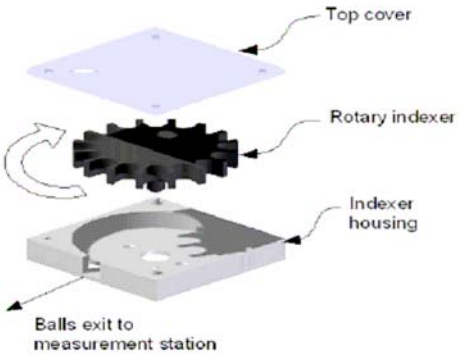

Figure 86 Rotary Indexer Concept

Figure 87 Prototyped Rotary Indexer [24]

A ball waiting in the ball release activated the first sensor; this in turn activated the release system, allowing the ball to travel into the rotary indexer. The second sensor was activated by a ball arriving in the indexer; this initiated a sequence of three steps of

the stepper motor, rotating the indexer by one slot (22.5˚). Balls were constantly fed into the unit; as a result the indexer operated on a continuous cycle, one ball being removed from the unit as another enters. Due to poor construction, problems arose with the reliability of the stepper motor; on many occasions, three steps of the stepper motor did not rotate the indexer by the required 22.5˚ and misalignment of the indexer drive shaft and the rotation axis of the stepper motor increased the torque required to rotate the indexer, causing the stepper motor to skip steps.

As the project developed it was decided that the total amount of balls in the queue for measurement at any one time would be seven (two reference balls and five sample balls), as mentioned in Section 3.2.2. Therefore, an indexer with 16 slots was no longer required and after some deliberation it was decided that the concept of a rotary indexer was too elaborate and a simple method of stacking the balls vertically in a queue would prove less problematic.

4.2.2.2 Vertical Queue Concept

The direct approach taken with the vertical queue method involves stacking the balls in the required sequence and using a miniature single acting, spring-return pneumatic cylinder, for ejecting the balls from the queue and guiding them onto the locating platform. Figure 88 shows the proposed operation of the vertical queue and ball insertion mechanism. When the set of balls arrive, the pin cylinder remains retracted (a). To insert a ball into the ball locator, the pin cylinder extends, pushing the first ball in the ball locator (b). This sequence is repeated until all the balls have been successfully measured.

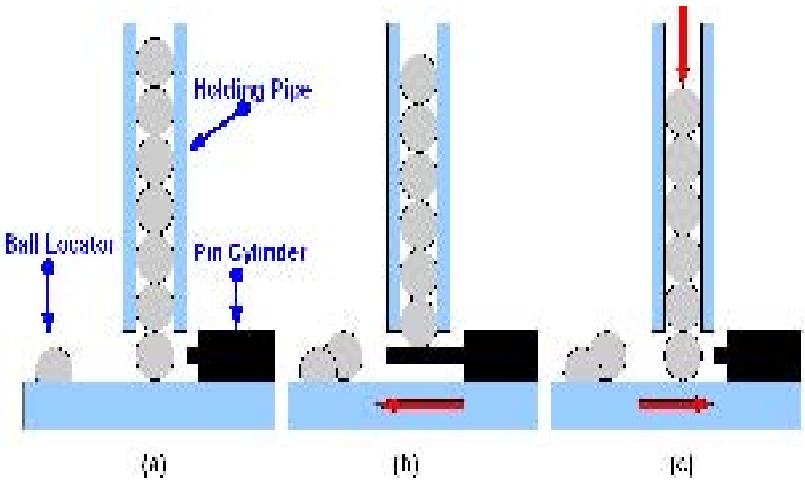

Figure 88 Vertical Queue Method

A working prototype was designed and constructed, again as an undergraduate project [66]. The base of the prototype consisted of two embedded spheres to directly replicate the original ball locator platform of the measuring instrument, Figure 89. The initial concept also incorporated a separate clamping device, to hold the sample balls against the ball locator during the measurement process. The clamp was designed to apply pressure on the upper half of the ball; therefore providing a downward force on the ball eliminating the possibility of the ball being disrupted during the measurement process. The clamp consisted of a single acting, spring-return pneumatic cylinder with an attached wire shaft and a second wire shaft attached to a mounting block, Figure 90 (a) and (b).

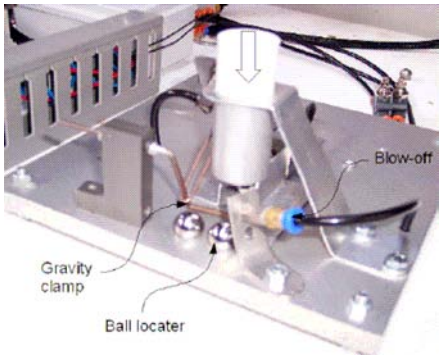

Figure 89 Vertical Queue Prototype [24]

The clamp was opened by fully extending the cylinder, causing the clamp to rotate upwards away from the ball locator, allowing a ball to be inserted or removed. On release, the cylinder would spring return, causing the clamp to rotate freely onto the sample ball holding the ball in place. The weight of the clamp alone applied a downward force to the sample.

The implementation of this clamping technique proved to be more difficult than anticipated as positioning of the pivot was achieved by trial and error. It was determined early in the design stage that the clamping force would need to have a line of action that would act through the centre of the ball in a downward direction, as this would provide the optimum constraint. To ensure a consistent clamping action, the optimum position for the pivot was found to be just behind the ball locater. This was important as a varying ball size had to be accommodated and clamping had to be consistent throughout the range.

4.2.2.3 Ball Ejection System

After some deliberation and experimentation it was found that a blast of air proved to be the simplest method of removing the ball; by carefully positioning a small air nozzle to one side of the ball locater, a short blast of compressed air is sufficient to

blow the ball out of the embedded spheres and off the replicated ball-locating platform. The air nozzle was held in place using a bracket as shown in Figure 90 (b).

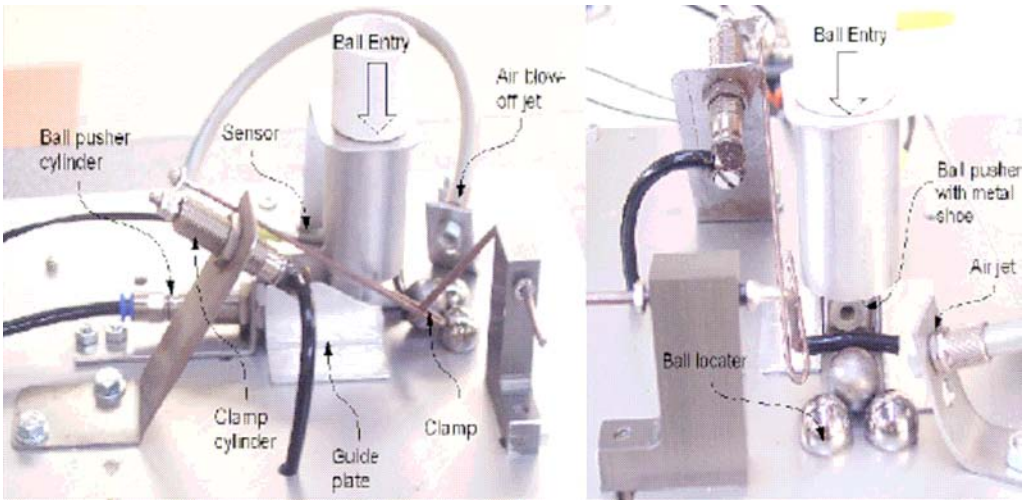

(a) **(b)**

Figure 90 Clamping Concept [24]

4.2.2.4 Delivery/Removal System

The concepts for the final production delivery system are all based on the vertical queue design method. The final production delivery/removal system was designed to overcome reliability and repeatability problems encountered with the initial vertical queue prototype. Also it was essential that the delivery/removal would have minimum influence on the functionality of the measuring instrument itself. Some key issues influencing the final design and fabrication are explained in detail below:

- The system must be flexible to cater for sample balls ranging from 10mm-14mm
- The delivery system must not contact the measuring instrument; contact would effect the performance of the precision instrument
- The ball locating platform is required to move vertically a minimum of 4mm, to cater for sample balls over the entire measurement range; therefore the ball locating platform is required to operate independently of the delivery/removal system
- To minimise the thermal effects on the metrology system, the measurement instrument is required to expand away from the measuring areas; therefore the delivery/removal system must not constrain the measuring instrument in any axis

- As the maximum and minimum reference standard balls are used continuously to calibrate the measuring instrument, the reference balls must be recycled to the normalizing tank after each calibration; the removal system is therefore required to distinguish between and separate reference and sample balls, and subsequently sort all reference balls into their required holding areas.
- The design must minimize the cycle time to deliver/remove a single ball from the locating platform; a single measuring instrument will be required to service 20-30 grinding/lapping machines with a minimum target measurement cycle time of 45 seconds

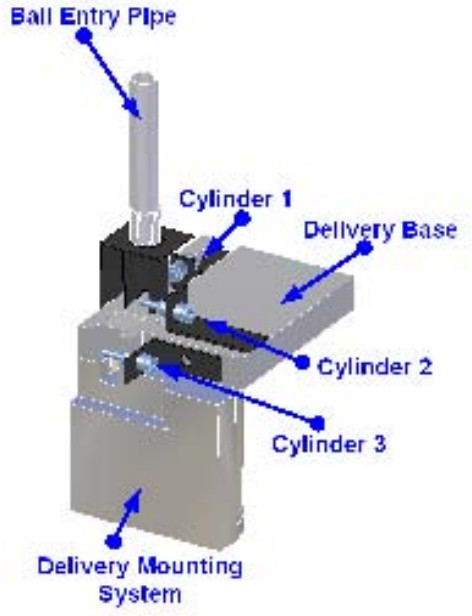

Figure 91 Delivery System Design

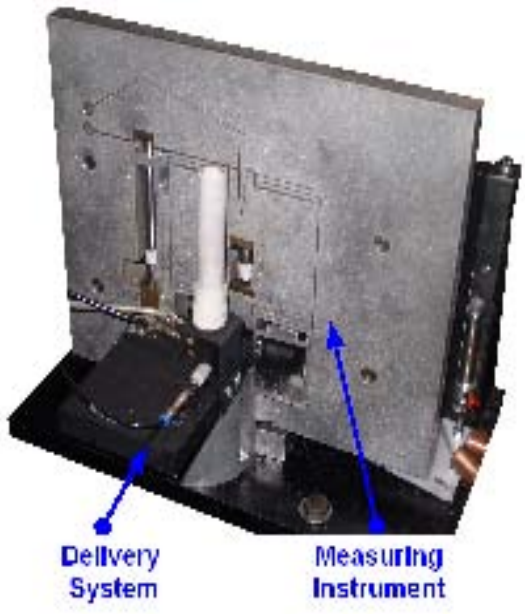

Figure 92 Finished Delivery System

The production delivery system design is shown in Figure 91 and Figure 92, the design consists of a ball entry pipe, base, mounting system and three miniature single acting, spring-return pneumatic cylinders. Cylinder 1 ejects the balls from the ball entry pipe and guides them into the slot in the base at Cylinder3.

The ball entry pipe is required to be flexible to cater for 10-14mm balls; therefore the minimum diameter of the pipe and exit slot height is 14.5mm. As shown in Figure 93 (a) small balls will settle differently than large balls within the 14.5mm pipe.

When a small ball is ejected from the vertical queue by cylinder 1, it is possible that a second small ball will drop down at the exit slot and consequently will be pushed out of the delivery pipe by the weight of the balls resting on top of it Figure 93 (c).

To overcome this problem Cylinder 2 was mounted at the exit slot of the ball entry pipe; this eliminates the chance of a second ball being ejected when Cylinder 1 is activated, Figure 93.

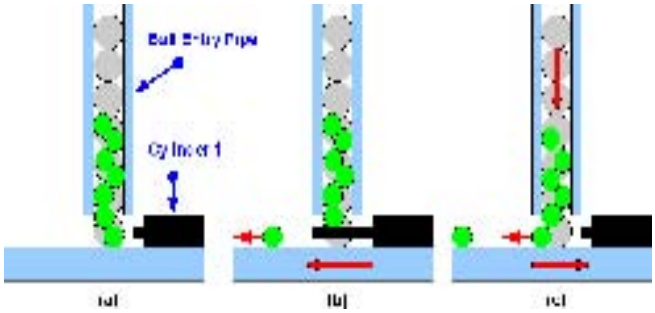

Figure 93 Delivery of Small Balls

As mentioned earlier the ball locator platform is required to move 4mm vertically on a linear guide. Also because of the potential interference with the measurement process the delivery system is mounted independently of the ball locator. To achieve a smooth transition of a ball between the stationary delivery system and the moveable ball-locating platform, the ball enters into a slot in the delivery base and rests on the precision gauge block attached to the locating platform. Subsequently under the force of gravity the ball is allowed to roll along the gauge block and settle against the embedded location spheres. As the difference in height increases between the locating platform and delivery system, the momentum of the ball entering the locating platform also increases. The variation in the ball approach velocity was found to reduce the consistency of ball location; increased velocity can cause the ball to bounce off the embedded spheres and exit the locating platform. This problem was eliminated by the Cylinder 3; the ball is stopped as it enters the locating platform, ensuring that all balls roll into the embedded spheres at a constant velocity.

The clamping device proposed in the vertical queue prototype has been removed: after extended testing it was found to lack adequate repeatability. The clamp did not operate uniformly throughout the complete range of sample balls and some forces applied to the ball by the clamp caused adverse movement of the ball. Also there was insufficient space for the clamping device between the ball locating platform and measuring instrument. Currently, to guarantee that contact is maintained between the ball and the two embedded spheres during the measurement process, the measuring

instrument and mounting system are positioned at an angle (approx.15˚):gravity is thereby employed as the clamping force.

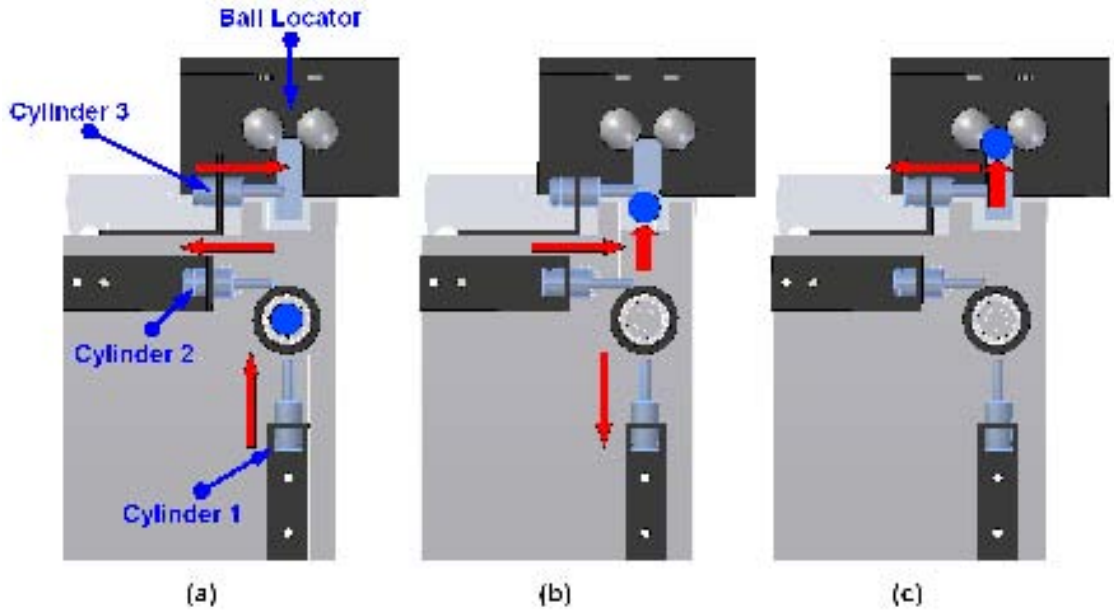

Figure 94 Operation of Delivery System

Figure 94 therefore demonstrates the operation of the delivery system. After temperature normalizing, the seven balls arrive at the ball entry pipe and are stacked vertically in the correct sequence. A countersunk hole in the base centres the first ball in relation to Cylinder 1. Cylinder 2 remains fully extended to stop the ball exiting the delivery pipe. To insert a ball for measurement, Cylinder 2 retracts and Cylinder 1 extends to push the first ball out of the ball entry pipe (Figure 94 (a)). Simultaneously Cylinder 3 extends to stop the ball as it drops onto the ball-locating platform (Figure 94 (b)). After half a second Cylinder 3 retracts, allowing the ball to gravity feed into the embedded spheres (Figure 94 (c)). Following the measurement process, the ball is removed using the air jet; while at the same time the delivery sequence of the second ball takes place. This cycle continues until all seven balls have been successfully measured. The cycle time to insert/remove a single ball is 1.5 seconds.

4.2.2.5 Ball Removal and Sorting

A continuous cycle of calibration followed by measurement of sample balls occurs; therefore to prepare for the next cycle, the reference balls must be recycled back to the temperature normalizing station after each calibration (Figure 83). The removal system is therefore required to distinguish between and separate reference and sample balls. Sample balls are subsequently delivered to a production ball disposal system and reference balls are delivered to the temperature normalizing station, where they are sorted into their specified holding pipes.

Figure 95 Divider System

The sequence of balls entering/exiting the measurement instrument remains constant. The minimum reference ball is measured setting the height of the location table and is immediately followed by the maximum reference ball: this serves to calibrate the instrument. Each of the five sample balls are then measured in turn by comparison with the calibration balls.

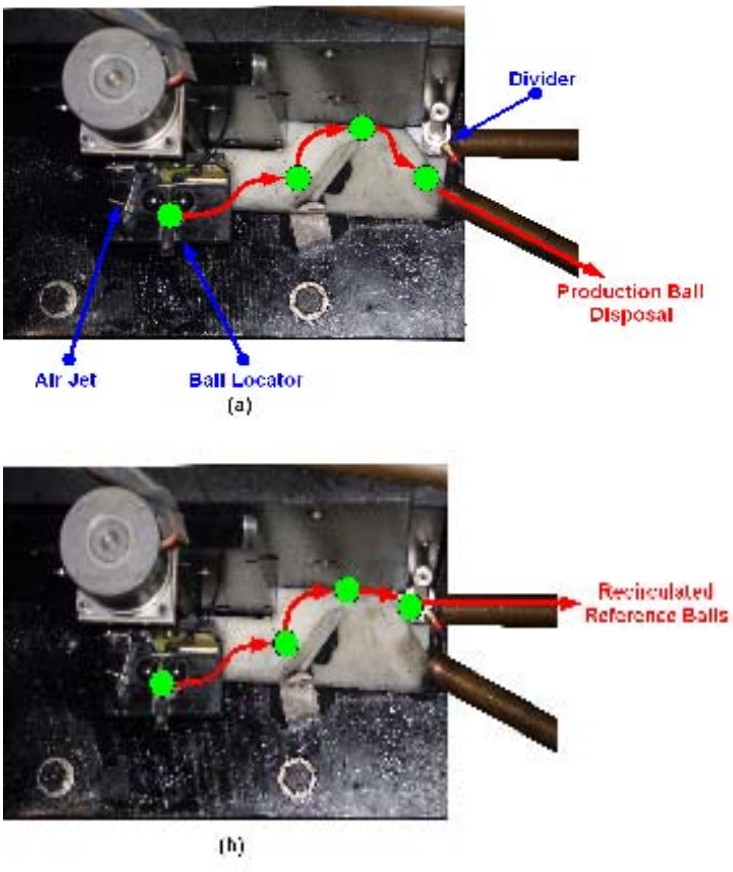

Figure 96 Route of Reference and Sample Balls

The ball divider system consists of a ball run-off, a pneumatic controlled divider and two separate exit pipes, Figure 95. The divider, which controls the route of each ball, is simply a single-acting spring return pneumatic actuator with an attached nylon end piece. During the

calibration process the divider is full retracted and for this reason when the reference balls are removed from the ball locator using the air jet they travel along the ball run-off and exit through the re-circulated reference ball pipe, Figure 96 (b). The divider extends following the calibration process; redirecting the five sample balls into the production ball disposal exit pipe (Figure 96(a)).

After their use in calibration, reference balls travel under gravity through Collecting Tank 2; the collector tank removes any excess fluid from the reference balls. Each ball continues from the collector tank and enters the component transfer mechanism, where a blast of air is used to lift the balls to the temperature-normalizing tank, Figure 83. Each reference ball has a designated holding pipe within the temperature-normalizing tank; hence each produced ball size requires two separate holding pipes (max and min reference ball). It is critical that each reference ball is returned to its designated holding pipe. Therefore a system is required to automatically separate and store the reference balls between measurements into these predetermined holding pipes.

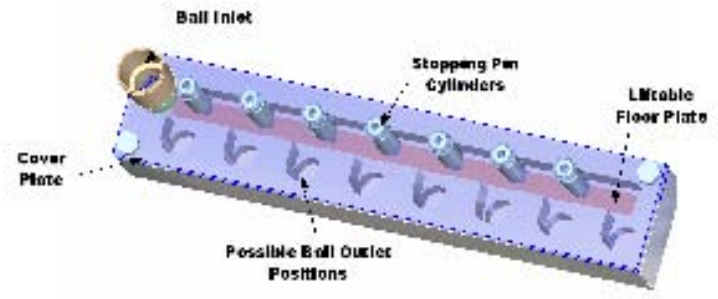

Figure 97 Concept Reference Ball Sorter [24]

The concept of the ball sorter is shown in Figure 97; the design consists of a base, retractable floor plate, a cover-plate and spring-return pneumatic cylinders. While the stainless steel floor is fully retracted, a reference ball enters the ball sorter at the ball inlet; the device is mounted at an angle (approx -25˚off vertical) to allow the reference ball to roll along the floor. Slots machined into the aluminium base (ball outlet positions), allow the reference balls to enter the holding pipes within the temperature normalising tank. The pneumatic cylinders determine which holding pipe a reference ball enters; the cylinders stop the ball at the desired holding pipe location. A pneumatic cylinder raises the retractable floor, Figure 98 (slots in the floor allow the stopping pin cylinders to pass through it). As the floor rises the reference ball falls into the appropriate holding pipe and is ready for the next measurement cycle.

After intensive testing, the ball sorter has proved very effective; the device has operated consistently and uniformly throughout the production range and the reliability of the device is very good.

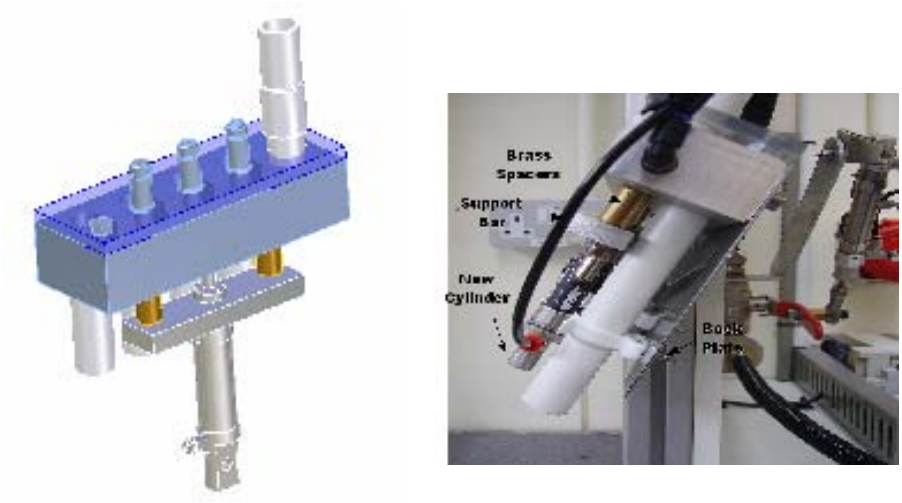

Figure 98 Production Ball Sorter

Having presented the system mechanical hardware (under the general umbrella of "Measurement Station Design"), the next chapter will discuss the electrical and electronic hardware (Section 5.1) linking to the system control (Section 5.2).

5 Electrical and Electronic Hardware and System Control

5.1 Electrical and Electronic Hardware

5.1.1 Introduction

This section discusses in detail the hardware used in the data acquisition, piezoelectric actuator control, ball locator platform control and the measurement display. This provides the essential background to the system structure related to the central controller and the LabView control software developed for implementation of the measurement system and its integration into the plant as presented in Section 5.2.

5.1.2 Data Acquisition and Piezoelectric Control

5.1.2.1 DAQ Hardware, Drivers and Application Software

The specific Data Acquisition hardware used for the automated piezo driven measurement instrument is a National Instruments PCI-6024E Multifunction DAQ as shown in Figure 99. The plug-in DAQ device resides in the PC; the device plugs into the PCI slot (Peripheral Component Interconnect specifies a computer bus for attaching peripheral devices to the computer motherboard) in the PC.

Figure 99 NI PCI-6024E Multifunction DAO

The PCI-6024E DAQ device contains 8 differential analog input channels, each having a resolution of 12bits (1 in 4,096) and a max sampling rate of 200 KSamples/s. The input signal ranges are shown in Figure 100. The device also contains 2 analog output channels with a resolution of 12bits and a max update rate of 10KHz. The range of the analog output voltage is ±10v. In addition to analog inputs/outputs, the PCI-6024E DAQ also contains 8 digital input/output channels.

Range	Bipolar
20 V	±10 V
10 V	±5 V
1 V	±500 mV
100 mV	±50 mV

Figure 100 Analog Input Signal Ranges

The space on the back of the PCI card is too small for the connection of signal input and outputs; therefore it is required to connect the PCI card to an external breakout box using a special cable. The type of breakout box used is a National Instruments BNC-2120 shielded connector block with signal-labelled BNC connectors; BNC (Bayonet Neill-Concelman) connectors are a very common type of RF connector used for terminating coaxial cable. The NI BNC-2120 is a desktop or DIN rail mountable breakout box that simplifies the connection of both analog and digital signals to the DAQ card while maintaining the integrity of measurements with a shielded enclosure and can be used as a connector block with the M series, E series and S series multifunction I/O DAQ devices.

Software transforms the PC and the DAQ hardware into a data acquisition, analysis and presentation tool. Driver software is the layer of software for communicating with the hardware; it forms the middle layer between the application software and the hardware. The driver software used for the piezo measurement instrument is National Instruments Traditional NI-DAQ Legacy; this is claimed to be robust software that makes it easy to access the functionality of the data acquisition hardware.

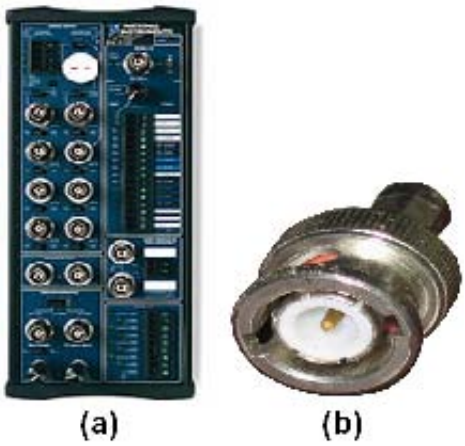

Figure 101 NI BNC-2120

The application software layer is used as a development environment in which a custom application is built that meets specific criteria. Application software adds analysis and presentation capabilities to driver software; the software sends the driver commands to acquire and generate signals and manipulates the raw data into a form that is understandable. As previously mentioned, the specific application software used in this project is National Instruments Labview version 8.

5.1.2.2 Piezoelectric Actuators

As mentioned in Section 3.2.2, the measurement instrument consists of a primary flexural-hinge guided stage driven by a piezoelectric actuator; in-built into the primary stage is a secondary flexural-hinge guided stage, which is driven by a second piezoelectric actuator. The primary piezo actuator is used to drive the stage through long-travel positioning and the secondary acts as a touch sensor to detect contact between the measurement stage and a sample or reference standard ball.

The primary piezoelectric actuator is a Physik Instrumente P-841.60 Closed-Loop Low Voltage Piezo Translator (LVPZT) with a maximum nominal displacement of 90μm and the touch sensor piezoelectric actuator is a Physik Instrumente P-841.10 Low Voltage Piezo Translator with a max nominal displacement of 15μm. These preloaded piezo translators shown in Figure 102 are high-resolution linear actuators for static and dynamic applications; the internal spring preload makes them ideal for dynamic applications. It is claimed by the vendor that they provide sub-millisecond response and sub-nanometer resolution.

These translators are equipped with what are claimed to be highly reliable multiplayer piezoelectric ceramic stacks protected by a non-magnetic stainless steel case. The standard translator tip and base have tapped holes; to help decouple off-axis or torque loads and to avoid bending moments and shear forces in the piezo ceramics, a ball tip has been fitted into the top piece of each individual translator. Due to the large forces involved, bolts screwed into each actuator base, mounted them within the measurement instrument.

There are two basic techniques for determining the position of piezoelectric motion systems: direct metrology and indirect metrology. With direct metrology, motion is measured at the point of interest; this can be done for example with an interferometer or capacitive sensor. However, indirect metrology involves inferring the position of the platform by measuring position or deformation at the actuator or other component in the drive train. Motion inaccuracies, which arise between the actuator and the platform, cannot be accounted for [4].

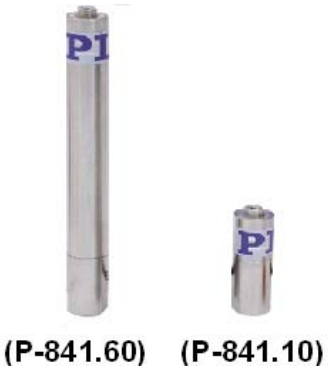

Figure 102 Piezoelectric Actuators

Using indirect metrology, the P-841.10 and P-841.60 piezo actuators include integrated ultra-high resolution strain gauge position sensors to sense the displacement of the actuators and operate with servo-control electronics.. A strain gauge sensor consists of a resistive film bonded to the piezo stack; when the film is stretched within its elastic limit it will become thinner and longer, changes that increase its electrical resistance. Conversely, when it is compressed such that it does not buckle, it will broaden and shorten; changes that decrease its electrical resistance. Strain generally causes a larger, but nearly proportional, fractional change in resistance [3].

Four resistors driven by a DC voltage form a Wheatstone bridge; this is used to measure an electrical resistance by balancing two legs of a bridge circuit. In the circuit in Figure 103, R_x is an unknown resistance to be measured and R_1, R_2 and R_3 are resistors of known resistance. If the ratio of the two resistances in the known leg (R_2/R_1) is equal to the ratio of the two in the leg (R_x/R_3) then the voltage between the two midpoints B and D will be zero and no current will flow through V_G. At the point of balance

$$R_2 / R_1 = R_x / R_3$$
$$\therefore R_x = (R_2 / R_1).R_3$$

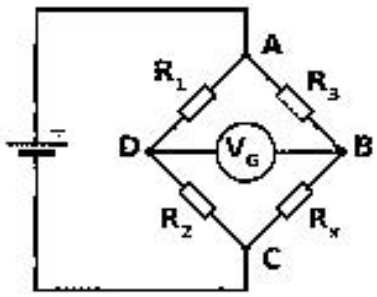

Figure 103 Wheatstone Bridge

If R_1, R_2 and R_3 known, the voltage through V_G can be used to calculate the value of R_x. If R_1, R_2 and R_3 are known to high precision, then R_x can be measured to high precision; very small changes in R_x disrupt the balance and are readily detected. When the bridge resistance changes, the sensor electronics convert the resulting voltage into a signal proportional to the displacement of the piezo stack.

The strain gauge configuration for both P-841.60 and P-841.10 piezoelectric actuators are shown in Figure 104 (a) and (b) respectively.

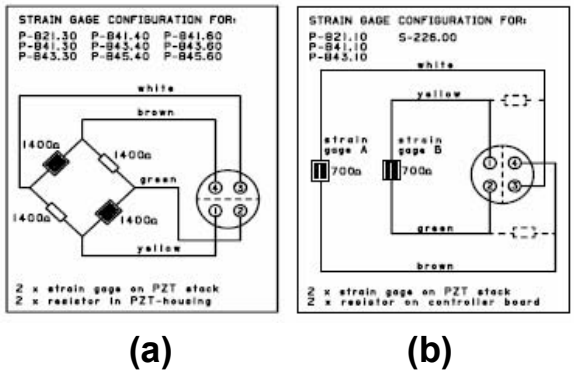

Figure 104 Strain Gauge Configuration

Both piezo position servo-controllers are calibrated with the specific piezoelectric actuators to achieve optimum displacement range, frequency response and settling time. The calibration is performed at the factory and a report, which plotted and

tabulated positioning accuracy was supplied with the piezo actuators. The vendor states that the equipment was tuned and tested with Zygo ZMI-2000 and ZMI-100 interferometers and their nanometrology calibration laboratories are seismically, electromagnetically and thermally isolated, with temperatures controlled to better than 0.25˚C/24hr. The displacement curves from the calibration documentation for both the P-841.10 and P-841.60 piezo actuators are shown in Figure 105.

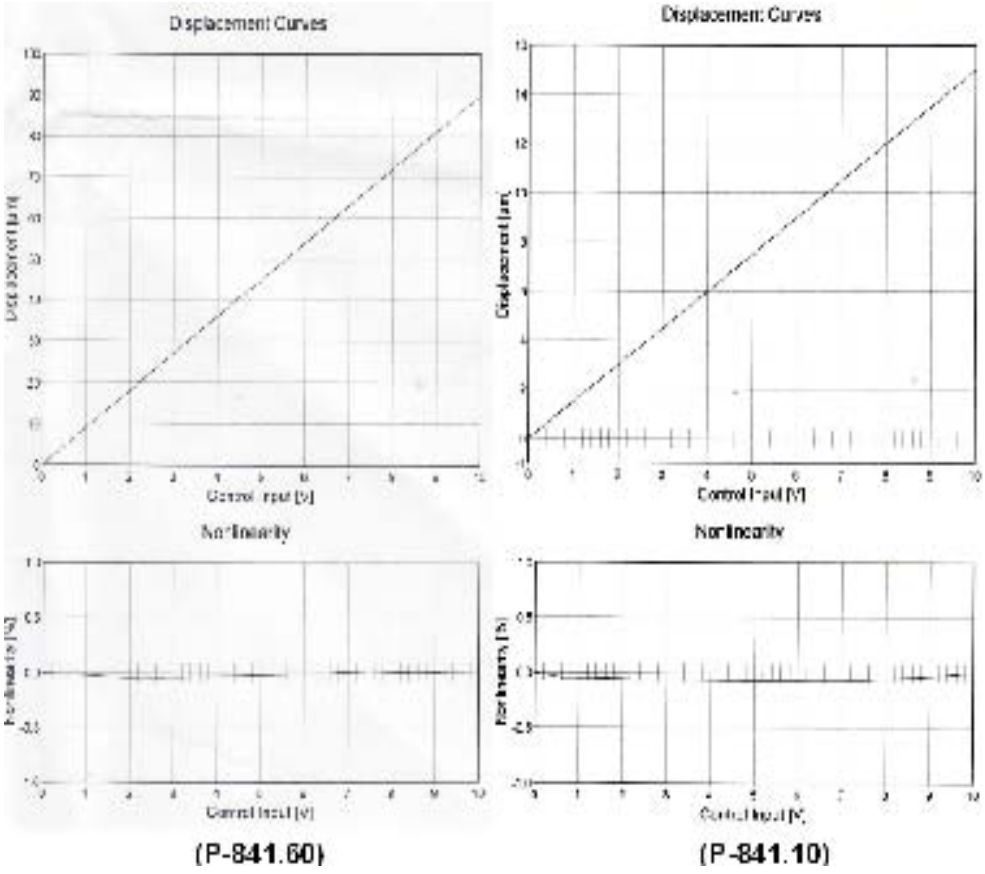

Figure 105 Displacement Curves

5.1.2.3 Piezoelectric Amplifier and Position Control

The electronics play a key role in the performance of piezoelectric actuators; ultra-low noise, high stability servo-controllers and linear amplifiers are essential because piezoelectric actuators respond with motion to even μvolt changes of the control voltage. Two separate Physik Instrumente E-610 LVPZT Piezo Amplifier and Position Servo-Controllers, control the P-841.10 and P-841.60 piezoelectric actuators, (Figure 106). This is a stand-alone amplifier and position servo-control board which is specifically configured for low voltage piezo actuators. Low voltage piezos generally operate within a nominal voltage range from 0 to +100v, although they can be used beyond their nominal operating voltage range; the maximal allowed voltage range covers –20 to +120v. This extended operating range gives 40% more expansion than the stated nominal values. Positive voltages cause the piezo to expand and negative voltages cause the piezo to retract; applying negative voltage to the piezo causes an electrical field opposed to the polarization direction and the piezo retracts. For example the P-841.10 piezo specified with 15μm nominal expansion can thus be used with a range of 21μm.

Figure 106 E-610 LVPZT Controller/ Amplifier

The specific type of E-610.SO amplifier/controller used in this project is the E-610.SO: this version controls strain gauge sensor equipped piezo actuators.

The E-610.SO controller/amplifier can be operated in four ways:

1. Open-Loop External Control (Amplifier Mode)

The output voltage is controlled by an analog signal ranging from –2 to +12v. Multiplying by the gain factor of 10, an output voltage of –20 to +120v results.

2. Open-Loop Manual Control (Power Supply Mode)

With 0v input signal, the output voltage can be set by an external, DC-offset potentiometer in the range of 0 to 100v.

3. Closed-Loop External Control (Position-Control Mode)

Displacement of the piezo actuator in this mode is controlled by an analog signal in the range of 0 to 10v. The controller is calibrated in such a way that 10v corresponds to maximum nominal displacement and 0v corresponds to zero displacement.

4. Closed-Loop Manual Control

With 0v input signal, displacement of the piezo actuator can be set by a DC-offset potentiometer in the range of zero to max nominal displacement.

The E-610 is a single-channel amplifier and position controller with an average output power of 6 watts. It consists of an amplifier, a sensor supply and a processing circuit. The latter includes a preamplifier, demodulator, different filters, proportional-integral (P-I) controller and a processing submodule for strain gauge sensors. The E-610 is suitable for static and dynamic applications; low voltage piezo actuators have high capacitances therefore the amplifiers are designed to supply appropriate high peak currents for dynamic applications. High stability, low noise, excellent linearity and stability allow the use of the E-610 in precision instruments.

The E-610 amplifier/controller is designed as a EURO-board plug in module; the two amplifier/controllers are mounted in separate rack-mount chassis located side by side within a specially developed control cabinet. To facilitate operation of the E-610 LVPZT Piezo Amplifier and Position Servo-Controllers in the control cabinet, the unit is supplied with a solderable socket matching the 32-pin main connector as shown in Figure 107; the 32 pins used all carry

Figure 107 32-Pin Connector and Control Cabinet Mount Sockets

even number designations and are in two rows “a” and “c”. This connector allows the E-610 units to be removed from each of the rack- mount chassis without the need to disconnect any wires. A panel-mount coaxial socket (Lemo ERN.00.250 CTL) is used for bringing the piezo drive-voltage lines on the 32-pin connector outside the control cabinet to interface with the piezos within the measurement instrument, see Figure 107. A second panel-mount socket, this time a 4-conductor (Lemo ERA.0S.304.CLL) is used to interface the strain gauge sensor excitation and readout lines with the 32-pin connector within the control cabinet, see Figure 107.

PZT output, LEMO center*	a	2	c	PZT output*
PZT GND, LEMO shield*	a	4	c	PZT GND*
nc	a	6	c	nc
Monitor PZT out (100:1)	a	8	c	Internal use
Internal use	a	10	c	Amplifier input
10 kOhm pot (-10 V)	a	12	c	Pot wiper
10 kOhm pot (GND) & test GND	a	14	c	Pot 10 kOhm (GND) & test GND
+VCC supply	a	16	c	+VCC supply
-VCC supply	a	18	c	-VCC supply (connect to 20c for minimum noise)
Test GND	a	20	c	Test GND
Sensor monitor[1]	a	22	c	Sensor monitor GND, Test GND
Display sensor (adjust.)	a	24	c	Sensor excitation, see wiring diagram, 4-line LEMO pin 1*
Overflow (TTL)	a	26	c	Sensor readout signal, see wiring diagram, connect to 4-line LEMO pin 2*
Servo OFF/ON select	a	28	c	Sensor readout signal, see wiring diagram, LEMO pin 3*
Internal use	a	30	c	Sensor excitation GND, see wiring diagram, LEMO pin 4*
Protective GND	a	32	c	Protective GND

Table 12 32-Pin Main Connector Pin Assignments

Table 12 shows the pin assignments for the 32-pin main connector. In open-loop positioning mode, the position servo-control circuit is bypassed and the system works like an amplifier; the piezo drive voltage is proportional to the control signal input. The piezo output voltage can be monitored either directly in parallel with the piezo or on the main connector pin 8a, which carries a high-impedance output of $1/100^{th}$ the voltage of the piezo. The nominal input voltage is connected on pin 10c.

Closed-loop operation differs from open loop operation in that the analog control input signal is interpreted as a target position rather than a target voltage; closed-loop operation offers both drift-free and hystersis-free positioning. In this closed-loop position-controlled mode, it is the output of the proportional integrated controller that is used as an input to the amplifier; the piezo position is refined until the final position is reached e.g. the controller is calibrated so that 5v should give half the maximum nominal voltage. In this control mode the piezo position is directly proportional to the input signal of the module, while the piezo supply voltage may not be. The piezo supply voltage must remain in the range from –20 to +120v. If one of these limits is reached and the resulting expansion of the piezo does not match that specified by the control signal, a TTL signal (overflow) is output on pin 26a and illuminates a LED.

The operating mode, either voltage controlled (open-loop) or position controlled (closed-loop) is controlled by pin 28a on the main connector: connection of pin 28a to pin 14ac (GND) enables closed-loop (servo on) mode or leaving pin 28a open enables open-loop (servo off) mode.

Figure 108 graphs the E-610.SO supply voltage ranging from +10 to –2v and the resultant strain gauge feedback voltages for open-loop and closed-loop operation. It can be seen that the closed loop (yellow) response is linearised whereas the open loop is not.

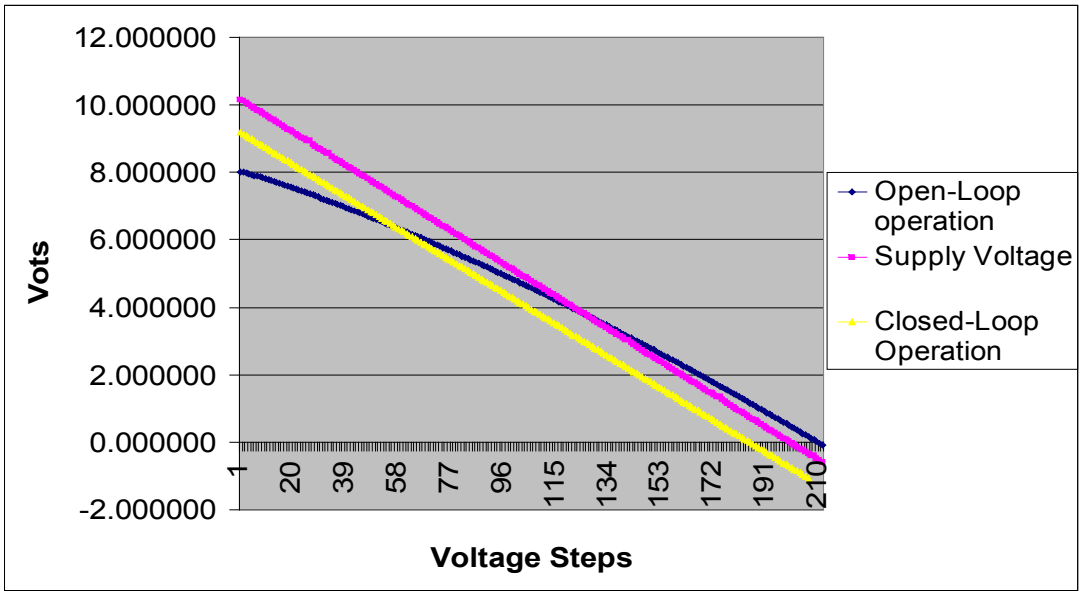

Figure 108 Open-Loop vs. Closed Loop Performance Graph

The application software controls the E-610.SO supply voltage; the software sends the driver commands to generate an analog output signal in the range of +10 to –2v. The supply voltage (purple series) is decremented in steps of 0.05v using the application software, generating 210 separate voltage points. The closed-loop and open-loop feedback voltage plots are directly proportional to the piezo actuator displacement resulting from the supply voltage. In open-loop mode it is clear that there is hysteresis within the system, while in closed-loop mode the piezo displacement is linearly proportional to the supply voltage.

In conclusion, closed-loop position servo-controlled mode eliminates undesirable behaviour such as hystersis and creep and offers superior linearity and repeatability than the open-loop mode. Knowing the exact location of the long-travel positioning piezo actuator when the stage contacts a ball bearing determines the quality of ball bearing measurement; therefore to ensure unbiased and precise ball measurements the primary piezo actuator is operated using the closed-loop mode.

The secondary touch sensor piezo is operated using the open-loop mode because it is only required to detect the sudden change in strain when the tip comes into contact with a ball bearing; it is not required for precise positioning.

Figure 109 illustrates the appropriate wiring of a single E-610.SO 32-Pin main connector. The pins are assigned to the piezo drive-voltage lines coaxial panel mount socket, strain gauge sensor excitation and readout lines 4-conductor panel mount socket, 24v power supply and the BNC-2120 breakout box; each wire is soldered to its dedicated pin. For ease of assembly all the soldered wires are constrained using terminal connector blocks; this groups all the connections and allows for organised cable routing, as shown in Figure 110.

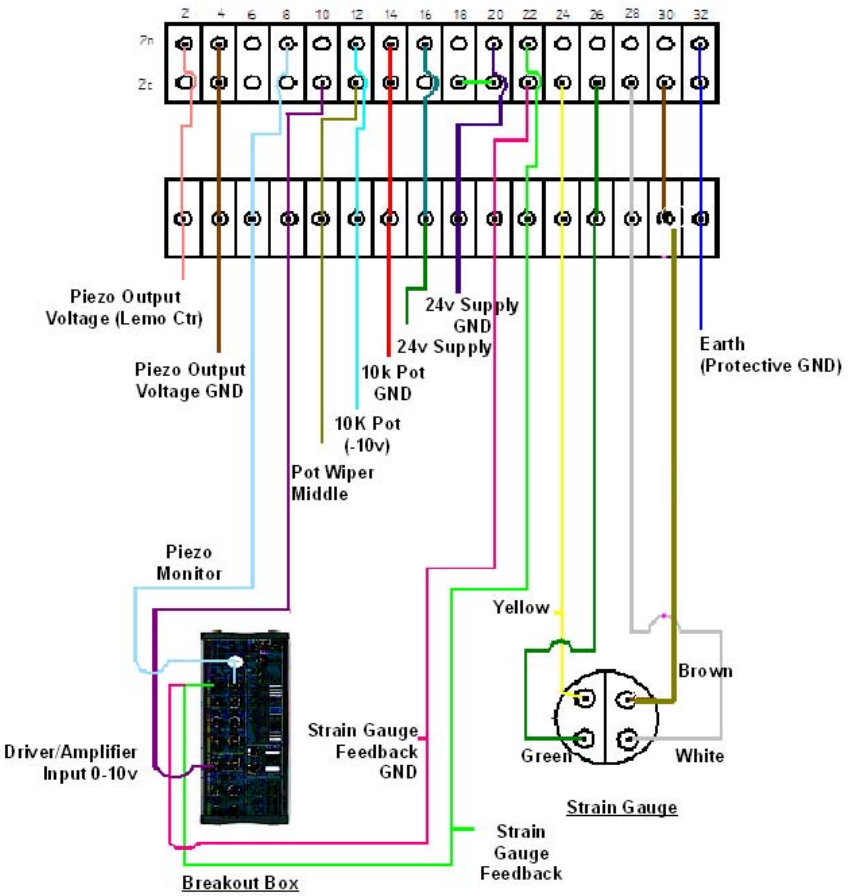

Figure 109 E-610.SO 32-Pin Main Connector Wiring Diagram

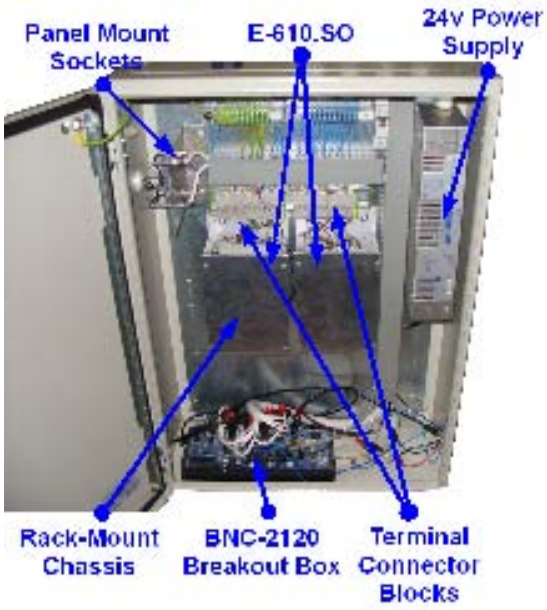

Figure 110 Control Cabinet

During the initial prototyping and testing period within the laboratory, the two E-610 LVPZT Piezo Amplifier/Position Servo-Controllers and all the required electronics were mounted on a mock-up board, as shown in Figure 111; this allowed all of the equipment to be completely tested before installing it into the dedicated control cabinet. The mock-up board also allowed various different equipment layouts to be analysed to determine the most efficient use of the control cabinet space; knowing the exact equipment layout before the installing it into the control cabinet simplified the process significantly.

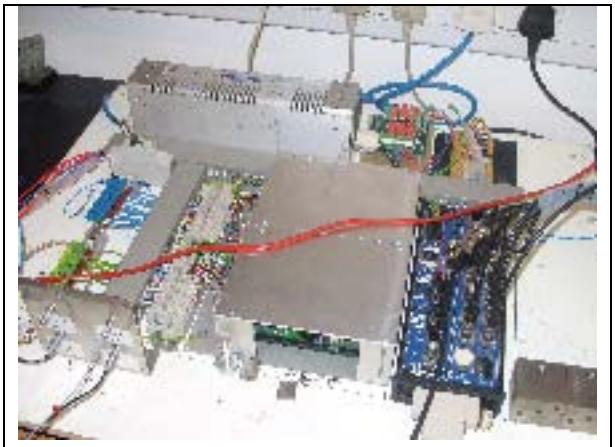

Figure 111 Mock-Up Board

The primary purpose of the control cabinet is to protect the sensitive circuitry in the piezo controllers from electrical noise. Electrical disturbance would interrupt, obstruct, or otherwise degrade or limit the effective performance of the circuits within the piezo controllers. The low voltage analog signal inputs and outputs from the DAQ device are very susceptible to electrical noise during transmission; sensor signals disturbed by an external power source can cause measurement errors and process malfunctions [51].

To reduce the electrical noise within the control cabinet and signal transmission, the following measures were carried out:

- All the cables are run as short as possible
- Each signal outgoing and return (positive and negative) lines are run together
- All cables are screened and the screen is grounded
- There are steel dividing walls within the cabinet between both piezo drivers and the power supply
- All the equipment is mounted on a grounded EMC (Electromagnetic Compatibility) compliant back plate

- Cables from different cable groups are physically separated. Cables can be categorised into four groups: I, II, III, IV

Group I: Very susceptible (analog signals, instrument lines)

Group II: Susceptible (digital signals, sensor cables, 24vDC switching signals, communication signals, e.g. field buses)

Group III: Noise source (control cable for inductive loads, unswitched power cables, contactors)

Group IV: Strong noise sources (output cables from frequency converters, supply cables for welding equipment, switched power cables)

- Noise generating and susceptible cables are crossed at right angles; cross lines from Group I, II and III, IV at right angles
- Cable screens are grounded at control cabinet entry and exit and to the devices

The importance of the above measures are illustrated in Figure 112; the bottom graph shows the strain gauge feedback from the P-841.10 piezo with the control cabinet door closed and the top graph shows the same signal, only this time the control cabinet door is left open. When the cabinet is closed the signal is stable, but when the door is open the signal becomes unstable and randomly drifts high or low.

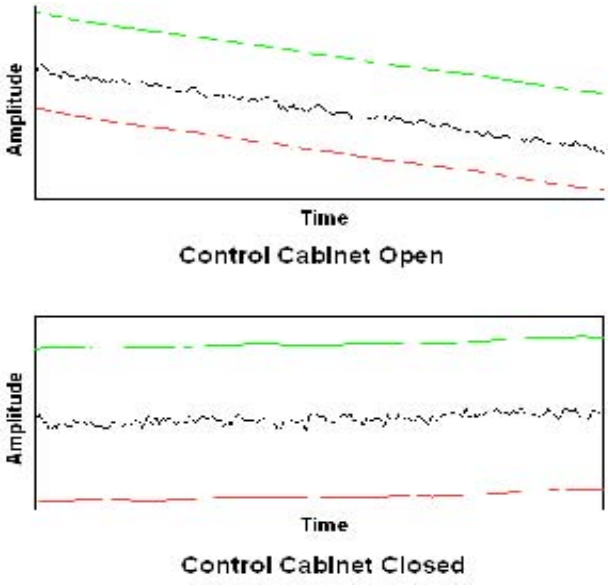

Figure 112 Disturbance due to Electrical Noise

In conclusion, the piezo controllers are very susceptible to external noise sources within the production facility. Without the appropriate measures taken to eliminate the electrical noise, the level of performance of the measurement instrument would be significantly decreased.

5.1.3 Ball Locator Platform

The specific range of balls required to be measured using the piezo measurement instrument is 10-13.494mm. To cater for the entire measurement range using a single measurement instrument, the measurement platform is required to move vertically at least 4mm independently of the flexure unit. This vertical movement is achieved by mounting the ball locator on a precision linear guide, which is driven by a stepper motor as shown in Figure 113.

5.1.3.1 Linear Motion Guide Actuator

The vertical motion is accomplished using a THK Linear Motion (LM) Guide Actuator KR201A+100LH; the LM guide actuator consists of LM guide rails, ball screw and support bearings, Figure 114. This is a high grade LM guide actuator with a lead of 1mm and has a maximum possible stroke length of 41.5mm. The U-shaped outer rail and the ball screw in the centre of the inner block provide high rigidity and precise positioning. The ball races are arranged at a contact angle of 45˚ in relation to one another so that each race of balls bears an equal load on the inner block in all four directions: radial, reverse-radial and the two lateral directions. The four raceways for loaded balls, which are formed into a circular-arc groove, allow balls to roll smoothly even under a preload; preloading eliminates clearances, provides high rigidity for the guideway and minimizes fluctuations in frictional resistance due to a fluctuating load. As a result, a high accuracy in the sun-micron can be can be obtained. To increase the service life of the guide, it is equipped with a grease nipple to eliminate wear on the rolling parts. The data sheet for the LM guide actuator KR201A+100LH is illustrated in Appendix C. The stepper motor is the essential control focus of this unit. Appendix G presents a detailed discussion on stepper motors and stepper motor controllers.

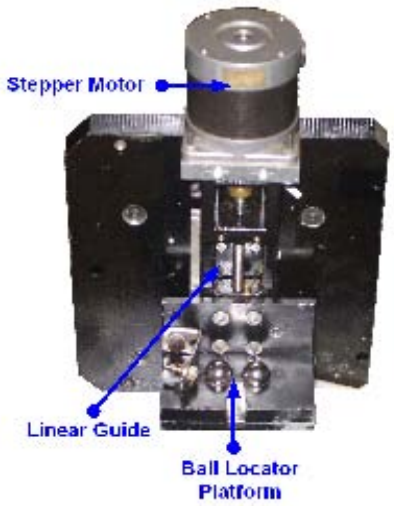

Figure 113 Ball Locator Platform Assembly

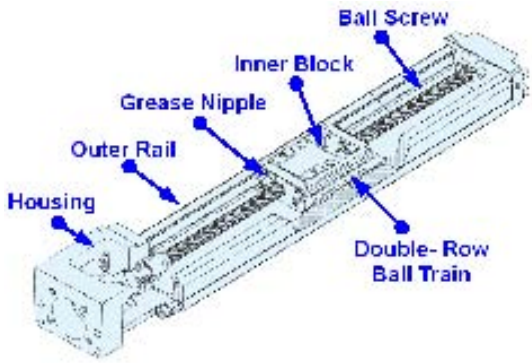

Figure 114 Construction of LM Guide Actuator

5.1.4 Measurement Display

A digital display unit is mounted on the control panel of each machine; this is controlled automatically by the central controller and is updated after each machine is sampled. This unit displays the average measured diameter and the time the sample was taken, allowing the operator to effortlessly identify the precise period in the cycle for each machine. Previously it was required for the operator to take and measure a sample from the each machine to determine the cycle time; this becomes very time consuming when dealing with twenty-four machines.

The measurement display concept originated during the initial stages of testing, when it was realised that having each measurement on the display unit would benefit the automation installation by allowing the operator to test the system. Using the measurement display unit it is possible for the operator to successfully make comparisons between the automated measurement instrument and the manual measurements plotted on the cut-down chart. Also, understanding that the level of automation through a larger scale system would develop over time, it was felt that the measurement display units enhance the confidence in the automation project and would give support to future investment.

The same communication method used between the central controller and the AS-I network controller is also used for the central controller to communicate with the measurement display unit; the central controller RS-232 signal is converted to RS-422 and transmitted across the facility using the same Cat-5 Ethernet cable as the AS-I controller, at the grinding machine location the signal is converted back to RS-232 for the measurement display unit to receive. Figure 115 illustrates the network structure used for the central controller to communicate with the measurement display unit.

The display unit is custom made to display sample measurements determined by the automated measuring instrument. All measurement display units are assigned a unique address with the aim of indicating what machine it is attached to; this addressing system allows a vast amount (99) of display units to communicate on one transmission line. The address of the intended measurement display unit precedes the measurement and time data. Each unit scans all inputs from the central controller on the RS-232/422 transmission line for its specific 8bit address preamble; once the unique address is recognised, the next string of data is processed into the correct format to display the date, time and average sample measurement.

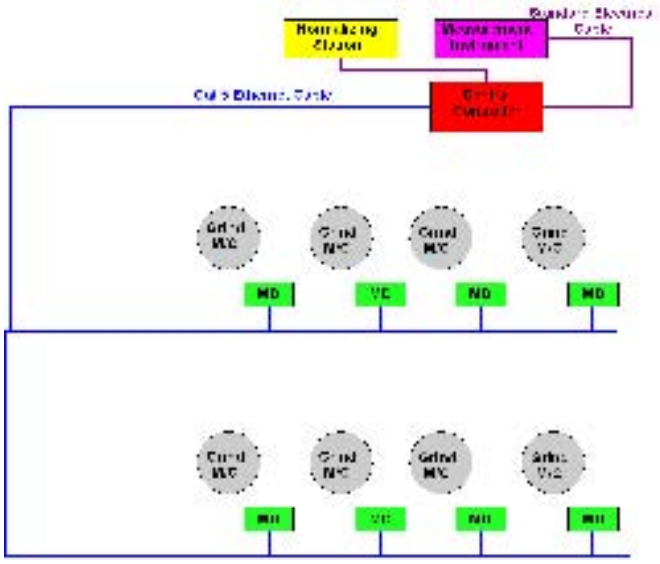

Figure 115 Measurement Display Network Overview

Figure 116 demonstrates a string of data sent by the central controller; this ASCII (American Standard Code for Information Interchange) format string is converted to binary and transmitted down the line; (ASCII is the most common format for text files in computers and on the internet, each alphabetic, numeric, or special character is represented with a 7bit binary number (string of seven 0s or 1s) i.e. 128 possible characters). The first two digits are the measurement display unit address; address 87 is the measurement display unit located at grinding machine no. 305. The next six digits are the average measurement data; the measurement in Figure 116 is 12.1234mm. The last four digits indicate the time the sample balls were measure; the sample in Figure 116 was measured at 11:40. When the display unit receives the binary code it converts this code into ASCII format and displays it on the LCD screen.

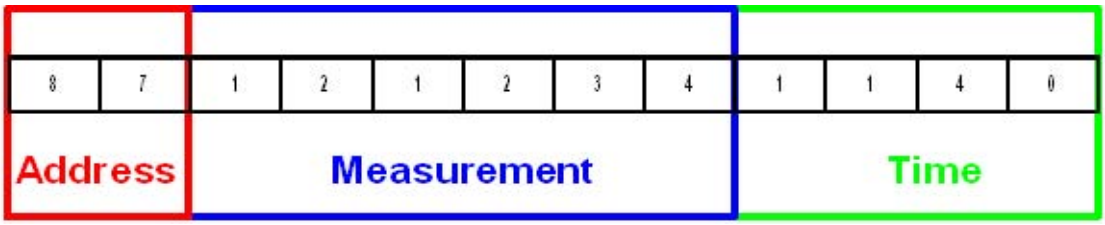

Figure 116 Measurement Display String

The process is completed using a programmed 16bit PIC Microcontroller working with a 5MHz instruction cycle. As shown in Figure 117, the main components in the electronic circuit are the PIC Microcontroller, a MAX232 chip to convert the RS-232 signal into a TTL level for the PIC to read, a voltage regulator to regulate the 24v DC supply to 5v for the PIC, a Liquid crystal display to display the measurements and a reset button. A heavy-duty electrical box houses the complete PCB board and LCD screen

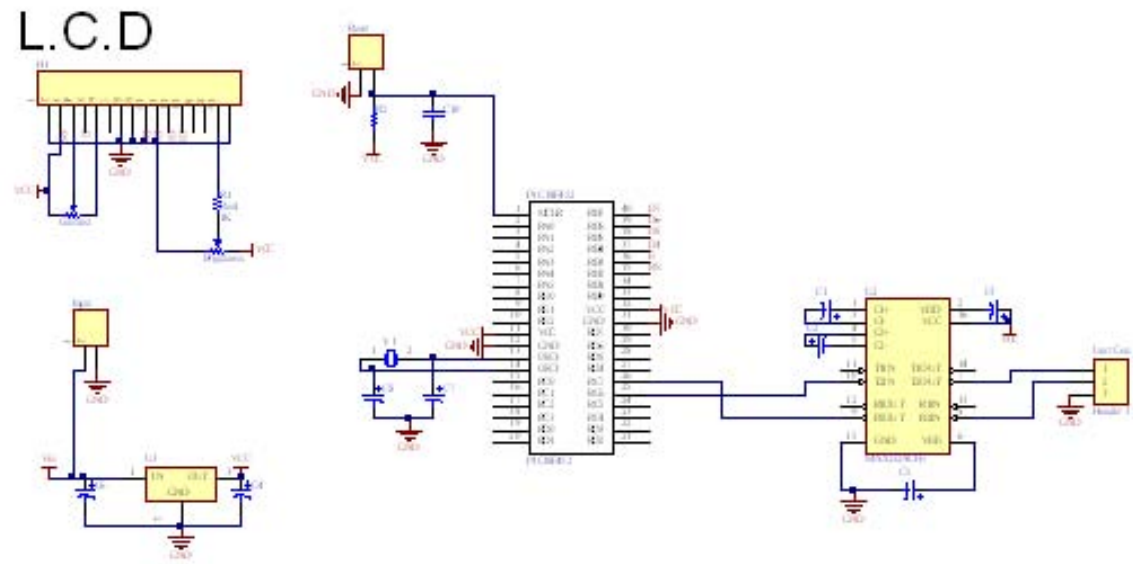

Figure 117 Measurement Display Schematic

Following the completion of the display unit the device operated flawlessly while linked to the central controller with a short cable using the RS-232 standard. However after the installation of a RS-232 to RS-422 interface converter and connection to the RS-232/422 network the display unit failed to operate. Investigation showed that the converter uses the control lines Clear To Send (CTS), Request To Send (RTS), Carrier Detect (CD) and Data Terminal Ready (DTR) from the RS-232 connection to power the device. The measurement display is only capable of receiving data; therefore under normal operation the control bits were not in place. To overcome this problem it was required to power the interface converter from an external source; RTS and DTR were connected to ground (-) and positive (+5v) respectively of a regulated external power supply.

Figure 118 Measurement Display

5.2 System Control

5.2.1 Introduction

This Chapter discusses in detail the control of the measurement process using the central controller; the central controller controls the piezo measurement instrument, ball-locating platform and temperature normalizing station. It also performs the SPC analysis and communicates with the AS-I central controller and measurement display unit. The central controller is a Labview VI operated using a PC.

The central controller VI can be broken down into eight sections: next

1. Analog and Digital I/O's
2. Piezoelectric Actuator Control
3. Ball Touch Detection
4. Ball Diameter Calculation
5. Write to File
6. Network Communication
7. Ball Locator Platform Control
8. Statistical Process Control

The complete measurement process operates in a series of steps as follows:

1. The central controller VI reads from the AS-I control network; the feedback received identifies the precise machines in operation at that moment in time.
2. Each machines in operation returns a "machine on" signal. Subsequently, the central controller sends a signal to each machine in operation requesting a ball sample.
3. The ball retrieval arm on each machine retrieves a sample from the machine turntable. After the sampling process, each machine sample is propelled to the temperature-normalizing station using the ball transfer system.
4. On arrival at the normalizing station each sample activates an individual proximity sensor; this allows the central controller to recognize which samples have arrived and the exact time of arrival. At this point, the

central controller starts the temperature-normalizing timer for each machine sample.

5. Following temperature normalizing, the central controller VI triggers the temperature-normalizing controller PLC to commence the ball delivery system.
6. Two reference standard balls and five production balls arrive at the measurement instrument.
7. The central controller triggers the ball delivery/removal system and the minimum reference ball is inserted into the measurement instrument; the fibre optic sensor activates when the ball is located accurately. Subsequently, the ball-locating platform is brought into range of the measurement instrument by means of the stepper motor driven linear motion guide actuator.
8. Calibration of the minimum reference ball commences.
9. Following the minimum reference ball calibration, the minimum reference ball is removed and the maximum reference is inserted into the ball-locating platform.
10. Calibration of the maximum reference ball commences.
11. Following the maximum reference ball calibration, the maximum reference ball is removed and the first sample ball is inserted into the ball-locating platform.
12. The sample ball measurement process continues until all the five sample balls are successfully measured.
13. After the measurement process, the central controller calculates the sample mean, the sample range, the sample variance and the sample standard deviation.
14. The central controller stores the date of measurement, the time of measurement and the actual five sample measurements to file.
15. The time of measurement and the sample mean is transmitted and displayed on each measurement display unit.
16. The central controller uses Statistical Process Control to calculate if the measurements taken lie within the control lines.

17. Machine Adjustment:

a. If the measured sample mean diameter is too large for the machine cycle time, the cut down rate has to be accelerated; therefore, a signal is sent to the grinding machine controller to increase the operating pressure.

b. If the measured sample mean diameter is too small for the machine cycle time, the cut down rate has to be decelerated; therefore, a signal is sent to the grinding machine controller to decrease the operating pressure.

5.2.2 Analog and Digital I/O's

Development of a measurement application that can acquire and generate signals requires the configuring of virtual channels using Measurement and Automation Explorer; Measurement and Automation Explorer (MAX) provides access to DAQ devices and allows an operator to create and edit channels, tasks, interfaces and virtual instruments. In addition to the standard tools, MAX can be used to configure, diagnose or test virtual channels within the system.

A physical channel is a terminal or pin at which one can measure or generate an analog or digital signal; every physical channel on a device has a unique name. Virtual channels are software entities that encapsulate the physical channel along with other channel specific information- range, terminal configuration, scaling information and type of measurement or generation.

The PCI-6024E (Section 5.1.2.1) device has sixteen analog input physical channels ranging from ai0 to ai15. Channels 0 through 7 can be configured in differential mode. When a channel is configured in differential mode, the channel is the positive input and the channel plus eight is the negative input. For instance, if Channel 1 is configured in differential mode, the positive is Channel 1, and Channel 9 is the negative input. The E series device also has two analog output channels, ao0 and ao1. The device has eight lines of digital input and output named Dev1/port0/line0 through Dev1/port0/line7; these lines belong to a single port, and the physical channel Dev/port0 refers to all eight lines at once. Table 13 shows the list of virtual channels and their channel specific information for the measurement instrument.

Virtual Channels				
Channel Name	**Channel Type**	**Description**	**Physical Channel**	**Range**
SGS1	Analog Input	P-841.1 SGS Feedback	AI0	10v (±5v)
SGS6	Analog Input	P-841.6 SGS Feedback	AI1	20v (±10v)
Controller Supply1	Analog Output	P-841.1 Controller Signal Input	AO0	20v (±10v)
Controller Supply6	Analog Output	P-84.6 Controller Signal Input	AO1	20v (±10v)
Step Input	Digital Output	Stepper Motor Step Input	DIO1	
Direction Control	Digital Output	Stepper Motor Direction Control	DIO0	

Table 13 Virtual Channels

The analog input channels and analog output channels all have a resolution of 12bits (1 in 4,096). Resolution is the smallest input signal change that a device can detect [52]; the number of bits used to represent an analog signal determines the resolution of the ADC (analog to digital converter). For example, a 3bit ADC divides the range into 2^3 or 8 divisions; a binary code between 000 and 111 represents each division. The ADC translates each measurement of the analog signal to one of the digital divisions.

The resolution and device range of a measurement device determine the smallest detectable change of the input signal called the code width; the smaller the code width, the more accurate the measurements are. The code width is calculated using the following formula:

$$CodeWidth = \frac{DeviceRange}{2^{\mathrm{Re}\,solution}}$$

Therefore the code width or the smallest detectable voltage change for the virtual channels SGS1 and SGS6 is 2.4mv and 4.8mv respectively. With the SGS1 and SGS6 DC signals, the attribute of greatest interest is how accurately (unbiased) the amplitude of the signal can be measured at a given point in time.

Figure 119 illustrates the section of the central controller block diagram that acquires and averages the strain gauge feedback analog inputs; each symbol on the block diagram represents a Labview subroutine (subVI), which can be another Labview program or a Labview library function.

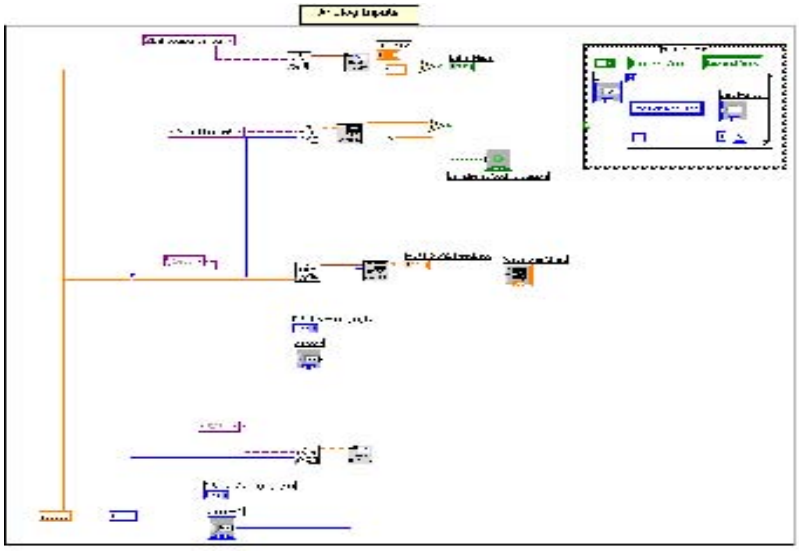

Figure 119 Central Controller Block Diagram that Acquires and Averages the Strain Gauge Feedback Analog Inputs

The central controller uses the AI Acquire Waveform VI to acquire the P-841.1 and the P-841.6 strain gauge feedback waveforms. The VI acquires a specified number of samples at a specified sample rate from a single channel and returns the acquired data; the AI Acquire Waveform VI performs a timed measurement of a waveform (multiple voltage readings at a specified sampling rate) on each of the strain gauge feedback channels. The number of samples and sample rate inputs define the waveform of data acquired. For example, if the number of samples is set to 10,000 and the max guaranteed sampling rate for analog input channel on the PCI-6024E device is 200KS/sec, the VI takes 0.05 seconds to acquire the 1,000 points.

Instantaneous DC measurements of a noisy signal can vary randomly and significantly. Averaging can yield a more useful reading if the strain gauge signals are rapidly changing or if noise exists on the lines; a more accurate measurement can be acquired by averaging out the noise that is superimposed on the desired level. The Basic Averaged DC-RMS VI is utilised by the central controller to average the acquired strain gauge feedback; this VI takes the waveforms in, applies a window to the signal and averages the DC and RMS values calculated from the windowed signal with the previous DC and RMS values according to the averaging type (linear within this project).

As soon as the strain gauge feedback signals are acquired and averaged, the central controller uses charts to display the data in a graphical form on the front panel. Shown on the chart is the current strain gauge measurement with data previously acquired. The strain gauge feedback charts are passed single values at a time; the central controller interprets the data as points on the chart and increments the x index by one starting at x = 0. The frequency at which the measurements are sent to the chart, determines how often the chart redraws. As previously mentioned, the central controller acquires measurements every 0.05 sec, therefore the charts are updated every 0.05 sec.

The virtual channels Controller Supply1 and Controller Supply2, control the input signal for the E-610.SO piezo driver devices; displacement of the piezo actuators is controlled by analog signals in the range of 0 to 10v. The analog output channels have a resolution of 12bits; therefore the finest allowable voltage step is 4.8mv.

Voltages can be generated in two ways; output voltage can be generated using a single DC signal or a time-varying (buffered) signal. Single-point analog outputs are used when the signal level at the output is more important than the rate at which the

output value changes, i.e. need to generate a steady DC value. With single-point analog outputs, the VI that produces the single update must be called every time an output voltage change is required on the output channel; therefore, the voltage can only change as fast as Labview calls the VI, this technique is called software timing. Sometimes the rate at which the output voltage varies is as important as the signal level, as in waveform generation. For example, if the DAQ device is could act as a function generator by using a VI that generates one cycle of a sine wave, stores one cycle of sine wave data in a waveform and programs the DAQ device to generate the values continuously from the waveform one point at a time at a specified rate.

The controller supply signal levels to the piezo drivers are more important than the rate of change; the piezo position is directly proportional to the piezo controller signal input. For this reason the measurement instrument is controlled by single-point analog outputs. The central controller single-point analog outputs are generated using the AO Update Channel VI; this VI writes a specified value to the controller supply output channels. The specified values are determined by the "P-841.6 Extended Value" and the "P-841.1 Extended Value" controls, which both have five digits of precision; changing the control value results in changing the analog output signal which in turn alters the piezo position.

The central controller VI controls the stepper motor that drives the ball-locating platform; the step input and motor direction is controlled using the digital lines D101 and D100 respectively. Digital lines and ports are important parts of a digital input/output system. A line is an individual signal and refers to a physical terminal; the data that a line carries are called bits, which are binary values that are 1 or 0. A port is a collection of digital lines, these lines are grouped into an 8bit port (port with eight lines); the PCI-6024E device has one 8bit port.

The digital signal is either

- 0v –0.8v = Logic Low
- 2v – 5v = Logic High

The digital lines D101 and D100 are controlled using the Write to Line VI; this VI sets the output logic state of a digital line to high or low on a specified digital channel. The line state is controlled using Boolean constants; line state is True for high logic and False for low logic.

5.2.3 Piezoelectric Actuator Position Control

The analog output signal that determines the displacement of the P-841.6 piezo actuator is controlled by "P-841.6 Extended Value" control; the displacement is altered by increasing or decreasing the voltage value of the control. The value of the "P-841.6 Extended Value" control is increased or decreased by incrementing or decrementing the voltage value by a specified step value; the voltage step is controlled by the "Step Size" control.

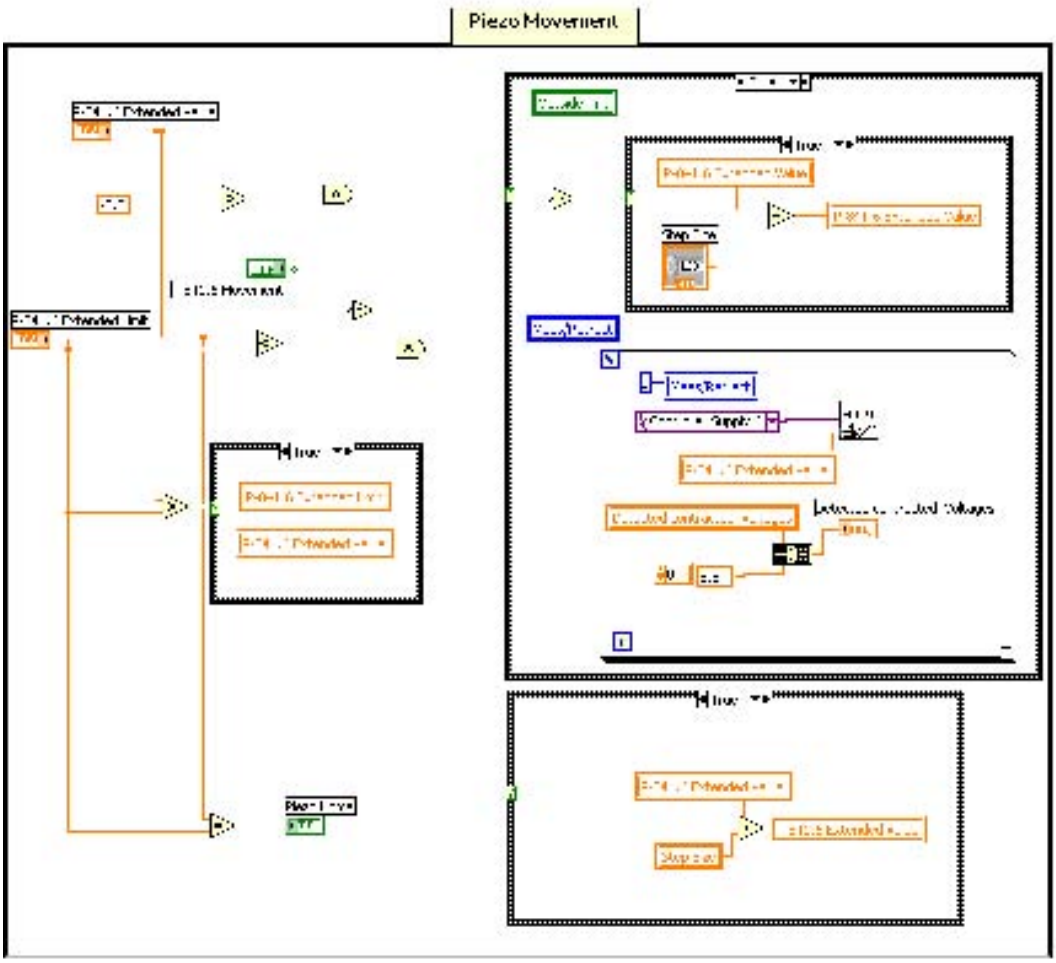

Figure 120 Central Controller Block Diagram that Controls the Piezo Actuator Position

Figure 120 illustrates the section of the central controller block diagram that controls the position of the P-841.6 piezo actuator. If the current "P-841.6 Extended Value" is greater than –0.5, and the "P-841.6 Movement" button is true, the True subdiagram of the case structure is selected; a case structure has two or more subdiagrams, or cases. Only one subdiagram is visible at a time and the structure executes only one case at a time; an input value determines which subdiagram executes.

At this point if the Boolean Not function after the Boolean indicator “Outside Limit” logic is true the “P-841.6 Extended Value” is continuously decremented by “Step Size”; a Not function computes the logical negation of the input. The Boolean indicator “Outside Limit” is activated when the measurement instrument makes contact with a sample ball during the measurement process, if there is no contact between ball and instrument the indicator is set false and if contact is made the indicator is set true.

The piezo continues to retract until the measurement instrument contacts a sample ball or the “P-841.6 Extended Value” is less than –0.5 (piezo fully retracted) or the “P-841.6 Movement” button is set false. When one of these instances occurs, the piezo automatically extends by incrementing the “P-841.6 Extended Value” until it is equal to “P-841.6 Extend Limit”, this limit set to 10v; therefore the output signal cannot exceed 10v and the max allowable piezo displacement is 90µm.

5.2.4 Ball Touch Detection

The strain gauge feedback from the P-841.10 touch sensor piezo actuator is acquired through the virtual channel SGS1. When a sample ball is in place the measurement process can begin; during this process the amplitude of the P-841.10 strain gauge feedback is constantly monitored. When the measurement instrument makes full contact with the sample ball, the strain on the piezo drops instantly because contacting the ball causes the piezo to compress. As mentioned previously it is this sudden change in feedback amplitude that is used to detect contact with the sample ball.

Illustrated in Figure 123, is the section of the central controller block diagram that determines when the measurement instrument makes contact with a sample ball. After the strain gauge feedback signal is acquired, a moving average of the signal is generated; the moving average is used to smooth out short-term fluctuations. The VI used to generate the moving average is the Mean PtByPt VI; this computes the mean of the values in the set of input data specified by the sample length. The sample length is the length of each set of incoming data, the VI performs a computation for each set of data and in this instance the sample length is set to 100 points.

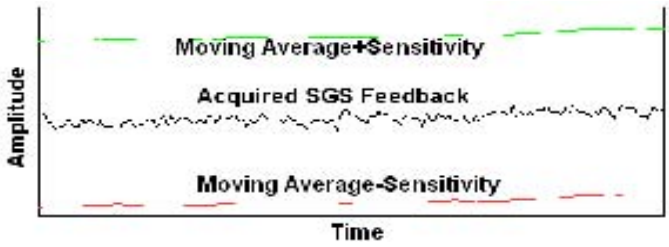

Figure 121 Acquired Strain Gauge Feedback Signal and Computed Moving Average

Once the moving average is computed, a sensitivity value of ±0.002v is applied to the averaged signal, (Figure 121); the moving average + sensitivity and moving average – sensitivity signals are constantly compared to the acquired SGS feedback signal to determine if contact is made between the measurement instrument and sample ball i.e. contact is made if the amplitude of the SGS signal suddenly falls below the moving average – sensitivity signal, see Figure 122.

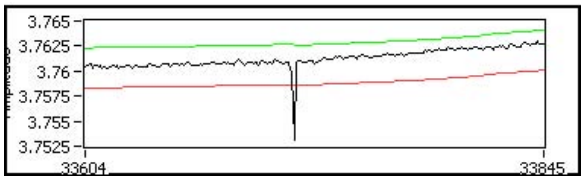

Figure 122 Amplitude of SGS Signal when Contact is made with Sample Ball

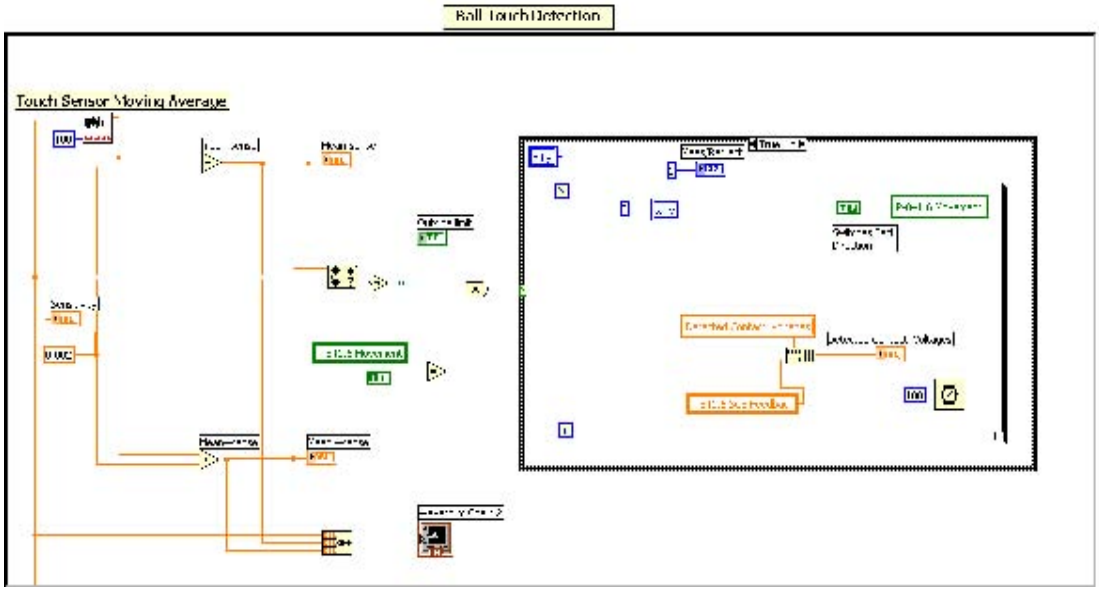

Figure 123 Central Controller Block Diagram that Controls Sample Ball Touch Detection

The central controller uses the In Range and Coerce VI to compare the acquired and averaged signals. This VI determines whether the acquired signal falls within a range specified by the upper limit and lower limit; the moving average + sensitivity and moving average – sensitivity signals are used to set the upper and lower limits. When the measurement instrument is not in contact with a sample ball, the acquired signal is within the range and when contact is made the signal suddenly drops below this range. If the signal is within the range the VI output "In Range" is set true and when outside the range, "In Range" is set false. A Boolean Not function is used to invert the "In Range" output to ensure that when there is no contact the "Outside Limit" LED is off and when contact is made the LED is turned on.

5.2.5 Ball Diameter Calculation

The expansion and contraction of the P-841.6 long travel piezo actuator is tracked by means of two strain gauges attached to it; the strain gauge feedback signal is acquired through the virtual channel SGS6. When a sample ball is in place the long travel piezo is retracted, the amplitude of the DC voltage feedback immediately prior to retraction is recorded. The exact amplitude of the voltage feedback is again recorded when the measurement instrument makes full contact with the sample ball. Having recorded the DC voltage feedback of the piezo actuator at point of contact and also prior to retraction, software based routine computes the actual distance travelled by the piezo actuator. This is then compared to the equivalent maximum and minimum reference ball travel distance to establish the actual diameter of the reference ball with a very high degree of confidence.

At the start of the measurement process when the piezo is retracted, the central controller VI instantly records the amplitude of the strain gauge feedback and saves into the "Detected Contracted Voltage" array and the voltage at the point of contact is recorded and saved into the "Detected Contact Voltage" array.

When the contracted and contact voltages are known, the difference between the two values is calculated to determine the change in voltage during the measurement process; the change in voltage is proportional to the actual distance travelled by the piezo actuator as shown in Figure 124.

Detected Contracted Voltage – Detected Contacted Voltage = Voltage Difference

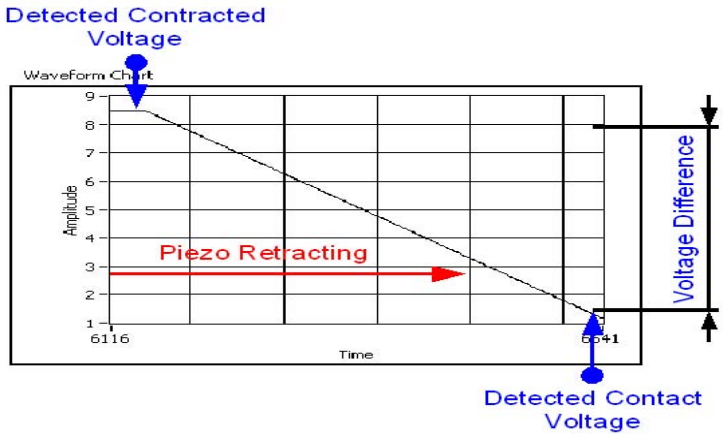

Figure 124 P-841.6 Feedback Chart

During the measurement instrument calibration process, the voltage difference for the minimum reference ball is calculated and stored in the "Vball1" indicator and the voltage difference for the maximum reference ball is calculated and stored in the "Vball2" indicator.

$$Voltage\ Difference\ for\ Min\ reference\ ball = Vball1$$
$$Voltage\ Difference\ for\ Max\ reference\ ball = Vball2$$

After the voltage difference for the measured sample ball is calculated, the voltage difference (D_v) between the sample ball difference and Vball1 is determined, see Figure 125; this establishes the difference in the strain gauge voltage feedback between the two balls and is used to calculate the difference in height between the two balls.

$$D_v = Vball1 - Sample\ Ball\ Voltage\ Difference$$

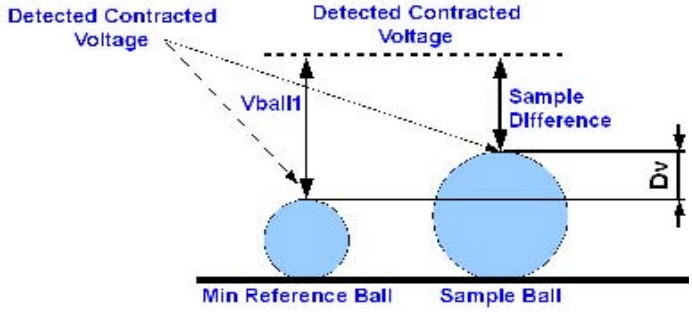

Figure 125 Calculate D_v

The voltage difference (Cv) between the minimum and maximum reference ball differences is also calculated:

$$C_v = Vball1 - Vball2$$

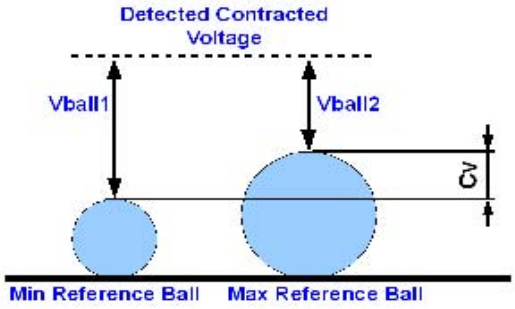

Figure 126 Calculate C_v

The maximum and minimum calibration ball diameters for each nominal ball diameter are known. The values for each nominal ball size are stored in a database and when a specific nominal ball diameter is measured the central controller calls the maximum and minimum reference ball diameters that match that specific nominal ball.

The central controller then calculates the difference in heights (C_d) in mm, between the maximum and minimum reference balls:

$$C_d = Max\,reference\,ball\,diameter - Min\,reference\,ball\,diameter$$

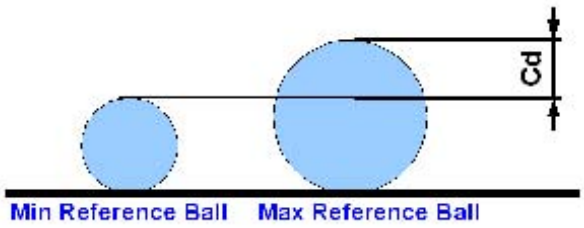

Figure 127 Calculate C_d

At this point, the amplitude change of the strain gauge voltage feedback for every mm of travel by the piezo actuator (V/mm) is calculated:

$$\frac{Voltage\,Dif\,between\,Min\,and\,Max\,ref\,ball\,Differences(C_v)}{Height\,Dif\,between\,Min\,and\,Max\,ref\,balls(C_d)} = Change\,in\,V\ per\,mm\,of\,Travel$$

$$V/mm = \frac{C_v}{C_d}$$

Once D_v and V/mm are known, the actual distance in mm between the top of the minimum reference ball and the top of the sample ball (Z) can be calculated as follows, see Figure 128:

$$Z = \frac{Dv}{\left(\frac{C_v}{C_d}\right)}$$

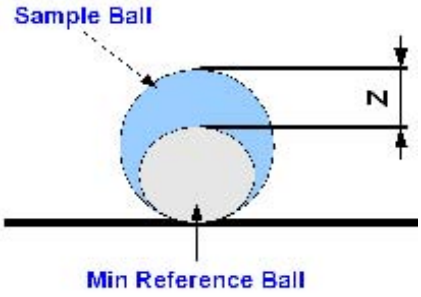

Figure 128 Calculate Z

The actual diameter of the sample ball is then simply calculated by adding the distance between the top of the reference ball and the top of the sample ball (Z) to the diameter of the minimum reference ball, see Figure 129.

$$Sample\ Ball\ Diameter = Z + Diameter\ of\ \min reference\ ball$$

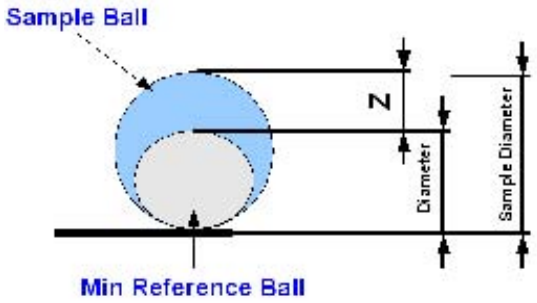

Figure 129 Calculate Ball Diameter

An example of a sample ball calculation is given below:

- Minimum Reference Ball Diameter = 13.0820mm
- Maximum Reference Ball Diameter = 13.1826mm
- The voltage difference for the minimum reference ball Vball1 = 8.07540v
- The voltage difference for the maximum reference ball Vball1 = 1.66659v
- Sample Ball Contracted Voltage = 8.5v
- Sample Ball Contact Voltage = 2.9061v

$$Sample\ Ball\ Voltage\ Difference = 8.5v - 2.9061v = 5.5939v$$

$$D_v = Vball1 - Sample\ Ball\ Voltage\ Difference = 8.0754v - 5.5939v = 2.4815v$$

$$C_v = Vball1 - Vball2 = 8.0754v - 1.66659v = 6.40881v$$

$$C_d = Max\ ref\ ball\ diameter - Min\ ref\ ball\ diameter = 13.1826 - 13.0820 = 0.1006mm$$

$$V/mm = \frac{C_v}{C_d} = \frac{6.40881v}{0.1006mm} = 63.705v/mm$$

$$Z = \frac{Dv}{\left(\frac{C_v}{C_d}\right)} = \frac{2.4815v}{63.705v/mm} = 0.038mm$$

$$\therefore Sample\ Ball\ Diameter = Z + Diameter\ of\ \min ref\ ball = 0.038 + 13.0820 = 13.1209mm$$

5.2.6 Write to File

Successful control of the production process by the measurement instrument allows for the development of information systems for effective data analysis. Meaningful data about each of the processes is obtained by saving each ball measurement to file; the date and time of measurement along with the actual five ball measurements of a machine sample are stored to file. Reviewing all cycle times and cut down rates for each nominal ball size, allows the quality engineer to gain more insight into the process variables.

Development of a file operation within Labview involves the following process:

1. Create or open a file. Indicate where an existing file resides or where the new file is to be created by specifying a file path.
2. After the file opens, write to the file
3. Close the file

The central controller saves the data in text files format because they are the most common and most portable. Text files are the easiest to use and share; almost any computer can read from or write to a text file; text files makes the data available to other applications, such as Microsoft Excel. If random access file reads or writes or if speed and compact disc space were crucial, binary files would prove more efficient than text files; storing binary data, such as an integer uses a fixed number of bytes on disk. For example, storing any number from 0 to 4 billion in binary format, such as 1, 1000 or 1,000,000 takes up 4 bytes for each number.

The central controller uses the Write Characters to File VI to save the sample measurement data; this VI writes a string of characters as lines to a file. Therefore, to write

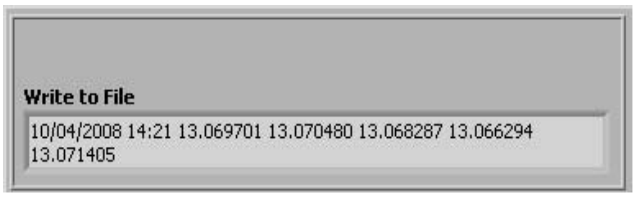

Figure 130 Measurement Data String

the data to file, the data must first be converted to a string as shown in Figure 130. To use the data in a spreadsheet file, the string is formatted as a spreadsheet string; this is a string that includes delimiters, such as tabs.

Figure 131 illustrates five different machine samples as viewed in Microsoft Excel; the machine sample data contains the date, time of measurement and the actual five ball measurements.

Date	Time	Sample1	Sample2	Sample3	Sample4	Sample5
27/03/2008	11:36	13.15301	13.1619	13.153	13.1514	13.15518
27/03/2008	12:00	13.15759	13.15288	13.15143	13.15419	13.15265
27/03/2008	12:13	13.15825	13.15403	13.16135	13.15246	13.15223
27/03/2008	12:22	13.15151	13.15358	13.15642	13.1616	13.15335
27/03/2008	12:30	13.15261	13.15547	13.15855	13.15453	13.15384

Figure 131 Measurement Data

5.2.7 Network Communication

The central controller communicates with the Actuator Sensor-Interface (AS-I) network and the Measurement Display Unit using the RS-232 asynchronous communication standard (see Appendix H). The Virtual Instrument Software Architecture (VISA) provides the programming interface between the hardware and the Labview development environment; VISA is a standard for configuring, programming and troubleshooting instrumentation systems comprising GPIB, VXI, PXI, Serial, Ethernet and/or USB interfaces. NI-VISA includes software libraries, interactive utilities and configuration programs through Measurement and Automation Explorer.

The central controller first configures the serial port using the VISA Configure Serial Port VI; this initialises the serial port specified by the VISA resource name to the specified settings. The VI configures, the COM1 serial port baud rate, data bits, parity, stop bits and flow control. The port is configured with a baud rate of 9600, 8 data bits, even parity, 2 stop bits and no flow control.

At the AS-I controller, the RS-232 interface block (FX2n-232if) is connected to the PLC to allow serial data communication between the AS-I PLC and the RS-232 interface on the central controller PC. The RS-232 interface block transmits data with the PC via buffer memories (BFM), each having 16bit RAM of memory. The buffer memory is configured to match the central controller communication format; selecting the specified details from Table 14 outlines the BFM communication format.

BFM #0: Communication format

Bit	Description	0	1	Initial value
b0	Data length	7 bit	8 bit	1 : 8 bit
b1 b2	Parity	(00) : None (01) : Odd (11) : Even		(11) : Even
b3	Stop bit	1 bit	2 bit	0 : 1 bit
b4 b5 b6 b7	Baud rate (bps)	(0011) : 300 (0100) : 600 (0101) : 1200 (0110) : 2400 (0111) : 4800 (1000) : 9600 (1001) : 19200		(1000) : 9600 bps
b8 b9	Control line	(00) : Not used (01) : Standard RS-232C (11) : RS-232C interlink connection mode		(00) : Not used
b10 b11	Addition of CR and LF	(00) : Not added (01) : CR only (11) : CR and LF		(00) : Not added
b12 b13	Availability of check sum and ASCII/HEX conversion	(00) : Not available (01) : ASCII/HEX conversion available (10) : Check sum available (11) : Check sum available, ASCII/HEX conversion available		(00) : Not available
b14	Send/receive buffer data length	16 bit	8 bit	0 : 16 bit
b15	Undefined (disabled)			0: Undefined

Table 14 Buffer Memory Communication Format

Depending on the selected format, a 16 bit binary number is generated and converted to Hexadecimal. An example of a selected format with the representing binary number and its Hexadecimal equivalent is shown in Figure 132.

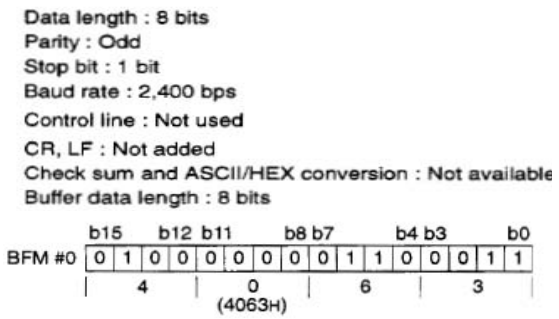

Figure 132 Buffer Memory Configuration Binary Number

The AS-I controller buffer memory is configured to match the central controller communication format by selecting the 16bit binary number: 0100 0000 1000 1111

The central controller VI uses the VISA Write to send data to the AS-I controller and the measurement display; VISA Write writes the data from write buffer to the COM1 serial port. When the write function is automatically selected, the decimal number in the “Serial Write” dialogue box (write buffer) is converted to an ASCII string and is combined with the ASCII start and stop bit string. This complete string is then written to the COM1 serial port in binary format. The start and stop bits allow the AS-I controller receiver to determine the start and end of each packet of data.

To receive data from the AS-I controller, the central controller uses the VISA Read VI; this reads the specified number of bytes from the COM1 serial port and returns the data to the "Serial Read" dialog box (read buffer). For the AS-I controller to send data, it is first required to be in send mode; send mode is activated when the AS-I controller receives the number 64 from the central controller. Once the controller is in send mode, it immediately sends whatever data is in the buffer memory to the central controller; the combination of AS-I slave inputs turned on at that specific moment in time, determines the value in the buffer memory.

During the automatic sampling process, the central controller requests ball samples every 15minutes from each machine currently in operation. Each time the period between ball samples has elapsed the central controller sends a signal to the AS-I controller to determine the exact machines currently in operation. Each specific combination of machines creates a different number in the buffer memory; this number is then transmitted to the central controller.

For example, if the number received at the central controller is 3, this means that just the grind machine is currently operating. The central controller then sends number 75 to the AS-I controller; the number 75 signals that samples are required from just the grind machine. If the number received at the central controller is 8, this means that just the lapping machine is currently in operation. In this instance, the central controller sends number 78; the number 78 signals that samples are required from just the lapping machine. But if the number received is 9, this means that both the lapping and grind machines are currently in operation and the central controller sends number 65 to signal both machines to send ball samples. Finally, if 0 is received, this means that no machines are currently in operation; when no machine is operating, the central controller checks continuously every 10 seconds until one of the machines begin operating.

5.2.8 Ball Locator Platform Control

The central controller VI controls the stepper motor that drives the ball-locating platform. The digital line D100 controls the direction of the motor; if the digital line is logic low, the motor rotates clockwise and if the digital line is logic high the motor rotates anti-clockwise.

The step input is controlled using the digital line D101; the step input pulse is created by constantly changing the line logic low and logic high. The amount of steps the motor turns is controlled by two controls "Steps Count" and "Target Steps", both located on the front panel of the central controller VI. The value located in the "Target Steps" is the required amount of steps the motor is required to turn and the value in "Steps Count" is a count of the amount of steps taken; the motor keeps rotating until the step count equals the amount of steps required.

Switching the digital line high and low using a case structure and a stacked sequence activates each step; a case structure consists of one or more subdiagrams, or frames that execute sequentially. When the amount of steps taken is less than the required steps, the case structure remains true, see Figure 133. The stacked sequence located in the true subdiagram of the case structure is then activated; the first subdiagram sets the digital line logic high. When this subdiagram is complete, the VI enters the next subdiagram where the digital line is set logic low. This logic high-low sequence keeps repeating and continues until the amount of steps taken equals the target amount of steps required.

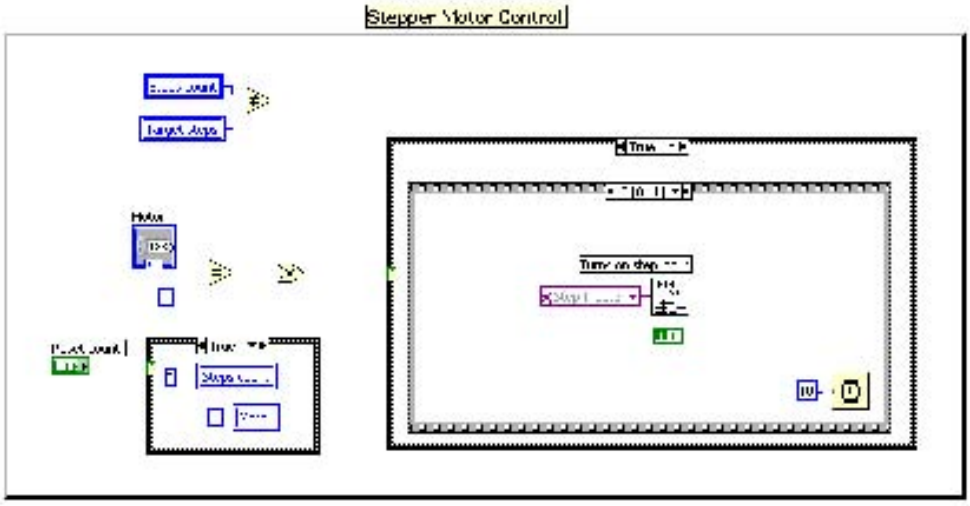

Figure 133 Central Controller Block Diagram that controls the Stepper Motor

5.2.9 Statistical Process Control

Statistical process control (SPC) is an effective method of monitoring a process through the use of control charts; the control chart is a tool used to determine if a manufacturing process is in a state of statistical control or not. If the chart indicates that the process is currently under control then it can be used with confidence to predict the future performance of the grinding process. If the chart indicates that the process is not in control, the pattern it reveals can help determine the source of variation to be eliminated to bring the process back into control; by collecting data from ball samples at various points within the process, the control chart allows significant change to be differentiated from the natural variability of the process. This is the key to effective process control and improvement; with an emphasis on early detection and prevention of problems, SPC has a distinct advantage over quality methods, such as inspection, that apply resources to detecting and correcting problems in the finished ball bearing.

A control chart consists of the following:

- Points representing measurements of ball bearing sample diameters taken from the process at different times (the data)
- A centre line, drawn at the desired ball bearing diameter mean
- Upper and lower control limits that indicate the threshold at which the process is considered statistically out of control
- Upper and lower warning limits, drawn as separate lines, 1.96 standard deviations above and below the centre line.

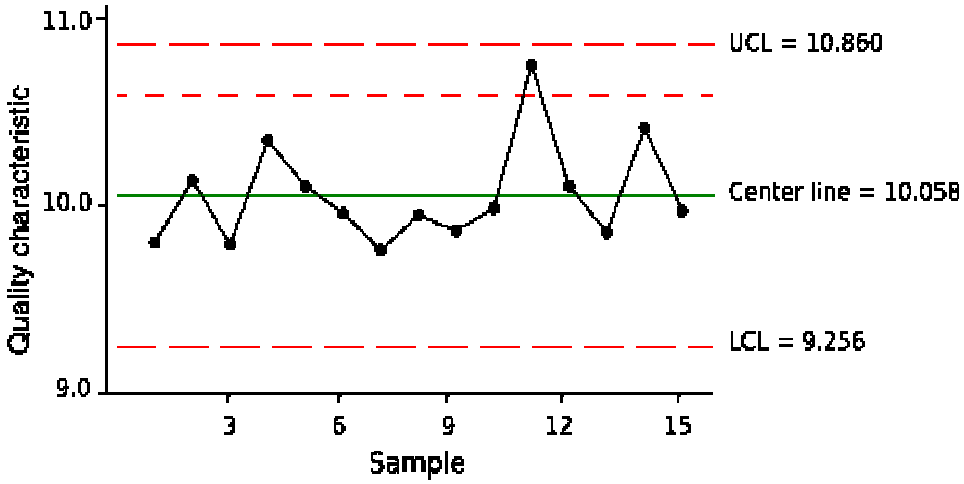

Figure 134 Typical Control Chart

The steps in constructing an X-bar control chart are as follows

1. Collect the data, select at least 20 successive sample ball subgroups, in which there are 5 balls to be measured in each subgroup. The letter "n" represents the number of samples and the letter "k" represents the number of subgroups.
2. Record the data on a data sheet; design the sheet so that it is easy to compute the X-bar values for each subgroup
3. Find the mean of each subgroup (X-bar)

$$Xbar = \frac{X1 + X2 + X3 + X4 + X5}{N}$$

4. Find the grand mean of all subgroups

$$Xdoublebar = \frac{N1 + N2 + N3 + N4 + N5....}{K}$$

5. Find the Control limits and the Warning limits using the following equations:

$$Control\ Limits = \mu \pm 3.09\frac{\sigma}{\sqrt{N}}$$

$$Warning\ Limits = \mu \pm 1.96\frac{\sigma}{\sqrt{N}}$$

Under the assumption that the variance of the process does not change, the successive sample means will be distributed normally around the actual mean. Without going into details regarding the derivation of these formulae, it is known that the distribution of the sample means will have a standard deviation of sigma (the standard deviation of individual measurements) over the square root of the sample size. It follows that approximately 95% of the sample means will fall within the limits μ ± 1.96 * Sigma/Square Root (n*)* and that approximately 99% of the sample means will fall within the limits μ ± 3.09 * Sigma/Square Root (n*)*.

The central controller VI block diagram constructs the control chart automatically and the resulting chart is plotted on the front panel; the control chart is updated after the each machine sample is successfully measured. The central controller uses a formula node to calculate the Control Limits and Warning Limits; a formula node is a convenient text-based node that is used to perform mathematical operations on the

block diagram. Access to any external code or wiring low-level arithmetic functions together to create equations is not required.

After each sample consisting of five balls is measured, the five measurements are averaged and the average is plotted automatically on the control chart. The central controller automatically interprets the data and determines if the process is out of control using the following guidelines:

A. One point outside the control limits
B. Eight successive points on the same side of the centreline
C. Six successive points that increase or decrease
D. Two out of three points that are on the same side of the centreline, both at a distance exceeding the Warning limit
E. Four out of five points that are on the same side of the centreline, four at a distance exceeding one sigma from the centreline

Each time the process goes out of control the central controller automatically records it to a specific file; the date and exact time when the process went out of control is recorded along with the sample average. This data will help to gain insight into the process, and will allow for process improvement and the detection of process problems.

In addition to reducing waste, it is anticipated that the SPC will lead to a reduction in the cycle time required to produce a batch of balls; this is partially due to a diminished likelihood that the final product will have to be reworked, but it may also result from using the SPC data to identify bottlenecks, wait times and other sources of delays within the process. Process cycle time reductions coupled with improvements in yield will make the SPC a valuable tool from both a cost reduction and a customer satisfaction standpoint.

6 Test Procedures and Results

6.1 Introduction

This chapter outlines the results of specific test procedures carried out on the automatic measurement instrument and the delivery system; The main focus in this Chapter is the performance of the measurement instrument: stability, measurement bias, repeatability and reproducibility were assessed and quantified. Also discussed are test procedures used to quantify the working parameters of the grinding machine and tests performed on the delivery system.

6.2 Ball Delivery Tests: Laboratory Prototyping

As mentioned in Section 4.2.2.2, a working prototype was designed and constructed to test the vertical queue delivery concept [66]; this initial prototype replicated the ball locator platform, using two embedded spheres to locate the sample ball and a blast of air to remove the ball. Also incorporated in this prototype is a separate clamping device to hold the ball in place during the measurement process.

Basic tests to determine how the device would perform under varying conditions were conducted, the results for which can be seen in Table 15 [66]. The results gathered demonstrate some system reliability based on a low level trial basis.

Air Pressure (Bar)	Test no.	Cycle Time T_c (sec)		Clamping Success	
		14mm Ball	10mm Ball	14mm Ball	10mm Ball
4	1	5.95	5.65	+	+
4	2	5.97	5.79	+	+
4	3	5.97	5.73	+	+
4	4	5.8	5.89	+	+
4	5	5.99	5.63	+	+
	Avg.	5.936	5.738		
3	1	5.82	5.89	+	+
3	2	6.02	5.97	+	+
3	3	6.01	5.68	+	+
3	4	5.82	6.08	+	+
3	5	5.74	6.3	+	+
	Avg.	5.882	5.984		
2	1	5.94	5.77	+	-
2	2	5.85	5.69	+	+
2	3	5.89	5.89	+	+
2	4	5.74	5.83	+	+
2	5	5.74	6.13	+	+
	Avg.	5.832	5.862		

Table 15 Ball Delivery Prototype Test Results

Analysis of the results demonstrate that the cycle time for the initial prototype to remove a sample ball, insert a new sample ball and to clamp the ball is 6 seconds; it is

assumed that the minute variations are caused by timing errors within the experiment set-up. However, analysis of the clamping mechanism shows that the 10mm ball yielded one misalignment in clamping while using a pressure of 2 bar. In conclusion, this misalignment is due to the inherent fact that the smaller ball has slightly more compliance in the system. This led to the changes in the construction of the location system as mentioned in Section 4.2.2.2: the diameter of the embedded spheres was increased to 15mm and were embedded 5.5mm into the platform, the distance between them was increased to 20mm.

6.3 Grind Machine Operating Parameters

Successful automation of the statistical process control (SPC) and the feedback to the grind machine requires a lot of knowledge about the grind process; knowledge of the stock removal rate per unit of pressure is required to determine the grind cut down chart data. The amount of stock removed after each hour of grinding determines if the process is in control, and if the hydraulic pressure on the balls is to be increased or decreased.

The first step in constructing the cut-down chart involved gathering a significant amount of data to determine the actual stock removal rate for each operating pressure. The basic objective of the grind process is to remove as much stock as possible while using as little energy as possible and maintaining an acceptable level of quality. The stock removal rate and the energy used are directly related. To increase the stock removal rate, the pressure on the balls must be increased; this pressure increase results in a greater power consumption by the motor used to drive the rotating stone. Ball roundness is the most important quality characteristic in the grinding process. Ball roundness is also affected by the pressure on the balls, the higher the pressure on the balls, the poorer the roundness the balls.

The pressure on the balls during the grinding process can range from 800 to 1400 PSI. On start up, the pressure is set to 800 PSI for approximately thirty minutes to allow the ball lot to cycle through the grind machine until there is no variation in colour between balls; this ensures each ball has been through the machine an adequate amount of times to remove all high spots that could damage the grinding stone at high pressure. After the variation is removed the machine is then switched to automatic mode. In automatic mode setting the amperage of the motor, rotating the stone, controls the pressure; the current is generally held between 30A and 40A, which will exert an operating pressure between 1100 and 1400 PSI. While running normal product at +10μm above the dump size, the machine is put into a round-up cycle by reducing the pressure to 800 PSI.

The three main factors analysed during the construction of the cut-down chart are:

1. Stock Removal Rate
2. Ball Roundness
3. Electrical current requirements for each pressure

The pressure versus stock removal rate test procedures took place over two weeks. Five different operating pressures were analysed on a one by one basis, 1000, 1100, 1200, 1300 and 1400PSI; each operating pressure ran for ten hours, the diameter and roundness of a five-ball sample was measured hourly.

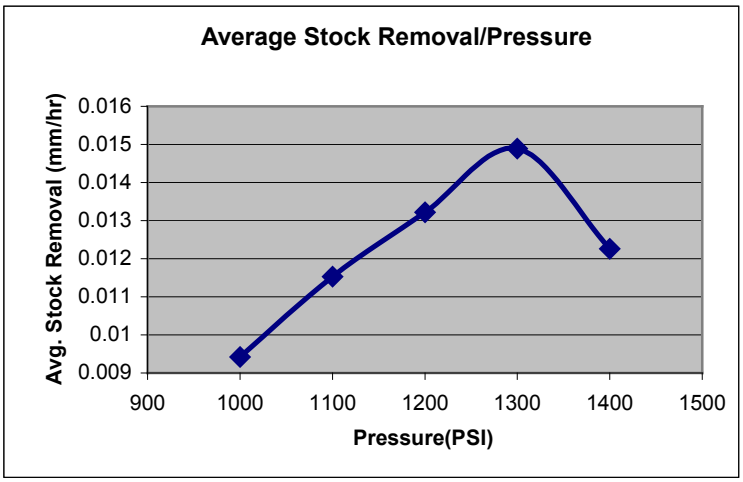

Figure 135 Average Stock Removal for Each Operating Pressure

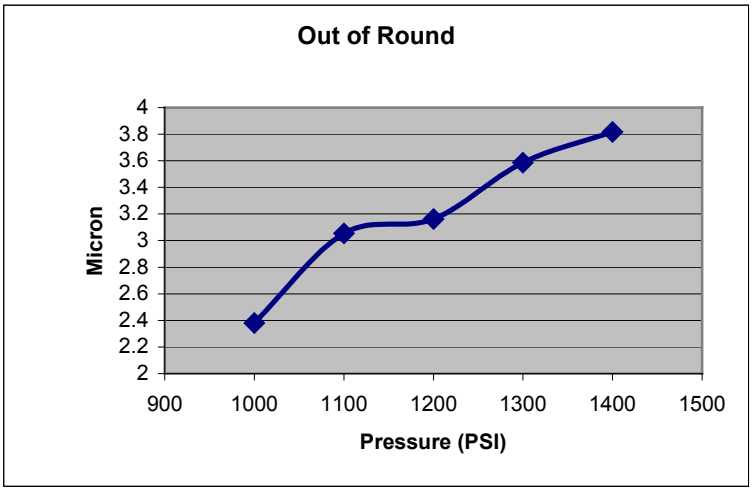

Figure 136 Average Out of Roundness Value for Each Operating Pressure

Considering the three main factors outlined above, an operating pressure of 1200PSI proved to be most efficient; the average stock removal rate per hour is 13.22µm and the average out of roundness value is 3.162µm, as shown in Figure 135 and Figure 136 respectively. The operating current at this pressure ranged between 33 and 40 amps.

All nominal ball sizes entering the grind process are required to be 150µm above the required finished size; i.e. a 13.494mm ball is 13.644mm (13.494mm +150µm)

entering the grind process. All nominal ball sizes leaving the grind process are required to be 20µm above the required finished size; i.e. a 13.494mm ball is 13.514mm (13.494 +20µm leaving the grind process. Therefore, the actual stock removed during the grind process is 130µm.

The nominal ball sizes entering the grind process have a tolerance of + 25.4µm (0.001"), a 13.494mm ball entering the grind process can vary from 13.644mm to 13.6694mm in diameter. As a result, the stock removed during the grind process can vary from 130µm to 155.4µm; this increases the stock to be removed by 19.5%.

Table 16 shows the "theoretical" grind process cut-down data for a 13.494mm ball: during the initial start up of the company this data was used to develop the process cut-down charts. The theoretical data does not give a true representation of the actual cut-down rates within the grind process. Analysis of the data suggests that a total of 194.6µm is removed throughout the process; this is far greater than the 130 to 155.4µm stock removal currently required. Furthermore, the theoretical data demonstrates an hourly stock removal rate of up to 25.4µm; the maximum stock removal rate obtained during the pressure versus stock removal tests was 14.89µm/hr. This stock removal rate was obtained while running the grind machine at 1300PSI: operating the machine at this constant pressure is not economically viable in terms of power consumption; therefore a stock removal rate of 25.4µm is known to be impractical.

Cycle Time	Stock Removal mm/Hr	Cumulative Stock Removal	Actual Diameter	UCL	LCL
0	0	0	13.644	13.6540	13.6340
1	0.0064	0.0064	13.637	13.6470	13.6270
2	0.0127	0.0191	13.6249	13.6349	13.6149
3	0.0127	0.0318	13.6122	13.6222	13.6022
4	0.0192	0.0510	13.593	13.6030	13.5830
5	0.0254	0.0764	13.5676	13.5776	13.5576
6	0.0254	0.1018	13.5422	13.5522	13.5322
7	0.0254	0.1272	13.5168	13.5268	13.5068
8	0.0254	0.1526	13.4914	13.5014	13.4814
9	0.0140	0.1666	13.4774	13.4874	13.4674
10	0.0140	0.1806	13.4634	13.4734	13.4534
11	0.0140	0.1946	13.4494	13.4594	13.4394

Table 16 Theoretical Cut-Down Data

Cycle Time	Stock Removal mm/Hr	Cumulative Stock Removal	Actual Diameter	UCL	LCL
0	0	0	13.644	13.6590	13.6290
1	0.0060	0.0060	13.6380	13.6480	13.6280
2	0.0132	0.0192	13.6248	13.6348	13.6148
3	0.0132	0.0324	13.6116	13.6216	13.6016
4	0.0132	0.0456	13.5984	13.6034	13.5934
5	0.0132	0.0588	13.5852	13.5902	13.5802
6	0.0132	0.0720	13.5720	13.5770	13.5670
7	0.0132	0.0852	13.5588	13.5638	13.5538
8	0.0132	0.0984	13.5456	13.5506	13.5406
9	0.0132	0.1116	13.5324	13.5344	13.5304
10	0.0132	0.1248	13.5192	13.5212	13.5172
11	0.0100	0.1348	13.5092	13.5112	13.5072

Table 17 Proposed Cut-Down Data

Table 17 contains the proposed grind process cut-down data; this data is derived using the results from the actual pressure versus stock removal tests. The start-up cycle operates at two pressures; at the initial start-up the machine operates for thirty minutes at 800PSI and then increases 1000PSI for a further 30 minutes. The total amount of stock removed during the start-up cycle is 6μm.

After the ball variation is removed, the grind machine operates in automatic mode; the machine operates at 1200PSI in automatic mode. The machine remains in automatic mode for nine hours, removing 118.8μm of stock. At this point, the product is +10μm above the dump size and the machine starts the round-up cycle; during the round-up cycle the machine pressure is set to 800PSI for one hour and 10μm of stock is removed.

Figure 137 shows the theoretical cut-down rate and the proposed cut-down rate for the 13.494mm ball during this grind process; the broken red line indicates the required finish size for the grind process. The proposed cut-down rate is plotted along with upper and lower control limits; as a result of the large tolerance entering the grind process, the control limits tighten throughout the process to ensure the variability within the batch is very small and that the actual finished size is controlled to a tight tolerance.

A full-scale test was conducted using the automated system to evaluate the proposed cut-down rate across 13mm diameter product. A sample was taken from the machine every eight minutes, each sample consisted of five balls: therefore over the 11.19 hour cycle time, 390 balls were measured in total (all ball measurements are

located in Appendix D). Each ball sample was picked from the grind machine using the automatic retrieval arm and transported to the normalizing station using the delivery-piping network. Following temperature normalizing, each sample ball diameter was measured using the automated piezo measurement instrument. The average of the five sample ball measurements were plotted on the developed cut-down chart and also displayed on the measurement display unit located at the grind machine.

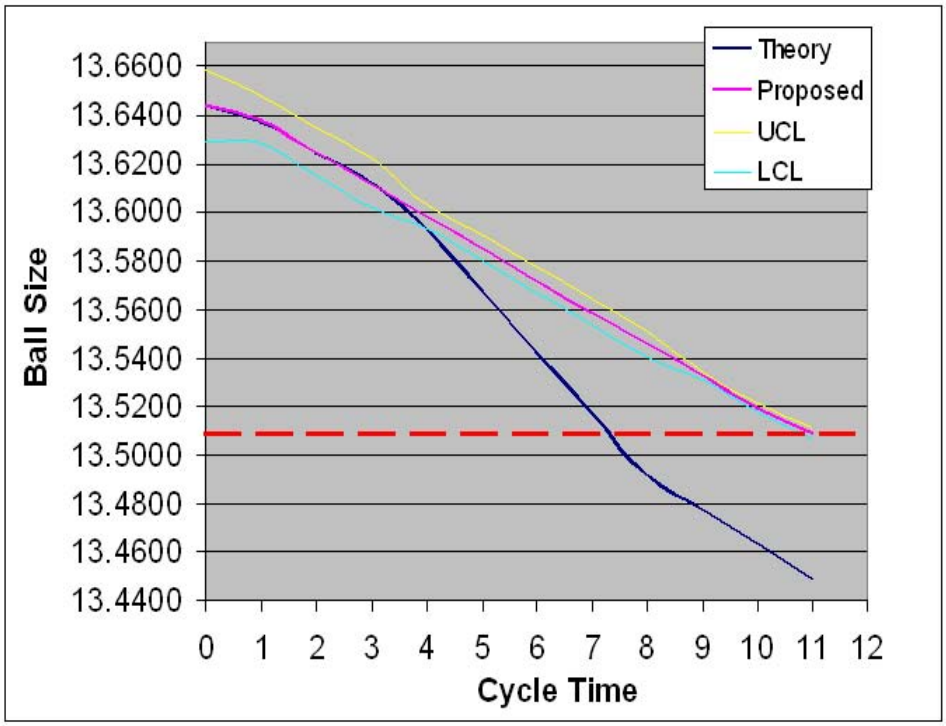

Figure 137Graph of Theoretical Cut-Down Rate and Proposed Cut-Down Rate

The cut-down chart resulting from the proposed cut-down rate test procedure is shown in Figure 138; this chart plots the average sample ball measurement against cycle time. Analysis of the cut-down chart indicates that the actual cycle time for the batch of balls is 11hrs 19mins; this matches closely the 11hrs approximation determined from the proposed grind process cut-down data.

The manual cut-down chart used by the machine operators throughout the test is illustrated in Appendix D.

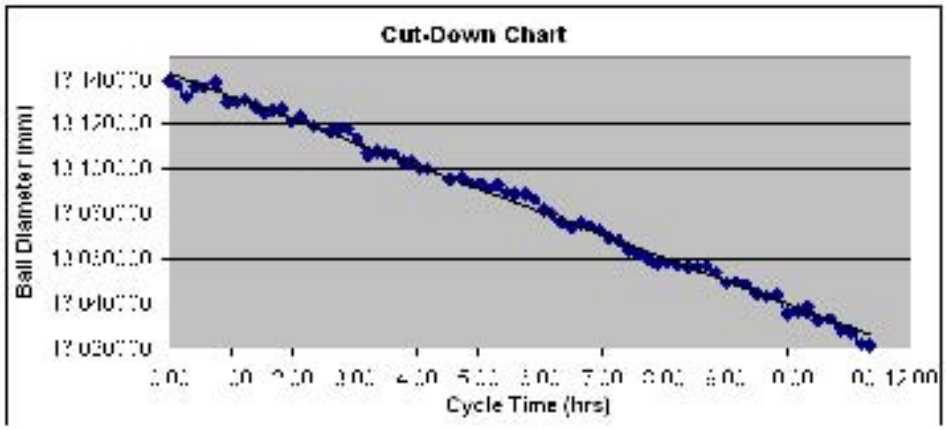

Figure 138 Plot of Test Sample Measurements

6.4 Measurement Instrument Stability

To determine if the stability of the measurement instrument is acceptable a 13.1318 mm reference standard ball was selected and measured at numerous different times; the ball was measured five times, twice a day for eight days. The readings were taken at differing times to represent when the measurement system is actually being used, this would account for warm-up, ambient or other factors that may change during the day. A X-bar and R chart were constructed to illustrate the data; other than normal control chart analyses, there is no known index for stability. The test results are shown in Table 18.

Piezo Measurement Unit									
Run	Date	Time	Sample1	Sample2	Sample3	Sample4	Sample5	Average Diameter	Range
1	04/04/2008	09:48	13.131826	13.131353	13.131608	13.13192	13.131512	13.131644	0.000567
2	04/04/2008	10:46	13.131798	13.132084	13.13198	13.132308	13.131628	13.131960	0.000680
3	05/04/2008	10:51	13.131825	13.131569	13.131998	13.131908	13.131723	13.131805	0.000429
4	05/04/2008	10:57	13.131882	13.131726	13.13159	13.131988	13.131772	13.131792	0.000398
5	07/04/2008	11:02	13.131791	13.13129	13.131887	13.131787	13.132088	13.131769	0.000798
6	07/04/2008	11:09	13.131882	13.132077	13.131444	13.131672	13.131564	13.131728	0.000633
7	08/04/2008	11:13	13.13128	13.13144	13.13189	13.131918	13.131681	13.131642	0.000638
8	08/04/2008	11:20	13.131982	13.13166	13.13131	13.131289	13.131487	13.131546	0.000693
9	09/04/2008	11:31	13.131564	13.131663	13.131644	13.131667	13.131664	13.131640	0.000103
10	09/04/2008	11:38	13.131717	13.131697	13.131469	13.131965	13.131866	13.131743	0.000496
11	10/04/2008	12:13	13.13197	13.132087	13.131947	13.131721	13.131741	13.131893	0.000366
12	10/04/2008	15:06	13.131675	13.131985	13.13121	13.13191	13.131917	13.131739	0.000775
13	11/04/2008	15:11	13.131882	13.1312	13.132307	13.132077	13.132084	13.131910	0.001107
14	11/04/2008	15:39	13.132182	13.1323	13.131642	13.131615	13.131849	13.131918	0.000685
15	12/04/2008	15:48	13.13129	13.13209	13.131848	13.132068	13.131854	13.131830	0.000800
16	12/04/2008	15:53	13.132119	13.132069	13.132101	13.131902	13.132065	13.132051	0.000217

Table 18 Measurement Instrument Stability Results

Firstly, each sub-group mean and range was calculated. R-bar is the mean of sub-group ranges and is given by:

$$Rbar = \frac{1}{g}\sum R = \frac{0.009385}{16} = 0.000586563$$

Where g is the number of sample sub-groups.

X-barbar is the is the mean of the sub-group means and is given by:

$$Xbarbar = \frac{1}{g}\sum Xbar = \frac{210.108608}{16} = 13.131788$$

The control limits on sub-group R values are given by:

$$UCL = D_4 Rbar = (2.114)(0.000586563) = 0.001237$$
$$LCL = D_3 Rbar = (0)(0.000586563) = 0$$

Here D_3 and D_4 are constants, which depend on the number of individual measurements in each sub-group and can be found from the multipliers for the range chart table.

The control limits of the X-bar chart can be established based on the standard deviation, i.e.:

$$UCL = \mu + 3\sigma$$
$$LCL = \mu - 3\sigma$$

The sub-group standard deviation can be estimated using:

$$3\sigma = A_2 Rbar = (0.577)(0.000586563) = 0.0003384$$
$$UCL = 13.1318 + 0.0003384 = 13.1321$$
$$LCL = 13.1318 - 0.0003384 = 13.1314$$

Here A2 is a constant, which depends on the number of individual measurements in each sub-group and can be found from the factors for the X-bar chart table.

Figure 139 and Figure 140 illustrate plots of the X-bar chart and R chart respectively. Analysis of the control charts indicates that the measurement process is stable as it remains within the limits and there are no obvious special cause effects visible.

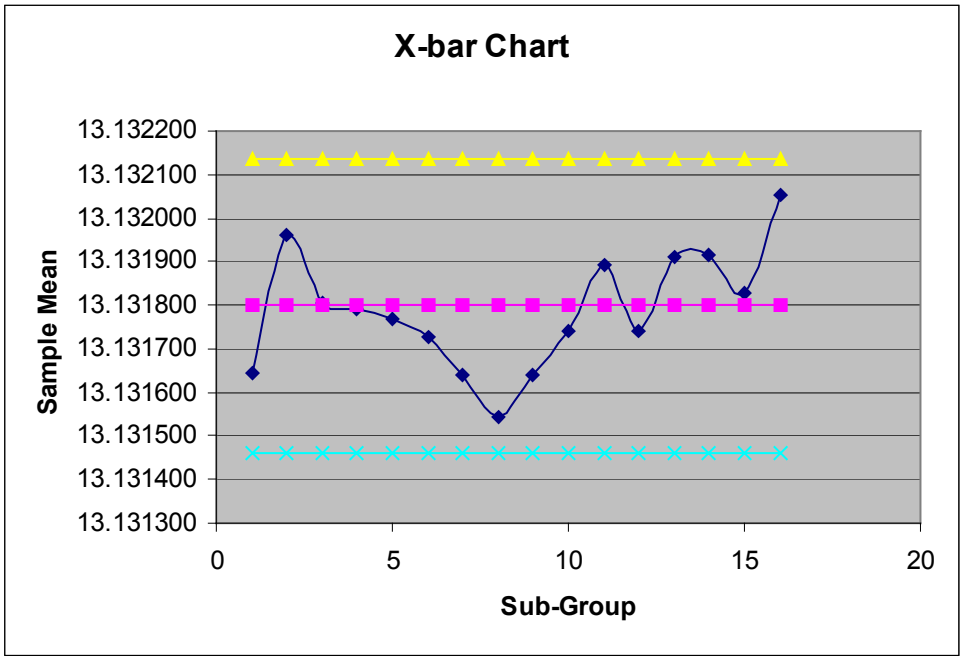

Figure 139 X-bar Chart

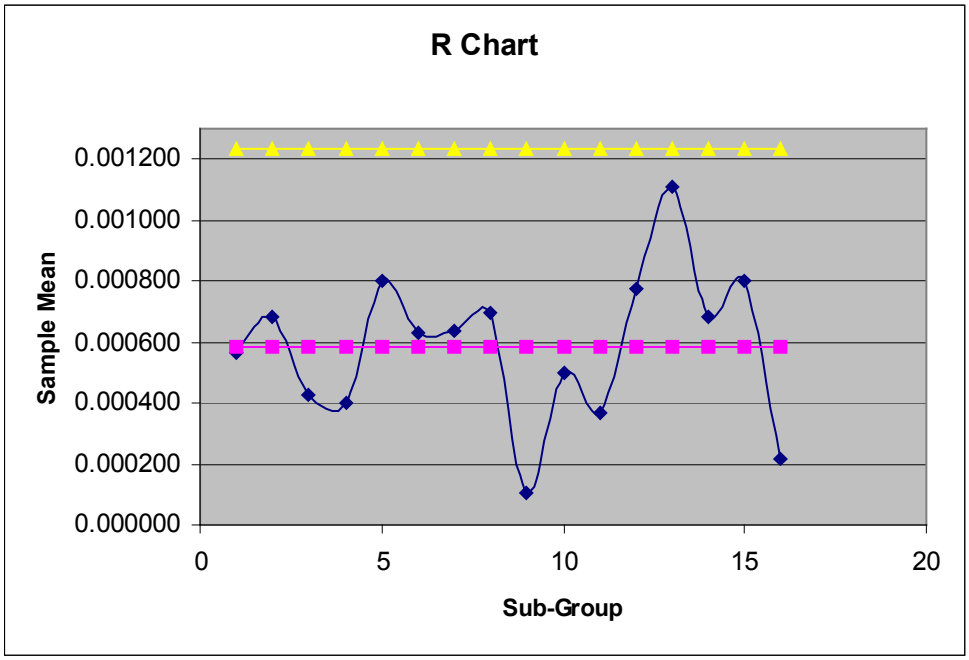

Figure 140 R Chart

6.5 Measurement Instrument Bias

Since an X-bar and R chart were used to measure the stability of the measurement instrument, this data can also be used to evaluate bias. The control chart analysis indicated that the measurement instrument is stable within limits; therefore it is acceptable to proceed with the bias study.

$Xbarbar = 13.131788$

The bias is computed by subtracting the reference value from X-barbar

$bias = Xbarbar - reference\,value = 13.131788 - 13.1318 = 0.00002$

Also, the standard deviation of the measurements can be used as an approximation for the repeatability of the measurement system.

$$\sigma_{repeatability} = \frac{Rbar}{d_2} = \frac{0.000586563}{2.326} = 0.00025217$$

Where d_2 is based on the sub-group size (m) and the number of sub-groups (g). Next, the t statistic is determined for the bias; the uncertainty for bias is given by σ_b:

$$\sigma_b = \frac{\sigma_r}{\sqrt{gm}} = \frac{0.00025217}{\sqrt{(16)(5)}} = 0.00002819$$

$$t = \frac{bias}{\sigma_b} = \frac{0.00002}{0.00002819} = 0.709$$

Bias is acceptable at the α level if zero falls within the 1-α confidence bounds around the bias value:

$$Bias - \left[\sigma_b\left(t_{v,1-\alpha/2}\right)\right] \le zero \le Bias + \left[\sigma_b\left(t_{v,1-\alpha/2}\right)\right]$$

Where v is found using the d2 tables and $t_{v,1-\alpha/2}$ is found using the standard t tables. The α level which is used depends on the level of sensitivity which is needed to evaluate/control the process and is associated with the loss function of the process; the value of 0.05 (95% confidence) is used here.

$$0.00002 - \left[0.000047105\right] \le zero \le 0.00002 + \left[0.000047105\right]$$
$$-0.0000271 \le zero \le 0.000067105$$

Since zero falls within the confidence interval of the bias (-0.0000271, 0.000067105), it can be assumed that the measurement bias is acceptable assuming that the actual use of the measurement instrument will not introduce additional sources of variation.

6.6 Measurement Instrument Repeatability and Reproducibility

A study of the repeatability and reproducibility of the measurement instrument was performed using the Average and Range method; this is an approach that provides an estimate of both repeatability and reproducibility for the measurement instrument, but not their interaction.

Five balls were chosen from the grind process; each ball was measured three times in a random order by the measurement instrument and the results noted. This exact measurement process was repeated two more times on the same five balls within an eight-hour period. Figure 141 shows the data collection sheet on which all the study results are recorded. R-bar (a, b, c) is the average of all ranges within each run and R-barbar is the average off all ranges. X-bar difference is the difference between the maximum and minimum of X-bar (a, b, c). Part Average is the sum of the measurements for each trial, for each part divided by the number of runs. Part range is calculated by subtracting the smallest part average from the largest part average.

	Part						
Run/Trial No	1	2	3	4	5	Average	
1	13.153005	13.1529	13.153002	13.151401	13.15518	13.1530972	
2	13.153591	13.15288	13.151434	13.151188	13.154651	13.1527496	
3	13.151251	13.15403	13.152347	13.152455	13.156227	13.1532612	
Average	13.152616	13.15327	13.152261	13.1516813	13.1553527	13.153036	X-bar(a)
Range	0.00234	0.001142	0.001568	0.001267	0.001576	0.0015786	R-bar(a)
1	13.151809	13.15258	13.155417	13.151597	13.156348	13.15355	
2	13.15201	13.15247	13.155547	13.150632	13.153839	13.1528998	
3	13.152844	13.15123	13.155334	13.150852	13.155392	13.1531308	
Average	13.152221	13.15209	13.1554327	13.151027	13.155193	13.1531935	X-bar(b)
Range	0.001035	0.001347	0.000213	0.000965	0.002509	0.0012138	R-bar(b)
1	13.152963	13.1523	13.152297	13.151731	13.155401	13.1529382	
2	13.152527	13.15129	13.153382	13.151978	13.154842	13.1528042	
3	13.153966	13.15253	13.152954	13.151441	13.155833	13.1533438	
Average	13.153152	13.15204	13.1528777	13.1517167	13.1553587	13.1530287	X-bar(c)
Range	0.001439	0.001233	0.001085	0.000537	0.000991	0.001057	R-bar(c)
Part Average	13.152663	13.15247	13.1535238	13.151475	13.1553014	0.00382644	Part Range
					R-barbar=	0.00128313	
					X-bar Differences=	0.0001648	
					Range UCL=	0.00331048	

Figure 141 Repeatability and Reproducibility Study Collection Sheet

The repeatability or equipment variation (EV) is determined by multiplying the average range (R-barbar) by constant K1; K1 depends upon the number of trials used in the study and is equal to the inverse of d_2.

$$EV = Rbarbar \times K1 = (0.0012831)(0.5908) = 0.000758mm$$

The reproducibility or appraiser variation is determined by multiplying the maximum average appraiser difference (X-bar Difference) by a constant K2; K2 depends upon the number of appraisers used in the study and again is the inverse of d_2. Since the appraiser variation is contaminated by the equipment variation, it must be adjusted by subtracting a fraction of the equipment variation. Therefore the appraiser variation is calculated by

$$AV = \sqrt{(Xbar\,dif \times K2)^2 - \frac{(EV)^2}{nr}} = \sqrt{(0.0001648 \times 0.5231)^2 - \frac{(0.000758)^2}{15}} = 0$$

n = number of parts and r = number of trials

The appraiser value is zero because the value under the square root is negative. Reproducibility is often referred to as the between appraiser variability; this is often true for manual instruments influenced by the skill of the operator. However it is not true for automated measurement instrument because an operator is not a major source of variation, therefore the zero appraiser variation is justified.

The measurement system variation for repeatability and reproducibility (GRR) is calculated by adding the square of the equipment variation and the square of the appraiser variation, and taking the square as follows:

$$GRR = \sqrt{(EV)^2 + (AV)^2} = \sqrt{(0.000758)^2 + 0^2} = 0.000758$$

The measurement system variation is the same as the equipment variation because the appraiser variation is zero.

The part variation (PV) is determined by multiplying the range of part averages (Part Range) by a constant K3; K3 depends on the number of parts used in the study and is the inverse of d_2.

$$PV = Part\,Range \times K3 = 0.0038264 \times 0.4030 = 0.001542mm$$

The total variation from the study is calculated by summing the square of both the repeatability and reproducibility variation and the part variation and taking the square root as follows:

$$TV = \sqrt{(GRR)^2 + (PV)^2} = \sqrt{0.000758^2 + 0.001542^2} = 0.001718mm$$

Once the variability for each factor in the study is determined, it can be compared to the total variation. The percent the equipment variation (%EV) consumes of the total variation is calculated by:

$$\%EV = 100\left[\frac{EV}{TV}\right] = 100\left[\frac{0.000758}{0.001718}\right] = 44.12\%$$

The percent that the other factors consume of the total variation can be similarly calculated as follows:

$$\%AV = 100\left[\frac{AV}{TV}\right] = 100\left[\frac{0}{0.001718}\right] = 0\%$$

$$\%GRR = 100\left[\frac{GRR}{TV}\right] = 100\left[\frac{0.000758}{0.001718}\right] = 44.12\%$$

$$\%PV = 100\left[\frac{PV}{TV}\right] = 100\left[\frac{0.001542}{0.001718}\right] = 89.75\%$$

This variation or capability will permanently exist within the measuring instrument because this study measures the random error variation within the measurement instrument.

6.7 Delivery System

To achieve a smooth transition of a ball between the stationary delivery system and the moveable ball-locating platform, the ball enters into a slot in the delivery base and rests on the precision gauge block attached to the locating platform. Using the force of gravity the ball is allowed to roll along the gauge block and settle against the embedded spheres. As mentioned in Section 4.2.2.4, the variation in the ball approach velocity between ball sizes is eliminated by the Cylinder 3; all balls are decelerated as they enter the locating platform, ensuring that the complete range of balls roll into the embedded spheres at a constant velocity. The delivery system is required to be flexible to cater for balls ranging from 10mm to 14mm; therefore the slot in the delivery base is required at least 14mm wide. Consequently, it is inevitable that the location variation of a small ball in the slot of the delivery base will be greater than that of a larger ball; as a result it is possible for a small ball to roll off centre along the gauge block and settle incorrectly against the embedded spheres.

The measuring instrument and mounting system is positioned at an angle; therefore the momentum of balls over the entire measurement range entering the locating platform is determined by the size of the angle. The occurrence of incorrectly positioned balls is eliminated by adjusting Cylinder 3 and controlling the angle of the measuring instrument and mounting system.

A study of the delivery system was undertaken to determine the repeatability; the study consisted of repeatedly inserting a 10mm ball onto the ball locator platform using the delivery system.

Table 19 displays the results of the delivery system while the measurement instrument and mounting system are positioned at an angle of 2.5˚. On the 7^{th}, 9th ^{and} 67^{th} trial, the balls were not positioned centrally between the two embedded spheres.

The same test was repeated, but this time the measurement instrument and mounting system are positioned at an angle of 1.5˚ and Cylinder 3 was adjusted to locate the ball on the centre of the gauge block. The results are shown in Table 20; during this run the delivery system proved to be 100% repeatable.

Trial	Result	Trial	Result	Trial	Result	Trial	Result	Trial	Result
1	+	21	+	41	+	61	+	81	+
2	+	22	+	42	+	62	+	82	+
3	+	23	+	43	+	63	+	83	+
4	+	24	+	44	+	64	+	84	+
5	+	25	+	45	+	65	+	85	+
6	+	26	+	46	+	66	+	86	+
7	Fail	27	+	47	+	67	Fail	87	+
8	+	28	+	48	+	68	+	88	+
9	+	29	+	49	+	69	+	89	+
10	+	30	+	50	+	70	+	90	+
11	+	31	+	51	+	71	+	91	+
12	+	32	+	52	+	72	+	92	+
13	+	33	+	53	+	73	+	93	+
14	+	34	+	54	+	74	+	94	+
15	Fail	35	+	55	+	75	+	95	+
16	+	36	+	56	+	76	+	96	+
17	+	37	+	57	+	77	-	97	+
18	+	38	+	58	+	78	+	98	+
19	+	39	+	59	+	79	+	99	+
20	+	40	+	60	+	80	+	100	+

Table 19 Run1 2.5°

Trial	Result	Trial	Result	Trial	Result	Trial	Result	Trial	Result
1	+	21	+	41	+	61	+	81	+
2	+	22	+	42	+	62	+	82	+
3	+	23	+	43	+	63	+	83	+
4	+	24	+	44	+	64	+	84	+
5	+	25	+	45	+	65	+	85	+
6	+	26	+	46	+	66	+	86	+
7	+	27	+	47	+	67	+	87	+
8	+	28	+	48	+	68	+	88	+
9	+	29	+	49	+	69	+	89	+
10	+	30	+	50	+	70	+	90	+
11	+	31	+	51	+	71	+	91	+
12	+	32	+	52	+	72	+	92	+
13	+	33	+	53	+	73	+	93	+
14	+	34	+	54	+	74	+	94	+
15	+	35	+	55	+	75	+	95	+
16	+	36	+	56	+	76	+	96	+
17	+	37	+	57	+	77	-	97	+
18	+	38	+	58	+	78	+	98	+
19	+	39	+	59	+	79	+	99	+
20	+	40	+	60	+	80	+	100	+

Table 20 Run2 1.5°

7 Conclusion

7.1 Introduction

A piezo actuated flexural stage for sub-micron precision measurement has been presented. The design was developed to fit the specified design criteria of the 0.1μm measurement accuracy being targeted by the company. The design features the use of solid flexures to transmit motion from a low voltage piezo actuator to the measurement surface. An array of flexure hinges was used to achieve the required range of movements for amplification of the actuator range and uniform linear movement of the contact surface. Taking advantage of the inherent material compliance, flexures are wear free and provided they are not distorted beyond their elastic limit, their line of action will remain constant throughout their life. The flexure stage is manufactured from a single piece of material to provide a monolithic mechanism which eliminates interface wear. Displacements of flexures are smooth and continuous at all levels, therefore displacements of the stage can be accurately predicted from the application of known forces, a characteristic very important for nanopositioning.

The final measurement instrument consists of a primary flexural-hinge guided stage driven by a low voltage piezoelectric actuator; in-built into the primary stage is a secondary flexural-hinge guided stage, which again is driven by a low voltage piezoelectric actuator. The primary piezo actuator is used to do the measurement and the secondary acts as a touch sensor to detect contact between the measurement stage and the product.

The precise motion that results from low voltage piezo actuators is of prime importance for nanopositioning; piezo actuators can perform sub-nanometer moves at high frequencies and they have no rotating or sliding parts to cause friction. Also, piezo actuators can generate high forces; depending on the extension of the actuator, both actuators used in this design can generate up to 1000N.

The expansion and contraction of the piezo actuators is tracked by means of two strain gauges attached to Wheatstone bridges: strain gauges were chosen for their ability to sense displacements in the sub-micron range. In addition, strain gauges are relatively inexpensive and allow for a compact design since they are attached to the ceramic stack within the protective housing.

7.2 Review of Objectives

The objective of the overall project was the total automation of the long established and universal labour intensive batch production technology of ball production. Within this overall objective, the objectives of this specific project are specified and reviewed below:

Objective 1: *Research and develop a 'piezo-flexure-based' sensor system for multi-diameter ball bearing tolerance measurement to 0.1micron accuracy using FEA simulation and, flexure design analysis*

Outcome: The measurement instrument was designed and built to achieve a measurement accuracy of 0.1μm. Tests performed on the instrument reveal that the instrument is stable and the bias is acceptable. Analysis of the test results shows the measurement accuracy currently being achieved with the instrument is 1μm and the repeatability of the device is 0.758μm. The next stage in this will yield the 0.1μm targeted accuracy. Recommendations for this achievement are given at the end of this chapter

Objective 2: *Simulate, design and build the measurement instrument to meet the production requirements of the client plant.*

Outcome: The prototype production instrument was designed on the basis of experience gained on Prototype 1. The design process consisted of design and redesign of different models using developed mathematical and CAD models. Subsequently the construction of the production measuring unit then took place; construction included the manufacture and assembly of the measuring unit, which consists of the wire eroded flexure stage, piezo actuators and preload shims. A complete mounting system that would help to keep environmental variability such as thermal effects and vibration to a minimum also had to be designed and manufactured. The resulting unit consisted of a motor and precision vertical platform assembly, heavy duty instrument chassis, instrument base, instrument table, delivery system, divider system and a ball locator platform

A ball fixturing system consisting of two embedded spheres, which locates the test ball during the measurement process, was implemented. This arrangement ensures

that centres of differing diameter balls are located relative to the measuring tip along the Y-axis. Mathematical models were created to represent the ball locator, the objective being to minimise the X-axis variation by varying the diameter of the locating spheres, the distance between them and the depth that the spheres are embedded into the locator. A compromise was reached and implemented between the need to minimise the ball foot print along the X-axis and the need for stability of the ball at the location spheres.

Objective 3: *To test, prove and validate this measurement instrument in the Laboratory.*

Outcome: Once the measurement unit was fully operational, a great deal of testing was carried out to determine the optimum settings for parameters such as: the sampling frequency and the number of samples to take; the averaging type and the number of points to average for the moving average; the sensitivity of ball detection; piezo increment size; settings for the ball locator fibre optic sensor.

Subsequently, the entire measurement unit was completely debugged to eliminate all detected errors in the software control of the unit and in the mechanical reliability of the unit. A full demonstration of the measuring unit in a laboratory environment took place and the specifications of the unit capabilities were generated.

The net result of all this, is that the reliability of the unit was greatly improved and the demonstration confirmed yet again the feasibility of the piezo based measurement instrument.

Objective 4: *Install and commission the instrument in the plant for the target production requirements: this includes the necessary temperature, humidity and vibration isolation and service access.*

Outcome: In October 2007, the measurement unit was installed in the production line

The mounting system protects the measuring instrument, chassis and instrument base from the vibratory motions of the supporting surface. It was desired to further isolate the measurement instrument and mounting system by enclosing the complete system in a temperature controlled room. This never came to fruition since the required

space is not available within the facility; this remains to be implemented in the next phase of the project.

Objective 5: *Prove and validate the instrument on-site for the in-process measurement task. This involves the full integration of the measurement station with the grinding machines to allow closed-loop feedback control*

Outcome: Tests of the measuring unit took place within the production facility; these tests confirmed that the measurement instrument will service current requirements of 1μm accuracy and is capable of successfully handling two machines.

At this point the measurement unit is integrated both physically and electronically with the automated production system for the grinding process and the lapping process. The automatic sampling system and measuring system were seamlessly linked to the central controller; the central controller controls the piezo measurement instrument, ball-locating platform, temperature normalizing station and communicates with the grinding machine and measurement display through the network.

Objective 6: *Study and improve the performance of the measurement system over a lengthy production cycle*

Outcome: When the system linkage was complete the first demonstration of the combined system took place on the mass grinding machines. The demonstration consisted of the measurement unit controller sending a signal across the network to the grinding machine at the far side of the plant to take sample components from the machine and delivering the sample balls to the temperature normalizing station using the developed air conveyor. After temperature normalizing has occurred, the sample components were measured and the reference components recycled to normalizing station. Using the developed automated Statistical Process Control program, calculations took place to see if the process was in or out of control. Next a signal was sent back to the grinding machine to automatically adjust the stock removal rate of the machine by adjusting the hydraulic pressure of the machine.

At this point any weaknesses in the system began to be uncovered; therefore a great deal of time was spent improving and debugging to increase the overall reliability of the system. This included the software debugging and continuous improvement of

Labview programs that control the measurement unit (piezo actuators, stepper motor and platform), RS-232/422 network, S.P.C, ball delivery system and machine control feedback.

The measurement system is currently very reliable: software debugging eliminated errors with the control of the measurement instrument and greatly increased the reliability of the network.

Objective 7: *To develop a measurement display unit to assist the operator to interface with each machine and to ease the change over from manual to automatic control.*

Outcome: A digital display unit has been developed that displays the latest sample measurement and the time of measurement for samples taken from the grinding machine. This is controlled automatically from the central controller by means of the RS-232/422 network and is updated after each machine is sampled. The display unit is mounted on the control panel of the grinding machine and is expected to help in the change over from the manual to the automated system: the operator will be able to see the actions of the central controller whilst standing beside his machine.

7.3 Summary of Results

Each section of the measurement instrument displayed an acceptable and convincing level of results. These results can be carried forward and analysed to assist with the most effective development of the system.

7.3.1 Measurement Instrument Bias

Bias is the difference between the true value (accepted reference value) and the observed average of measurements of the diameter of the same reference ball. Bias is the measure of systematic error as contrasted to random error; a larger systematic difference from the accepted reference value is reflected by a larger bias value. Results obtained from section 6.5 show that the measurement bias is acceptable since zero falls within the confidence interval of the bias (-0.0000271, 0.000067105).

7.3.2 Measurement Instrument Stability

Stability is the total variation in the measurements obtained with the measurement instrument on the same ball over an extended time period. Stability measures the change in systematic errors over time. Systematic errors, which change during an experiment, are usually easy to detect; measurements show trends with time rather than varying randomly about the mean. Analysis of the control charts obtained from the stability test in Section 6.4 indicates that the measurement process is stable since there are no obvious special cause effects visible.

7.3.3 Measurement Instrument Repeatability and Reproducibility

Repeatability is the precision of the measurement instrument under repeatability conditions. Repeatability conditions are conditions where independent test results are obtained with the same method on the same balls in the same production area using the measurement instrument within short intervals of time. This variation or capability will permanently exist within the measuring instrument; repeatability is the random error variation from successive trials under defined conditions of measurement. From Section 6.6 the repeatability of the measurement instrument is 0.758μm or 44.12% of the total variation. To further improve the performance of the measurement instrument it is anticipated that a repeatability of at least 0.5μm will be required in the future

Reproducibility is different from repeatability: Reproducibility relates to the agreement of test results with different operators, test apparatus and laboratory

locations. From Section 6.6, the reproducibility is calculated as zero or 0% of the total variation; reproducibility is often referred to as the between appraiser variability; this is often true for manual instruments influenced by the skill of the operator. However it is not true for automated measurement instrument because an operator is not a major source of variation, therefore the zero appraiser variation is justified.

The part variation is calculated as 1.542μm or 89.75% of the total variation; therefore the vast majority of the variation within the measurements can be associated with the variation within the balls. The total variation from the study is calculated as1.718μm.

7.3.4 Grind Machine Operating Parameters

The three main factors analysed during the construction of the cut-down chart were:

- Stock Removal Rate
- Ball Roundness
- Electrical current requirements for each pressure

Considering the three main factors, an operating pressure of 1200PSI proved to be most efficient; the average stock removal rate per hour is 13.22μm, the average out of roundness value is 3.162μm and the operating current at this pressure is economically viable (ranging between 33 and 40 amps).

The proposed grind process cycle consists of three stages: Start-up, automatic mode and round-up. The start-up cycle operates at two pressures; at the initial start-up the machine operates for thirty minutes at 800PSI and then increases 1000PSI for a further 30 minutes. The total amount of stock removed during the start-up cycle is 6μm.

After the ball variation is removed, the grind machine operates in automatic mode; the machine operates at 1200PSI in automatic mode. The machine remains in automatic mode for nine hours, removing 118.8μm of stock. At this point, the product is +10μm above the dump size and the machine starts the round-up cycle; during the round-up cycle the machine pressure is set to 800PSI for one hour and 10μm of stock is removed.

Tests of the proposed cut-down rate were carried out and analysis of the cut-down chart indicates that the actual cycle time for the batch of balls is 11hrs 19mins, compared to the 11hrs approximation determined from the proposed grind process cut-

down data, validating the proposed cut-down rate. This cut-down rate will standardise the grinding process cycle time and will aid forecasting of future production; cycles times with the manual system ranged from 11-15hrs.

7.3.5 Ball delivery

Ball delivery consists of the ball delivery/removal and sorting system and the ball locating. The ball delivery system and sorting system were problematic during the initial set-up period when dealing with varying ball sizes, but after the system was properly adjusted to cater for the varying ball size the system operated successfully.

The delivery system proved to be 100% repeatable once the angle of the mounting system was adjusted from 2.5˚ to 1.5˚.

7.3.6 Measurement Display

The measurement display unit to assist the operator to interface with each machine is mounted on the control panel of the grind machine; this is controlled automatically by the central controller and is updated after each machine is sampled. The display unit scans all inputs from the central controller on the RS-232/422 transmission line for its specific 8bit address preamble; once the unique address is recognised, the next string of data is processed into the correct format to display the date, time and average sample measurement, allowing the operator to effortlessly identify the precise period in the cycle for each machine. It is anticipated that the display unit will assist in the ongoing acceptance of the automation process by the operators as well as the production management personal.

7.3.7 Central Controller

The development of the SPC control allows for automatic monitoring of the grinding process and feedback control to the machine from which the samples are being taken. The result from this is a more efficient and controlled process. It is anticipated by the management that significant improvements will arise in product quality.

The amount of communication required for the two machines in this project is relatively low. The current network system is however considered more than capable of dealing with all the traffic of the plant when full integration is achieved..

7.4 Conclusions

The main objectives within this project were the development of a high-speed, high-precision measurement instrument to meet the requirements of the plant for the future and the development of a measurement station to integrate with the selected machines and a temperature normalizing system within a plant wide automation scheme.

During the initial design period of the measurement instrument, general analytical equations for calculating the stiffness, displacement and resonance of this measurement stage were developed. The numerical results obtained from this were compared with those found using finite element simulation and were found to be consistent. The optimal stage design was found using the analytical equations and the stage was machined from Aluminium 7075 using wire erosion. The primary flexural-hinge guided stage has an effective stiffness of 5.524 N/μm and a natural frequency of 385.43Hz. The maximum displacement of the primary piezo is 57.97μm and has a rise time of 55.5μsec. In-built into the primary stage is a secondary flexural-hinge guided stage; the secondary flexural-hinge guided stage has a linear stiffness of 1.44 N/μm and a natural frequency of 749.4Hz. The measurement instrument is integrated electronically with the central controller and is also physically integrated with the temperature normalizing station: its performance is considered very satisfactory in terms of both of these

The mounting system for the measurement instrument consists of an instrument chassis, instrument base and instrument table. The mounting system not only serves a functional purpose in terms of the chassis for the measuring instrument to operate correctly, but also to protect the measuring instrument, chassis and instrument base from the vibratory motions of the supporting surface. The mounting system does not isolate the measurement instrument from thermal disturbances or electrical noise. Thermal disturbances to the instrument decrease its measurement accuracy and repeatability. Electrical disturbance interrupt, obstruct and limit the effective performance of the circuits within the piezo controllers; electrical noise decreases the sensitivity of the instrument causing the measurement accuracy and repeatability of the instrument to be decreased. Therefore, to obtain the required measurement accuracy of 0.1μm, the device must be enclosed in a temperature controlled room and be completely

isolated from any electrical disturbances. This remains to be achieved in the next phase of the project.

The complete automated system which consists of the sampling and measuring system is controlled by the central controller; the central controller is linked to the piezo measurement instrument, ball-locating platform, temperature normalizing station and communicates with the AS-I central controller and measurement display unit using the developed network. The central controller schedules the retrieval of samples from the grinding machine, determines the period of temperature normalizing, performs the measurement process, carries out S.P.C based on the measurements obtained, displays the average measurement on the measurement display unit and creates closed loop feedback to the grinding machine by adjusting the operating pressure. Its operation is considered very satisfactory for the current two machine control project.

A significant amount of valuable data was gathered concerning the working limitations of particular equipment within this harsh working environment. Invaluable knowledge was gained which outlined the level of complexity required in the installation of an automated measurement system for the complete grinding process. It also became evident that the level of automation within the proposed sampling and measuring process would be a gradual achievement. From the level of fault finding and constant readjustment required during the operation of the automated system, it is estimated that there would need to be constant technical support to maintain an automated sampling and measurement system for a 24 machine system for perhaps one year after its implementation.

In conclusion, the objectives of the project were in large realised and the results can be used as a vital building block for the design and development of a commercial system if the investment is deemed feasible by the associated manufacturing plant.

7.5 Future Work

7.5.1 Temperature controlled enclosure:

An inescapable feature of the ball bearing manufacturing industry is the difficult working conditions: very high levels of acoustic and electrical noise, vibration, heat generation as well as high humidity all arising from the huge metal removal processes involved. For this reason, the piezo measurement instrument is located in a reasonably undisturbed section of the facility, 200 meters away from the mass grinding machines. Further isolation is required using an enclosed temperature controlled room.

The benefits of this enclosure would be:

1. Complete isolation of the measurement instrument from thermal and vibrational disturbances, which would improve the measurement capability of the instrument.
2. Isolate the complete system from the production plant atmosphere, which would decrease the likelihood of solid particles from the air entering the coolant surrounding the measuring instrument and building up on equipment.
3. Enhance the level of control of the coolant within the temperature normalizing station; tighter tolerances of the temperature controlled fluid will ensure that the thermal expansion of the sample balls and reference balls remain equal, improving the performance of the measurement instrument.

7.5.2 Sample return:

After the measurement process the five sample balls are currently dumped. When the system is expanded to 24 machines the amount of balls being dumped will be completely unacceptable. For example, if each machine is sampled every 15 minutes, 11,520 balls will be dumped daily. Therefore a system must be developed to send the each 5-ball sample back to its specific machine. The major issue in this process is that the samples would have to be stored, cooled, measured and returned to the batch within 10 minutes to keep the returned ball at the same diameter as the rest of the batch and not cause problems for the continued grinding process.

7.5.3 Direct Metrology

Position feedback of the flexural stages is provided using indirect metrology; strain gauges attached to the piezo actuators sense the displacement of the actuators. However, this type of metrology ignores any motion inaccuracies, which arise between the actuator and the measurement surface. Therefore to increase the measurement accuracy and repeatability of the instrument to 0.1μm, it is recommend that the displacement of the measurement surface should be sensed using direct metrology. With direct metrology the motion of the measurement surface should be measured closer to the critical point of action.

7.5.4 Under Fluid Measurement

Under fluid measurement is worth researching. Provision has been made for this in the design of the measurement tank. Specifically heating as well as recirculation of the fluid for complete mixing and precise fluid level control via a fluid weir within the measurement tank have been arranged. It is not yet known however, what effect of the partial immersion of the balls in the fluid will have on the measurement.

7.5.5 Ball Clamping

Further work can be done to see if more positive clamping of the balls during the measurement process would be of benefit. Indications from our work to date suggests that the gravity fixturing implemented here is satisfactory.

7.5.6 Vibrating Touch Sensor

Further research and development of the vibrating touch sensor is worth while. This method of touch sensing was used by Prototype 1; during the measurement the flexure hinges were oscillated at resonance. When the measurement tip makes full contact with a sample ball, this has the effect of adding stiffness to the system; they vibrate in unison. This additional stiffness increases the resonant frequency of the system; the magnitude of the vibration of the measurement tip is therefore decreased. It is this sudden change in feedback wave amplitude that could be used to detect contact with a sample ball and with further development it could help to achieve the desired 0.1μm measurement accuracy.

7.5.7 Multi-Touch Measurement

To increase the measurement speed and measurement resolution, further work could by carried out on the control of the piezo actuators. The primary piezo actuator could be positioned with a series of decreasing step sizes once the initial ball touch is detected; this will ensure that the contact strain on the touch sensor piezo remains constant for each ball measurement.

References

[1] Elmustafa1 A. A., Lagally M.G., *'Flexural-hinge guided motion nanopositioner stage for precision machining: finite element simulations'*, Elsevier Publishers, J. Intern. Soc. for Prec. Eng. & Nanotechnology 25 (2001) 77–81

[2] Woronko A., Huang J., Altintas Y., *'Piezoelectric tool actuator for precision machining on conventional CNC turning centers'*, Elsevier Publishers, J. Intern. Soc. for Prec. Eng. & Nanotechnology 27 (2003) 335–345

[3] Smith S.T., Chetwynd D.G. *'Foundations Of Ultraprecision Mechanism Design'*, Gordon, and Beach Science Publishers, 1992.

[4] Physik Instrumente, "*The world of Micro-and Nanopositioning*", 2005/2006

[5] Qing Yao, Dong J., Ferreira P.M., *'Design, analysis, fabrication and testing of a parallel-kinematic micropositioning XY stage'* Elsevier Publishers, Intern J. of Machine Tools and Manufacture 47(2007) 946-961

[6] Strassberger M., Waller H., '*Active noise reduction by structural control using piezo-electric actuators'*, Pergamon Publishers, Mechatronics 10 (2000) 851-868

[7] ISO 5725-1 *Accuracy (trueness and precision) of Measurement Methods and Results- Part1; General Principles and Definitions* 1994

[8] ISO 3290 *Rolling Bearings – Balls – Dimensions and Tolerances 3rd Edition*

[9] Wemyss T., Phelan J., *'The Mechanical Design of a 3-Axis Nano-Contouring Stage'*, Waterford Institute of Technology, 24th International Manufacturing Conference 2007

[10] ANSYS, Version 8.0, Ansys Inc.

[11] Aluminium Information, www.aircraftspruce.com , accessed 12/04/08

[12] Alcoa 7075 data sheet

[13] Matweb Material Data Aluminium 7075

[14] The Aluminium Association

[15] ASM Aerospace Specification Metals Inc, ASM Materials Data Sheet, accessed 06/06/08

[16] T Doiron T., Beers J., "*The Gauge Block Handbook"* Dimensional Metrology Group, Precision Engineering Division, National Institute of Standards and Technology

[17] Precision granite, www.precisiongraniteuasa.com accessed 19/04/08

[18] Starrett, Tru-stone technologies www.tru-stone.com accessed 19/04/08

[19] Itp Group, Coordinate Measuring Machine (CMM) Manufacture, www.itpgroup.co.uk accessed 10/05/08

[20] http://www.farrat.com/vibration_theory.html accessed 15/05/08

[21] http://www.wikipedia.org/ accessed 01/05/08

[22] Snowden J.C *"Vibration and shock in Damped Mechanical Systems",* J.Wiley and sons, London, 1968

[23] Measurement Systems Analysis Work Group, *"Measurement Systems Analysis Reference Manual"*, third edition, Daimler Chrysler Corporation, Ford Motor Company, General Motors, 2002

[24] Shouldice, C., *"Total Automation of In-Line Quality Measurement System"* WIT MEng Thesis, 2008.

[25] *BIPM, IEC, IFCC, ISO, IUPAC, IUPAP, OIML: International Vocabulary of Basic and General Terms in Metrology*, 2nd edition 1993, ISBN 92-67-01075-1

[26] IS0 3534-2:1993, *Statistics - Vocabulary and symbols - Part 2: Statistical quality control*.

[27] IS0 3534-3:1985, *Statistics - Vocabulary and symbols - Part 3: Design of experiments*.

[28] Marriott F.H.C. "*A Dictionary of Statistical Terms",* 5th edition, The International Statistical Institute, Published by Longman Scientific and Technical.

[29] McNaught A.D, Wilkinson A., *"IUPAC Compendium of Chemical Terminology* 2nd edition*"* Publisher, International Union of Pure and Applied Chemistry: Research Triangle Park, US (NY)

[30] http://dictionary.reference.com/browse/commensurate accessed 23/06/08

[31] www.timken.com accessed 23/06/08

[32] Carlisle, R. P. "*Scientific American Inventions and Discoveries: All the Milestones in Ingenuity"*, John Wiley & Sons, 2004.

[33] Rowland, K. T. "*Eighteenth Century Inventions"*,University of Michigan, 1974.

[34] SKF Product Information 401 *"Bearing failures and their Causes"*

[35] NIST/SEMATECH *"e-Handbook of Statistical Methods".*
http://www.itl.nist.gov/div898/handbook/index.htm accessed 25/06/08

[36] Adishesha P.K, *"Effect of Steel Making and Processing Parameters on Carbide Banding in Commercially Produced ASTM 52100 Bearing Steel",* Bearing Steel

Technology, ASTM STP 1419, J.M. Beswick, Ed., American Society for Testing and Materials International, West Conshohocken, PA, 2002

[37] Engineers Edge, "Solutions by Design", http://www.engineersedge.com accessed 03/07/08

[38] Guo Y.B., Liu C.R., *"Mechanical Properties of Hardened AISI 52100 Steel in Hard Machining Processes",* School of Industrial Engineering, Purdue University, West Lafayette, IN 47907

[39] Amiot B., "*Technical Requirements for Steel Balls for Bearings",* SNR Roulements, ER000611L

[40] Eschmann, P., "*Ball & Roller Bearings: Theory, Design & Application",* 2nd Edition.

[41] Harris, A., "*Rolling Bearing Analysis",* 3rd Edition. John Wiley & Sons, Inc., 1991.

[42] Houghton, P. S., "*Ball & Roller Bearings",* Elsevier Science Publishing Company, Inc., 1976

[43] Werner, K., Madelung, O.W., "*AS-Interface – The Actuator Sensor Interface for Automation*", Carl Hanser Verlag Munchen Wien, 1994

[44] Profibus Standard EN 50170 (DIN 19245)

[45] Profinet Standard IEC 61158/ IEC 61784

[46] Hodson, P., *"Local Area Networks",* 4th Edition, Continuum Publishers, 2003, ISBN: 0-8264-5866-1.

[47] National Instruments Developer Zone http://zone.ni.com/dzhp/app/main accessed 16/07/08

[49] "*Hawkins Electrical Guide"*, 2nd Edition, Volume 1, Theodore Audel and Company

[50] Jones, D., J., "*Control of Stepping Motors*", The University of Iowa, Department of Computer Science

[51] Holland, A., "*Is Electrical Interference Crippling Your Control System? Understand It And You Can Defeat It*", Holland Technical Skills.

[52] Labview Measurements Manual

[53] Labview User Manual

[54] Moaveni, S., "*Finite Element Analysis Theory and Application with ANSYS"*, Prentice Hall International Limited.

[55] Diracdelta.co.uk., "*Science and Engineering Encyclopaedia*", http://www.diracdelta.co.uk/ accessed 22/07/08

[56] Lobontiu, N., "*Compliant Mechanisms: Design of Flexure Hinges*", Published by CRC Press, 2002, ISBN 08493113678

[57] Jones, R.V., "*Parallel and Rectilinear Spring Movements*", Journal of Scientific. Instrumentation

[58] Jones, R.V., "*Some Parasitic Deflexions in Parallel Spring Movements*", Journal of Scientific. Instrumentation

[59] Reeds, J., Hansen S., Otto O., Carroll A., McCarthy D., Radley J., "*High Speed Precision X-Y Stage",* Journal of. Scientific Technology

[60] Martens M., Waller H., "*Vibration control of a mechanical structure with piezoelectric actuators - a comparison of bimorph and stack actuators"*. In: Actuators 98, Proceedings of the 6th International Conference on New Actuators, Bremen, Germany.

[61] Chetwynd D.G., *"Linear Translation Mechanisms for Nanotechnology Applications"*, Measurement and Control, 24

[62] Miyashita M., Yoshioka J., "Development of Ultra-Precision Machine Tools for Micro-Cutting of Brittle Materials" Japan Society of Precision Engineering, 16(1)

[63} Sclater N., Chironis N.P., "Mechanisms and Mechanical Devices Sourcebook" Published by MvGraw-Hill Professional, 2007, ISBN 0071467610, 9780071467612.

[64] Wemyss T., Phelan J., *"Development of a Flexure Based Sub-Micron Measurement Instrument for use in a Noisy Environment"*, Waterford Institute of Technology, 24th International Manufacturing Conference 2007.

[65] Private conversation with K. Murphy, Waterford Institute of Technology

[66] Fenlon, N, Irish, K. *"Development of a High-Speed Ball Feeding and Location Mechanism"* WIT Bachelor of Science Project Report, 2007.

Appendix A
Material Properties

Charcoal Black Granite Physical Properties:

TRU-STONE TECHNOLOGIES

Charcoal Black Granite Physical Properties

Absorption % by weight	0.09
Density lbs/ft^3 (kg/m^3) Conv: lb/ft^3x16.0283=kg/m^3	170.9 (2,740)
Modulus of Rupture lbs/in^2 (Mpa) Conv: x,xxxpsi/145=Mpa	2,510 (17.3)
Compressvie Strength lbs/in^2 (Mpa) Conv: x,xxxpsi/145=Mpa	26,200 (181)
Abrasion Resistance Ha (mm)	88.5
Flexural Strength lbs/in^2 (Mpa) Conv: x,xxxpsi/145=Mpa	2,450 (16.9)
Flexural Modulus of Elasticity **Parallel to Rift Direction** lbs/in^2 (Gpa) Conv: x.xxE+06psi/.145=Gpa	7.80E+06 (53.8)
Flexural Modulus of Elasticity **Perpendicular to Rift Direction** lbs/in^2 (Gpa) Conv: x.xxE+06psi/.145=Gpa	8.00E+06 (55.1)

AISI 1006 Steel Plate Physical Properties

AISI 1006 Steel, cold drawn

Categories: Metal; Ferrous Metal; Carbon Steel; AISI 1000 Series Steel; Low Carbon Steel

Material Notes: The composition shown above is for structural shapes, plates, strip, sheets, and welded tubing only. Semifinished products for forging, hot-rolled and cold finished bars, wire rods, and seamless tubing have a magnesium range of 0.25 - 0.40%.

Applications: Soft, very ductile, used in applications which require severe bending and welding such as panels for automobiles or appliances. Also used in magnet core applications.

Key Words: UNS G10060, ASME 5041, ASTM A29, ASTM A510, ASTM A545, FED QQ-W-461, MIL SPEC MIL-S-11310 (CS1006), SAE J403, SAE J412, SAE J414

Vendors: No vendors are listed for this material. Please click here if you are a supplier and would like information on how to add your listing to this material.

Physical Properties	Metric	English	Comments
Density	7.872 g/cc	0.2844 lb/in³	

Mechanical Properties	Metric	English	Comments
Hardness, Brinell	95.0	95.0	
Hardness, Knoop	113	113	Converted from Brinell hardness.
Hardness, Rockwell B	55.0	55.0	Converted from Brinell hardness.
Hardness, Vickers	98.0	98.0	Converted from Brinell hardness.
Tensile Strength, Ultimate	330 MPa	47900 psi	
Tensile Strength, Yield	285 MPa	41300 psi	
Elongation at Break	20.0 %	20.0 %	In 50 mm
Reduction of Area	45.0 %	45.0 %	
Modulus of Elasticity	205 GPa	29700 ksi	Typical for steel
Bulk Modulus	140 GPa	20300 ksi	Typical for steel
Poissons Ratio	0.290	0.290	Typical For Steel
Machinability	50.0 %	50.0 %	Based on AISI 1212 steel. as 100% machinability. The machinability of Group I bar, rod, and wire products can be improved by cold drawing.
Shear Modulus	80.0 GPa	11600 ksi	Typical for steel

Electrical Properties	Metric	English	Comments
Electrical Resistivity	0.0000174 ohm-cm	0.0000174 ohm-cm	Typical steel

Thermal Properties	Metric	English	Comments
CTE, linear 20°C	12.6 µm/m-°C	7.00 µin/in-°F	0-100°C
CTE, linear 250°C	13.5 µm/m-°C	7.50 µin/in-°F	0-300°C (68-570°F)
CTE, linear 500°C	14.2 µm/m-°C	7.89 µin/in-°F	0-500°C (68-930°F)
CTE, linear 1000°C	13.7 µm/m-°C	7.61 µin/in-°F	0-1000°C
Specific Heat Capacity	0.481 J/g-°C	0.115 BTU/lb-°F	50-100°C

Material Components Properties	Metric	English	Comments
Carbon, C	<= 0.0800 %	<= 0.0800 %	
Iron, Fe	99.43 - 99.75 %	99.43 - 99.75 %	
Manganese, Mn	<= 0.450 %	<= 0.450 %	
Phosphorous, P	<= 0.0400 %	<= 0.0400 %	
Sulfur, S	<= 0.0500 %	<= 0.0500 %	

References for this datasheet.

M1006A

AISI E 52100 Steel Physical Properties

AISI E 52100 Steel

Categories: Metal; Ferrous Metal; Alloy Steel; Carbon Steel; AISI 5000 Series Steel; High Carbon Steel; Low Alloy Steel

Material Notes: 52100 has metallurgical and processing characteristics similar to alloy T8-9. HRC tests taken after 1 hour at tempering temperature.

Key Words: UNI 100 Cr 6 (Ital.), U.S. 534 A 99, U.S. 535 A 99, ASTM A 295, ASTM A295, ASTM A519, ASTM A535, ASTM A646, ASTM A711, MIL SPEC MIL S 900, MIL SPEC MIL S 7420, MIL SPEC MIL S 22141, SAE J404, SAE J412, SAE J770, DIN 1.3505, AISI 52100, AISI 100 C 6 (Ital.), UNS G52986, AMS 6440, AMS 6441, AMS 6444, AMS 6447, ASTM A322, ASTM A331, ASTM A507

Vendors: Click here to view all available suppliers for this material.

Please click here if you are a supplier and would like information on how to add your listing to this material.

Physical Properties	Metric	English	Comments
Density	7.81 g/cc	0.282 lb/in³	annealed

Mechanical Properties	Metric	English	Comments
Hardness, Knoop	870	870	Converted from Rockwell C hardness.
Hardness, Rockwell C	62.0	62.0	quenched in oil from 150°C tempered.
	64.0	64.0	quenched in water from 150°C tempered.
	64.0	64.0	quenched in oil
	65.0	65.0	quenched in water
Hardness, Vickers	940	940	Converted from Rockwell C hardness.
Modulus of Elasticity	210 GPa	30700 ksi	
Bulk Modulus	140 GPa	20300 ksi	Typical for steels.
Poissons Ratio	0.300	0.300	Calculated
Machinability	40.0 %	40.0 %	spheroidized annealed and cold drawn. Based on 100% machinability for AISI 1212 steel.
Shear Modulus	80.0 GPa	11600 ksi	Typical for steel

Electrical Properties	Metric	English	Comments
Electrical Resistivity	0.0000219 ohm cm	0.0000219 ohm cm	Typical 5000 series steel

Thermal Properties	Metric	English	Comments
CTE, linear 20°C	11.9 µm/m-°C @Temperature 23.0 - 280 °C	6.61 µin/in-°F @Temperature 73.4 - 536 °F	annealed
	12.5 µm/m °C @Temperature 20.0 - 200 °C	6.94 µin/in °F @Temperature 68.0 - 392 °F	hardened
Specific Heat Capacity	0.475 J/g °C	0.114 BTU/lb °F	Typical 5000 series steel
Thermal Conductivity	46.6 W/m-K	323 BTU-in/hr-ft²-°F	Typical steel

Material Components Properties	Metric	English	Comments
Carbon, C	0.980 - 1.10 %	0.980 - 1.10 %	
Chromium, Cr	1.45 %	1.45 %	
Iron, Fe	97.0 %	97.0 %	
Manganese, Mn	0.350 %	0.350 %	
Phosphorous, P	<= 0.0250 %	<= 0.0250 %	
Silicon, Si	0.250 %	0.250 %	
Sulfur, S	<= 0.0250 %	<= 0.0250 %	

Aluminium 7075-T6 Physical Properties

Aluminum 7075-T6; 7075-T651

Categories: Metal; Nonferrous Metal; Aluminum Alloy; 7000 Series Aluminum Alloy

Material Notes: General 7075 characteristics and uses (from Alcoa): Very high strength material used for highly stressed structural parts. The T7351 temper offers improved stress-corrosion cracking resistance.

Applications: Aircraft fittings, gears and shafts, fuse parts, meter shafts and gears, missile parts, regulating valve parts, worm gears, keys, aircraft, aerospace and defense applications; bike frames, all terrain vehicle (ATV) sprockets.

Data points with the AA note have been provided by the Aluminum Association, Inc. and are NOT FOR DESIGN.

Composition Notes:
A Zr + Ti limit of 0.25 percent maximum may be used with this alloy designation for extruded and forged products only, but only when the supplier or producer and the purchaser have mutually so agreed. Agreement may be indicated, for example, by reference to a standard, by letter, by order note, or other means which allow the Zr + Ti limit.
Aluminum content reported is calculated as remainder.
Composition information provided by the Aluminum Association and is not for design.

Key Words: Aluminium 7075-T6; Aluminium 7075-T651; UNS A97075; ISO AlZn5.5MgCu; Aluminium 7075-T6; Aluminium 7075-T651; AA7075-T6

Vendors: Click here to view all available suppliers for this material.

Please click here if you are a supplier and would like information on how to add your listing to this material.

Physical Properties	Metric	English	Comments
Density	2.81 g/cc	0.102 lb/in³	AA; Typical

Mechanical Properties	Metric	English	Comments
Hardness, Brinell	150	150	AA; Typical; 500 g load; 10 mm ball
Hardness, Knoop	191	191	Converted from Brinell Hardness Value
Hardness, Rockwell A	53.5	53.5	Converted from Brinell Hardness Value
Hardness, Rockwell B	87.0	87.0	Converted from Brinell Hardness Value
Hardness, Vickers	175	175	Converted from Brinell Hardness Value
Ultimate Tensile Strength	572 MPa	83.0 ksi	AA; Typical
Tensile Yield Strength	503 MPa	73.0 ksi	AA; Typical
Elongation at Break	11.0 %	11.0 %	AA; Typical; 1/16 in. (1.6 mm) Thickness
	11.0 %	11.0 %	AA; Typical; 1/2 in. (12.7 mm) Diameter
Modulus of Elasticity	71.7 GPa	10400 ksi	AA; Typical; Average of tension and compression. Compression modulus is about 2% greater than tensile modulus.
Poissons Ratio	0.330	0.330	
Fatigue Strength	159 MPa @# of Cycles 5.00e+8	23000 psi @# of Cycles 5.00e+8	completely reversed stress; RR Moore machine/specimen
Fracture Toughness	20.0 MPa-m½	18.2 ksi-in½	K(IC) in S-L Direction
	25.0 MPa-m½	22.8 ksi-in½	K(IC) in T-L Direction
	29.0 MPa-m½	26.4 ksi-in½	K(IC) in L-T Direction
Machinability	70.0 %	70.0 %	0-100 Scale of Aluminum Alloys
Shear Modulus	26.9 GPa	3900 ksi	
Shear Strength	331 MPa	48000 psi	AA; Typical

Electrical Properties	Metric	English	Comments
Electrical Resistivity	0.00000515 ohm-cm	0.00000515 ohm-cm	AA; Typical at 68°F

Thermal Properties	Metric	English	Comments
CTE, linear 68°F	23.6 µm/m-°C	13.1 µin/in-°F	AA; Typical; Average over 68-212°F range.
CTE, linear 250°C	25.2 µm/m-°C	14.0 µin/in-°F	Average over the range 20-300°C
Specific Heat Capacity	0.960 J/g-°C	0.229 BTU/lb-°F	
Thermal Conductivity	130 W/m-K	900 BTU-in/hr-ft²-°F	AA; Typical at 77°F
Melting Point	477 - 635.0 °C	890 - 1175 °F	AA; Typical range based on typical composition for wrought products 1/4 inch thickness or greater. Homogenization may raise eutectic melting temperature 20-40°F but usually does not eliminate eutectic melting.
Solidus	477 °C	890 °F	AA; Typical
Liquidus	635.0 °C	1175 °F	AA; Typical

Processing Properties	Metric	English	Comments
Annealing Temperature	413 °C	775 °F	
Solution Temperature	466 - 482 °C	870 - 900 °F	
Aging Temperature	121 °C	250 °F	

Material Components Properties	Metric	English	Comments
Aluminum, Al	87.1 - 91.4 %	87.1 - 91.4 %	
Chromium, Cr	0.180 - 0.280 %	0.180 - 0.280 %	
Copper, Cu	1.20 - 2.00 %	1.20 - 2.00 %	

Aluminium 6082-T6 Physical Properties

Aluminum 6082-T6

Categories:	Metal; Nonferrous Metal; Aluminum Alloy; 6000 Series Aluminum Alloy
Material Notes:	Material specs taken from SAPA / Indalex manual on extrusions. Data points with the AA note have been provided by the Aluminum Association, Inc. and are NOT FOR DESIGN. **Composition Notes:** Composition information provided by the Aluminum Association and is not for design.
Key Words:	EU Numerical EN-AW-6082; EU Chemical AlSi1MgMn; AA6082; Sweden: SS-EN-AW-6082; Aluminium 6082-T6
Vendors:	Click here to view all available suppliers for this material. Please click here if you are a supplier and would like information on how to add your listing to this material.

Physical Properties	Metric	English	Comments
Density	2.70 g/cc	0.0975 lb/in³	AA; Typical

Mechanical Properties	Metric	English	Comments
Hardness, Vickers	95.0	95.0	
Tensile Strength, Ultimate	290 MPa	42100 psi	wall thickness < 5 mm
	310 MPa	45000 psi	wall thickness > 5 mm
Tensile Strength, Yield	250 MPa	36300 psi	wall thickness < 5 mm
	260 MPa	37700 psi	wall thickness > 5 mm
Elongation at Break	10.0 %	10.0 %	

Thermal Properties	Metric	English	Comments
Thermal Conductivity	170 W/m-K	1180 BTU-in/hr-ft²-°F	

Material Components Properties	Metric	English	Comments
Aluminum, Al	95.2 - 98.3 %	95.2 - 98.3 %	As remainder
Chromium, Cr	<= 0.250 %	<= 0.250 %	
Copper, Cu	<= 0.100 %	<= 0.100 %	
Iron, Fe	<= 0.500 %	<= 0.500 %	
Magnesium, Mg	0.600 - 1.20 %	0.600 - 1.20 %	
Manganese, Mn	0.400 - 1.00 %	0.400 - 1.00 %	
Other, each	<= 0.0500 %	<= 0.0500 %	
Other, total	<= 0.150 %	<= 0.150 %	
Silicon, Si	0.700 - 1.30 %	0.700 - 1.30 %	
Titanium, Ti	<= 0.100 %	<= 0.100 %	
Zinc, Zn	<= 0.200 %	<= 0.200 %	

Aluminium 6082-T4 Physical Properties

Aluminum 6082-T4

Categories:	Metal; Nonferrous Metal; Aluminum Alloy; 6000 Series Aluminum Alloy
Material Notes:	Material specs taken from SAPA / Indalex manual on extrusions. Data points with the AA note have been provided by the Aluminum Association, Inc. and are NOT FOR DESIGN. **Composition Notes:** Composition information provided by the Aluminum Association and is not for design.
Key Words:	EU Numerical EN-AW-6082; EU Chemical AlSi1MgMn; AA6082; Sweden: SS-EN-AW-6082; Aluminium 6082-T4
Vendors:	Click here to view all available suppliers for this material. Please click here if you are a supplier and would like information on how to add your listing to this material.

Physical Properties	Metric	English	Comments
Density	2.70 g/cc	0.0975 lb/in³	AA; Typical

Mechanical Properties	Metric	English	Comments
Hardness, Vickers	65.0	65.0	
Tensile Strength, Ultimate	205 MPa	29700 psi	
Tensile Strength, Yield	110 MPa	16000 psi	
Elongation at Break	14.0 %	14.0 %	
Shear Strength	126 MPa	18300 psi	Calculated

Thermal Properties	Metric	English	Comments
Thermal Conductivity	170 W/m-K	1180 BTU-in/hr-ft²-°F	

Material Components Properties	Metric	English	Comments
Aluminum, Al	95.2 - 98.3 %	95.2 - 98.3 %	As remainder
Chromium, Cr	<= 0.250 %	<= 0.250 %	
Copper, Cu	<= 0.100 %	<= 0.100 %	
Iron, Fe	<= 0.500 %	<= 0.500 %	
Magnesium, Mg	0.600 - 1.20 %	0.600 - 1.20 %	
Manganese, Mn	0.400 - 1.00 %	0.400 - 1.00 %	
Other, each	<= 0.0500 %	<= 0.0500 %	
Other, total	<= 0.150 %	<= 0.150 %	
Silicon, Si	0.700 - 1.30 %	0.700 - 1.30 %	
Titanium, Ti	<= 0.100 %	<= 0.100 %	
Zinc, Zn	<= 0.200 %	<= 0.200 %	

Appendix B
Circuit Diagrams

Physik Instrumente E-610 LVPZT Piezo Amplifier and Position Servo-Controller Circuit Diagram

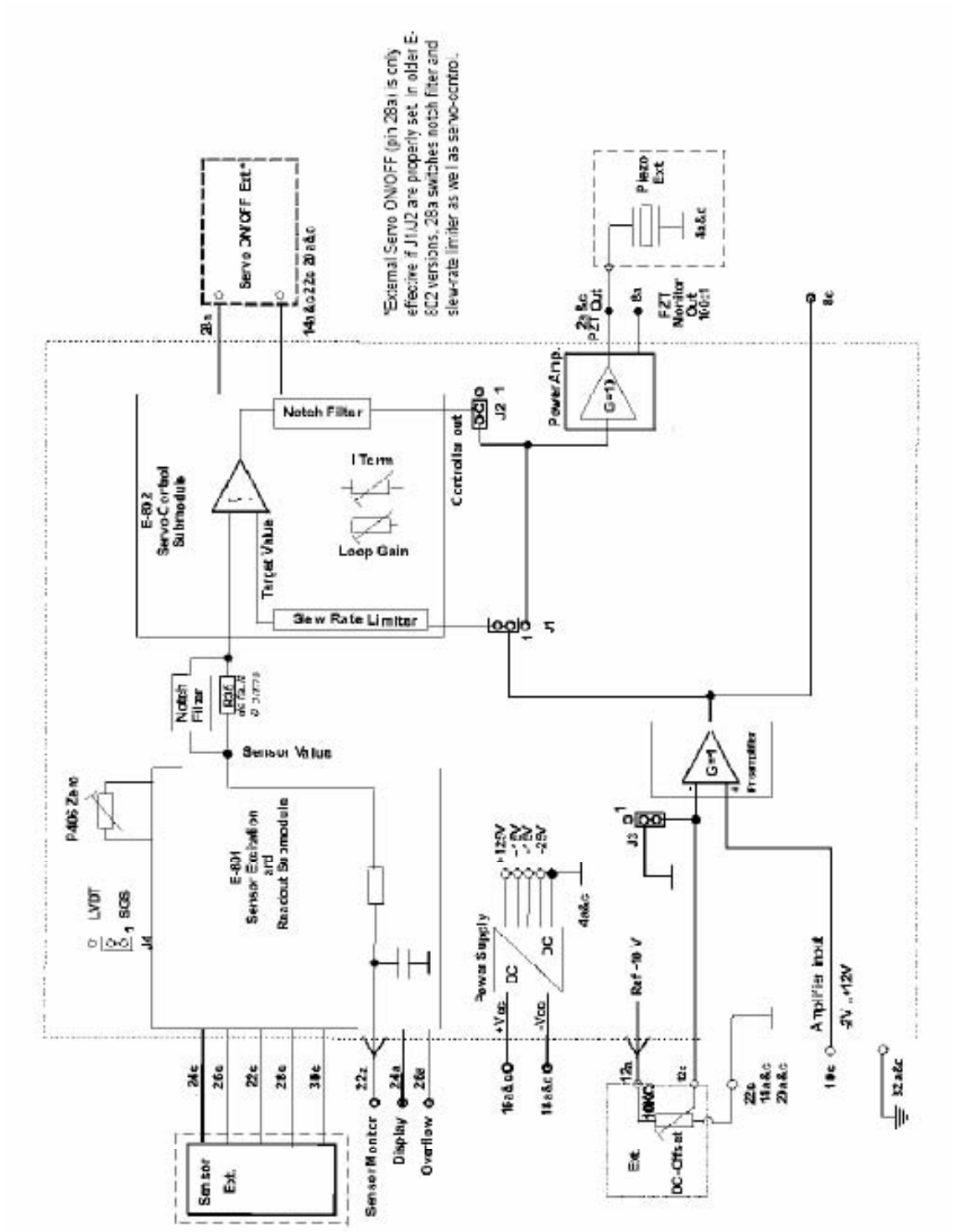

Measurement Display Circuit Diagram

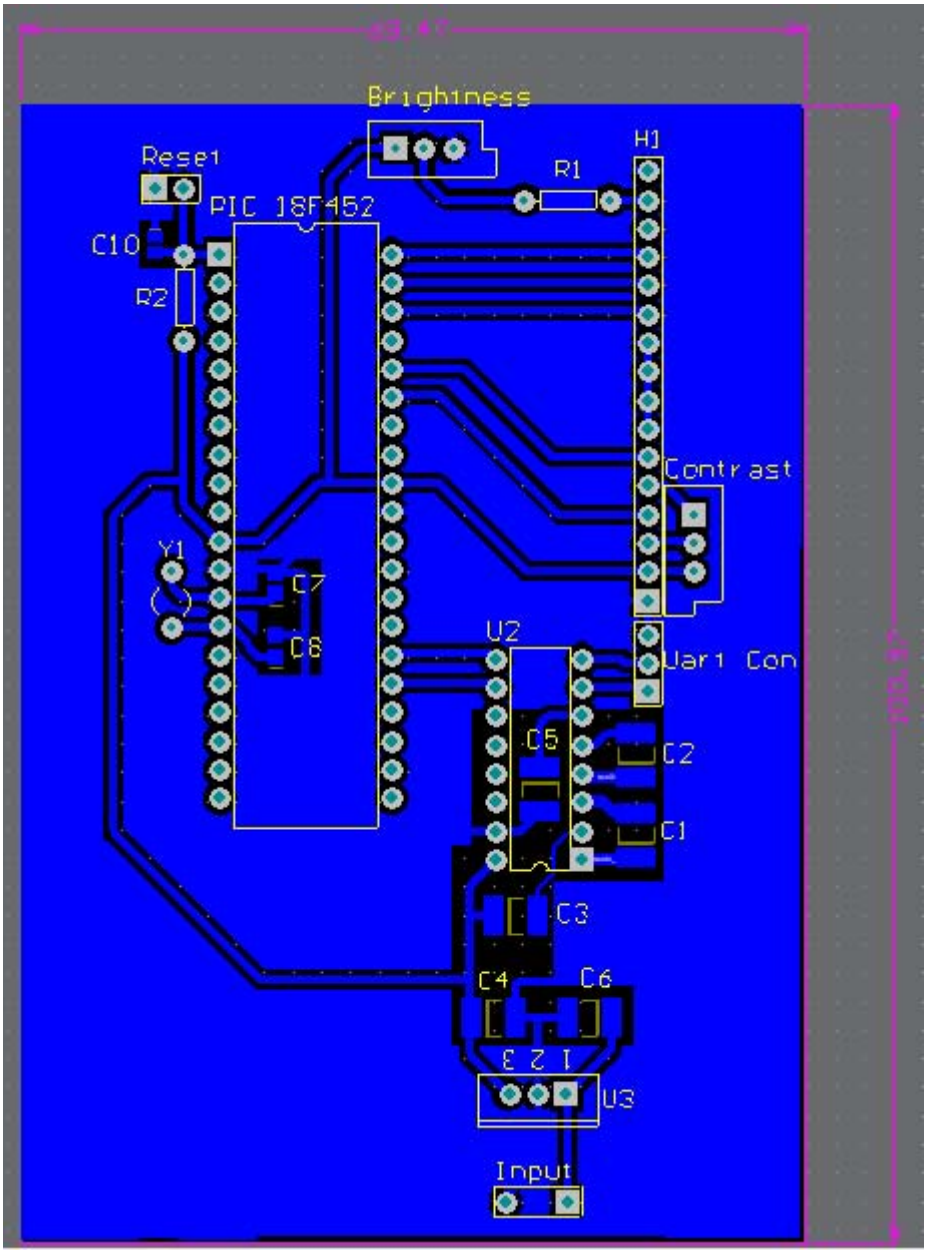

Patton Electronics Model 222N9 Ultra-miniature RS-232 (EIA-574) to RS-422 Interface Converter Circuit Diagram

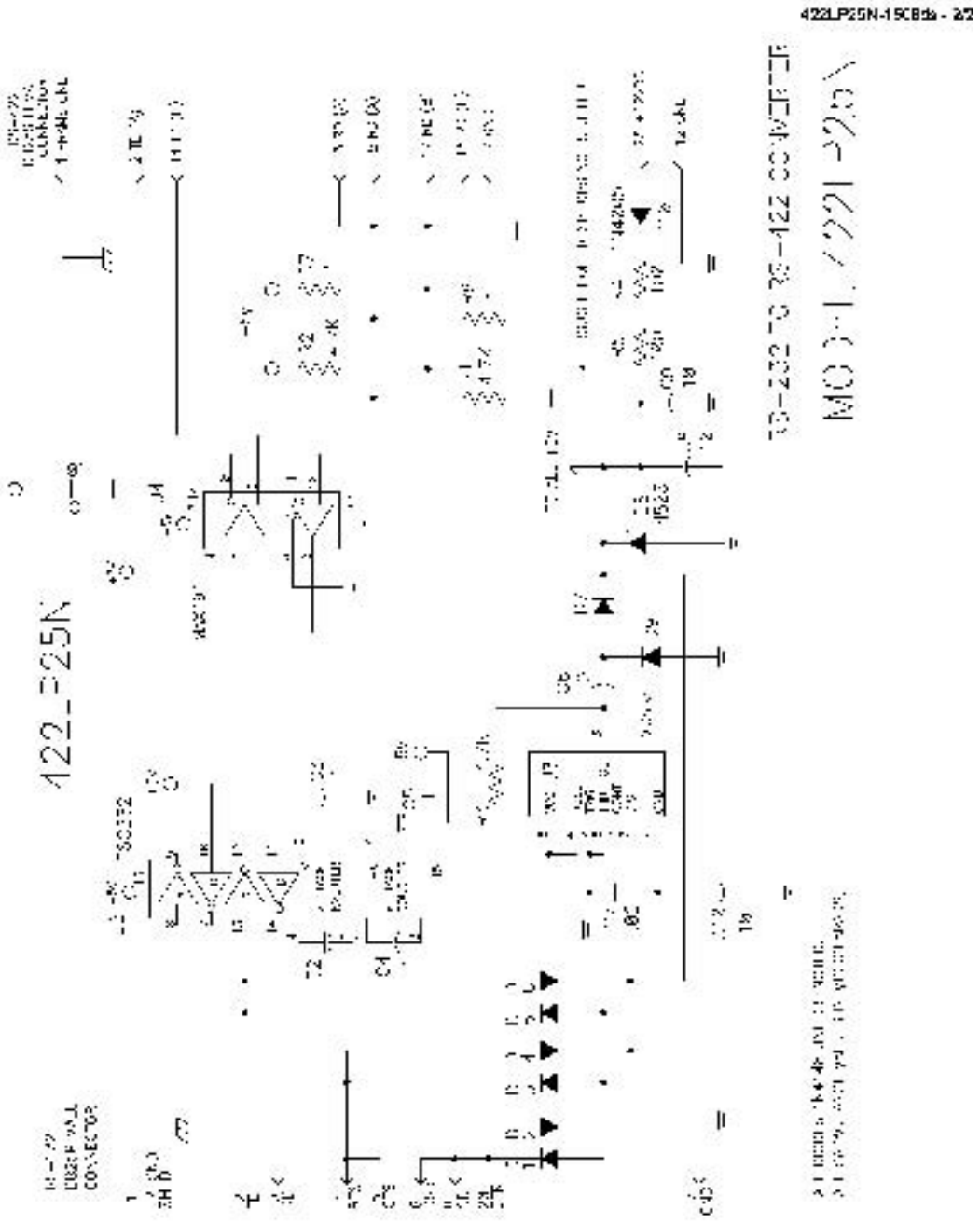

Appendix C
Datasheets and Specifications

Patton Electronics Model 222N9 Ultra-miniature RS-232 (EIA-574) to RS-422 Interface Converter Specifications

Transmission Format:	Asynchronous
Data Rate:	0 to 19,200 bps (no strapping)
Control Signal:	CTS (Pin 8) turns ON immediately after the terminal raises RTS (Pin 7). DSR (Pin 6) and DCD (Pin 1) turn ON immediately after the terminal raises DTR (Pin 4).
Transmit Line:	4 wire, unconditioned line (2 twisted pairs)
Transmit Mode:	Full Duplex, 4-wire
Transmit Level:	0 dBm
Line Connection:	RJ-11 or RJ-45 jack or 5 screw terminal posts (4 wires and 1 ground) and a strain relief insert. Works well with data signals only.
Power Supply:	None required, uses ultra low power from EIA data and control signals
Surge Protection:	Compliant with IEC 801.5 level 2, 1kV (Model 222N9S Only)
Size:	2.50" x 1.2" x .75"

THK Linear Motion (LM) Guide Actuator KR201A+100LH Specifications

Model No.	Rail length	Positionnig accuracy reproducibility	Positionnig	Running parallelism	Backlash	Starting torque [Ncm]
KR15	75	±0.003	0.020	0.010	0.002	0,8
	100					
	125					
	150					
	175					
	200					
KR20	100	±0.003	0.020	0.010	0.003	1,2
	150					
	200					
KR26	150	±0.003	0.020	0.010	0.003	4
	200					
	250					
	300					
KR30H	150	±0.003	0.020	0.010	0.003	15
	200					
	300					
	400					
	500		0.025	0.015		
	600					
KR33	150	±0.003	0.020	0.010	0.003	15
	200					
	300					
	400					
	500		0.025	0.015		
	600					
KR45H	340	±0.003	0.025	0.015	0.003	15
	440					
	540					
	640					17
	740		0.030	0.020		
KR46	340	±0.003	0.025	0.015	0.003	15
	440					
	540					
	640					17
	740		0.030	0.020		
KR55	980	±0.005	0.035	0.025	0.003	17
	1080					
	1180		0.040	0.030		20
KR65	980	±0.005	0.035	0.025	0.005	20
	1180					
	1380		0.040	0.030		22

High-Grade Nitrile (NBR) Rubber Anti-Vibration Material Specifications

www.farrat.com

NBR

Description: An elastic vibration damping material with high shock and vibration damping

NBR 40-8, NBR 60-8, NBR 70-8, NBR 70-15, NBR 70-25, NBR 80-25 Tread both sides (T2)
NBR 70-5P1, NBR 70-15P1 Tread one side.
Plain for adhesive bonding
Applications
Passive Isolation
e.g. Sensitive equipment such as scientific, measuring and test equipment.
Active Isolation
e.g. Pumps, compressors, power presses, forging machines, diesel generators, Hydraulic equipment, granulators, material handling equipment

Construction
Moulded from high grade nitrile (NBR) rubber in various hardnesses to suit desired natural frequency and isolation efficiency.

Oil and Chemical Resistance: Excellent
Full chemical resistance, table available on request
Damping C/Cc: 0.09
Coefficient of Friction (dry): 0.8-0.9
Ratio Dynamic to Static Modulus: 4
Working temperature range deg. C: - 30 to + 120
Standard Sheet Sizes;1000 x 500mm plus Strips and Pads

Cut with bandsaw or waterjet; Holes: drill or punch

NBR							
	Hard-ness Irhd	Thick-ness mm	Tread	Compr. Modulus Ecs N/mm2	Maximum Loading Pressure N/mm2	kg/cm2	SSPC* N/mm/mm2
NBR	40	8	T2	3.4	0.5	5	0.43
NBR	60	8	T2	7	1	10	0.88
NBR	70	8	T2	12	1.5	15	1.50
NBR	70	15	T2	12	1.5	15	0.80
NBR	70	25	T2	12	1.5	15	0.48
NBR	80	25	T2	28	2	20	1.12
NBR	70	5	P1	16	1.5	15	3.20
NBR	70	15	P1	16	1.5	15	1.07
Tread Key T2 Tread both sides, P1 Tread one side, P2 No tread either side							

*SSPC Specific static spring constant.

Appendix D
Test Results

Grind Machine Operating Parameter Test: Pressure versus Stock Removal Test Results

1000		
Cycle Time	Stock Removed (mm/hr)	Out of Round
0	0	0.0009652
1	0.00994664	0.00109728
2	0.00887984	0.00073152
3	0.0086741	0.00076708
4	0.00867156	0.00098044
5	0.010922	0.00047244

1100		
Cycle Time	Stock Removed (mm/hr)	Out of Round
0	0	0.00099314
1	0.00915543	0.00102616
2	0.01185418	0.00091948
3	0.0115786	0.00064008
4	0.01319784	0.00078232
5	0.01184402	0.00089916

1200		
Cycle Time	Stock Removed (mm/hr)	Out of Round
0	0	0.00062992
1	0.01126236	0.00059944
2	0.0129667	0.00046228
3	0.01317498	0.00099568
4	0.01276858	0.0010414
5	0.01593596	0.00138684

1300		
Cycle Time	Stock Removed (mm/hr)	Out of Round
0	0	0.00138684
1	0.01432306	0.00058928
2	0.0144145	0.0005334
3	0.01541526	0.00073152
4	0.01481582	0.00133604
5	0.015494	0.00086868

1300		
Cycle Time	Stock Removed (mm/hr)	Out of Round
0	0	0.00074676
1	0.01008126	0.00088392
2	0.0126365	0.00089916
3	0.01306322	0.00092456
4	0.01346708	0.00088392
5	0.01206246	0.00096012

Pressure	Avg. Stock Removal (mm/hr)	Out of Round
1000	0.009418828	0.00083566
1100	0.011526266	0.000876723
1200	0.013221716	0.0008593
1300	0.014892528	0.000907627
1400	0.012262104	0.000883073
1500		

Pressure	Actual Avg. Out of Round (micron)
1000	2.38
1100	3.054
1200	3.162
1300	3.587
1400	3.817
1500	

Proposed Cut-Down Rate Test Results

Piezo Measurement Unit

Run	Date	Time	Relative Time	Sample1	Sample2	Sample3	Sample4	Sample5	Average Diameter
1	09/04/2008	13:09	00:00	13.137729	13.135308	13.139734	13.141835	13.140663	13.139054
2	09/04/2008	13:17	00:08	13.14325	13.142802	13.134717	13.135179	13.131833	13.137556
3	09/04/2008	13:26	00:17	13.136341	13.1323	13.128985	13.133017	13.130382	13.132205
4	09/04/2008	13:35	00:26	13.145918	13.133962	13.136344	13.128733	13.137811	13.136554
5	09/04/2008	13:43	00:34	13.140714	13.130914	13.134243	13.132318	13.141627	13.135963
6	09/04/2008	13:55	00:46	13.13126	13.127462	13.162517	13.135805	13.134862	13.138381
7	09/04/2008	14:05	00:56	13.125049	13.127042	13.130007	13.134369	13.131668	13.129627
8	09/04/2008	14:14	01:05	13.124475	13.130876	13.129187	13.133492	13.130176	13.129641
9	09/04/2008	14:22	01:13	13.128863	13.125267	13.128864	13.125972	13.144871	13.130767
10	09/04/2008	14:32	01:23	13.124285	13.127443	13.13084	13.126487	13.128157	13.127442
11	09/04/2008	14:41	01:32	13.125284	13.122673	13.12432	13.126514	13.125288	13.124816
12	09/04/2008	14:50	01:41	13.120331	13.122337	13.12597	13.129352	13.132047	13.126007
13	09/04/2008	14:59	01:50	13.125834	13.119916	13.131776	13.128004	13.127051	13.126516
14	09/04/2008	15:08	01:59	13.11903	13.118558	13.121172	13.122374	13.120005	13.120228
15	09/04/2008	15:17	02:08	13.12396	13.119455	13.120031	13.122891	13.127865	13.122840
16	09/04/2008	15:28	02:19	13.124293	13.124003	13.115914	13.112571	13.115933	13.118543
18	09/04/2008	15:45	02:36	13.116933	13.113287	13.11445	13.11647	13.11934	13.116096
19	09/04/2008	15:54	02:45	13.117997	13.123033	13.116125	13.113748	13.115173	13.117215
20	09/04/2008	16:03	02:54	13.116774	13.114185	13.114944	13.120056	13.120037	13.117199
21	09/04/2008	16:12	03:03	13.109065	13.11814	13.114287	13.111163	13.112885	13.113108
22	09/04/2008	16:22	03:13	13.106461	13.104576	13.105945	13.105257	13.114664	13.107381
1	10/04/2008	10:27	03:13	13.106398	13.107439	13.10814	13.104997	13.099005	13.105196
2	10/04/2008	10:36	03:22	13.107093	13.107902	13.110268	13.105271	13.109965	13.108100
3	10/04/2008	10:44	03:30	13.107026	13.103888	13.111296	13.10167	13.110583	13.106893
4	10/04/2008	10:52	03:38	13.106945	13.108895	13.105006	13.106243	13.107414	13.106901
5	10/04/2008	11:01	03:47	13.101548	13.097954	13.110975	13.107808	13.098229	13.103303
6	10/04/2008	11:09	03:55	13.109784	13.098886	13.107382	13.099572	13.100947	13.103314
7	10/04/2008	11:17	04:03	13.099441	13.100588	13.100371	13.099886	13.099167	13.099891
8	10/04/2008	11:25	04:11	13.100639	13.099451	13.101893	13.100916	13.097564	13.100093
10	10/04/2008	11:47	04:33	13.099173	13.09634	13.09306	13.094202	13.092624	13.095080
11	10/04/2008	11:58	04:44	13.09918	13.094182	13.093006	13.098718	13.094391	13.095895
12	10/04/2008	12:07	04:53	13.093291	13.093996	13.100948	13.089911	13.08958	13.093545
13	10/04/2008	12:15	05:01	13.096742	13.093609	13.09291	13.094324	13.089583	13.093434
14	10/04/2008	12:24	05:10	13.093805	13.090034	13.090052	13.091322	13.09005	13.091053
15	10/04/2008	12:32	05:18	13.09045	13.086601	13.102089	13.089744	13.09382	13.092541
16	10/04/2008	12:41	05:27	13.089627	13.085816	13.087712	13.096841	13.086539	13.089307
18	10/04/2008	12:49	05:35	13.088845	13.088437	13.087083	13.087297	13.090351	13.088403
19	10/04/2008	13:00	05:46	13.084361	13.090779	13.089405	13.089386	13.089642	13.088715
20	10/04/2008	13:09	05:55	13.083831	13.084297	13.080506	13.096894	13.084743	13.086054
21	10/04/2008	13:18	06:04	13.078614	13.084488	13.081801	13.07859	13.082523	13.081203
22	10/04/2008	13:26	06:12	13.079546	13.077063	13.079323	13.079808	13.081843	13.079517
23	10/04/2008	13:35	06:21	13.0738	13.075351	13.074768	13.078234	13.076362	13.075703
24	10/04/2008	13:44	06:30	13.07751	13.071067	13.073741	13.072984	13.072641	13.073589
25	10/04/2008	13:53	06:39	13.078726	13.075455	13.075016	13.075225	13.071749	13.075234
26	10/04/2008	14:02	06:48	13.080524	13.072027	13.07146	13.075318	13.070881	13.074042
27	10/04/2008	14:11	06:57	13.072061	13.073701	13.070885	13.070389	13.07469	13.072345
28	10/04/2008	14:21	07:07	13.069701	13.07048	13.068287	13.066294	13.071405	13.069233
29	11/04/2008	10:12	07:07	13.068164	13.068517	13.061943	13.073345	13.075167	13.069427
30	11/04/2008	10:22	07:17	13.066273	13.070637	13.065803	13.067675	13.066292	13.067336
31	11/04/2008	10:31	07:26	13.065195	13.068875	13.064484	13.060211	13.061339	13.064021
32	11/04/2008	10:40	07:35	13.059513	13.062248	13.062015	13.068567	13.058442	13.062157
33	11/04/2008	10:50	07:45	13.059133	13.054986	13.059923	13.059025	13.064598	13.059533
34	11/04/2008	10:59	07:54	13.059527	13.058853	13.057419	13.05671	13.054945	13.057491
35	11/04/2008	11:08	08:03	13.058574	13.057552	13.058709	13.054785	13.059491	13.057822
36	11/04/2008	11:18	08:13	13.057025	13.057024	13.054137	13.059176	13.0575	13.056972
37	11/04/2008	11:28	08:23	13.051361	13.052206	13.057465	13.057224	13.060883	13.055828
38	11/04/2008	11:37	08:32	13.051416	13.05244	13.052913	13.073156	13.051971	13.056379
39	11/04/2008	11:47	08:42	13.04963	13.061879	13.054519	13.052129	13.064648	13.056561
40	11/04/2008	11:56	08:51	13.052173	13.050429	13.051114	13.053048	13.060497	13.053452
41	11/04/2008	12:06	09:01	13.04758	13.04836	13.047579	13.048805	13.0519	13.048845
42	11/04/2008	12:15	09:10	13.049548	13.050107	13.05022	13.046902	13.049883	13.049332
43	11/04/2008	12:25	09:20	13.050155	13.055786	13.045407	13.046808	13.044725	13.048576
44	11/04/2008	12:35	09:30	13.045659	13.043416	13.043089	13.043791	13.044496	13.044090
45	11/04/2008	12:44	09:39	13.043048	13.042019	13.043778	13.041444	13.042581	13.042574
46	11/04/2008	12:54	09:49	13.043626	13.043294	13.043388	13.043406	13.042361	13.043215
47	11/04/2008	13:05	10:00	13.033901	13.033923	13.034156	13.036898	13.03748	13.035272
48	11/04/2008	13:15	10:10	13.03495	13.038555	13.033793	13.036357	13.036121	13.035955
49	11/04/2008	13:25	10:20	13.036261	13.036279	13.033014	13.033491	13.040657	13.035940
50	11/04/2008	13:35	10:20	13.0378	13.036623	13.038977	13.04107	13.035918	13.038078
51	11/04/2008	13:45	10:30	13.02817	13.036503	13.029957	13.029492	13.037181	13.032261
52	11/04/2008	13:55	10:40	13.027446	13.028119	13.036574	13.036346	13.034515	13.032600

Proposed Cut-Down Rate Test Manual Cut Down Chart

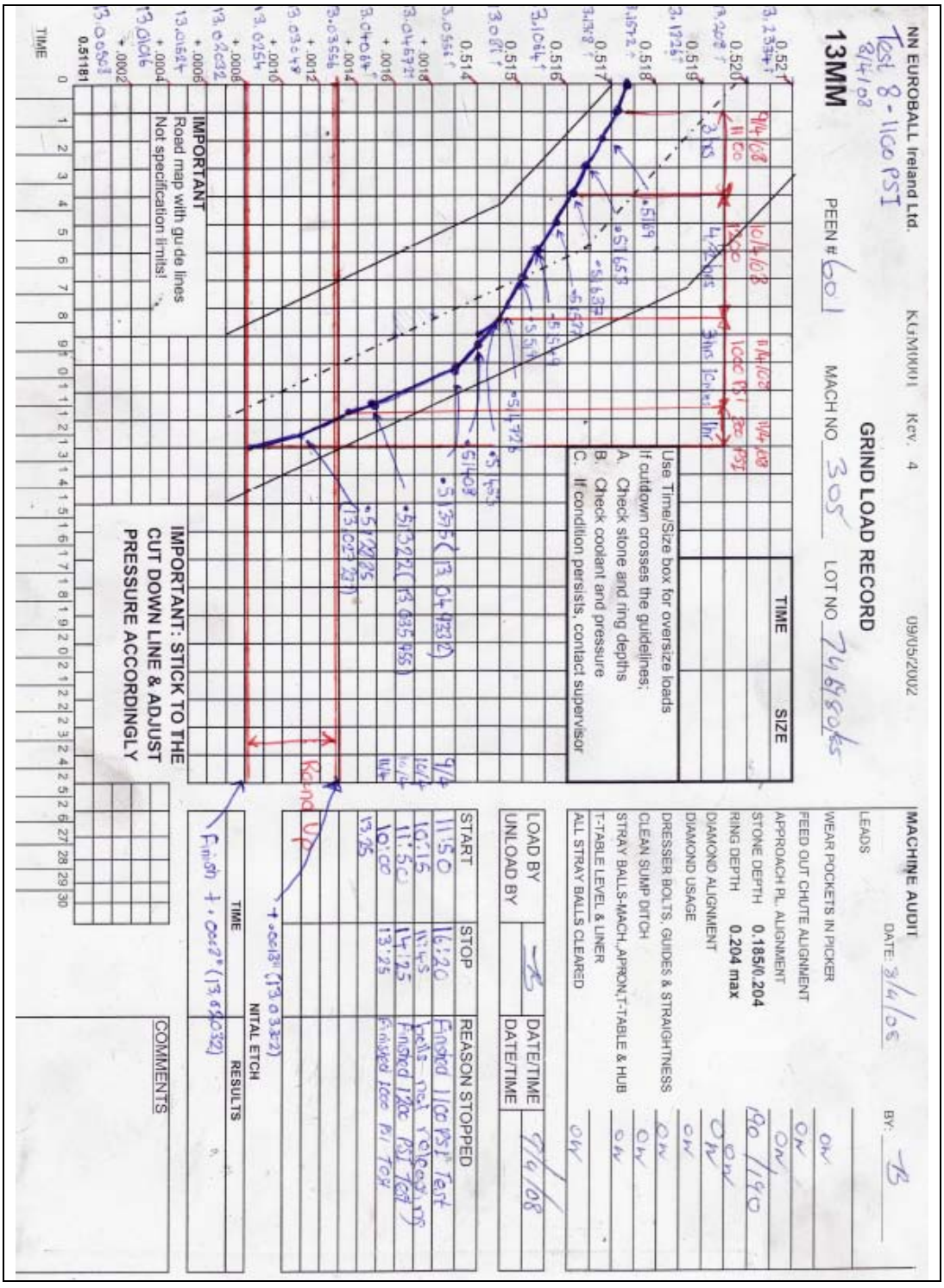

Grinding Process Measurements

Date	Time	Sample1	Sample2	Sample3	Sample4	Sample5
27/03/2008	11:36	13.15301	13.1619	13.153	13.1514	13.15518
27/03/2008	12:00	13.15759	13.15288	13.15143	13.15419	13.15265
27/03/2008	12:13	13.15825	13.15403	13.16135	13.15246	13.15223
27/03/2008	12:22	13.15151	13.15358	13.15642	13.1616	13.15335
27/03/2008	12:30	13.15261	13.15547	13.15855	13.15453	13.15384
27/03/2008	12:38	13.15284	13.15123	13.15833	13.15785	13.15239
27/03/2008	12:48	13.15206	13.1523	13.1523	13.16473	13.1614
27/03/2008	12:56	13.15153	13.15129	13.15338	13.15198	13.15484
27/03/2008	13:05	13.15477	13.15253	13.15215	13.15144	13.15283
27/03/2008	13:14	13.1522	13.1538	13.15244	13.15667	13.15644
28/03/2008	11:14	13.1521	13.16145	13.15488	13.1575	13.15062
28/03/2008	11:26	13.14992	13.15279	13.15232	13.15398	13.15421
28/03/2008	11:37	13.14803	13.14733	13.14803	13.14874	13.14874
28/03/2008	11:48	13.1484	13.15226	13.15273	13.22309	13.18228
28/03/2008	12:06	13.14995	13.14904	13.14801	13.1478	13.15259
28/03/2008	12:19	13.14834	13.15305	13.14995	13.14949	13.15133
28/03/2008	12:30	13.1491	13.1505	13.14794	13.15126	13.14887
28/03/2008	12:41	13.15823	13.15412	13.15467	13.1494	13.15134
28/03/2008	12:54	13.14814	13.14866	13.1541	13.14743	13.14845
28/03/2008	13:06	13.14554	13.14694	13.1481	13.14812	13.14914
28/03/2008	14:21	13.14736	13.14783	13.14878	13.14659	13.1466
28/03/2008	14:47	13.1469	13.1462	13.14905	13.1483	13.15547
28/03/2008	14:58	13.14941	13.1518	13.15225	13.14847	13.14869
01/04/2008	10:40	13.1318	13.2334	13.18252	13.18244	13.18221
01/04/2008	10:45	13.18222	13.18221	13.18245	13.18222	13.18221
01/04/2008	10:48	13.18245	13.18244	13.18222	13.18228	13.18245
01/04/2008	11:02	13.18223	13.23324	13.2334	13.18273	13.18322
01/04/2008	11:11	13.18266	13.18319	13.18293	13.18318	13.18266
01/04/2008	15:18	13.14953	13.14977	13.14983	13.14908	13.14977
01/04/2008	15:30	13.14921	13.14299	13.14276	13.14462	13.14797
01/04/2008	15:59	13.14826	13.14562	13.14182	13.14305	13.14423
01/04/2008	16:20	13.14027	13.14289	13.14001	13.14027	13.14241
02/04/2008	10:37	13.13798	13.1404	13.13774	13.14302	13.14109
02/04/2008	10:50	13.13925	13.14234	13.13753	13.15351	13.14685
03/04/2008	14:24	13.13095	13.08292	13.17743	13.13029	13.08489
04/04/2008	09:48	13.13183	13.13135	13.13161	13.13373	13.13301
04/04/2008	10:46	13.082	13.1826	13.13232	13.13231	13.13233
04/04/2008	10:51	13.13233	13.13233	13.1321	13.13231	13.13232
04/04/2008	10:57	13.082	13.1826	13.13229	13.13229	13.13717
04/04/2008	11:02	13.13719	13.13229	13.13229	13.13229	13.13229
04/04/2008	11:09	13.082	13.1826	13.13244	13.13217	13.13256
04/04/2008	11:13	13.13268	13.13244	13.1329	13.13292	13.13268
04/04/2008	11:20	13.082	13.1826	13.13231	13.13229	13.13229
04/04/2008	11:31	13.13266	13.13266	13.13264	13.13267	13.13266
04/04/2008	11:38	13.13272	13.1327	13.13247	13.13247	13.13247
04/04/2008	12:13	13.13197	13.13209	13.13195	13.13172	13.13174
04/04/2008	15:06	13.13068	13.13119	13.13121	13.13119	13.13122
04/04/2008	15:11	13.082	13.1826	13.13231	13.13208	13.13208
04/04/2008	15:39	13.082	13.1826	13.13106	13.13106	13.13108
04/04/2008	15:43	13.13108	13.1306	13.13082	13.13057	13.13058
04/04/2008	15:48	13.082	13.1826	13.13185	13.13207	13.13185
04/04/2008	15:53	13.13232	13.13207	13.1323	13.1323	13.13207

07/04/2008	13:39	13.20369	13.07764	13.08133	13.08221	13.08651
07/04/2008	13:46	13.13263	13.13294	13.13337	13.13384	13.15265
07/04/2008	14:03	13.13417	13.12962	13.12848	13.13254	13.12796
07/04/2008	14:12	13.12619	13.13219	13.12706	13.12813	13.12687
07/04/2008	14:20	13.133	13.13232	13.13115	13.13068	13.13207
07/04/2008	14:29	13.13628	13.1293	13.13024	13.13198	13.13221
07/04/2008	14:41	13.13184	13.12824	13.13301	13.1314	13.14312
07/04/2008	14:50	13.12555	13.1246	13.12532	13.12871	13.12508
07/04/2008	14:58	13.12528	13.12528	13.13958	13.12978	13.13148
07/04/2008	15:07	13.12499	13.12499	13.124	13.1273	13.12499
07/04/2008	15:16	13.12102	13.12432	13.12717	13.12266	13.12432
07/04/2008	15:25	13.12345	13.1299	13.12323	13.1246	13.12447
07/04/2008	15:34	13.12128	13.12103	13.12644	13.12622	13.11934
07/04/2008	15:43	13.12342	13.11916	13.11941	13.12156	13.1213
07/04/2008	15:52	13.11747	13.11794	13.11912	13.12277	13.12465
07/04/2008	16:01	13.12077	13.11932	13.11883	13.11652	13.11597
07/04/2008	16:10	13.11691	13.11667	13.11957	13.11738	13.12262
07/04/2008	16:19	13.11455	13.11905	13.11618	13.12031	13.11548
07/04/2008	16:28	13.12392	13.11651	13.11676	13.12894	13.11526
07/04/2008	16:37	13.11342	13.1122	13.11414	13.11578	13.1122
07/04/2008	16:47	13.11774	13.11253	13.11583	13.11469	13.11252
07/04/2008	16:56	13.10914	13.11298	13.11086	13.11489	13.11271
07/04/2008	17:06	13.10877	13.11367	13.11105	13.11207	13.11699
08/04/2008	10:29	13.10869	13.10777	13.10945	13.10993	13.11134
08/04/2008	11:04	13.11174	13.1093	13.10793	13.11174	13.1069
08/04/2008	11:12	13.10898	13.1054	13.12435	13.10608	13.10492
08/04/2008	11:22	13.10834	13.10928	13.10615	13.10664	13.10568
08/04/2008	11:30	13.10602	13.10461	13.10053	13.10695	13.10695
08/04/2008	11:38	13.10064	13.09923	13.10189	13.10134	13.10213
08/04/2008	11:54	13.10839	13.1043	13.10073	13.10073	13.01879
08/04/2008	12:10	13.09526	13.09598	13.1	13.09667	13.0969
08/04/2008	12:18	13.09432	13.09581	13.09626	13.09476	13.0965
08/04/2008	12:31	13.09878	13.09026	13.09098	13.09809	13.08932
08/04/2008	12:39	13.09285	13.09047	13.09047	13.09504	13.09073
08/04/2008	12:52	13.08579	13.0898	13.08794	13.08887	13.08885
08/04/2008	13:01	13.08627	13.09582	13.08729	13.08678	13.09014
08/04/2008	13:10	13.08906	13.08742	13.08308	13.08668	13.08284
08/04/2008	13:18	13.08388	13.08483	13.08293	13.08102	13.08342
08/04/2008	13:27	13.0825	13.08301	13.08202	13.0811	13.08016
08/04/2008	13:36	13.07983	13.07791	13.07651	13.08315	13.08051
08/04/2008	13:54	13.07709	13.07901	13.07544	13.07474	13.07971
08/04/2008	14:07	13.07327	13.07302	13.07682	13.07256	13.07466
09/04/2008	13:09	13.13773	13.13531	13.13973	13.14184	13.14066
09/04/2008	13:17	13.14325	13.1428	13.13472	13.13518	13.13183
09/04/2008	13:26	13.13634	13.1323	13.12899	13.13302	13.13038
09/04/2008	13:35	13.14592	13.13396	13.13634	13.12873	13.13781
09/04/2008	13:43	13.14071	13.13091	13.13424	13.13232	13.14163
09/04/2008	13:55	13.13126	13.12746	13.16252	13.13581	13.13486
09/04/2008	14:05	13.12505	13.12704	13.13001	13.13437	13.13167
09/04/2008	14:14	13.12448	13.13088	13.12919	13.13349	13.13018
09/04/2008	14:22	13.12886	13.12527	13.12886	13.12597	13.14487
09/04/2008	14:32	13.12429	13.12744	13.13084	13.12649	13.12816

09/04/2008	14:41	13.12528	13.12267	13.12432	13.12651	13.12529
09/04/2008	14:50	13.12033	13.12234	13.12597	13.12935	13.13205
09/04/2008	14:59	13.12583	13.11992	13.13178	13.128	13.12705
09/04/2008	15:08	13.11903	13.11856	13.12117	13.12237	13.12001
09/04/2008	15:17	13.12396	13.11946	13.12003	13.12289	13.12787
09/04/2008	15:28	13.12429	13.124	13.11591	13.11257	13.11593
09/04/2008	15:36	13.142	13.14108	13.29949	13.29515	13.30817
09/04/2008	15:45	13.11693	13.11329	13.11445	13.11647	13.11934
09/04/2008	15:54	13.118	13.12303	13.11613	13.11375	13.11517
09/04/2008	16:03	13.11677	13.11419	13.11494	13.12006	13.12004
09/04/2008	16:12	13.10907	13.11814	13.11429	13.11116	13.11289
09/04/2008	16:22	13.10646	13.10458	13.10595	13.10526	13.11466
10/04/2008	10:27	13.1064	13.10744	13.10814	13.105	13.09901
10/04/2008	10:36	13.10709	13.1079	13.11027	13.10527	13.10997
10/04/2008	10:44	13.10703	13.10389	13.1113	13.10167	13.11058
10/04/2008	10:52	13.10695	13.1089	13.10501	13.10624	13.10741
10/04/2008	11:01	13.10155	13.09795	13.11098	13.10781	13.09823
10/04/2008	11:09	13.10978	13.09889	13.10738	13.09957	13.10095
10/04/2008	11:17	13.09944	13.10059	13.10037	13.09989	13.09917
10/04/2008	11:25	13.10064	13.09945	13.10189	13.10092	13.09756
10/04/2008	11:35	13.25648	13.32428	13.32225	13.30963	13.32473
10/04/2008	11:47	13.09917	13.09634	13.09306	13.0942	13.09262
10/04/2008	11:58	13.09918	13.09418	13.09301	13.09872	13.09439
10/04/2008	12:07	13.09329	13.094	13.10095	13.08991	13.08958
10/04/2008	12:15	13.09674	13.09361	13.09291	13.09432	13.08958
10/04/2008	12:24	13.09381	13.09003	13.09005	13.09132	13.09005
10/04/2008	12:32	13.09045	13.0866	13.10209	13.08974	13.09382
10/04/2008	12:41	13.08963	13.08582	13.08771	13.09684	13.08654
10/04/2008	12:49	13.08885	13.08844	13.08708	13.0873	13.09035
10/04/2008	13:00	13.08436	13.09078	13.08941	13.08939	13.08964
10/04/2008	13:09	13.08383	13.0843	13.08051	13.09689	13.08474
10/04/2008	13:18	13.07861	13.08449	13.0818	13.07859	13.08252
10/04/2008	13:26	13.07955	13.07706	13.07932	13.07981	13.08184
10/04/2008	13:35	13.0738	13.07535	13.07477	13.07823	13.07636
10/04/2008	13:44	13.07751	13.07107	13.07374	13.07298	13.07264
10/04/2008	13:53	13.07873	13.07546	13.07502	13.07523	13.07175
10/04/2008	14:02	13.08052	13.07203	13.07146	13.07532	13.07088
10/04/2008	14:11	13.07206	13.0737	13.07089	13.07039	13.07469
10/04/2008	14:21	13.0697	13.07048	13.06829	13.06629	13.07141
11/04/2008	10:12	13.06816	13.06852	13.06194	13.07335	13.07517
11/04/2008	10:22	13.06627	13.07064	13.0658	13.06768	13.06629
11/04/2008	10:31	13.0652	13.06888	13.06448	13.06021	13.06134
11/04/2008	10:40	13.05951	13.06225	13.06202	13.06857	13.05844
11/04/2008	10:50	13.05913	13.05499	13.05992	13.05903	13.0646
11/04/2008	10:59	13.05953	13.05885	13.05742	13.05671	13.05495

11/04/2008	11:08	13.05857	13.05755	13.05871	13.05479	13.05949
11/04/2008	11:18	13.05703	13.05702	13.05414	13.05918	13.0575
11/04/2008	11:28	13.05136	13.05221	13.05747	13.05722	13.06088
11/04/2008	11:37	13.05142	13.05244	13.05291	13.07316	13.05197
11/04/2008	11:47	13.04963	13.06188	13.05452	13.05213	13.06465
11/04/2008	11:56	13.05217	13.05043	13.05111	13.05305	13.0605
11/04/2008	12:06	13.04758	13.04836	13.04758	13.04881	13.0519
11/04/2008	12:15	13.04955	13.05011	13.05022	13.0469	13.04988
11/04/2008	12:25	13.05016	13.05579	13.04541	13.04681	13.04473
11/04/2008	12:35	13.04566	13.04342	13.04309	13.04379	13.0445
11/04/2008	12:44	13.04305	13.04202	13.04378	13.04144	13.04258
11/04/2008	12:54	13.04363	13.04329	13.04339	13.04341	13.04236
11/04/2008	13:05	13.0339	13.03392	13.03416	13.0369	13.03748
11/04/2008	13:15	13.03495	13.03856	13.03379	13.03636	13.03612
11/04/2008	13:25	13.03626	13.03628	13.03301	13.03349	13.04066
11/04/2008	13:35	13.0378	13.03662	13.03898	13.04107	13.03592
11/04/2008	13:45	13.02817	13.0365	13.02996	13.02949	13.03718
11/04/2008	13:55	13.02745	13.02812	13.03657	13.03635	13.03452
11/04/2008	14:06	13.02401	13.02187	13.02002	13.02071	13.02037
11/04/2008	14:16	13.02403	13.02709	13.02739	13.02907	13.02885
11/04/2008	14:27	13.02208	13.02117	13.02219	13.02357	13.02117
11/04/2008	14:34	13.02939	13.024	13.03519	13.02176	13.03211

Appendix E
Drawings

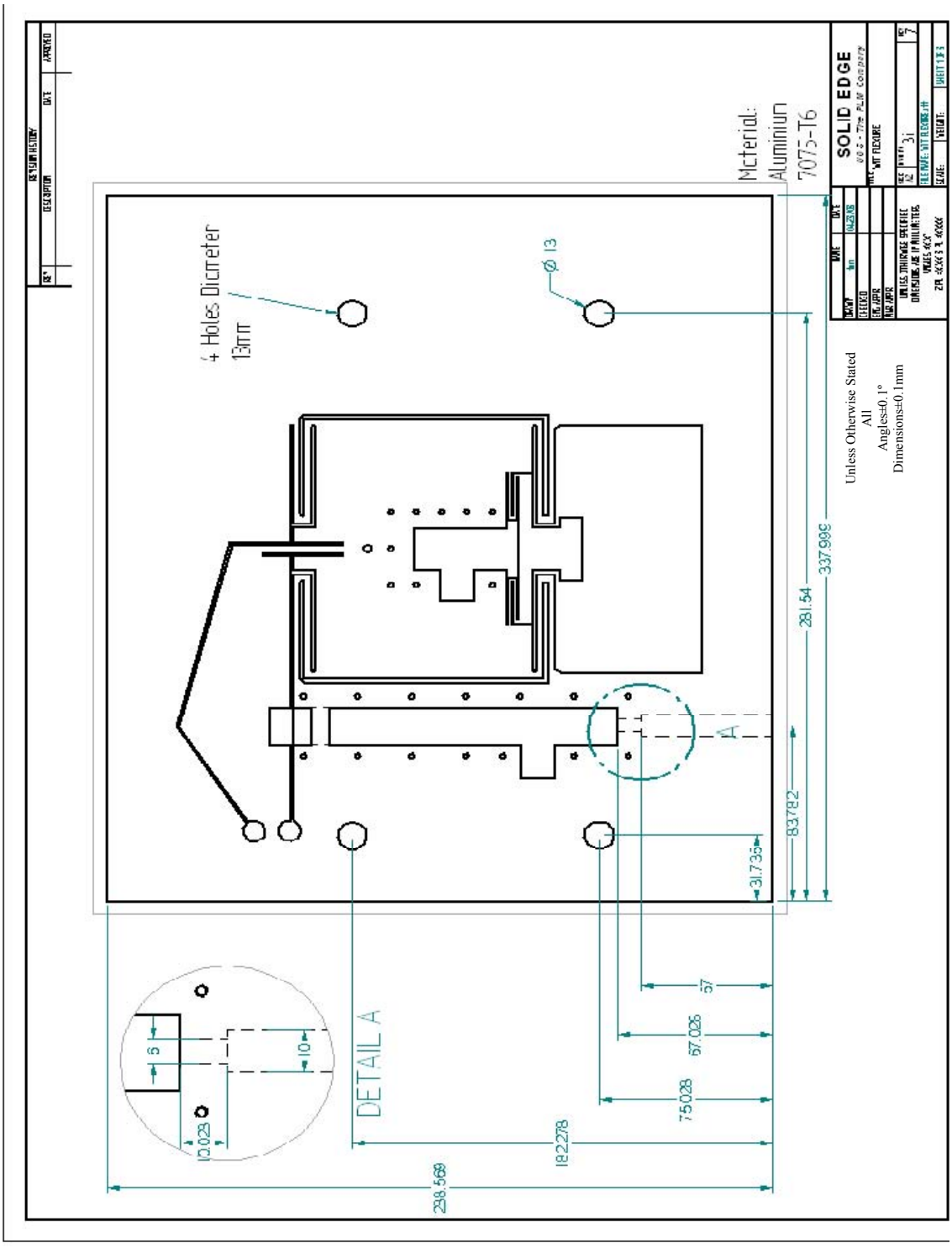
4 Holes Diameter 13mm
Ø 13
Material: Aluminium 7075-T6
Unless Otherwise Stated
All
Angles±0.1°
Dimensions±0.1mm
SOLID EDGE
DETAIL A
337.996
281.54
83.782
31.735
57
67.026
75.028
182.278
238.569
10.023
6
10

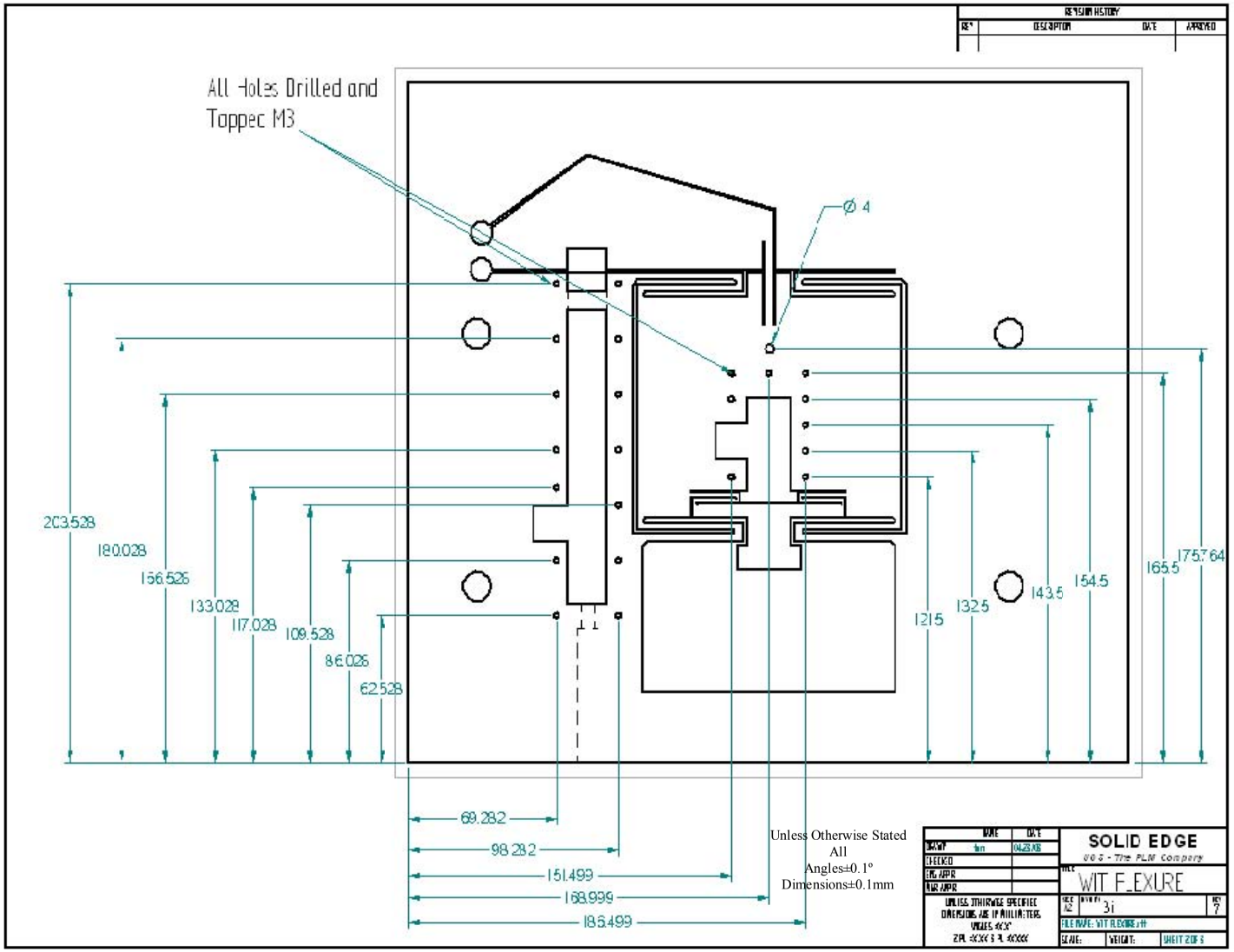
All Holes Drilled and Tappec M3
Ø 4
203.528
180.028
156.528
133.028
117.028
109.528
86.028
62.528
121.5
132.5
143.5
154.5
165.5
175.764
69.282
98.282
151.493
168.999
185.499
Unless Otherwise Stated
All
Angles±0.1°
Dimensions±0.1mm
SOLID EDGE
WIT F_EXURE

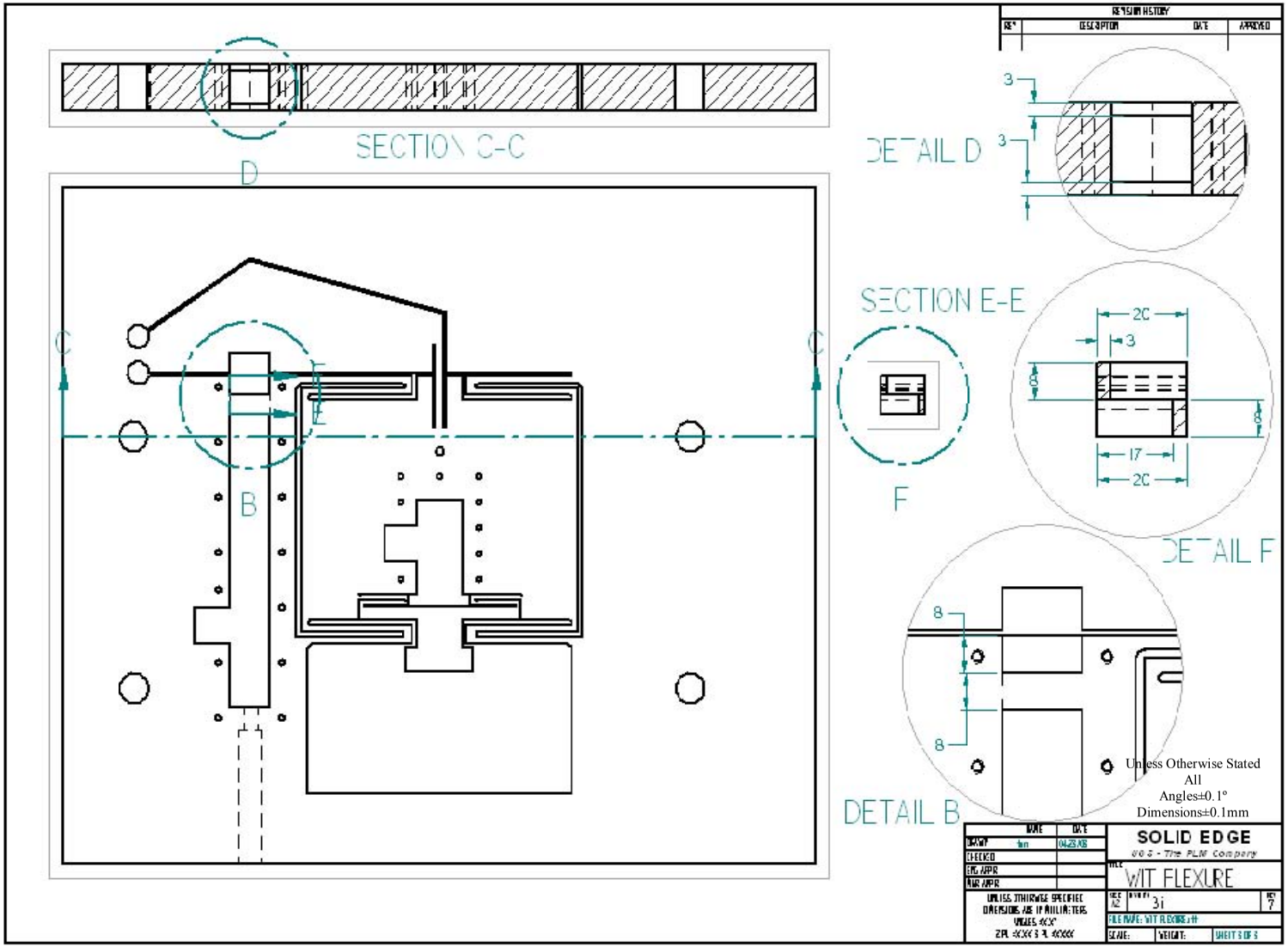
REVISION HISTORY
REV
DESCRIPTION
DATE
APPROVED
SECTION C-C
D
C
C
E
B
SECTION E-E
F
DETAIL D
3
3
DETAIL F
20
3
8
8
17
20
DETAIL B
8
8
Unless Otherwise Stated
All
Angles±0.1°
Dimensions±0.1mm
NAME
DATE
DRAWN
tim
04.23.08
CHECKED
ENG APPR.
MFG APPR.
UNLESS OTHERWISE SPECIFIED
DIMENSIONS ARE IN MILLIMETERS
SOLID EDGE
ST5 - The PLM Company
TITLE
WIT FLEXURE
SIZE
A2
DWG NO
3i
REV
7
FILE NAME: WIT FLEXURE.ipt
SCALE:
WEIGHT:
SHEET 3 OF 3

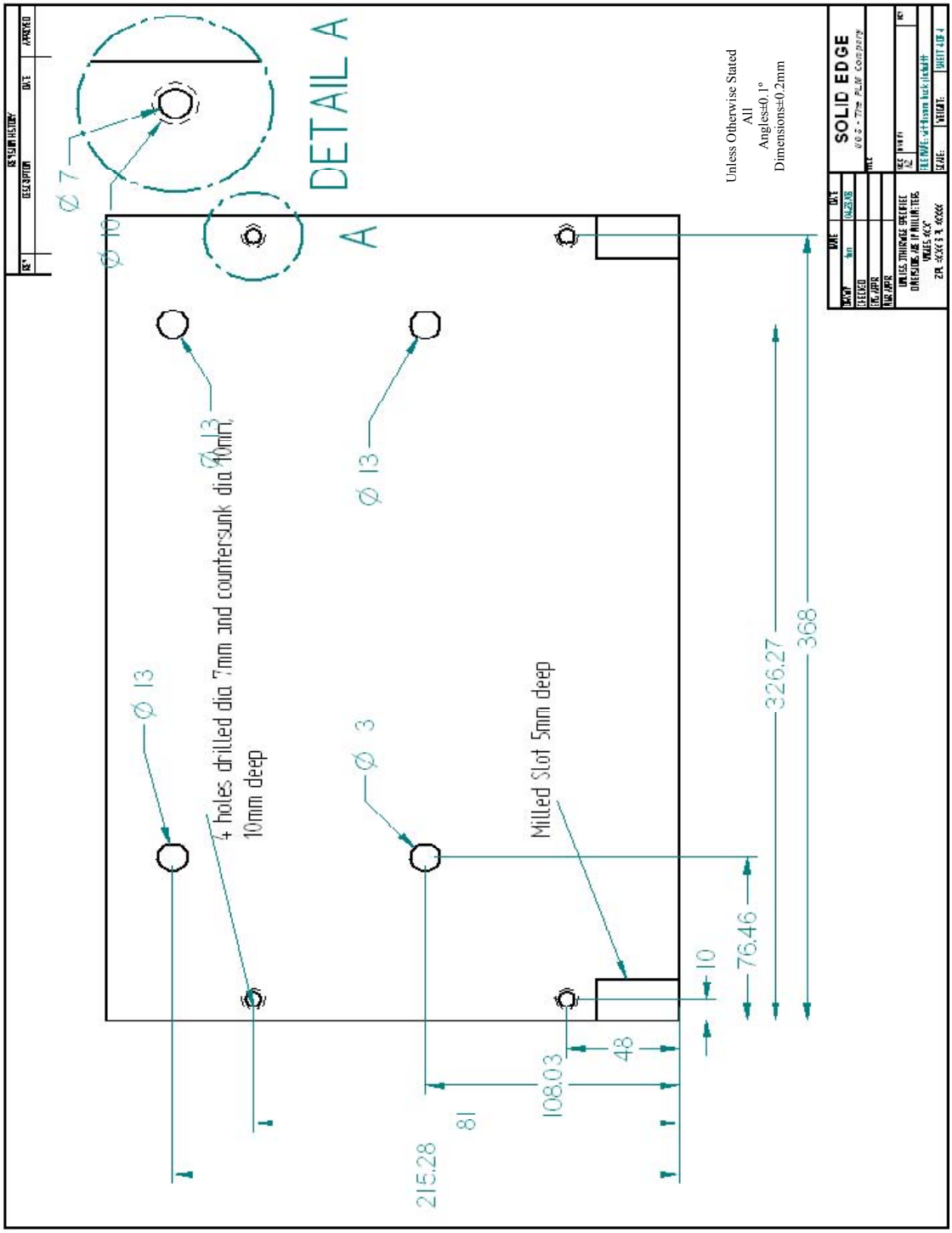
DETAIL A
A
Unless Otherwise Stated
All
Angles±0.1°
Dimensions±0.2mm
SOLID EDGE
Ø 7
Ø 10
Ø 13
Ø 13
4 holes drilled dia 7mm and countersunk dia 10mm
10mm deep
Ø 13
Ø 3
Milled Slot 5mm deep
368
326.27
76.46
10
48
108.03
81
215.28

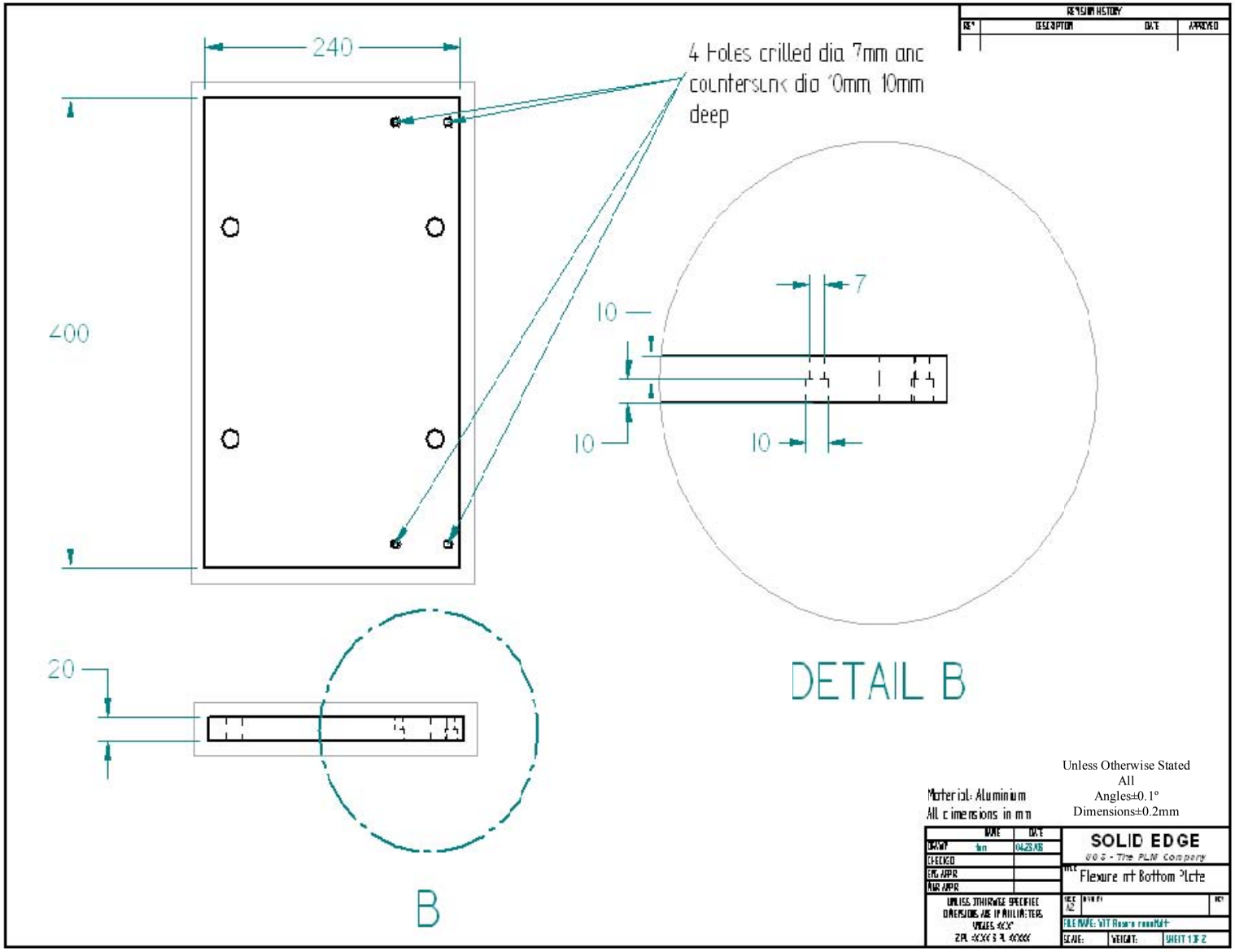
240
400
4 Holes drilled dia 7mm and
countersink dia 10mm 10mm
deep
7
10
10
10
DETAIL B
20
B
Material: Aluminium
All dimensions in mm
Unless Otherwise Stated
All
Angles±0.1°
Dimensions±0.2mm
SOLID EDGE
Flexure rt Bottom Plate

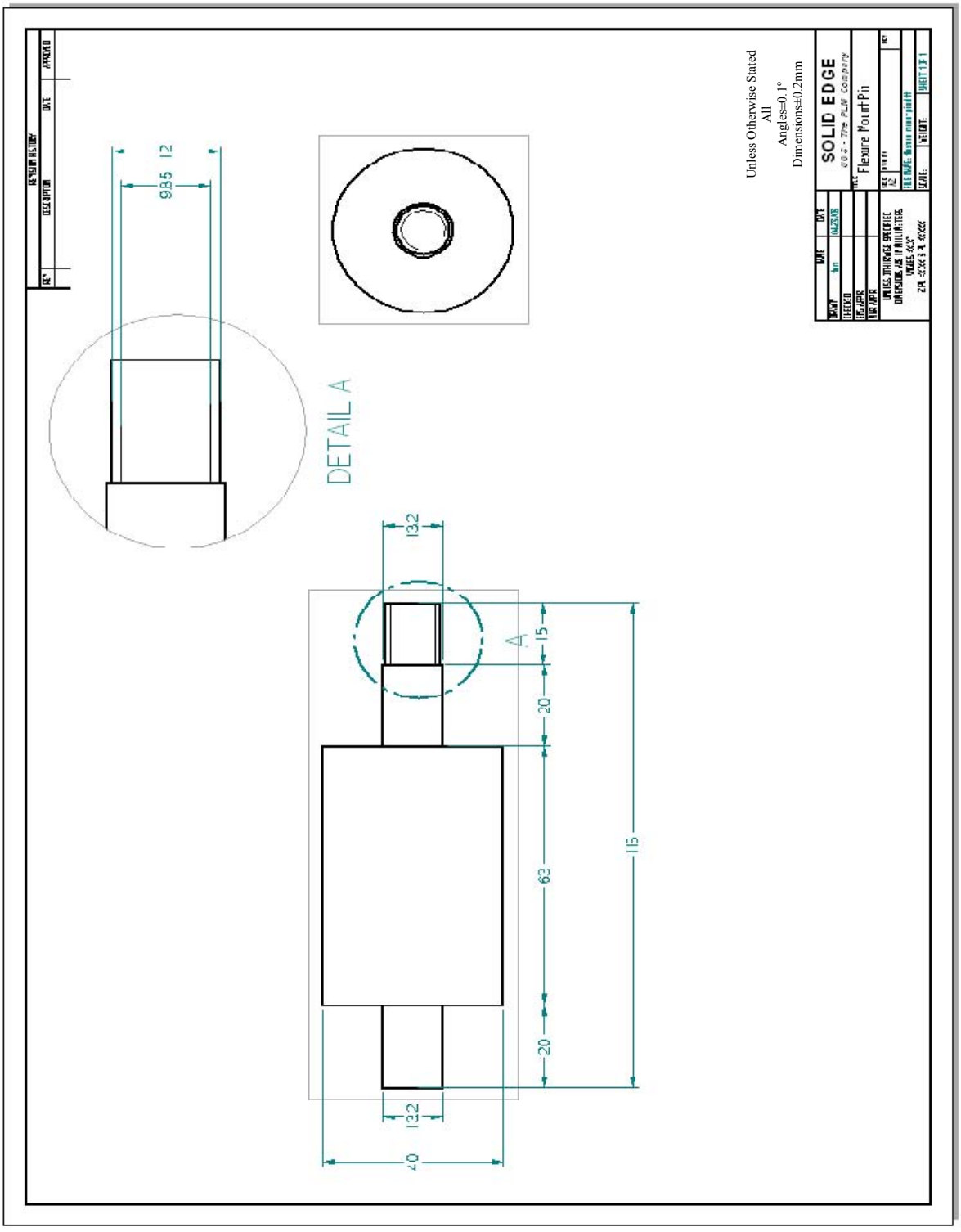
Unless Otherwise Stated
All
Angles±0.1°
Dimensions±0.2mm
SOLID EDGE
Flexure MountPin
DETAIL A
9.85
12
13.2
15
20
63
113
20
13.2
40

Appendix F
Data Acquisition

The fundamental task of all measurement systems is the measurement and/or generation of real-world physical signals; measurement devices help acquire, analyze and present the measurements taken. Data acquisition (DAQ) is the sampling of the real world to generate data that can be manipulated by a computer; acquire and convert physical signals such as voltage, current, pressure and temperature into digital formats and transfer them into the computer for storage, analysis and presentation. DAQ systems come in many different PC technology forms; scientists and engineers can choose from PCI, PXI, PCI Express, USB, parallel or serial ports for data acquisition in test, measurement and automation applications. As shown in the components to be considered when building a basic DAQ system are:

- Transducers and Sensors
- Signals
- DAQ Hardware
- Driver and Application Software

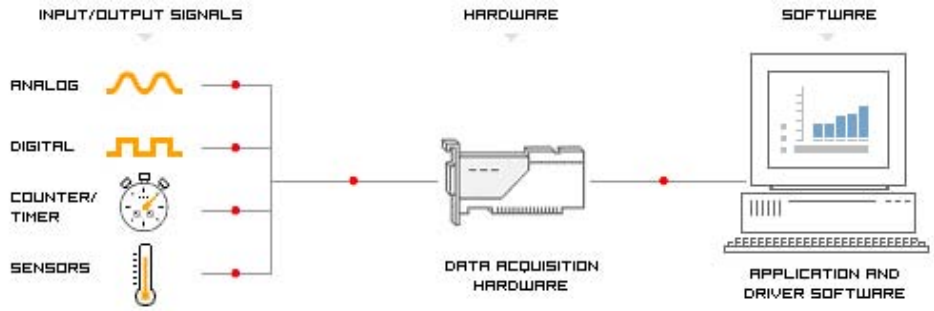

Figure 142 Data Acquisition Software

Data acquisition begins with the physical phenomenon to be measured. This physical phenomenon could be the temperature of a room, the intensity of a light source, the force applied to an object or many other things. In relation to the developed automated measurement instrument the physical phenomena being measured is the expansion of both the primary piezo actuator that functions to drive the stage through long-travel positioning and the secondary touch sensor piezo actuator.

A transducer is a device that converts a physical phenomenon into a measurable electrical signal, such as voltage or current. The ability of a DAQ system to measure different phenomena depends on the transducers to convert the physical phenomena into signals measurable by the DAQ hardware; on the measurement instrument, strain

gauges attached to both piezo actuators output DC signals that are amplified in preamplifier and outputted as an analog signal between 0 to 10v directly proportional to the piezo expansion. Transducer are identical with sensors in DAQ systems.

Transducer signals can be categorized into two groups, analog and digital. An analog signal can be at any value with respect to time; different types of analog signals include voltage, temperature, pressure, sound and load. The three primary characteristics of an analog signal include level, shape and frequency

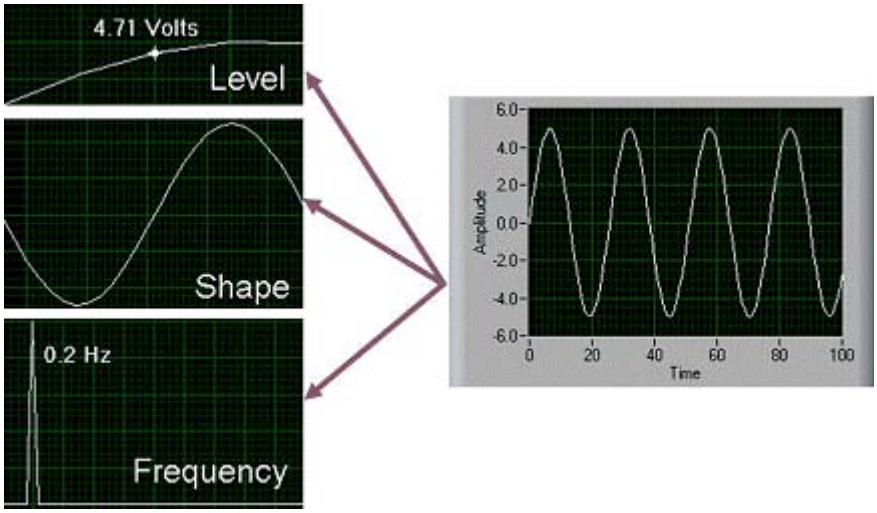

Figure 143 Primary Characteristics of an Analog Signal

Since analog signals can take on any value, the level gives vital information about the measured analog signal; the expansion of the piezo actuators is directly proportional to the level of the strain gauge feedback voltage.

Some signals are named after their specific shape- sine, square, sawtooth and triangle. The shape of an analog signal can be as important as the level; measuring the shape of the signal allows the peak values and the slope to be examined. Signals where shape is of interest generally change rapidly with respect to time.

All analog signals can be categorized by their frequency; frequency is a measure of the number of occurrences of a repeating event per unit time. Unlike the level or shape of a signal, frequency cannot be directly measured; the signal must be analysed using software to determine the frequency information. When frequency is the most important piece of information, it is important to consider both accuracy and acquisition speed. Although the acquisition speed for acquiring the frequency of a signal is less than the speed required for obtaining the shape of a signal, the signal must still be acquired fast enough that the relevant information is not lost while the analog signal is being

acquired. The condition that stipulates the acquisition speed is known as the Nyquist Sampling Theorem; this theorem states that a signal must be sampled at least twice as fast as the bandwidth of the signal to accurately reconstruct the waveform [47]. If the signal is not sampled sufficiently fast enough, the high frequency content will alias at a frequency inside the spectrum of interest; an alias is a false lower frequency component that appears in sampled data acquire at too low a sampling rate. Figure 144shows a sampled sine wave with an inappropriate acquisition speed, the dotted line indicates the aliased signal; two different sinusoids fit the same sample.

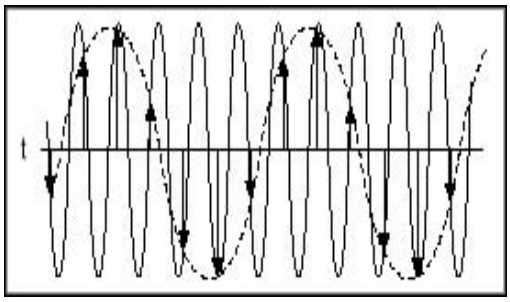

Figure 144 Sine Wave Demonstrating the Nyquist Frequency [47]

The second type of signal is a digital signal; a digital signal cannot take on any value with respect to time. Instead, a digital signal has two possible levels: high and low. Digital signals generally confirm to certain specifications that define characteristics of the signal and are commonly referred to as transistor-to-transistor logic (TTL); TTL specifications indicate a digital to be low when the level falls within 0 to 0.8v and the signal is high between 2 to 5v. As shown in Figure 145, the useful information that can be measured from a digital signal includes the state and the rate.

The state of a digital signal is essentially the level of the signal: on or off, high or low.

The rate of a digital signal defines how the digital signal changes state with respect to time. Unlike frequency, the rate of a signal measures how often a portion of a signal occurs.

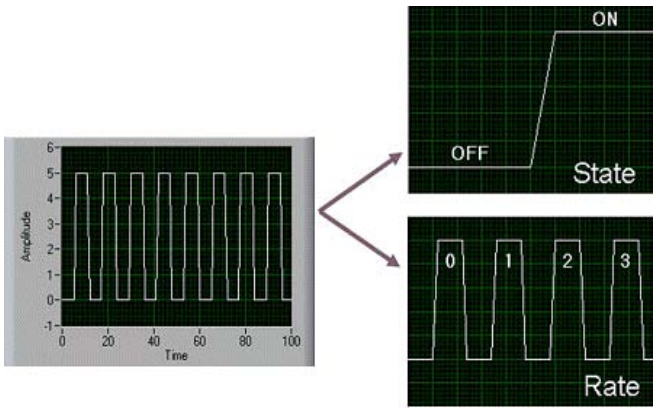

Figure 145 Primary Characteristics of a Digital Signal

DAQ hardware acts as the interface between the computer and the outside world. It primarily functions as a device

that digitises incoming analog signals so that the PC can interpret them. A DAQ measurement system is different from other measurement systems because the software in stalled on the PC performs the actual measurements; the DAQ device only converts the incoming signal into a digital signal the PC can use. Other data acquisition functionality includes:

- Analog Input/Output
- Digital Input/Output
- Counters/Timers
- Multifunction – a combination of analog, digital and counter operations on a single device

Appendix G
Stepper Motors

Stepper motors can be viewed as electric motors without commutators; a commutator is an electrical switch that periodically reverses the current direction in an electric motor, by reversing the current direction in the moving coil of a motors armature, a steady rotating force is produced [47]. Typically, all windings in a stepper motor are part of the stator and the rotor is a permanent magnet. The motor controller must handle all of the commutation externally; typically the motor and controller are designed so that the motor can be rotated in both directions and held in any fixed position.

For the locating platform application, there was a choice between using servomotors and stepping motors to drive the LM guide actuator. Both types of motors offer similar opportunities for precise positioning, but they differ in a number of ways. Servomotors require analog control systems of some type; this involves a potentiometer to provide feedbackabout the rotor position and some mix of circuitry to drive a current through the motor inversely proportional to the difference between the desired position and the current position.

In making a choice between stepper motors and servomotors, a number of issues must be considered. For example, the repeatability of positioning achieved with a stepper motor depends on the geometry of the rotor, while the repeatability of positioning with a servomotor generally depends on the stability of the potentiometer and other analog components in the feedback circuit.

During the design and construction of the ball locator platform, due to backlash within the ball screw there was some doubt about the level of performance of the LM guide actuator in terms of precise positioning and repeatability. For this reason, the simplest and cheapest drive which in this case was a stepper motor, was deemed appropriate to test the stability of the system. Stepper motors can be used in simple cost effective open-loop control systems; therfore a stepper motor should be adequate for the ball locating platform system which operates at low accelerations with static loads.

Stepper motors come in two varieties, permanent magnet and variable reluctance. The feel when no power is applied can generally tell the two apart; permanent magnet motors tend to “cog” when twisted, while variable reluctance motors almost spin freely. Stepper motors come in a wide range of angular resolution; the coarsest motors typically turn 90˚ per step, while high-resolution permanent magnet

motors are commonly able to handle 1.8˚ or even 0.72˚ per step. With an appropriate controller, stepper motors can be run in half steps and some controllers can handle smaller fractional steps or microsteps.

Stepper motors are constant-power devices (power = angular velocity x torque); as the motor speed increases, the torque decreases and vice-versa. As with all mechanical devices, stepper motors are manufactured to a certain tolerance; typically a standard motor has a tolerance of ± 5% non-accumulative error regarding the location of any given step. For example, this means that any step on atypical 200 steps per revolution (1.8º) motor will be within a 0.18º error range.

The specific stepper motor used to drive the ball locator platform is a McLennan 24v 1.8º 23HS-030 (Figure 113); this is unipolar permanent stepper motor. The rotor is a permanent magnet and the stator is made up of two coils or windings giving 4 poles. Each winding is wired with a centre tap; the centre taps of the windings are wired to the positive supply and the two ends of each winding are alternatively grounded to reverse the direction of the field provided.

In the 23HS-030 stepper motor, the permanent magnet lies North-South along the shaft. It is encased in two stacks each with 50 teeth around the rim; the teeth on the South stack are out of phase with the teeth on the North stack by half the gap between teeth. This means that at the same time the teeth on the North stack are being attracted by and thus lining up with the teeth on the currently magnetised pole of the stator, the teeth on the South stack are being repelled and thus lining up with the gaps between the teeth on that same pole.

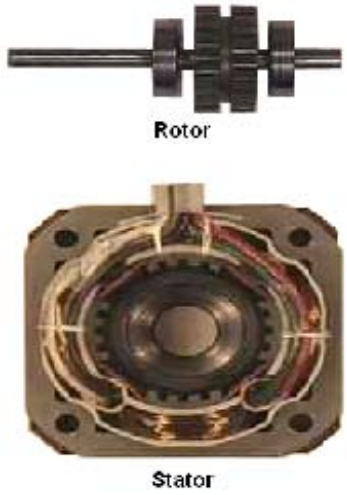

Figure 146 23HS-030

To make the motor shaft turn, first one of the poles is magnetised, which makes the stacks teeth to be attracted to that magnetised pole, as discussed above. When the stacks teeth are thus aligned to the first pole, they are slightly offset from the next pole; when the next pole is energised and the first is de-energised, the stacks rotates slightly to align with the energised pole and from there the process is repeated. Each of the slight rotations is called a step and allows the motor to turn a precise angle. As shown in Figure 147, flattening out the stator and rotor makes it easier to illustrate.

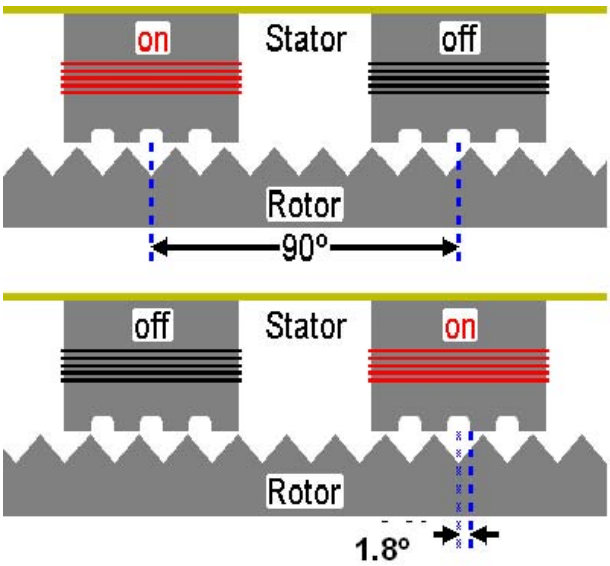

Figure 147 Stepper Motor Operation

With 50 teeth round the edge of the rotor and four poles excited individually in turn, the 23HS-030 stepper motor takes 200 steps per complete revolution; the spacing between the teeth is:

$$\frac{360°}{50} = 7.2°$$

When the teeth on the rotor are aligned with the teeth on the stator pole of the excited coil, they are misaligned by a quarter of that angle with the teeth on the next stator pole; therefore when the coil on that pole becomes energised instead, the rotor is pulled round through one quarter of the 7.2º producing a step of 1.8º.

Generally for this type of stepper motor:

Steps per Complete Revolution = Number of Poles x Number of Teeth on Rotor

As previously mentioned, the motor controller must handle all of the commutation externally; the circuitry is centred on a single issue, switching the current in each motor winding on and off, and controlling its direction. In Figure 148, the boxes are used to represent switches; a control unit, not shown, is responsible for providing the control signals to open and close the switches at the appropriate times in order to spin the motor. The control unit used is an Allegro UCN5804B BiMOS Unipolar Stepper motor Translator/Driver Chip; combining low-power logic with high-

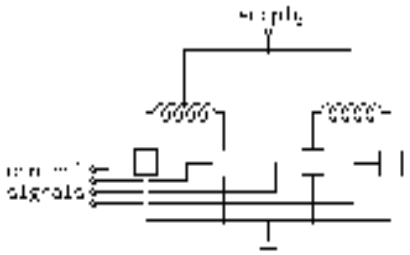

Figure 148 Typical Unipolar Stepper Motor Controller

current and high-voltage bipolar outputs, the UCN5804B provides complete control and drive for a four phase unipolar stepper motor with continuous current rating to 1.25A per phase and 35v. The logic section provides the sequencing logic, direction and output enable control with three drive formats: wave-drive (one-phase), two-phase and half-step. The wave-drive format consists of energizing one motor phase at a time in an A-B-C-D (or D-C-B-A) sequence. Two-phase drive energizes two adjacent phases in each opposing position (AB-BC-CD-DA); this sequence mode offers an improved torque-speed product and is less susceptible to motor resonance. Half step excitation alternates between one-phase and two-phase modes (A-AB-B-BC-C-CD-D-DA) providing an eight-step sequence. The two-phase drive format is selected to drive the ball locator platform.

The UCN5804B chip and all the required inputs and outputs are mounted on a PCB board. The circuit and its dedicated 24v power supply are mounted in control cabinet separate to the sensitive piezo driver modules; cables run between both control cabinets to power the 5v logic side of the circuit and to control the step input and motor direction using the BNC-2120 breakout. Figure 149 illustrates the appropriate wiring for the UNC5804B Translator/Driver Chip and 23HS-030 stepper motor.

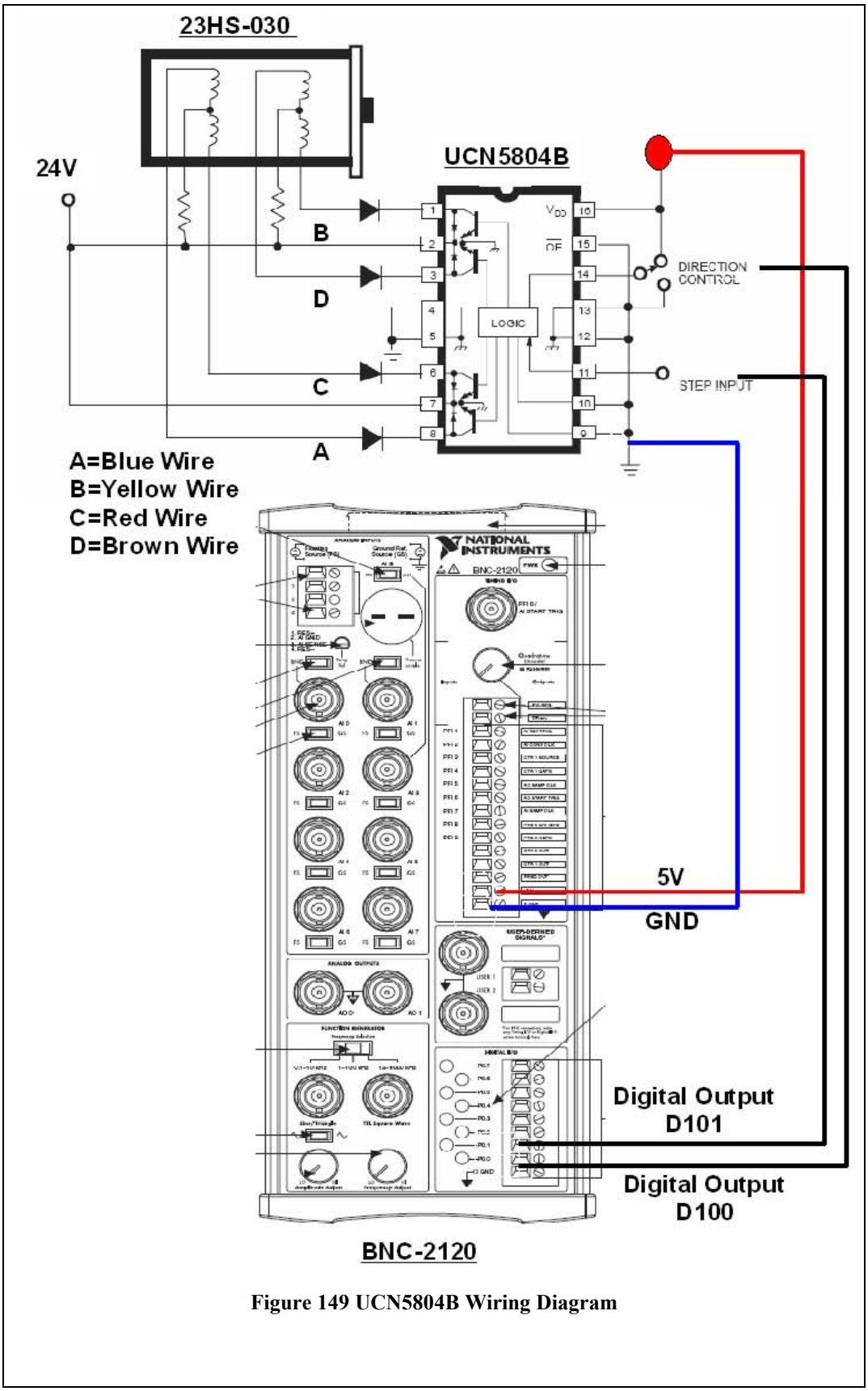

Figure 149 UCN5804B Wiring Diagram

Appendix H
Network Communication and Control

Introduction

The section of the chapter discusses the network installed on the plant floor and the method of communication between the Central Controller, AS-I Controller, Grind Machine Controller and the Measurement Display Unit. Figure 150 illustrates an overview of the complete network installed within the manufacturing facility.

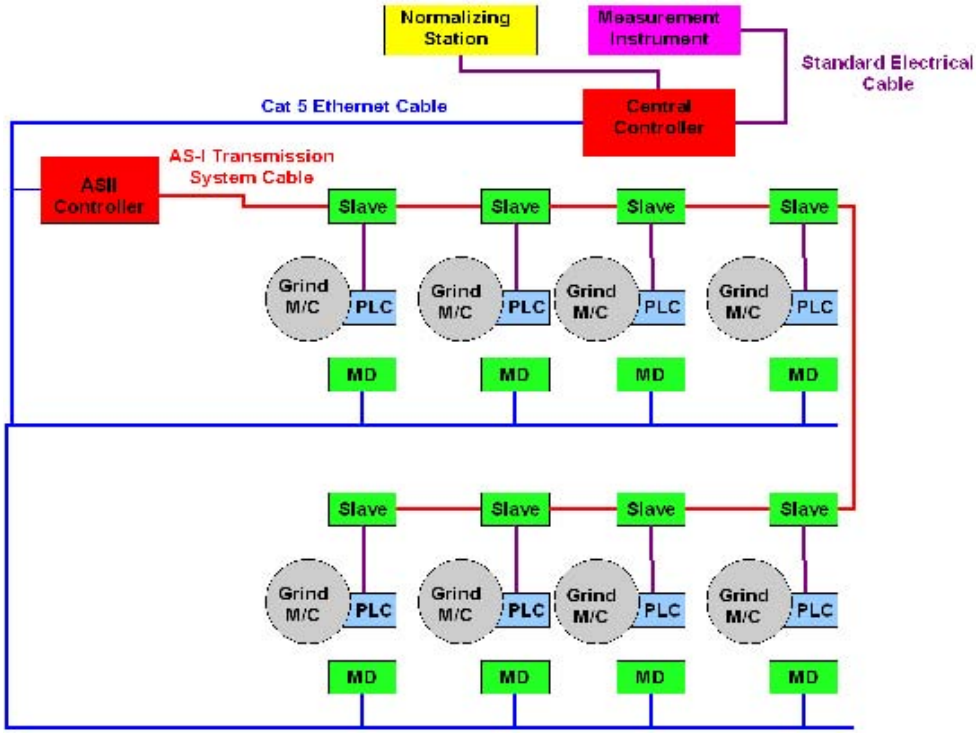

Figure 150 Network Overview

AS-I Field Bus Network

An AS-I network is used to communicate between the central controller and the machine controllers located on the plant floor; AS-I (abbreviation for Actuator Sensor Interface) is a bus system for low-level field applications in industrial automation. The objective in its creation was not a universal field bus for all areas of automation, but rather an economically reasonable system for lower field control. The AS-Interface was developed in order to network binary sensors and actuators to the higher control level; it is especially suited for field devices that are required to incorporate in a stand-alone local area automation network controlled by a PLC or PC. It is a low cost electromechanical connection system designed to operate over a two-wire cable carrying data and power. In traditional wiring, every single signalling transmitter and receiver is wired directly with the superior control; rampant cable trees and huge control

cubicles were the consequence. With the AS-I system the cables and primarily the assembly costs are reduced.

The AS-I network controller communicates with the central controller using the RS-232 standard. Figure 151 shows the AS-I network control system; within the AS-I system there are six main hardware components:

- RS-232 Module
- Programmable Logic Controller (PLC)
- AS-I Power Supply
- AS-I Master
- AS-I Slave Modules
- AS-I Cable

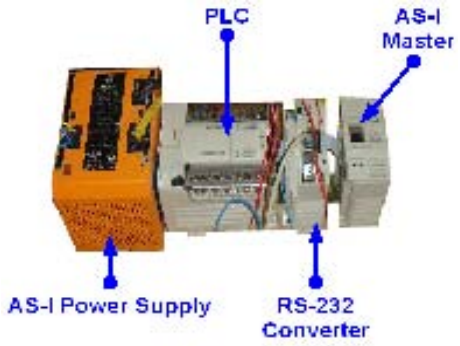

Figure 151 AS-I Network Controller

The data transfer between the central controller and the AS-I network controller is bi-directional. The signals sent from the central controller represent the request to retrieve samples from the grind machine and subsequently if required the command to change the machines operating parameters. The signals sent to the central controller correspond to the operating status of each machine at the time of sampling.

The RS-232 module allows the central controller to remotely communicate with the PLC controlling the AS-I network using the RS-232 standard. A programmable logic controller (PLC) is a digital computer used for automation of industrial processes. Unlike general-purpose computers, a PLC is designed for multiple inputs and output arrangements, extended temperature ranges, immunity to electrical noise and resistance to vibration and impact. Programs to control machine operation are typically stored in battery backed or non-volatile memory; this is computer memory that can retain the stored information even when not powered. A plc is an example of a real time system which responds to signals as fast as possible, or as they

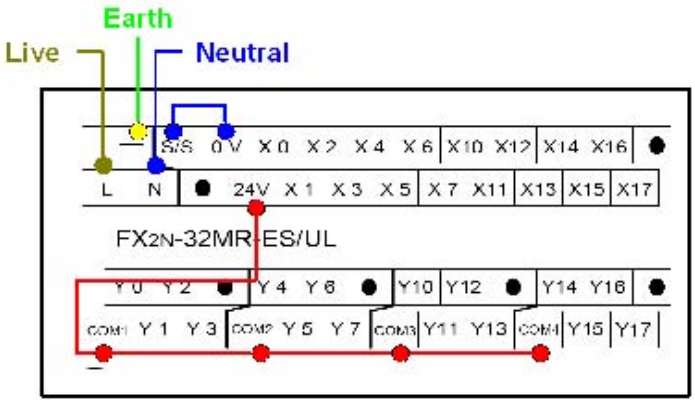

Figure 152 PLC Wiring

happen. The specific type of PLC used is a Mitsubishi FX2N-32MR ES/UL with a processing speed of just 0.08μs per logical instruction and program storage capacity of 8,000 steps. Figure 152 shows the PLC wiring, this Mitsubishi PLC contains 16 inputs and 16 outputs.

Any AS-I interface segment must be powered; this is accomplished by connecting an AS-I power supply. These supplies have certain unique characteristics regarding internal circuitry and output voltage; standard 24v DC power supplies cannot be used to directly power a segment. An AS-I power supply generates a regulated 30v DC supply with a high degree of stability and low residual ripple; it is used to supply the electronics of the network i.e. AS-I master, slaves as well as the connected sensors. The specific power supply used is an Ifm Electronic Power Supply AC 1209. The total length AS-I network cable in a single segment must be no more than 100 meters. If the total network length is required to be longer, repeaters can be used; as the repeater galvanically isolates any two segments a new power supply is required at the opposite side of the repeater. It is often stated that the maximum length of an AS-I network is 300 meters, created by using two repeaters. This is not true, what matters is not how many repeaters are used but rather how many repeaters ant data packet has to cross before reaching the master. Due to the tight timing constraints defined each packet can at most travel across two repeaters before reaching the master. This can allow for various types of network topologies:

1. Linear networks with the master mounted at one end can be 300 meters long
2. Linear network with 600m length can be constructed when the master is mounted in the middle segment
3. Star shaped networks with virtually no length limitation are possible

The AS-I master communicates with AS-I slave modules; the master exchanges information with slave modules, which are connected to the AS-I network. Slaves include the AS-I interface electronics and are the largest group of components that could include binary and analog I/O modules, lights, pushbuttons, sensors, valve control boxes and E-stops; in general any device that can exchange data with the PLC. The slaves cyclically exchange their data (information of the connected I/Os) with the master. Up to 31 slaves can be connected to a bus; each slave on the network must have a unique address. For AS-I the address space ranges from 0 to 31, where 0 cannot be

used but is reserved for automatic single node replacement. The specific type of slave modules used is Ifm Electronic Bus System AS-Interface, AC2411 Active Compactline, AS-I flat cable connection slave. Figure 153 shows the pin connections for the digital inputs and outputs.

inputs

M12 socket	pin
sensor supply L+	1
sensor supply L-	3
data input	2+4
functional earth	5

outputs

M12 socket	pin
external voltage -	3
switching output +	4
functional earth	5

Figure 153 AC2411 Slave Pin Connections

The protocol of the AS-Interface system ensures a simple extendibility. The AS-Interface network can be configured like any conventional electrical installation. Every AS-Interface slave is freely addressable and can get connected to the bus cable in any arbitrary place. This makes a modular construction possible, and due to the robust operating principle, there are no limits to the structure and any network topology can be used, as shown in Figure 154.

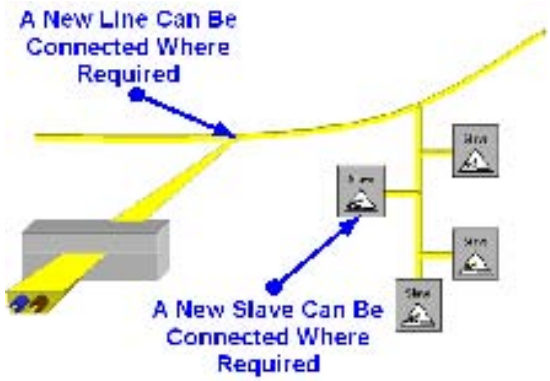

Figure 154 AS-I Network Topology

The AS-I master is the link to the higher-level control system; it organises the data traffic on the AS-I cable and automatically and when required makes the signals of the sensors and actuators available to higher-level system. After polling the signals, the master also transfers the parameter settings to the individual nodes, monitors the network continuously and runs diagnostic checks

As shown in Figure 155, each grinding machine controller PLC is attached to a separate slave on the transmission cable; the command signals are sent between the network controller and these slaves. This links the central controller directly to the inputs and outputs of the grinding machine controller; this allows the central controller to send specific numbers, which represent specific commands (i.e. number 76 may correspond to the command for grinding machine No.1 to pick a sample of five balls from turntable). When each number enters a specific data registers in the AS-I controller PLC the corresponding internal relay is programmed to activate and subsequently send the required signal to the desired slave. This slave signal in turn activates inputs on the grind machine plc, which executes the desired command.

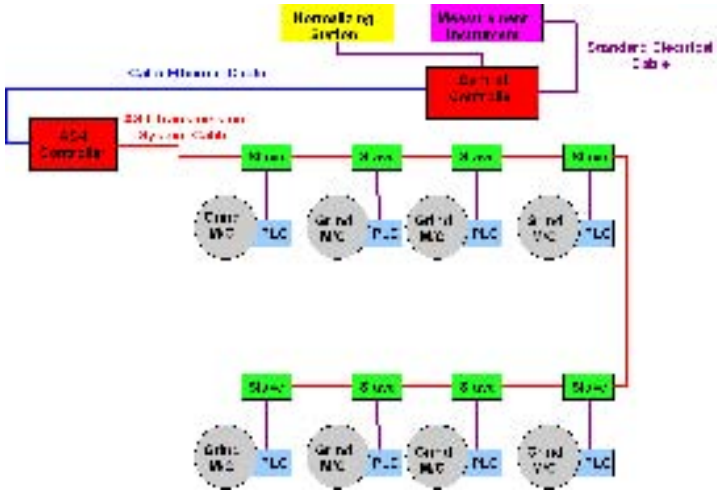

Figure 155 AS-I Network Overview

This AS-I installation utilizes the AS-Interface flat cable defined as part of the AS-Interface specifications. The shape of the cable does not matter (any other cable can be used) but the electrical characteristics of the selected cable matters greatly; to prevent problems due to improper cable it is highly recommended to use the AS-I flat cable. This cable is designed to make use of the cable piercing technology; when a slave module is installed on the network, piercing needles penetrate the cable and displace the internal copper strands without cutting them, as illustrated in Figure 156. This allows AS-I interface slaves to be installed anywhere on the network without cutting and preparing the cable first (i.e. removing cable jacket, stripping insulation and applying a ferule). The result is a faster installation without the chance of inadvertent shorts between the leads. The jacket of the cable is rubber; if slave modules need to be moved after they have been connected to cable this is possible without causing any problems.

The cable is “self-healing”, this means that the holes made by the contact blades in the rubber jacket of the cable close themselves.

There are several types of cable available; yellow cable is used in this installation to power AS-I slave modules and enable communication between the grind machine and the network controller. The AS-I black cable is used to supply the slave modules with 24v DC Auxiliary power. No communication takes place on this cable and similar to the yellow cable, the black is also produced with a jacket material to address the need for the piercing technology. The two leads inside the AS-I interface cable are brown (+lead) and blue (-lead) independent of the material makeup and the outer jacket colour.

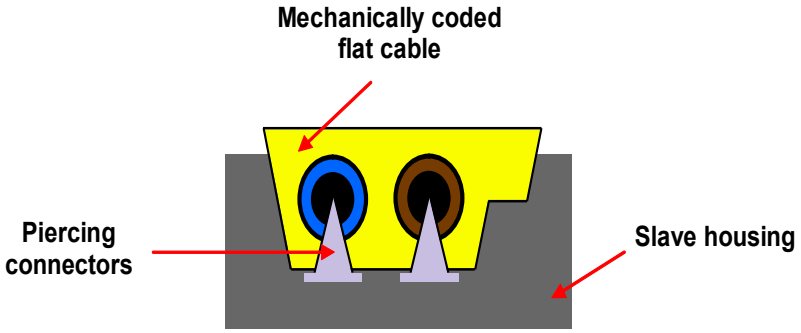

Figure 156 AS-I Interface Flat Cable with Piercing Technology

Serial Port RS-232/RS-422 Interface Converter

The central controller communicates with the AS-I network and the measurement display using the RS-232 standard; communication as defined in the RS-232 standard is an asynchronous serial communication. The word serial means that the information is sent one bit at a time down a single line and asynchronous means that the information is not sent in predetermined time slots. In asynchronous transmission, the receiver does not know when the next character is going to arrive and awaits the arrival of the next start bit to detect when a message starts. Also, there is no information within the character about the speed at which it is being sent i.e. there is nothing to tell the receiver how quickly it needs to sample the incoming signal in order to recover the transmitted data [46]. In contrast, synchronous transmission sends synchronization characters at the start of each block that represents a clock or trigger signal to allow the receivers clock to lock onto the sender's signal. The absence of a clock signal makes an asynchronous communication channel cheaper to operate; fewer lines are necessary in the cable. The disadvantages of asynchronous communication is that the receiver can start receiving at the wrong moment and extra bits that take up bandwidth are needed in the data stream to indicate the start and end of useful information.

In RS-232 communication data bits are sent with a predefined frequency known as the baud rate; baud rate is measured in bits per second. Both the transmitter and receiver must be programmed to use the same bit frequency; after the first bit is received, the receiver calculates at which moments the other data bits will be received and will check the line voltage levels at those moments. The maximum baud rate defined for RS-232 is 20kbps.

Communication using RS-232 means that the sending of data can start on each moment; if starting at each moment is possible, this can pose some problems for the receiver to know which is the first bit to receive. To overcome this problem each data packet is started with a start bit.

The data bits are sent directly after the start bit. Following the data bits, for error detecting purposes it is possible to add an extra bit known as a parity bit to the data packet automatically. The transmitter calculates the value of the bit depending on the information sent and the receiver performs the same calculation to check if the actual parity bit value corresponds to the calculated value. There are two variants of parity bits: even parity bit and odd parity bit. An even parity bit is set to 1 if the number of

ones in a given set of bits is odd, making the total number of ones including the parity bit, even. An odd parity bit is set to 1 if the number of ones in a given set of bits is even, making the total number of ones including the parity bit, odd.

Suppose that the receiver has missed the start because of noise on the transmission line and started on the first following data bit with a low value; this would cause garbled data to reach the receiver. Therefore a mechanism must be present to resynchronise the communication. To do this framing is introduced; framing means that all the data bits and parity bit are contained in a frame of start and stop bits. The period of time between the start and stop bits is a constant defined by the baud rate and the number of data and parity bits. The start bit is always a low value and the stop bit is always a high value. If the receiver detects a value other than a high value when the stop bit should be present on the line, it knows that there is a synchronisation failure; the device then tries to resynchronise on new incoming bits.

The RS-232 standard defines the voltage levels that correspond to logical one and logical zero levels; valid signals are plus ±3 to 15 volts. Logic one is defined as a negative voltage and logic zero is defined as a positive voltage.

Cable length is a big issue in relation to RS-232 communication; the standard has a maximum cable length of 15m or the cable length equal to a capacitance of 2500pF. The latter rule is frequently forgotten; this means that using a cable with low capacitance allows communication over longer distances e.g. if Cat-5 cable with a typical capacitance of 55pF/m is used, the maximum cable length is 45m.

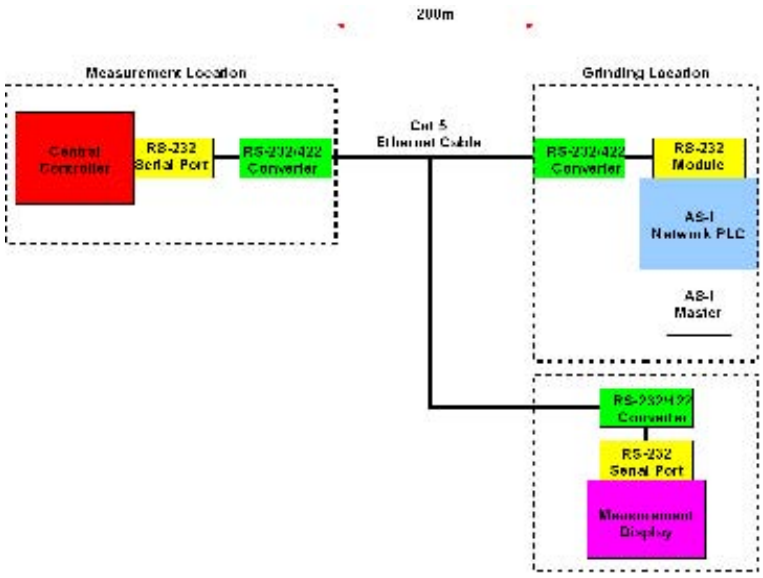

Figure 157 RS-232 to RS-422 Overview

As previously mentioned the very high levels of acoustic and electrical noise, vibration and humidity in the environment would have adverse effects on the measuring instrument. For this

reason, the piezo measurement instrument, the temperature normalizing station and the central controller will be situated in a designated measurement location in a reasonably undisturbed section of the facility, 200 meters away from the hard-grinding process. This introduces a problem for the communication between the central controller and the grinding process, where the AS-I network and the measurement display unit are located; the distance exceeds the max allowable cable length for RS-232 transmission. To overcome this problem, the RS-232 signal is converted to RS-422 and transmitted across the facility using Cat-5 Ethernet cable, at the grinding location the signal is converted back to RS-232 for the AS-I network controller and the measurement display unit to receive, see Figure 157.

The relatively short distances and low speed of the RS-232 standard serial interface has caused a demand for newer standards like RS-422; RS-422 provides for data transmission using serial balanced differential signalling. Balanced differential is what makes RS-422 different from RS-232. On RS-232 interfaces, the signals are sent on lines that share a common zero; the transmitter generates a single voltage that the receiver compares with a fixed reference voltage, both relative to a common ground connection shared by both ends. With Rs-422 each signal line consists of two wires twisted to reduce noise; the voltage difference between the two lines is an indication of the signal value rather than the voltage level. Twisting the lines helps to reduce the noise; the noise currents induced by an external source are reversed in every twist. Instead of amplifying each other as in a straight line, the reversed noise currents reduce each other's influence. Figure 158 explains this in more detail.

Looking at voltage differences rather than levels eliminates a lot of noise induced by external sources and allows for higher data rates and cable lengths compared to RS-232. To see why, consider a single ended system with a supply voltage V_s. The high logic level is V_s and the low logic level is 0v; the difference between the two levels is therefore V_s-0v = V_s. Consider a differential system with the same supply voltage. The voltage difference in the high state, where one wire is at V_s and the other at 0v, is V_s-0v = V_s. The voltage difference in the

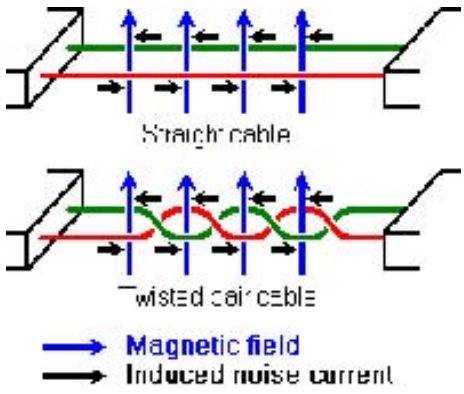

Figure 158 Noise in Straight and Twisted Pair Cables

low state, where the voltages on the wires are exchanged is 0v- V_s = - V_s. The difference between high and low logic levels is therefore V_s-(- V_s) = 2 V_s. This is twice the difference of the single ended and the result is that it takes twice as much noise to cause an error with the differential system as with the single ended system i.e. the noise immunity is doubled.

Another difference between RS-422 and RS-232 is the amount of receivers on the system. A RS-232 transmitter is only designed to serve on receiver, while a RS-422 transmitter can serve up to ten receivers in parallel; this allows one central control unit to send commands in parallel to up to ten slaves. Unfortunately, those slave devices cannot send information back over a shared interface line.

RS-422 transmitters and receivers are designed for point-to-point and multi-drop configurations but not multi-point. Point-to-point is a one transmitter and one receiver system. The second configuration is a one transmitter with two or more receivers normally connected in a daisy chain layout. The last type of configuration is multi-point, which uses two or more transmitters connected to one or more receivers.

A RS-422 driver is capable of transmitting data across 1,200 meters of cable, but not at maximum data rates. Cable length and data rate have an inverse effect on each other; when operating at either the recommended maximum cable or data the other cannot be obtained. For instance, it is not possible to operate at 1,200 meters when operating at 10 Mb/s or vice versa. A chart displaying the recommended operational region of a typical RS-422 standard interface is shown in Figure 159, other interface standards are also shown for comparison.

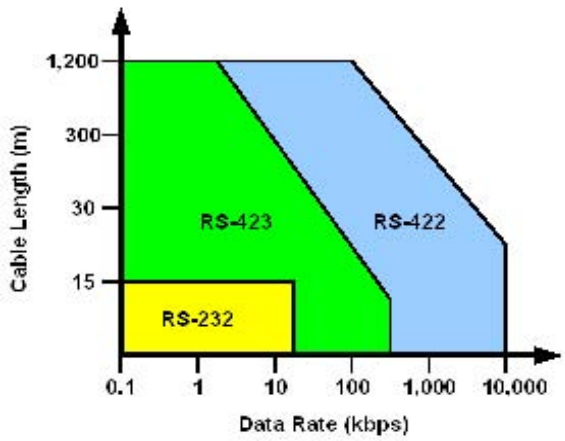

Figure 159 Interface Standards Operating Regions

A RS-232 to RS-422 interface converter installed at both the transmitter and receiver ends of the network allows for the RS-232 signal generated from the central controller to be transmitted across the facility using RS-422 and successfully received by the RS-232 standard AS-I network controller and measurement display unit. The central controller can also receive signals from the AS-I network controller on the same line.

The specific converter used is a Patton Electronics Model 222N9 Ultra-miniature RS-232 (EIA-574) to RS-422 Interface Converter, as shown in Figure 160; this allows PC, terminals and laptops employing the RS-232/ DB-9 interface to communicate with devices using RS-422 balanced electrical signals. The 222N9 converter is housed in an ultra-miniature ABS plastic enclosure measuring 6.35cm x 3cm x 1.9cm. Facilitating bi-directional data conversion over two twisted pair, the interface converter supports data rates up to 19.2 Kbps over distances up to 1,200 meters.

Figure 160 Patton Electronics RS-232 to RS-422 Interface Converter

The interface converter is easy to install and requires no pre-configuration. To function properly the converter must have two twisted pairs of metallic wire; these wires must be dry, unconditioned metallic wire between 19 and 26 AWG (American Wiring Gauge, a U.S. measurement standard of the diameter of non-ferrous wire: the smaller the AWG number, the thicker the wire). The specific type of cable used for the RS-422 transmission is Category 5 cable; this cable includes four twisted pairs in a single shielded cable jacket and uses balanced lines to help preserve a high signal-to-noise ratio. Cat 5 cable typically has three twists per inch of each twisted pair of 24 gauge copper wires within the cable.

When connecting two interface converters it is necessary to use a “cross over” cable. At the central controller interface converter, one pair of wires is connected to XMT+ and XMT- (transmit positive and negative)

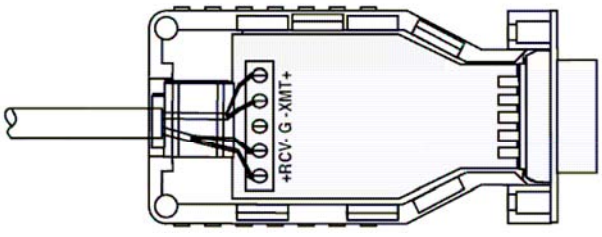

Figure 161 Interface Converter Wiring

and a second pair of wires connected to RCV+ and RCV- (receive positive and negative), as shown in Figure 161. At the opposite end of the transmission line, the interface converters connected to the AS-I controller and the measurement display are wired opposite to the central controller converter i.e. central controller XMT+ connected to AS-I controller RCV+. Table 21 below shows the wiring for the interface converters cross over cable.

222N9 RS-232 to RS-422 Interface Converter		
Central Controller Converter	**Cable Colour**	**AS-I Controller and Measurement Display Converter**
XMT+	BLUE	RCV+
XMT-	BLUE/WHITE	RCV-
RCV+	GREEN	XMT+
RCV-	GREEN/WHITE	XMT-

Table 21 222N9 RS-232 to RS-422 Interface Converter

Once the Model 222N9 is properly installed, it operates transparently as if it were a standard cable connection. Operating power is derived from the RS-232 data and control signals; there is no ON/OFF switch. All data from the RS-232 interface including flow control information is passed straight through.

Appendix I
Ball Locator Mathematical Model

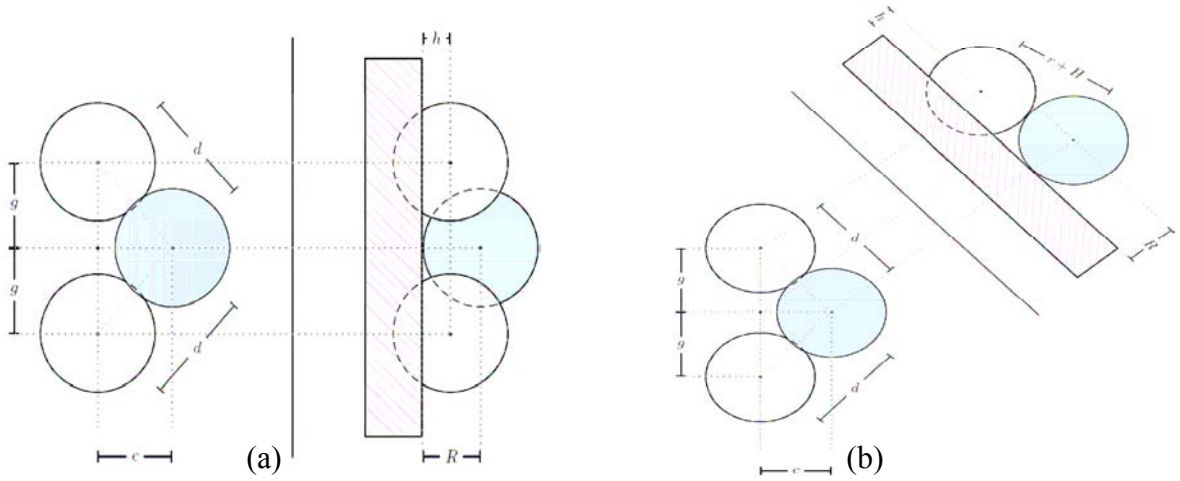

Figure 162 (a) Plan and Side View (b) Plan and Plane of Contact Side View

Using mathematical software and the mathematical models, an optimal configuration has been found by Kieran Murphy [65].

The problem can be specified using the parameters shown in Fig.43 (a) and (b)

Fixed Input:

- g is half the horizontal distance between the centers of the embedded spheres $(r \le g \le R + r)$
- h is the height of the center of both the embedded spheres above the mounting plate $(0 \le h \le r)$
- r is the radius of both the embedded spheres $(5 \le r \le 6.25)$

Variable Input:

- R is the radius of the measurement ball $(5 \le R \le 6.25)$

Output:

- d is the horizontal distance between the center of an embedded sphere and the center of a measurement ball
- c is the horizontal distance between the origin and the center of a measurement ball

The length d can be calculated from the plane of contact side view Fig.43 (b) using properties of right angle triangles

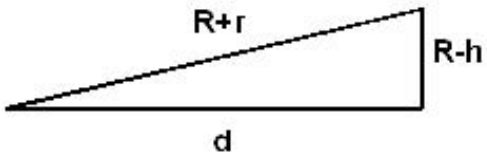

$$H^2 = O^2 + A^2$$
$$A^2 = H^2 - O^2$$
$$\Rightarrow d^2 = (R+r)^2 - (R-h)^2$$
$$d^2 = R^2 + Rr + Rr + r^2 - R^2 + Rh + Rh + h^2$$
$$\therefore d^2 = 2R(r+h) + r^2 - h^2$$

The length c can be calculated from the plan Fig.43 (a), again using properties of right angle triangles

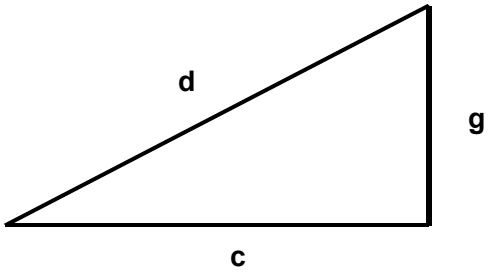

$$c^2 = d^2 - g^2$$
$$c^2 = (R+r)^2 - (R-h)^2 - g^2$$
$$c^2 = 2R(r+h) + r^2 - h^2 - g^2$$

Of interest are values of the parameters g, h and r, which minimize the variation in c arising from varying the diameter of the measurement ball from 10mm-13mm (radius R over the interval R_{min}=5 to R_{max}=6.25)

$$\min_{g,h,r} \left| c_{g,h,r}(R_{\max}) - c_{g,h,r}(R_{\min)} \right|$$

Or on defining function (generated by Kieran Murphy)

$$f(g,h,r) = \left| \sqrt{2R_{MAX}(r+h) + r^2 - h^2 - g^2} - \sqrt{2R_{MIN}(r+h) + r^2 - h^2 - g^2} \right|$$

Of interest is the following constrained optimization problem

$$\min_{g,h,r} \quad f(g,h,r)$$

$$R_{MiN} \le r \le R_{MAX}$$

subject $0 \le h \le r$

$$r \le g \le R_{MIN} + r$$

The radius of the embedded spheres, the distance of the center of the embedded spheres above the mounting plate and the distance between the embedded spheres are 6.25, 0 and 14mm respectively for the configuration shown in Figure 163. With this configuration the max location variation on the Y-axis between a 10mm and 13.5mm ball is 1.00757mm.

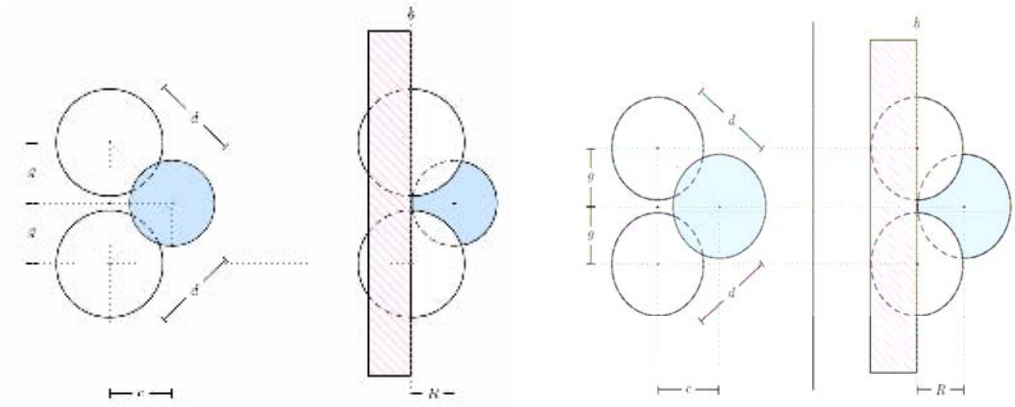

Figure 163 Test Configuration

Figure 164: the location variation in the seating point over the targeted range of ball sizes has been reduced to 0.89762mm. The optimal configuration requires that two spheres of radius 5mm are embedded 5mm into the mounting plate and the distance between the centres of the spheres is 10mm

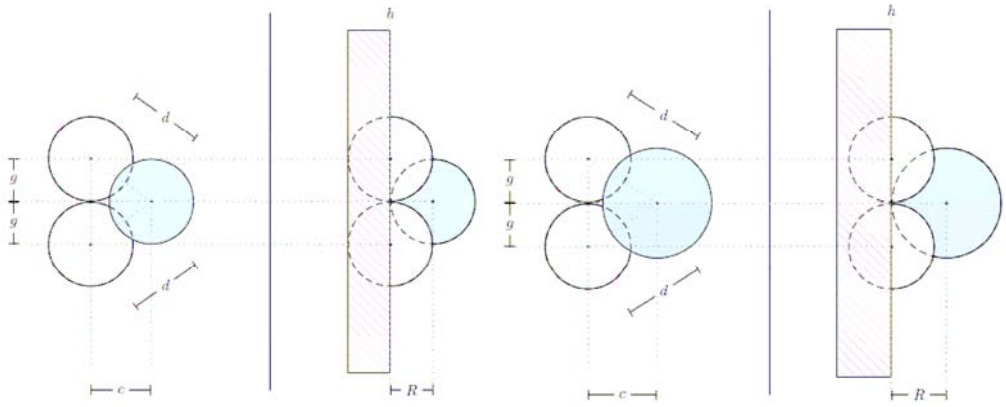

Figure 164 Optimal Configuration